January 2016

Density Functional Theory Calculations Complement Mass Spectrometry Experiments in the Investigation of Biomass Fast Pyrolysis and Ion-Molecule Reaction Mechanisms

Mckay Whetton Easton
Purdue University

Graduate School Form
30 Updated 12/26/2015

PURDUE UNIVERSITY
GRADUATE SCHOOL
Thesis/Dissertation Acceptance

This is to certify that the thesis/dissertation prepared

By Mckay Easton

Entitled
Density Functional Theory Calculations Complement Mass Spectrometry Experiments in the Investigation of Biomass Fast Pyrolysis and Ion-Molecule Reaction Mechanisms

For the degree of Doctor of Philosophy

Is approved by the final examining committee:

Fabio H. Ribeiro Co-chair	Jeffrey Greeley
Hilkka I. Kenttamaa Co-chair	Lyudmila Slipchenko
John J. Nash	

To the best of my knowledge and as understood by the student in the Thesis/Dissertation Agreement, Publication Delay, and Certification Disclaimer (Graduate School Form 32), this thesis/dissertation adheres to the provisions of Purdue University's "Policy of Integrity in Research" and the use of copyright material.

Approved by Major Professor(s): Fabio H. Ribeiro

Approved by: John A. Morgan 7/1/2016

Head of the Departmental Graduate Program Date

DENSITY FUNCTIONAL THEORY CALCULATIONS COMPLEMENT MASS SPECTROMETRY EXPERIMENTS IN THE INVESTIGATION OF BIOMASS FAST PYROLYSIS AND ION-MOLECULE REACTION MECHANISMS

A Dissertation

Submitted to the Faculty

of

Purdue University

by

Mckay Whetton Easton

In Partial Fulfillment of the

Requirements for the Degree

of

Doctor of Philosophy

August 2016

Purdue University

West Lafayette, Indiana

สำหรับภรรยา สำหรับลูก ๆ

ACKNOWLEDGEMENTS

I must begin by acknowledging my advisor, Professor Fabio Ribeiro, for his support and flexibility in aiding me during my time at Purdue. One of the main reasons I chose to attend Purdue University was to work on a project related to DFT. Unfortunately, the project lost funding after my first year and I was left without an advisor and without a project. Fabio was willing to work with me to create a new project related to DFT and establish important collaborations with Argonne National Labs, and Dr. John Nash and Professor Hilkka Kenttämaa from the chemistry department at Purdue. Although he has not been able to provide me with technical advice, he ensured that I had ample opportunity for growth.

I cannot say enough about the benefit I have received by collaborating with the chemistry department. Dr. Nash has been insightful and encouraging throughout our interactions. In the early days of my research when I felt that my calculations were not running as I hoped or intended, every meeting with Dr. Nash would instill in me greater vision and drive to tackle the difficult problems associated with the project. Without his expertise, I would not have been able to accomplish more than a modicum of DFT research.

The collaboration with Professor Kenttämaa has also been a highlight of my experiences at Purdue. She exudes an unrivaled level of enthusiasm and optimism. I am

excited to continue my work under her tutelage as a post-doctoral researcher and anticipate learning a whole new set of skills from her vast knowledge of mass spectrometry. It is very obvious to me that Professor Kenttämaa has great respect and regard for those within her circle of influence, which I reciprocate.

Numerous other people have been influential for me, including my other committee members, Professor Jeffrey Greeley and Professor Lyudmila Slipchenko. I have learned valuable skills from each of them from class lectures and one on one interactions. Other important influences are Professor Nicholas Delgass, Professor Rakesh Agrawal, and Professor Mahdi Abu-Omar. I also have learned valuable teaching skills from Professor David Corti, for whom I was a teaching assistant for a semester.

I must acknowledge so many past and present graduate students with whom I worked so closely. Specifically, Dr. John Degenstein, Priya Murria, and Ravi Yerabolu have made invaluable contributions to my work with their experimental work and arousing scientific discussions. I have interacted with many talented people in both the school of chemical engineering (Dr. Piotr Gawecki, Dr. Sara Yohe, Dr. Vinod Kumar Venkatakrishnan, Dr. Dhairya Mehta, Dr. Harshavardhan Choudhari, Emre Gencer, Taufik Ridha, Richard Caulkins, Ian Smith, Abhijit Talpade, Ishant Khurana, Shankali Pradhan, Dr. Myles Thomas, Dr. Kevin Brew, Dr. Nathan Carter, Dr. Erik Sheets, and Dr. Chuck Hages) as well as the chemistry department (Dr. Matt Hurt, Dr. Huaming Sheng, Dr. Jinshan Gao, Dr. Chris Marcum, Dr. James Riedeman, Hanyu Zhu, Joann Max, Jacob Milton, and Josh Yu). There are countless other friendships I have developed while at Purdue that have inspired me and encouraged me.

Most importantly, I must thank my family. My success has been 30 years in the making by my parents, David and Chris Easton, and my siblings, Evan Easton, Garrett Easton, and Annie Bryan. They crafted me to be a lover of education. My talented wife, Sheri, and my beautiful children, Dallin, Connor, and Bennett, are my motivation to be the best version of myself.

Finally, I must acknowledge the financial support for this project as part of the Center for Direct Catalytic Conversion of Biomass to Biofuels (C3Bio), an Energy Frontier Research Center (EFRC) funded by the U.S. Department of Energy (DOE), Office of Science, Basic Energy Sciences (BES), under Award #DE-SC0000997.

TABLE OF CONTENTS

Page

LIST OF TABLES ix

LIST OF FIGURES xii

ABSTRACT xxiv

CHAPTER 1. INTRODUCTION 1

1.1 Research Objectives 3

1.2 Thesis objectives 3

CHAPTER 2. MASS SPECTROMETRIC STUDIES OF FAST PYROLYSIS OF CELLULOSE 5

2.1 Introduction 5

2.2 Experimental Methods 7

2.3 Results and Discussion 8

2.4 Conclusions 12

CHAPTER 3. FAST PYROLYSIS OF ^{13}C-LABELED CELLOBIOSES: GAINING INSIGHTS INTO THE MECHANISMS OF FAST PYROLYSIS OF CARBOHYDRATES 15

3.1 Introduction 15

3.2 Methods 16

3.3 Results and Discussion 18

3.4 Conclusions 23

CHAPTER 4. DEHYDRATION PATHWAYS FOR GLUCOSE AND CELLOBIOSE DURING FAST PYROLYSIS 25

4.1 Introduction 25

4.2 Computational Methods 26

Page

4.3 Results and Discussion....28
4.3.1 Maccoll Elimination and Dehydration.... 28
4.3.2 Pinacol Ring Contraction.... 35
4.3.3 Cyclic Grob Fragmentation.... 40
4.3.4 Aldol Condensation Rearrangement.... 45
4.3.5 Alcohol condensation.... 48
4.3.6 Retro-Diels Alder Reaction.... 53
4.4 Conclusions....55
CHAPTER 5. COMPUTATIONAL RESULTS ON CELLOBIOSE FRAGMENTATION GIVE CLUES TO CELLULOSE DEPOLYMERIZATION DURING FAST PYROLYSIS 57
5.1 Introduction....57
5.2 Methods....60
5.3 Results and Discussion....61
5.3.1 Catalytic Glucose formation via Maccoll Elimination 64
5.3.2 Hydrolysis/Alcoholysis.... 67
5.3.3 Reducing vs. Non-reducing End Chemistry 68
5.4 Conclusions....71
CHAPTER 6. EXPLORING THE MECHANISMS OF FAST PYROLYSIS OF HEMICELLULOSES VIA TANDEM MASS SPECTROMETRY AND QUANTUM CHEMICAL CALCULATIONS: A SYNTHETIC MODEL COMPOUND STUDY 73
6.1 Introduction....73
6.2 Methods....73
6.3 Results and Discussion....74
6.4 Conclusions....81
CHAPTER 7. COMPUTATIONAL AND EXPERIMENTAL INVESTIGATION OF ION-MOLECULE REACTIONS TO IDENTIFY PROTONATED SULFONE AND AROMATIC CARBOXYLIC ACID FUNCTIONALITIES 84
7.1 Introduction....84

Page

7.2 Methods....85
7.3 Results and Discussion....86
7.3.1 Protonated carboxylic acid model compounds 86
7.3.2 Protonated sulfone model compounds 94
7.4 Conclusions....95
CHAPTER 8. SUMMARY 98
REFERENCES 100
VITA 304

LIST OF TABLES

Table Page

4.1. Transition state and reaction Gibb's free energies in kcal/mol for Maccoll eliminations of glucose calculated for 298.15 K and 873.15 K at the M06-2X/6-311++G(d,p)//M06-2X/6-311++G(d,p) level of theory. 29

4.2. Transition state and reaction Gibb's free energies in kcal/mol for Maccoll elimination of cellobiose calculated at 298.15 K and 873.15 K at the M06-2X/6-311++G(d,p)// M06-2X/6-311++G(d,p) level of theory. 32

4.3. Transition state and reaction energetics in kcal/mol for Pinacol ring contraction of glucose calculated at the M06-2X/6-311++G(d,p)//M06-2X/6-311++G(d,p) level of theory at 298.15 K and 873.15 K. 37

4.4. Transition state and reaction free energies in kcal/mol for Pinacol ring contraction of cellobiose calculated at the M06-2X/6-311++G(d,p)// M06-2X/6-311++G(d,p) level of theory at 298.15 K and 873.15 K..... 40

4.5. Transition state and reaction free energies in kcal/mol for cyclic Grob fragmentations of glucose calculated at the M06-2X/6-311++G(d,p)//M06-2X/6-311++G(d,p) level of theory at 298.15 K and 873.15 K..... 43

4.6. Transition state and reaction free energies in kcal/mol for cyclic Grob fragmentation of glucose calculated at the M06-2X/6-311++G(d,p)// M06-2X/6-311++G(d,p) level of theory at 298.15 K and 873.15 K..... 45

Table Page

4.7. Barrier heights in kcal/mol for transformations between Pinacol products and Grob products via aldol rearrangement. All calculations were carried out at the M06-2X/6-311++G(d,p)//M06-2X/6-311++G(d,p) level of theory at 873.15K. 47

4.8. Transition state and reaction free energies in kcal/mol for alcohol condensation reactions of glucose calculated at the M06-2X/6-311++G(d,p)//M06-2X/6-311++G(d,p) level of theory at 298.15 K and 873.15 K. 51

4.9. Comparison of rDA reaction barriers (Gibb's free energy) in kcal/mol for the cyclic alkene products of the Maccoll eliminations of glucose and both rings of cellobiose. Calculations were performed using the M06-2X/6-311++G(d,p)//M06-2X/6-311++G(d,p) level of theory at 873.15 K. 55

5.1. Low energy conformers of cellobiose-water complexes and their electronic energy, enthalpy, and Gibb's free energy (all in kcal/mol) relative to cellobiose and water with no interaction, calculated using the M06-2X/6-311++G(d,p)//M06-2X/6-311++G(d,p) level of theory at the temperatures listed. 62

5.2. Low energy conformers of cellobiosan-water complexes and their electronic energy, enthalpy, and Gibb's free energy (all in kcal/mol) relative to cellobiosan and water with no interaction, calculated using the M06-2X/6-311++G(d,p)//M06-2X/6-311++G(d,p) level of theory at the temperatures listed. 63

5.3. Lowest Gibb's free energy (in kcal/mol) conformers of water complexes with various molecules, calculated at the M06-2X/6-311++G(d,p)//M06-2X/6-311++G(d,p) level of theory at 873.15 K. 64

Table Page

5.4. Complexation energy and transition state energy for Maccoll elimination of cellobiose by hydrogen transfer from C3 catalyzed by various molecules. Calculations performed at the M06-2X/6-311++G(d,p)//M06-2X/6-311++G(d,p) level of theory at 873.15K. 67

5.5. Reaction barriers for hydrolysis and glycosidic bond cleavage for the intermediates along the “GA loss” pathway. Calculations done with M06-2X/6-311++G(d,p)//M06-2X/6-311++G(d,p) at 873.15 K and energies are reported in kcal/mol. 72

6.1. Elemental compositions, proposed structures of fast pyrolysis products as well as m/z values of their ions for xylobiose and xylotriose. 77

LIST OF FIGURES

Figure Page

2.1. The carbohydrate molecules studied here contain two to six glucose units coupled to each other in a linear manner via β(1-4) linkages, just as in cellulose. 6

2.2. Positive ion mode mass spectra showing the ionized primary products of the fast pyrolysis of cellobiose (top) and cellohexaose (bottom) ionized by APCI with ammonium hydroxide. The ions whose relative abundances differ the most are indicated with dotted lines. Two isomers of levoglucosan were observed, levoglucosan itself (ion of m/z 180) and another isomer (ion of m/z 163). All the structures shown for cellobiose have been identified[29] by CAD mass spectral comparison using authentic compounds. 9

2.3. Positive ion mode mass spectra showing the primary products of the fast pyrolysis of cellotriosan (top) and cellulose (bottom) ionized by APCI with ammonium hydroxide. Some of the ions having the same m/z ratio are indicated with a dotted line. 11

2.4. A positive ion mode mass spectrum showing the primary products of the fast pyrolysis of cellobiosan (m/z 342) ionized by APCI with ammonium hydroxide. The ions of m/z 85, 127, 145, 163, 180, and 195 are also formed for cellotriosan, cellopentosan and cellulose. The ion of m/z 324 results from the loss of H2O from the ion of m/z 342. 12

Figure Page

2.5. A simple schematic of the major fast pyrolysis pathways proposed for oligosaccharides formed from cellulose during fast pyrolysis upon addition of water. The cleavages indicated in red are thought to occur in the middle of a cellulose chain. The cleavages indicated in blue and green likely occur only at the reducing terminals, which for long chains of cellulose represent a small overall fraction of the total units. Hence, they are minor pathways. 14

3.1. Positive ion-mode mass spectra showing the ionized initial fast-pyrolysis products (either as ammonium adducts or protonated molecules) of (a) glucopyranosyl[1-^{13}C]glucose and (b) unlabeled cellobiose ionized by APCI with ammonium hydroxide dopant. The structures of the intact molecules are shown at the far right in each spectrum. The products that are ^{13}C-labeled in the top spectrum are connected with red dotted lines to the corresponding unlabeled products in the lower spectrum. 16

3.2. Positive ion-mode mass spectra showing the ionized initial fast-pyrolysis products (either as ammonium adducts or protonated molecules) of (a) [1-^{13}C]glucopyranosylglucose and (b) glucopyranosyl[3-^{13}C]glucose ionized by APCI with ammonium hydroxide dopant. The structures of the intact molecules are shown at the far right in each spectrum. The only product that is labeled in the top spectrum but unlabeled in the bottom spectrum is glucose, as indicated by a red dotted line. The ion labeled with * corresponds to an unknown impurity. 21

Figure Page

3.3. Calculated free energies (kcal mol^{-1}) of intermediates and transition states (square brackets) for the formation of levoglucosan from cellobiose via consecutive losses of one glycolaldehyde (GA) and two ethenediol (EDL) molecules (which are likely to eventually tautomerize to glycolaldehyde) at 25°C (top pathway) and 600°C (bottom pathway) obtained at the M06-2X/6-311++G(d,p)//M06-2X/6-311++G(d,p) level of theory. The location of a ^{13}C label at C-1 in the reducing end is indicated by a red circle, at C-3 by a blue circle, and at C-5 by a green circle. The mass-to-charge (m/z) ratios are for unlabeled cellobiose. 24

4.1. Numbering scheme for cellobiose. Atoms on non-reducing end indicated by primed numbers. 27

4.2. An example mechanism of Maccoll elimination for glucose, depicting GLC32Mac (3 indicates the carbon site where the C-O bond is broken; 2 indicates the carbon site where the C-H bond is broken). 29

4.3. All eight possible Maccoll eliminations of β-D-glucopyranose. The numbers near the arrows indicate barrier heights (Gibb's free energy) in kcal/mol calculated at the M06-2X/6-311++G(d,p)//M06-2X/6-311++G(d,p) level of theory at 873.15 K. The reaction codes indicate the reactant (GLC=glucose), the respective carbon sites from which OH and H are lost during dehydration, and the reaction type (Mac=Maccoll).31

Figure Page

4.4. All the 16 possible Maccoll eliminations of cellobiose. The numbers by the arrows indicate barrier heights (Gibb's free energy) in kcal/mol calculated at the M06-2X/6-311++G(d,p)//M06-2X/6-311++G(d,p) level of theory at 873.15 K. The reaction codes indicate the reactant (CB=cellobiose), the respective carbon sites from which OH and H are lost during dehydration, and the reaction type (Mac=Maccoll). 33

4.5. Comparison of transition state energies in kcal/mol for Maccoll eliminations of glucose (GLC) and each glucose ring in cellobiose: reducing end (CBr) and non-reducing end (CBnr). 35

4.6. Example Pinacol ring contraction mechanism, depicting GLC12Pin. The reaction code indicates the reactant (GLC=glucose), the respective carbon atoms that break a C-O bond and form a C=O bond (C1 and C2 in this case), and the reaction type (Pin=Pinacol rearrangement). 36

4.7. Pinacol ring contraction mechanisms for β-D-glucopyranose. The numbers by the arrows indicate the Gibb's free energy in kcal/mol calculated at the M06-2X/6-311++G(d,p)//M06-2X/6-311++G(d,p) level of theory at 873.15 K. The reaction codes indicate the reactant (GLC=glucose), the respective carbon sites from which a C-O bond is broken and a C=O bond is formed, and the reaction type (Pin=Pinacol rearrangement). 37

4.8. Mechanism for water loss and ring contraction of glucose protonated at O2. 38

Figure Page

4.9. Pinacol ring contraction reactions for cellobiose. The numbers by the arrows indicate the Gibb's free energy barriers in kcal/mol calculated at the M06-2X/6-311++G(d,p)//M06-2X/6-311++G(d,p) level of theory at 873.15 K. The reaction codes indicate the reactant (CB=cellobiose), the respective carbon sites from which a C-O bond is broken and a C=O bond is formed, and the reaction type (Pin=Pinacol rearrangement). 39

4.10. Generalized cyclic Grob fragmentation mechanism. 41

4.11. The cyclic Grob fragmentation reactions of β-D-glucopyranose with Gibb's free energy barriers in kcal/mol calculated at the M06-2X/6-311++G(d,p)//M06-2X/6-311++G(d,p) level of theory at 873.15 K. The reaction codes indicate the reactant (GLCeq = "equatorial" glucose, GLCax = "axial" glucose), the respective carbon atoms that break a C-O bond and form a C=O bond, and the reaction type (Grob=cylic Grob fragmentation). In the case of GLC53Grob, the C-O bond is not broken but transforms from an ether to a hydroxyl group. 42

4.12. The cyclic Grob fragmentation reactions of cellobiose with Gibb's free energy barriers in kcal/mol calculated at the M06-2X/6-311++G(d,p)//M06-2X/6-311++G(d,p) level of theory at 873.15 K. The reaction codes indicate the reactant (CBeq = "equatorial" cellobiose, CBax = "axial" cellobiose), the respective carbon atoms that break a C-O bond and form a C=O bond, and the reaction type (Grob=cylic Grob fragmentation). In the case of CB53Grob and CB5'3'Grob, the C-O bond is not broken, but transforms from an ether to a hydroxyl group. 44

Figure Page

4.13. Generalized aldol rearrangement mechanism. 46

4.14. Interconversion between Pinacol ring contraction products and cyclic Grob fragmentation products via aldol rearrangement. 46

4.15. Potential energy surface in kcal/mol for the formation and interconversion of Pinacol ring contraction and cyclic Grob fragmentation products of glucose. Calculations were performed at the M06-2X/6-311++G(d,p)//M06-2X/6-311++G(d,p) level of theory at 873.15 K. 47

4.16. Generalized alcohol condensation reaction mechanism. 48

4.17. Alcohol condensation reactions for β-D-glucopyranose. Each product can be formed in two ways depending on which OH group leaves as water and which OH loses a hydrogen atom. The locations of the lost OH and H are indicated by the reaction numbers (*i.e.* GLC13Cond loses the OH at C1 and the H at C3 whereas GLC31Cond loses the OH at C3 and the H at C1.). Gibb's free energy barriers in kcal/mol were calculated at the M06-2X/6-311++G(d,p)//M06-2X/6-311++G(d,p) level of theory at 873.15 K. 50

4.18. Most likely condensation reactions of cellobiose. Reaction codes indicate the reactant (CB=cellobiose, CBN=cellobiosan), the respective carbon sites for C-O cleavage and C-O ether formation, and the reaction type (Cond=alcohol condensation). Numbers indicate the Gibb's free energy in kcal/mol of the transition state relative to the reactants. Calculations were performed at the M06-2X/6-311++G(d,p)//M06-2X/6-311++G(d,p) level of theory at 873.15 K. 52

Figure Page

4.19. Potential energy surface in kcal/mol for levoglucosan formation from cellobiose through a cellobiosan intermediate, including conformational changes. Calculations were performed at the M06-2X/6-311++G(d,p)//M06-2X/6-311++G(d,p) level of theory at 873.15K..... 52

4.20. Generalized representation of the retro-Diels Alder reaction. Each R group can be either carbon- or oxygen-centered. 53

4.21. The rDA reactions of the cyclic alkene fragments formed upon glucose dehydration. Numbers above the arrows are the Gibb's free energy barriers in kcal/mol calculated at the M06-2X/6-311++G(d,p)//M06-2X/6-311++G(d,p) level of theory at 873.15 K. The labels on the left side of the reactions indicate the dehydration reaction that formed the cyclic alkene. 53

Figure Page

4.22. The rDA reactions of the cyclic alkene fragments formed upon cellobiose dehydration. Numbers above the arrows are the Gibb's free energy barriers in kcal/mol calculated at the M06-2X/6-311++G(d,p)//M06-2X/6-311++G(d,p) level of theory at 873.15 K. The labels on left side of the reactions indicate the dehydration reaction that formed the cyclic alkene. Two of the rDA transition states (CB2'3'Mac and CB4'5'Mac) were not compatible with a one-step concerted mechanism, but rather a two-step mechanism with a loosely bound zwitterionic intermediate. Reported here are the heights for the rate-limiting barriers.Cyclic alkenes arising from saccharide dehydration are likely to fragment further through a retro-Diels Alder reaction, since the calculated barriers for rDA are so low—between 39.3 and 55.2 kcal/mol (Table 4.9). In general, the reactions of cellobiose have larger barriers than the corresponding reactions of glucose. This is probably due to the additional intramolecular hydrogen bonds that must break during the transition for cellobiose. A comparison of the results obtained for glucose and cellobiose rDA is provided in Table 9. 54

5.1. Depiction of the "hydroxymethylene-assisted glycosidic bond cleavage" (HAGBC) reaction of a generalized glucosaccharide. 58

5.2. Comparison of conformations of cellobiose-water complexes CB_WAT_6 and CB_WAT_9. Distances of hydrogen bonds (dashed lines) displayed in angstroms. . 63

Figure Page

5.3. Maccoll elimination by hydrogen transfer from C3 to the glycosidic oxygen in isolation (A), with external water or methanol (B), external formic acid (C), external glucose (D), and possible cellobiose self-catalysis (E). Calculations performed at the M06-2X/6-311++G(,dp) level of theory at 873.15 K for reactions in (A)-(D)..... 66

5.4. Reaction pathways for alcoholysis of cellobiose. 68

5.5. Cellobiose fragmentation via hydrolysis, HAGBC, and reducing end unravelling. Reaction free energies and reaction barriers (in square brackets) were calculated at the M06-2X/6-311++G(d,p)//M06-2X/6-311++G(d,p) level of theory at 873.15 K. * Denotes a calculated barrier with an explicit water molecule present, relative to the water complexed reactant. Dashed arrows correspond to reactions that contradict the experimental study of Degenstein et al.[28] 69

6.1. Structures of compounds used as model compounds in this study: (a) β-1,4-xylobiose and (b) β-1,4-xylotriose. 74

6.2. Positive ion mode mass spectra showing ionized initial products of fast pyrolysis of (a) β-1,4-xylobiose and (b) β-1,4-xylotriose, ionized by atmospheric pressure chemical ionization with ammonium hydroxide as dopant. All peaks shown in the mass spectra correspond to ammonium adducts of products generated upon pyrolysis. 75

6.3. Free energies (kcal mol^{-1}) of intermediates and transition states (square brackets) for the formation of β-D-xylopyranosyl-glyceraldehyde (ions of m/z 240) and β-D-xylopyranosyl-glycoaldehyde (ions of m/z 210) from xylobiose at 600°C calculated at the M06-2X/6-311++G(d,p)//M06-2X/6-311++G(d,p) level of theory..... 79

Figure Page

6.4. Calculated free energy barriers (kcal mol^{-1}) for 1,2-dehydration and cleavage of the glycosidic linkage via Maccoll elimination at 600°C calculated at the M06-2X/6-311++G(d,p)//M06-2X/6-311++G(d,p) level of theory. Reaction codes indicate respective carbon sites that cleave C-O and C-H bonds. 80

6.5. Pathways for the formation of product molecules yielding ions with m/z 222 via water loss from xylobiose (XB) followed by loss of ethendiol or loss of water from xylopyranosylglyceraldehyde (XGRA). Reaction free energies and barriers (in brackets) calculated at the M06-2X/6-311++G(d,p)//M06-2X/6-311++G(d,p) level of theory at 600°C relative to xylobiose. Numbers with * indicate the barrier of the rate determining step in the two-step process of ring-opening and loss of ethenediol. 83

7.1. The mass spectrum of protonated benzoic acid measured after 300 ms of reaction with TMMS (spectrum A). The most abundant product ion (m/z 227) corresponds to adduct-MeOH. The other product ion (m/z 137) corresponds to proton transfer product. The MS^3 spectrum measured after collision-activated dissociation (CAD) of TMMS adduct-MeOH (spectrum B). The fragment ion (m/z 195) corresponds to TMMS adduct-2MeOH. The MS^4 spectrum measured after CAD of TMMS adduct-2MeOH (spectrum C). The most abundant fragment ion corresponds to CO_2 loss. The other fragment ion corresponds to loss of a molecule with MW of 90. 88

Figure Page

7.2. Proposed reaction pathways and calculated potential energy surfaces for the formation of different reaction products upon reaction of protonated aromatic benzoic acid with TMMS reagent and upon CAD of the product ions, calculated at the M06-2X/6-311++G(d,p) level of theory. A) Spontaneous proton transfer and formation of TMMS adduct-MeOH upon reaction of protonated benzoic acid with TMMS. B) Formation of adduct-2MeOH upon CAD of adduct-MeOH. C) Characteristic losses of molecules of MW of 44 Da (solid line) and 90 Da (dashed line) upon CAD of adduct-2MeOH. 89

7.3. Transition state structure for the loss of CO_2 from benzoic acid TMMS adduct-2MeOH calculated at the M06-2X/6-311++G(d,p) level of theory. 90

7.4. The mass spectrum of protonated 2-hydroxybenzoic acid measured after 300 ms of reaction with TMMS (A).Spontaneous formation of TMMS adduct (m/z 275), adduct-MeOH (m/z 243) and adduct-2MeOH (m/z 211) is observed. MS3 spectrum measured after collision activated dissociation (CAD) of TMMS adduct-MeOH (B). The fragment ion (m/z 211) corresponds to TMMS adduct-2MeOH. MS4 spectra measured after CAD of TMMS adduct-2MeOH. The most abundant fragment ion corresponds to the loss of MW 30Da (formaldehyde loss). The other fragment ion corresponds to a neutral loss of MW 44Da (CO2 loss). 91

Figure Page

7.5. Proposed reaction pathway and potential energy surface for the formation of different reaction products and fragments formed upon reaction of 2-hydroxybenzoic acid with TMMS reagent, calculated with the M06-2X/6-311++G(d,p) level of theory for A) spontaneous proton transfer and formation of TMMS adduct-MeOH, B) formation of adduct-2MeOH upon isolation and CAD of adduct-MeOH, and C) characteristic losses of MW of 44 Da (solid line) and 30 Da (dashed line) observed upon CAD of adduct-2MeOH. 92

7.6. The mass spectrum of protonated dimethylsulfone (m/z 95) measured after 300 ms of reaction with TMMS (spectrum A). The most abundant product ion (m/z 199) corresponds to TMMS adduct-MeOH. The other product ion is the protonated TMMS reagent (m/z 137). MS3 spectrum measured after collision activated dissociation (CAD) of TMMS adduct-MeOH (spectrum B). The fragment ions of m/z 75, 105 and 123 are diagnostic to sulfone functionality. 95

7.7. Proposed reaction mechanism (A) and calculated potential energy surface (B) (M06-2X/6-311++G(d,p) level of theory) for the spontaneous formation of TMMS adduct-MeOH and endergonic formation of abundant diagnostic fragment ion (m/z 105) upon CAD of the adduct-MeOH of protonated analytes containing sulfone functionality. The pathway for the formation of the fragment ion (m/z 105) is assumed to be a barrierless pathway (Gibbs free energy (ΔG) is reported in kcal/mol). 96

ABSTRACT

Easton, Mckay W. Ph.D., Purdue University, August 2016. Density Functional Theory Calculations Complement Mass Spectrometry Experiments in the Investigation of Biomass Fast Pyrolysis and Ion-Molecule Reaction Mechanisms. Major Professor: Fabio Ribeiro.

Biomass fast-pyrolysis, or the rapid heating in the absence of oxygen, is a promising method for biomass conversion necessary for a renewable energy economy. Although kinetic models of cellulose pyrolysis have existed since the 1970s, current models and hypothesized reaction networks fail to explain the product distribution even for a simple model compound, the cellulose dimer, cellobiose. A novel approach of using mass spectrometry to instantly characterize fast pyrolysis vapors allows for identification of initial products to help delineate the reaction pathways that dictate the final product distribution of fast pyrolysis of biomass and model compounds. The use of this set-up to study fast pyrolysis of glucosaccharide-based compounds, such as cellobiose, ^{13}C-labeled cellobiose, cellohexaose, cellotriosan, and cellulose has revealed that the reaction pathway of unraveling the reducing end of the polysaccharide by multiple losses of glycolaldehyde (or isomer) is competitive with the well-established mechanism of levoglucosan production via nucleophilic attack of the hydroxymethylene group at the anomeric carbon concerted with glycosidic bond cleavage. Computational investigation on the reaction barriers of this reducing end unraveling mechanism in tandem with

levoglucosan production and hydrolysis may be able to qualitatively account for the observed products of cellobiose pyrolysis. These reaction mechanisms appear to be relevant also for fast pyrolysis of hemicellulose model compounds, specifically xylans.

CHAPTER 1. INTRODUCTION

The current energy market demands and steady decline of non-renewable energy sources has sparked attention in the field of biofuels.[1,2] While cellulosic ethanol has been implemented into the current infrastructure by fuel blending, there is promise in obtaining higher-energy bio-oil by fast-pyrolysis of biomass, followed by downstream upgrading via catalytic hydrodeoxygenation.[2,3] The H_2Bioil process introduced recently in the literature[2] utilizes pyrolysis with fast heating rates for higher yields of oil and minimal char formation versus standard pyrolysis heating rates,[4] and has nearly twice the carbon recovery potential of cellulosic ethanol production by fermentation, with a theoretical carbon efficiency of about 70%. Carbon efficiencies greater than 50% have already been achieved.[3] Fast-pyrolysis is a process of rapid heating in the absence of oxygen to prevent combustion. The final product of biomass fast-pyrolysis is 60-75 wt % condensable vapors, 15-25 wt % char, and 10-20 wt % permanent gases.[5,6] While fast-pyrolysis is not without its challenges,[7] a significant advantage of fast-pyrolysis over other processes such as gasification and fermentation is that more of the larger fuel-range compounds stay intact rather than decompose into gases or char, making it a worthy subject of research.

Lignocellulosic biomass is a complex mixture of cellulose, lignin, hemicellulose, and inorganic material with crystalline and amorphous regimes. The complexity of the

structure of biomass is a source of difficulty in understanding the process by which it breaks down under pyrolytic conditions. Cellulose is a biopolymer of glucoses bound via β(1→4) glycosidic linkages with a degree of polymerization up to 500 and is also the most abundant biopolymer, making up between 40% and 60% of the total mass of the biomass. The products that are commonly observed upon fast pyrolysis of oligosaccharides include sugars (such as glucose), anhydrosaccharides (such as cellobiosan and levoglucosan), furans (such as furfural and 5-hydroxymethylfurfural), light oxygenates (such as formic and acetic acids, glyceraldehyde, formaldehyde, and glycolaldehyde), permanent gases (such as CO and methane), water, and char.[6] The ability to understand and model the chemistry of fast pyrolysis will assist future researchers in their efforts to tailor the product distribution prior to downstream catalytic upgrading.

Although cellulose fast pyrolysis has been considered since the 1970s,[8–10] the mechanisms that dictate the product distribution are still poorly understood. Early models of cellulose pyrolysis employed lumped kinetics and parameters[8–14] but using density functional theory (DFT) to elucidate elementary reactions has led to significant improvement to recent models.[15–18] The growth of DFT over the past several decades[19] provides a systematic way to investigate elementary reactions that may take place during the fast pyrolysis event. The application of DFT to the mechanistic study of the decomposition of smaller glucosaccharides, such as glucose, cellobiose, and cellotriose, is more tractable than the direct study of cellulose but can still provide insights into the underlying mechanisms of fast pyrolysis.[20,21]

1.1 Research Objectives

While current models of pyrolysis are a vast improvement from the early days of the field, the "brute force" method of incorporating all possible reactions is an exhaustive task. It has been my interest to advance the understanding of feasible reaction networks that are applicable to biomass pyrolysis by developing and evaluating potential reaction mechanisms for model compounds of cellulose, hemicellulose, and lignin. This computational work, coupled with mass spectrometric experimental results obtained using novel techniques has led to significant findings. The complementary mix of MS experiments and DFT has also been applied to the development of methods for the characterization of drug metabolites by ion-molecule reactions.

1.2 Thesis objectives

This dissertation can be divided into three general sections: cellulose fast pyrolysis mechanisms, hemicellulose fast pyrolysis mechanisms, and ion-molecule reactions of trimethoxymethylsilane (TMMS) with protonated drug model compounds. CHAPTER 2 provides an introduction to cellulose pyrolysis by comparing the behavior of several model compounds, including cellobiose, cellohexaose, and cellotriosan. This comparison provides justification for the study of cellobiose to understanding cellulose decomposition. The next chapter shows the usefulness of combining experimental and computational work by exploring the fast pyrolysis of isotopically labeled cellobiose. A large number of reactions and mechanisms are discussed in CHAPTER 4 and CHAPTER 5, including dehydration, retro-aldol condensation, retro-Diels Alder reaction, glycosidic bond cleavage, and hydrolysis. The culmination of this section is presented in CHAPTER

5, which proposes a general scheme for cellulose depolymerization. Chapter 6 presents computational and experimental results on fast pyrolysis of hemicellulose model compounds (xylobiose and xylotriose). Finally, CHAPTER 7 highlights the results obtained upon examination of reactions of TMMS with protonated compounds containing carboxylic acids, sulfones and other functionalities.

CHAPTER 2. MASS SPECTROMETRIC STUDIES OF FAST PYROLYSIS OF CELLULOSE

2.1 Introduction

Fast pyrolysis (rapid heating in an inert atmosphere) is an attractive alternative for the conversion of biomass to fuels or valuable chemicals since it is a relatively simple and scalable process.[6,15,20,22–26] Most studies on the mechanisms and pathways of fast pyrolysis of biomass have focused on fast pyrolysis of cellulose since it is the simplest polymer in biomass.[6,15,20,22–26] Unfortunately, even for cellulose, the final fast pyrolysis products (often referred to as biooil in the literature) are a complex unstable mixture of molecules having an oxygen content too high to be used (directly) as a fuel.[6,15,20,22–26] Upgrading this mixture is hindered by its extreme complexity, which arises from numerous competing and consecutive reactions both during and after pyrolysis.[6,15,20,22–26] Currently, no agreement exists in the literature on the mechanisms (e.g., radical, ionic, or neither) of fast pyrolysis reactions of cellulose, the sequence of these reactions, or the identity of the primary products of fast pyrolysis, although anhydro-oligomers in general have been proposed as intermediates several times.[6,15,20,22–28] As background for the computational investigations contained in this thesis, my collaborators have performed vital experimental work on cellulose and model compounds. The results from these experiments provide empirical evidence for the mechanisms proposed herein.

With the aim of gaining a deeper understanding of the fast pyrolysis of cellulose, which may allow better control over the final products, the primary products of fast

pyrolysis of cellulose, cellobiose, cellotriose, cellotetraose, cellopentaose, and cellohexaose (Figure 2.1), as well as cellobiosan, cellotriosan and cellopentosan, have been determined using a previously described mass spectrometry methodology.[29] Primary products, as considered here, are the very first products to evaporate from the hot surface (at 600°C) where pyrolysis occurs.

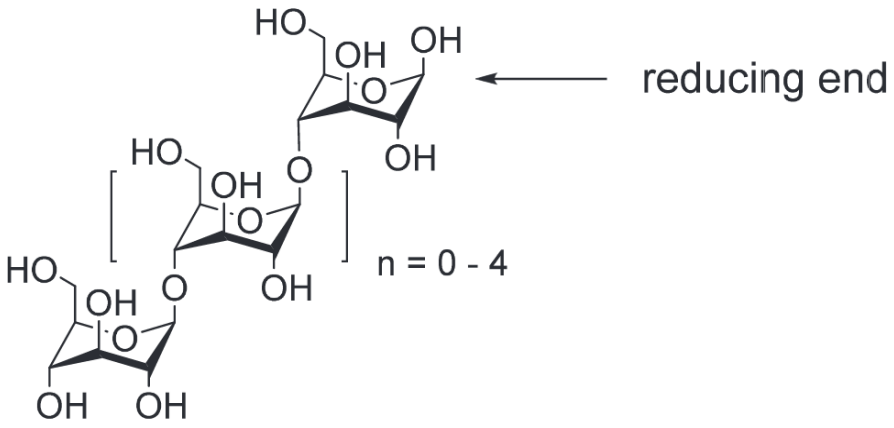

Figure 2.1. The carbohydrate molecules studied here contain two to six glucose units coupled to each other in a linear manner via β(1-4) linkages, just as in cellulose.

The reactor configuration utilized in this work was specifically designed to detect the primary products and not to allow them to undergo further reactions.[29] It has been previously reported that pyrolysis reactor configuration is of critical importance to the product distribution of fast pyrolysis of cellulose.[6,23,24] Hence, the primary products detected here may not be the same detected in a reactor of a different design. The gaseous molecules were ionized via atmospheric pressure chemical ionization (APCI) using either chloroform in methanol (negative ion mode; Cl^- attachment) or ammonium hydroxide in water (positive ion mode; NH^{+4} or proton attachment) in order to ensure that all products were ionized and detected.[29] Based on previous model compound studies, both methods have been found to ionize all major pyrolysis products of cellobiose (some minor

products were ionized by only one of the two methods).[29] Hence, only the positive ion mode results are discussed below. The structures of most of the ions formed from cellobiose and cellulose have been examined[29,30] previously by using MS^2 experiments (i.e., by isolating them and subjecting them to collision-activated dissociation (CAD)). When necessary, the structures of the fragment ions were examined by isolating them and subjecting them to CAD (MS^3 experiment).[29] Where possible, structures were confirmed by analyzing authentic compounds. High resolution mass spectral data needed to determine elemental compositions of the ions were collected using a Thermo Scientific LQIT/Fourier-transform ion cyclotron resonance mass spectrometer.[29] Similar studies were carried out in this research by my collaborators for the fast pyrolysis products of selectively labeled cellobiose molecules.

2.2 Experimental Methods

The pyrolysis method employed here by my collaborators is based on the coupling of a very fast-heating (up to 20,000°C s^{-1}) Pyroprobe 5200 (CDS Analytical, Oxford, PA) to a Thermo Scientific LTQ linear quadrupole ion trap (LQIT) mass spectrometer (Waltham, MA) through a custom-built adaptor.[29] The pyrolysis probe uses a resistively-heated platinum ribbon (2.1 mm x 35 mm x 0.1 mm). The pyrolysis probe was placed inside the atmospheric pressure chemical ionization (APCI) source of the linear quadrupole ion trap and the ribbon was heated up to 600°C at a rate of 1,000°C s^{-1}. The primary products of pyrolysis evaporated into a nitrogen atmosphere at 100°C in the ion source and were quenched. The gaseous molecules were ionized via APCI using ammonium hydroxide in water (positive ion mode; NH^{+4} or proton attachment). The structures of the ions were examined by CAD in MS2 and MS3 experiments and their

elemental compositions were determined by high-resolution measurements by using a Thermo Scientific LQIT/Fourier-transform ion cyclotron resonance mass spectrometer. It should be noted here that we are currently unable to determine mass balance for this pyrolysis experiment. However, quantitation of the pyrolysis products was performed using pyrolysis-GC/MS set-up.

2.3 Results and Discussion

The primary products of fast pyrolysis of cellobiose, the simplest compound studied, are shown in Figure 2.2 (top).[29,30] The relative abundances of the ions reflect the relative abundances of the products that produced them, as verified earlier by using authentic compounds.[29] Only ten major products were observed (with an abundance of at least 10% compared to the most abundant product) and they are consistent with those recently reported in the literature.[29,30] The unambiguously identified products include hydroxymethylfurfural (protonated molecule; m/z 127), levoglucosan (NH_4^+ adduct; m/z 180), glucose (NH_4^+ adduct; m/z 198), glucopyranosyl-β-glycolaldehyde (NH_4^+ adduct; m/z 240; note that this product is formed[30] by loss of two glycolaldehyde units (or isomers) from cellobiose), and cellobiosan (NH_4^+ adduct; m/z 342).[29] Based on our preliminary computational studies, formation of cellobiosan has the lowest energy barrier of these reactions.[30] Two levoglucosan isomers were generated: one that forms an NH_4^+ adduct (m/z 180) like the authentic compound and one that does not (protonated molecule; m/z 163).[29,30] This finding is in agreement with an earlier report wherein the structure (anhydroglucofuranose) was proposed for the second isomer.[31] It is also noteworthy that levoglucosan is not the major primary product of fast pyrolysis although it is a major final product.[15,22,24,25] In prior reports that utilized on-stream fast pyrolysis-

GC/MS, the largest molecules that were observed for cellulose (and oligosaccharide) pyrolysis were levoglucosan and its isomers.[15,25] This may be explained by the high final temperature of about 300°C typically used in GC analysis, which opens the possibility for secondary reactions of larger primary products. Further, the pyrolysis-MS reactor discussed here achieves both pyrolysis and downstream analysis in as little as 125 + 57 ms whereas a pyrolysis-GC/MS reactor requires from 2 up to 30 minutes, depending on the elution times of the products.

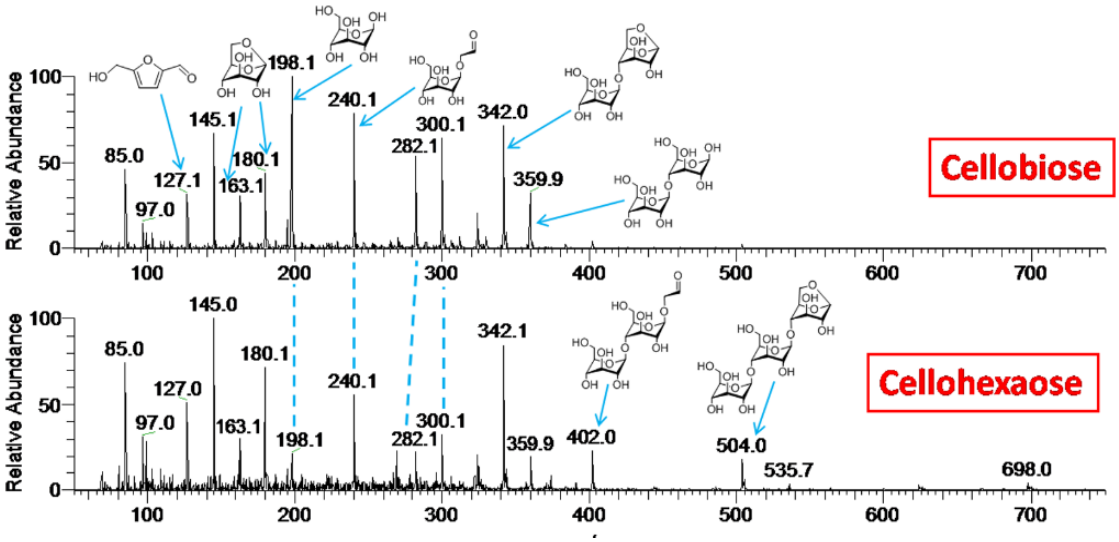

Figure 2.2. Positive ion mode mass spectra showing the ionized primary products of the fast pyrolysis of cellobiose (top) and cellohexaose (bottom) ionized by APCI with ammonium hydroxide. The ions whose relative abundances differ the most are indicated with dotted lines. Two isomers of levoglucosan were observed, levoglucosan itself (ion of m/z 180) and another isomer (ion of m/z 163). All the structures shown for cellobiose have been identified[29] by CAD mass spectral comparison using authentic compounds.

All the major products observed upon fast pyrolysis of cellobiose were also observed for cellotriose, cellotetraose, cellopentaose, cellohexaose, and even cellulose, albeit with different relative abundances. Specifically, the abundances of glucopyranosyl-β-glycolaldehyde (m/z 240; dominant product for cellobiose formed via loss of two glycolaldehyde molecules (or isomers)), glucose (m/z 198), cellobiose that has lost a

glycolaldehyde molecule (or isomer; m/z 300), and cellobiose that has lost both a glycolaldehyde molecule (or isomer) and a water molecule (m/z 282), decrease systematically proceeding from the dimer to trimer, tetramer, pentamer, hexamer and cellulose. For example, Figure 2.2 shows a comparison of the primary products of fast pyrolysis of cellobiose (top) and cellohexaose (bottom). It is obvious that the four products listed above (highlighted with dotted lines in Figure 2.2) have substantially lower abundances for cellohexaose than for cellobiose. For cellulose, their abundances are even lower, as shown in Figure 2.3 (bottom). These findings suggest that the four products described above are somehow associated with the terminal glucose units because the ratio of the terminal units to the total number of glucose units decreases as the size of the oligomer increases. Indeed, the end-group-to-monomer ratio has been reported to be a vital descriptor of cellulose pyrolysis chemistry.[20,26]

In addition to the products observed for cellobiose, the oligomers studied generated two larger products: a molecule likely to be cellobiopyranosyl-β-glycolaldehyde (NH_4^+ adduct; m/z 402) and cellotriosan (NH_4^+ adduct; m/z 504; verified by comparison of its CAD mass spectrum to an authentic sample). Cellulose also produced a very small amount of cellotetrosan (NH_4^+ adduct; m/z 666; verified by comparison of its CAD mass spectrum to an authentic sample; Figure 2.3, bottom). Hence, cellotriosan appears to be the largest product with a significant abundance that is able to efficiently escape the hot pyrolysis surface for cellotriose and the larger oligosaccharides as well as cellulose during fast pyrolysis at 600°C.

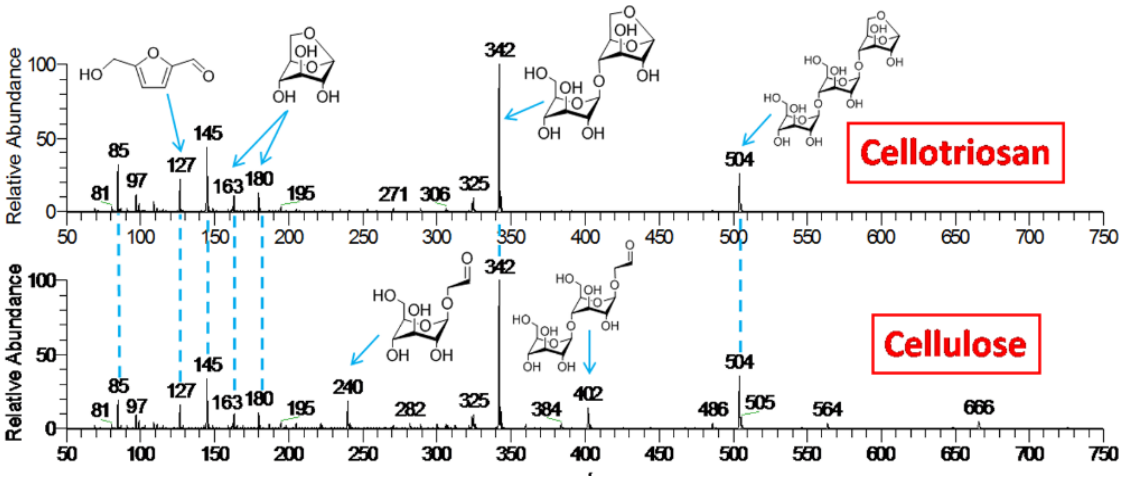

Figure 2.3. Positive ion mode mass spectra showing the primary products of the fast pyrolysis of cellotriosan (top) and cellulose (bottom) ionized by APCI with ammonium hydroxide. Some of the ions having the same m/z ratio are indicated with a dotted line.

Inspired by above observations, fast pyrolysis of cellotriosan was also performed. Cellobiosan dominates this product distribution. However, all major products observed for cellobiose and the oligomers were also observed, with the following exceptions: glucose (m/z 198), glucopyranosyl-β-glycolaldehyde (m/z 240), the product corresponding to cellobiose that has lost a glycolaldehyde molecule (or isomer; m/z 300) and the product corresponding to cellobiose that has lost both a glycolaldehyde (or isomer) and a water molecule (m/z 282). These are the four products mentioned above to be somehow associated with the terminal glucose units. Since the reducing end in cellotriosan has been modified compared to cellotriose, and cellotriose yields these four products but cellotriosan does not, the formation of these four products is likely to depend on the presence of the reducing end in cellotriose. The same is true for cellobiosan (Figure 2.4) except that no ions larger than m/z 342 (ionized cellobiosan) were observed. The mechanisms of these fragmentations are currently being investigated using quantum chemical calculations. The most surprising finding made in this study is

that the fast pyrolysis product distribution of cellotriosan (and cellopentosan) is nearly identical to that of cellulose (Figure 2.3). The most significant differences are the formation of glucopyranosyl-β-glycolaldehyde (m/z 240) and cellobiopyranosyl-β-glycolaldehyde (m/z 402) for cellulose but not for cellotriosan (or cellopentosan).These two products correspond to cellotriose that has lost two glycolaldehyde molecules (or isomers) (m/z 402) and cellobiose that has undergone the same losses (m/z 240). These findings suggest that the fast pyrolysis of cellulose may be initiated predominantly via two competing processes—formation of anhydro-oligosaccharides, such as cellobiosan, cellotriosan and cellopentosan (major route), and elimination of glycolaldehyde (or isomeric) units from the reducing end of oligosaccharides formed from cellulose during fast pyrolysis (minor route leading to products of m/z 240 and 402; Figure 2.5).

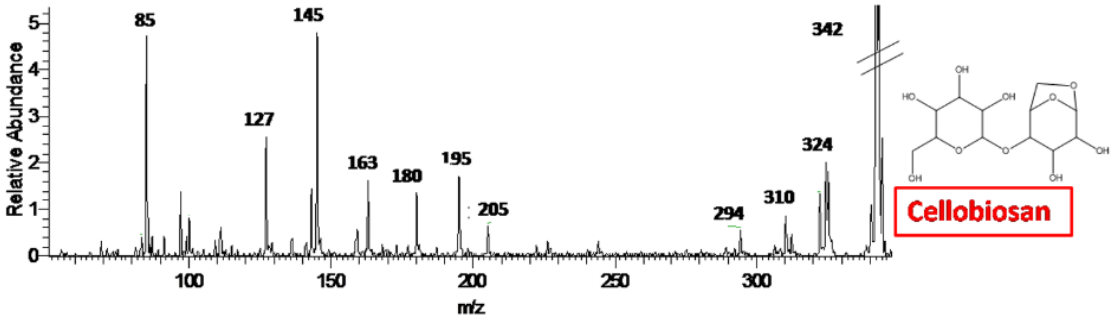

Figure 2.4. A positive ion mode mass spectrum showing the primary products of the fast pyrolysis of cellobiosan (m/z 342) ionized by APCI with ammonium hydroxide. The ions of m/z 85, 127, 145, 163, 180, and 195 are also formed for cellotriosan, cellopentosan and cellulose. The ion of m/z 324 results from the loss of H2O from the ion of m/z 342.

2.4 Conclusions

The above results suggest that molecules larger than cellotriosan are not able to efficiently leave the heated surface during fast pyrolysis of oligosaccharides at 600°C. Instead, they undergo further degradation on the hot surface. The observation of very similar primary product distributions for fast pyrolysis of cellotriosan and cellulose

suggests that cellotriosan presents an excellent small-molecule surrogate for cellulose, and it should be a much better choice than glucose, which has been considered previously.[20,26]

Based on the primary products observed for cellotriosan and cellulose, fast pyrolysis of cellulose under the conditions used here may be initiated predominantly via two competing pathways. One involves the formation of small anhydro-oligosaccharides (but not predominantly levoglucosan, as suggested in the literature[15,20,22,24–26]) that either evaporate from the hot pyroprobe surface or degrade to yield most of the other primary products (major pathway). The other involves elimination of glycolaldehyde (or isomeric) molecules from the reducing end of small oligosaccharides formed from cellulose during pyrolysis upon addition of water to yield volatile cellobiopyranosyl-β-glycolaldehyde and glucopyranosyl-β-glycolaldehyde molecules (ions of m/z 240 and 402; Figure 2.5). Reactions of the primary products of fast pyrolysis are currently under investigation in order to understand better how the final fast pyrolysis products are formed. These reactions may explain why levoglucosan is a major final fast pyrolysis product but not a major primary product.

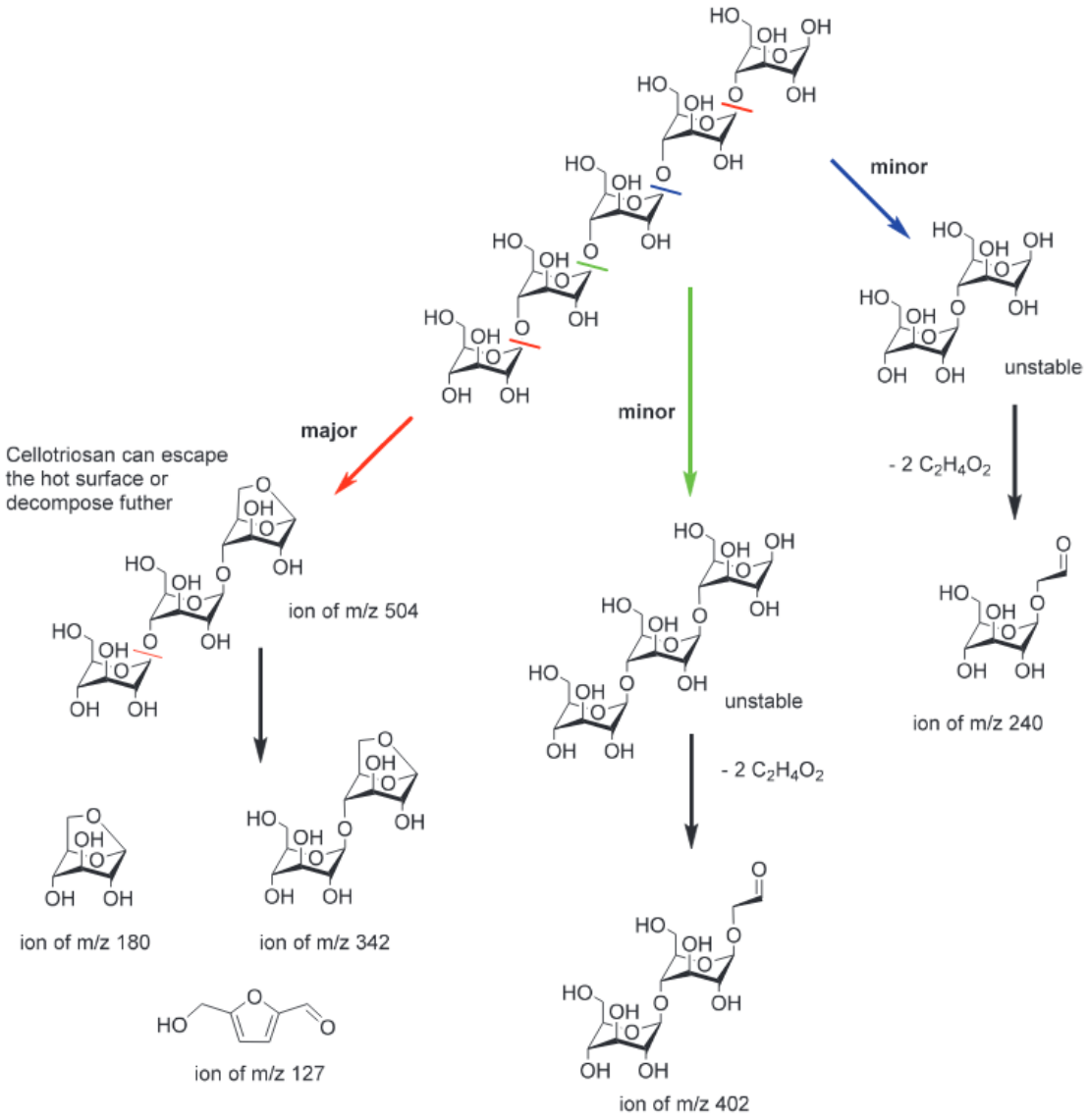

Figure 2.5. A simple schematic of the major fast pyrolysis pathways proposed for oligosaccharides formed from cellulose during fast pyrolysis upon addition of water. The cleavages indicated in red are thought to occur in the middle of a cellulose chain. The cleavages indicated in blue and green likely occur only at the reducing terminals, which for long chains of cellulose represent a small overall fraction of the total units. Hence, they are minor pathways.

CHAPTER 3. FAST PYROLYSIS OF ^{13}C-LABELED CELLOBIOSES: GAINING INSIGHTS INTO THE MECHANISMS OF FAST PYROLYSIS OF CARBOHYDRATES

3.1 Introduction

As stated above, fast pyrolysis is an efficient method for converting biomass to a low energy-density liquid (bio-oil) that can be further upgraded for use as fuel.[5] Optimization of fast pyrolysis to maximize the yields of compounds containing six or more carbons, which represent some of the most valuable potential end products, requires detailed knowledge of the dominant pyrolysis reactions.[7] However, the pathways and mechanisms (*e.g.*, stepwise radical or ionic or concerted) of fast pyrolysis reactions are still largely unknown even for cellulose, the simplest component of biomass, as well as for analogous di- and oligosaccharides.[7,25] The goal of this study was to explore these mechanisms by using selective ^{13}C-isotope labeling since this has not been performed previously.

The inherent capability of mass spectrometers to separate ions that differ in their mass-to-charge ratios (such as those with and without a ^{13}C label) makes the combination of this technique with fast pyrolysis of selectively labeled carbohydrates a powerful approach for mechanistic studies. The experimental results obtained[30] by my collaborators upon examination of the initial fast-pyrolysis products of unlabeled cellobiose (a glucose dimer with the same linkage as in cellulose; see Figure 3.1) and four selectively ^{13}C-labeled cellobioses by tandem mass spectrometry are presented here as a

background for my computational studies. It should be noted that “initial" products are defined here as the products that first leave the heated surface of the fast-pyrolysis probe.

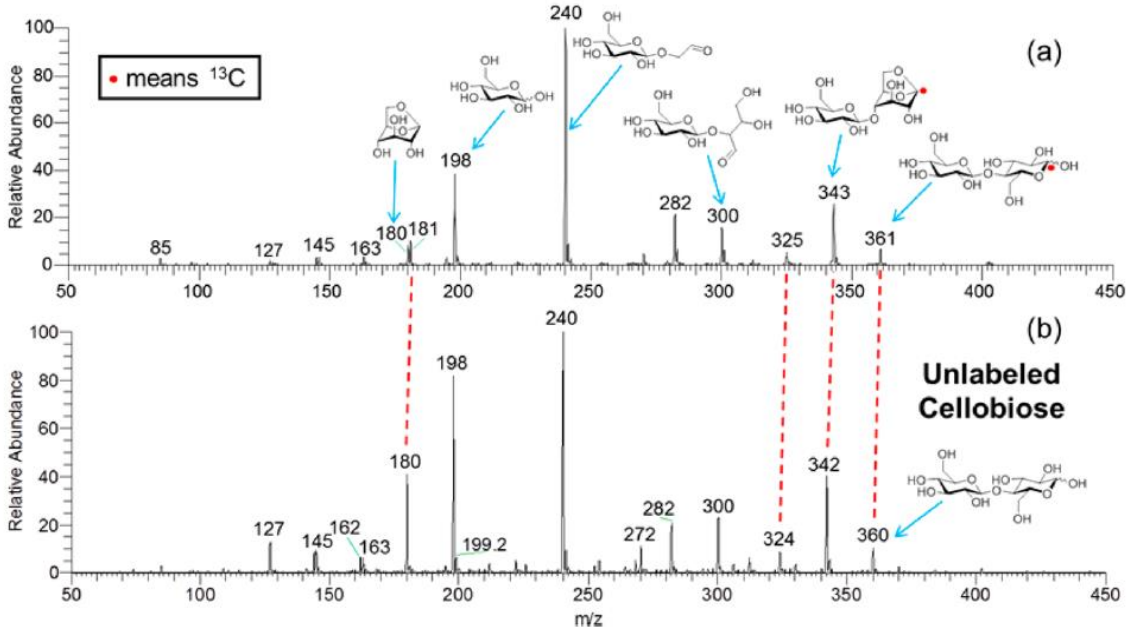

Figure 3.1. Positive ion-mode mass spectra showing the ionized initial fast-pyrolysis products (either as ammonium adducts or protonated molecules) of (a) glucopyranosyl[1-^{13}C]glucose and (b) unlabeled cellobiose ionized by APCI with ammonium hydroxide dopant. The structures of the intact molecules are shown at the far right in each spectrum. The products that are ^{13}C-labeled in the top spectrum are connected with red dotted lines to the corresponding unlabeled products in the lower spectrum.

3.2 Methods

The pyrolysis/tandem mass spectrometry technique utilized here has been described in detail in the literature.[29] It combines a pyrolysis probe that can be heated very fast (up to 20 000°C s^{-1}) with a Thermo Scientific linear quadrupole ion trap (LQIT) mass spectrometer. This technique was used to study the initial fast-pyrolysis products of cellobiose and four selectively ^{13}C-labeled cellobioses: commercially available [1-^{13}C]glucopyranosylglucose and glucopyranosyl[1-^{13}C]glucose (Omicron Biochemicals, South Bend, IN) as well as glucopyranosyl[3-^{13}C]glucose and glucopyranosyl[5-^{13}C]glucose (synthesized according to literature procedures).[32,33] The pyrolysis probe uses

a resistively heated at platinum ribbon (2.1 mm x 35 mm x 0.1 mm), which was placed inside the atmospheric-pressure chemical ionization (APCI) source of the LQIT. The ribbon was heated to 600°C at a rate of 1000°C s^{-1}. The initial products of pyrolysis evaporated from the heated surface into a nitrogen atmosphere at 100°C (at atmospheric pressure) in the ion source and were quenched. It should be noted that this approach is very different from that used in laboratory pyrolysis reactors, since laboratory pyrolysis reactors generally utilize heated surfaces in combination with heated gaseous environments. A soft ionization method, APCI with ammonium hydroxide dopant, was utilized to ionize the products since this method typically generates[29] only one ion (either the NH_4^+ adduct or the protonated molecule) without fragmentation for each product molecule of the type of interest here. The reactor and analysis suites were designed to prevent fragmentation of the pyrolysis products. Mass balances cannot be obtained using this new methodology; however, relative abundances of the products were determined, and much larger pyrolysis products were detected than reported previously.[6,20,29] Each reported mass spectrum is a result of a weighted average (based on total ion current) of the individual mass spectra measured during pyrolysis. No significant changes were detected in the product distribution during cellobiose pyrolysis; in other words, the relative abundances were constant during pyrolysis.

The structures of most of the ions were examined by using MS^2 experiments (*i.e.*, by isolating them and subjecting them to collision-activated dissociation (CAD)). When necessary, the structures of the fragment ions were examined by isolating them and subjecting them to further CAD (MS^3 experiment). High-resolution data needed to determine the elemental compositions of the ions were collected using an LQIT/Fourier-

transform ion cyclotron resonance mass spectrometer coupled with the pyrolysis probe as described above.

Geometry optimizations and energy calculations were performed by the Gaussian09[34] program on 12-core AMD Opteron 6176 processors at the M06-2X/6-311++G(d,p)[35,36] level of theory. Gibb's free energies were calculated using statistical mechanics assuming an ideal gas with vibrational temperatures computed from a full Hessian calculation. Transition states possess exactly one negative eigenvalue while minima possess all positive eigenvalues for the Hessian.

3.3 Results and Discussion

The ionized initial fast pyrolysis products of unlabeled cellobiose are shown in Figure 3.1b, and they are in agreement with those reported previously.[29] As discussed above, the identified products include hydroxymethylfurfural (protonated molecule of m/z 127), levoglucosan (NH_4^+ adduct of m/z 180 and a protonated molecule of m/z 163), glucose (NH_4^+ adduct of m/z 198), and β-D-glucopyranosylglycolaldehyde (NH_4^+ adduct of m/z 240). β-D-Glucopyranosylglycolaldehyde is likely formed upon the loss of two glycolaldehyde (or isomeric) molecules from cellobiose upon fast pyrolysis. On the other hand, the pyrolysis product generating ions of m/z 300 (NH_4^+ adduct) is formed via the loss of a single glycolaldehyde (or isomeric) molecule from cellobiose, and the product generating ions of m/z 282 (NH_4^+ adduct) is formed via the loss of glycolaldehyde (or isomeric) molecule and water from cellobiose. Evidence in support of these products being initial products instead of secondary products was obtained from the previously determined structure of the β-D-glucopyranosylglycolaldehyde product.[29] The glycosidic bond (*i.e.*, the C-O bond at the oxygen atom on the carbon adjacent to the ring oxygen) in

this pyrolysis product is still in the same position and has the same stereochemistry (β-1) as in cellobiose. If β-D-glucopyranosyl-glycolaldehyde were not an initial product but instead the result of recombination of smaller initial products, one would expect a mixture of linkage positions and stereochemistry. These larger products (>162 Da) are typically not seen with pyrolysis/GC-MS methodologies because of their thermal instability and low volatility, which may at least partially explain the incomplete mass balance of previous oligosaccharide pyrolysis studies.[6,20] The results presented here are in agreement with recent mechanistic studies suggesting that glycolaldehyde may form directly from cellobiose (or a longer glucosaccharide) rather than through a glucose intermediate.[37–39]

The ionized initial fast-pyrolysis products of glucopyranosyl-[1-^{13}C]glucose (with the label at the reducing end or the end containing a free hydroxyl group on the carbon adjacent to the ring oxygen) are shown in the mass spectrum in Figure 3.1a. Comparison of these products to those produced from unlabeled cellobiose (Figure 3.1b) revealed that only one product is partially ^{13}C-labeled (levoglucosan, NH_4^+ adducts of m/z 180 and 181), while all of the others are either completely labeled or do not contain the label at all. Specifically, cellobiosan (NH_4^+ adduct of m/z 343) and the product formed via loss of water from cellobiosan (NH_4^+ adduct of m/z 325) are completely ^{13}C-labeled, as expected, while all of the other products are unlabeled (Figure 3.1a). For example, glucose, β-D-glucopyranosylglycolaldehyde and β-D-glucopyranosylerythrose contain intact rings that originate exclusively from the non-reducing end since they have no label. The formation of glucose from the non-reducing end of cellobiose must occur via scission of the aglyconic bond (*i.e.*, the other C-O bond of the oxygen atom involved in

the glycosidic linkage) rather than the glycosidic bond as previously proposed.[25,40] In the literature, the only mechanisms that explain formation of glucose involve glycosidic bond cleavage and thermohydrolysis, which form glucose either from the reducing end only or from the reducing and non-reducing ends in equal amounts, respectively.[15,25,41] On the contrary, the present results indicate that the formation of glucose occurs exclusively from the non-reducing end of cellobiose (within the detection limits of our pyrolysis/MS experiment). This observation suggests that there is at least one additional glucose formation pathway that has not been proposed in the literature. Work is underway to explore alternate reaction pathways that explain formation of glucose from the non-reducing end.

The results also demonstrate that the first glycolaldehyde (or isomeric) molecule eliminated from cellobiose upon pyrolysis contains the ^{13}C label (NH_4^+ adduct of m/z 300); this process must involve the loss of ^{13}C-1 and most likely C-2 of the reducing end of cellobiose. Identification of the origin of the initially eliminated glycolaldehyde on the basis of carbon labeling indicates that certain mechanisms may be more feasible than others. For example, the retro-aldol mechanism considered here and elsewhere results in the elimination of glycolaldehyde from the C-1 and C-2 positions.[15,41] On the other hand, 1,2-dehydration followed by retro-Diels-Alder reaction would result in elimination of glycolaldehyde from the C-5 and C-6 positions.

Levoglucosan must be formed via at least two pathways since two different ions (NH_4^+ adducts of m/z 180 and 181, corresponding to ammoniated molecules with and without the ^{13}C label) are produced. Hence, levoglucosan is likely formed from both the reducing and non-reducing ends of cellobiose. The ionized initial fast-pyrolysis products

of another labeled cellobiose, [1-^{13}C]glucopyranosylglucose, with a ^{13}C label in the non-reducing end, are shown in the mass spectrum in Figure 3.2a. Comparison of these products to those obtained for unlabeled cellobiose revealed that all of the ionized products with m/z values greater than 180 contain the ^{13}C label. These results support the above conclusion that glucose is produced exclusively from the non-reducing end of cellobiose. Further, both labeled and unlabeled levoglucosan were observed, in agreement with the above proposal that more than one mechanism must lead to levoglucosan and that it is likely to be formed from both the reducing and non-reducing ends. Finally, the results show that the first two glycolaldehyde (or isomeric) molecules eliminated from cellobiose come from the reducing end.

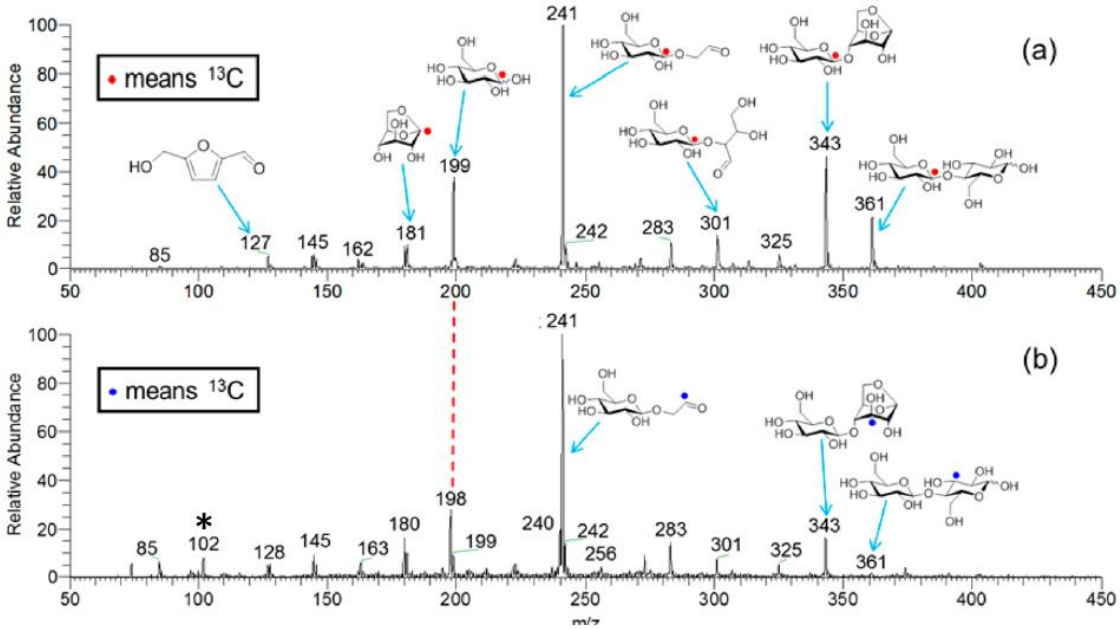

Figure 3.2. Positive ion-mode mass spectra showing the ionized initial fast-pyrolysis products (either as ammonium adducts or protonated molecules) of (a) [1-^{13}C]glucopyranosylglucose and (b) glucopyranosyl[3-^{13}C]glucose ionized by APCI with ammonium hydroxide dopant. The structures of the intact molecules are shown at the far right in each spectrum. The only product that is labeled in the top spectrum but unlabeled in the bottom spectrum is glucose, as indicated by a red dotted line. The ion labeled with * corresponds to an unknown impurity.

In order to explore the mechanism for the elimination of the second glycolaldehyde (or isomeric) molecule from the reducing end of cellobiose (to yield the NH_4^+ adduct of m/z 240 for the unlabeled cellobiose), a third ^{13}C-labeled cellobiose, glucopyranosyl[3-^{13}C]glucose, was synthesized. The ionized initial fast-pyrolysis products of this compound are shown in the mass spectrum in Figure 3.2b. The presence of a major ion of m/z 301 (containing ^{13}C) supports the above finding that the first glycolaldehyde (or isomeric) molecule eliminated from cellobiose upon pyrolysis contains C-1 and C-2 of the reducing end (i.e., to form the ion of m/z 301). Furthermore, since elimination of the second glycolaldehyde (or isomeric) molecule yields an ion of m/z 241 (containing ^{13}C), this glycolaldehyde unit must contain C-5 and C-6 of the reducing end. Examination of a fourth ^{13}C-labeled compound, glucopyranosyl[5-^{13}C]glucose, confirmed all of the above conclusions. In particular, the elimination of C-5 of the reducing end in the second eliminated glycolaldehyde (or isomeric) molecule was verified by the observation of β-D-glucopyranosylglycolaldehyde with no ^{13}C.

My contribution to this research, quantum chemical calculations[34] at the M06-2X/6-311++G(d,p)//M06-2X/6-311++G(d,p) level of theory[36,35] revealed a low-energy pathway (at 25°C and 600°C) for the consecutive elimination of one glycolaldehyde and two isomeric ethenediol molecules from cellobiose, eventually producing levoglucosan (Figure 3.3) (it is well-known that ethenediol converts readily into its tautomer glycolaldehyde; therefore, β-D-glucopyranosylethenediol was assumed to readily tautomerize to β-D-glucopyranosylglycolaldehyde). This pathway is consistent with the ^{13}C-labeling results described above. Work to identify additional pathways leading to levoglucosan and the other observed products is in progress.

3.4 Conclusions

In conclusion, identification of the initial fast-pyrolysis products of selectively ^{13}C-labeled cellobioses using a previously reported[29] experimental method has been demonstrated by my collaborators to be a powerful approach for exploring the details of the initial reactions in the fast pyrolysis of cellobiose. Several products that are likely to be produced by consecutive glycolaldehyde (or isomer) eliminations from the reducing end of cellobiose, including levoglucosan, were observed. Literature mechanisms proposed for the fast pyrolysis of cellobiose are not consistent with the results reported here.[25] Quantum chemical calculations revealed a feasible low-energy pathway for some of the products observed. Since many of the initial products have molecular weights greater than those of the final pyrolysis products reported for cellobiose in the literature,[6,20] these initial products may be intermediates in the formation of the final products, which include light oxygenated hydrocarbons.

Minimization of the production of low-molecular-weight oxygenated hydrocarbons is an important goal for fast pyrolysis of cellulose in order to maximize the production of fuel and high-value chemical products. Knowledge of the fragmentation pathways occurring during fast pyrolysis of smaller carbohydrates will contribute to the knowledge of fast pyrolysis of cellulose and ultimately fast pyrolysis of whole biomass, possibly enabling the tailoring of the product distribution obtained upon fast pyrolysis of whole biomass.

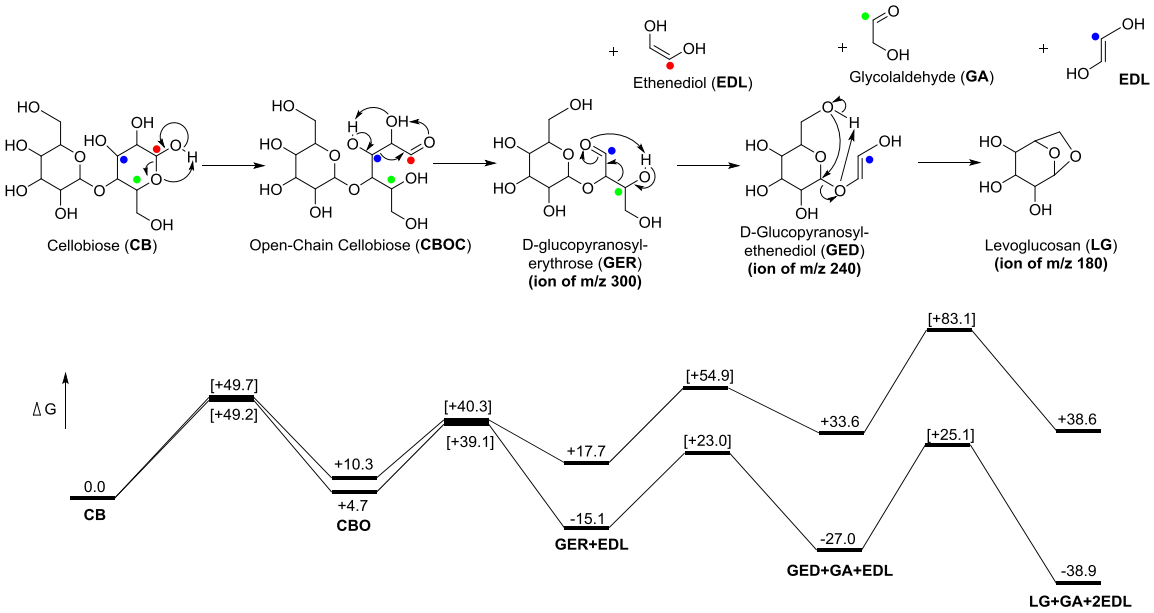

Figure 3.3. Calculated free energies (kcal mol^{-1}) of intermediates and transition states (square brackets) for the formation of levoglucosan from cellobiose via consecutive losses of one glycolaldehyde (GA) and two ethenediol (EDL) molecules (which are likely to eventually tautomerize to glycolaldehyde) at 25°C (top pathway) and 600°C (bottom pathway) obtained at the M06-2X/6-311++G(d,p)//M06-2X/6-311++G(d,p) level of theory. The location of a ^{13}C label at C-1 in the reducing end is indicated by a red circle, at C-3 by a blue circle, and at C-5 by a green circle. The mass-to-charge (m/z) ratios are for unlabeled cellobiose.

CHAPTER 4. DEHYDRATION PATHWAYS FOR GLUCOSE AND CELLOBIOSE DURING FAST PYROLYSIS

4.1 Introduction

As stated previously, Cellulose is the most abundant biopolymer in biomass, making up between 40% and 60% of the total biomass, depending on the feedstock.[5,42] While early mechanistic models of cellulose depolymerization during pyrolysis used lumped kinetic parameters and unknown "active cellulose" intermediates,[9] current kinetic models have been developed to utilize an understanding of the elementary reactions that may occur during pyrolysis.[15] The specific mechanisms of cellulose fast pyrolysis, including elementary reactions, are under active debate.[25,27,43,44] For computational studies on thermal degradation of cellulose, both glucose and cellobiose have been used as model compounds. In recent experiments, glucose and cellobiose were considered constituents of the "active cellulose" intermediate of cellulose pyrolysis, which is likely to undergo dehydration.[45] Water accounts for 41 wt% of the pyrolysis products of glucose,[6] 24 wt% of cellobiose pyrolysis products,[6] and up to ~40 wt% of the products of cellulose pyrolysis,[3,6,37] indicating that dehydration must occur.

Several water loss mechanisms for glucosaccharides have been reported in the literature, including 1,2-dehydration,[15,37,45–47] Pinacol rearrangement,[37] "Tandem Alkaline Pinacol Rearrangement/Retro Aldol Fragmentation" (TAPRRAF),[39] cyclic Grob fragmentation (CGF),[37,39] and generalized alcohol condensation. These mechanisms have

been used to explain the cleavage of C-C and C-O bonds that leads to fragments such as formic acid, formaldehyde, glycolaldehyde, and erythrose, as well as many other oxygenated hydrocarbons upon fast pyrolysis. Formation of some of these products has also been explained by a retro-aldol condensation mechanism[48] and a retro-ene mechanism.[39] Some mechanisms, such as retro-Diels-Alder, have not been thoroughly explored computationally. Cellotriose has been the focus of some computational studies with the focus on Pinacol ring cleavage, dehydration and retro-Diels-Alder mechanisms.[49] Some computational work has been performed on selected reactions of cellobiose,[25,30,44,50,51] but a comprehensive survey on the dehydration and retro-Diels-Alder decomposition of cellobiose is notably absent in the literature. In this thesis, Maccoll elimination,[52] Pinacol rearrangement,[53] cyclic Grob fragmentation, condensation cyclization, retro-aldol condensation, and retro-Diels-Alder reactions of glucose and cellobiose are reported and compared.

4.2 Computational Methods

Conformational analysis was accomplished with the MacroModel program as part of the Schrödinger software package[54] using MCMM[55] torsional sampling with the MMFF94s force field.[56] DFT calculations were performed on 12-core AMD Opteron 6176 processors with the Gaussian09 program.[34] The labeling of the atoms in cellobiose and the dihedral angles along the glycosidic linkage (shown in Figure 4.1) are according to convention.

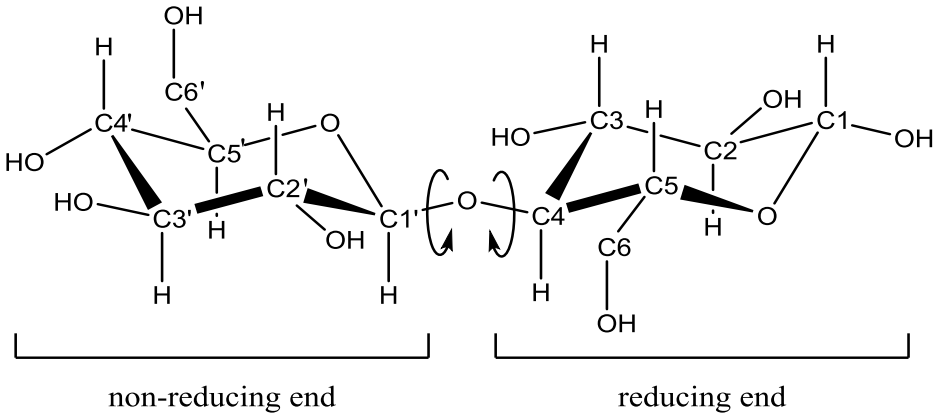

Figure 4.1. Numbering scheme for cellobiose. Atoms on non-reducing end indicated by primed numbers.

It is important to select the most appropriate conformation of cellobiose for calculations since pyrolysis is an inherently multi-phase process[7] and cellobiose can adopt different conformations depending on its state. Crystallographic data on solid cellobiose[57] indicates that in the solid state, the molecule is in the syn-form, the hydroxymethylene groups being on opposite sides of the rings relative to each other, which is the conformation most closely resembling the crystalline cellulose form Iα as present in native plant matter.[5,58] On the other hand, previous work[25,59] has shown that the energetically most favorable conformation of cellobiose in the gas phase is the anti-form, where the hydroxymethylene groups are cis to each other. A conformational change of the crystal structure may occur when the particles enter the melt phase of pyrolysis.[60,61] However, liquid phase simulations with the SMD solvation model indicate that the crystal-like syn-conformation is lower in energy than the gas-phase conformation in the liquid phase.[62] Furthermore, conformational changes in cellulose become increasingly more difficult as the number of neighboring cellulose chains increases due to intermolecular interactions.[63] Since the goal of this research was to accurately model

native cellulose, the syn-conformation of cellobiose was selected as the starting point for calculations.

B3LYP[64–67] has often been used in literature since it can accurately predict molecular structure,[68] but it has a tendency to underestimate the energies of transition structures.[69,70] M06-2X is among the best functionals for calculating barrier heights, particularly for unimolecular reactions and hydrogen atom transfer reactions.[35] M06-2X has been shown to accurately replicate results obtained using MP4(SDQ) and has been used extensively in literature for studying sugar chemistry.[25] The chosen basis set is 6-311++G(d,p) as suggested in literature.[71] All geometry optimizations were followed by a full Hessian calculation to guarantee that the minima had all positive eigenvalues and the transition states had exactly one negative eigenvalue. Intrinsic reaction coordinate calculations confirmed that the appropriate reactants and products were associated with each transition state. Thermal corrections for internal energy, enthalpy, and Gibb's free energy were calculated using statistical mechanics, assuming an ideal gas and using the harmonic oscillator approximation.

4.3 Results and Discussion

4.3.1 Maccoll Elimination and Dehydration

Maccoll elimination involves cleavage of a C-O bond with a concerted hydrogen atom transfer from a β-carbon to the oxygen atom to form a C-C double bond and eliminate either H_2O or another compound with a new hydroxyl functionality.[52,72] When referring to a Maccoll elimination, two numbers will be used to describe the carbon sites that break a C-O bond and a C-H bond, respectively (see Figure 4.2). Glucose can

undergo Maccoll elimination via eight different reactions while cellobiose has 16 possible reactions (see Figure 4.3 and Figure 4.4). Each of the Maccoll eliminations of glucose (or cellobiose) leads to an alkene, one (two) of which is (are) terminal alkenes and 7 (14) of which are cyclic alkenes that can undergo a retro-Diels Alder reaction. See Table 4.1 for calculated reaction barriers and overall changes in Gibb's free energy at room temperature and at the pyrolysis temperature (600 ^{o}C).

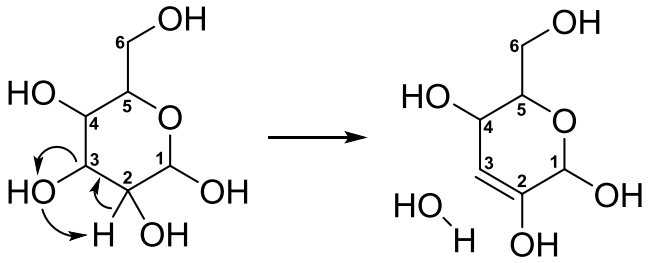

Figure 4.2. An example mechanism of Maccoll elimination for glucose, depicting GLC32Mac (3 indicates the carbon site where the C-O bond is broken; 2 indicates the carbon site where the C-H bond is broken).

Table 4.1. Transition state and reaction Gibb's free energies in kcal/mol for Maccoll eliminations of glucose calculated for 298.15 K and 873.15 K at the M06-2X/6-311++G(d,p)//M06-2X/6-311++G(d,p) level of theory.

Reaction	298.15 K		873.15 K	
	TS ΔG	Rxn ΔG	TS ΔG	Rxn ΔG
GLC12Mac	69.4	5.72	65.9	-17.9
GLC21Mac	81.9	-0.75	80.4	-25.3
GLC23Mac	74.6	1.12	72.3	-22.6
GLC32Mac	77.4	4.52	73.6	-20.1
GLC34Mac	75.9	4.40	74.3	-20.7
GLC43Mac	75.5	-2.46	73.8	-25.7
GLC45Mac	78.1	1.27	75.0	-23.3
GLC65Mac	71.6	1.16	70.1	-22.2

The lowest Maccoll elimination barrier for glucose is 65.9 kcal/mol calculated for GLC12Mac (see Table 4.1 and Figure 4.3), which involves a loss of a hydroxyl group from C1 and a loss of a hydrogen atom from C2. The product from this reaction is anhydrous glucose with a double bond between carbons C1 and C2 (Figure 4.3), which may be an intermediate to levoglucosan formation via attack of the hydroxymethylene group at the anomeric carbon.[50] The reaction with the largest barrier is GLC21Mac, where the hydroxyl group is lost from C2 while the hydrogen atom is lost from C1. The anomeric carbon (C1) has more positive charge than the other carbon atoms since it is attached to two electron-withdrawing oxygen atoms,[37,73] which may explain why the transition state energy for removing the OH group from C1 (reaction GLC12Mac) is 14.5 kcal/mol lower than the transition state energy for removing the hydrogen atom from C1 (reaction GLC21Mac).

Seven of the eight Maccoll elimination reactions for glucose result in a cyclic alkene. The GLC65Mac reaction is unique because it forms a terminal alkene at the C5 position. It has the second lowest barrier at 70.1 kcal/mol. The remaining Maccoll elimination reactions involve the loss of an exocyclic hydroxyl group at C2, C3, or C4. The barrier heights for these five reactions are within 2.7 kcal/mol of each other, suggesting that each of these reactions is equally competitive.

Comparison of the Maccoll eliminations for glucose and cellobiose reveal some similarities in the trends for the barrier heights of analogous water loss reactions (see Figure 4.4 and Table 4.2). The lowest barriers for cellobiose involve the removal of an oxygen from the anomeric carbon, just like for glucose, slightly favoring the breakage of

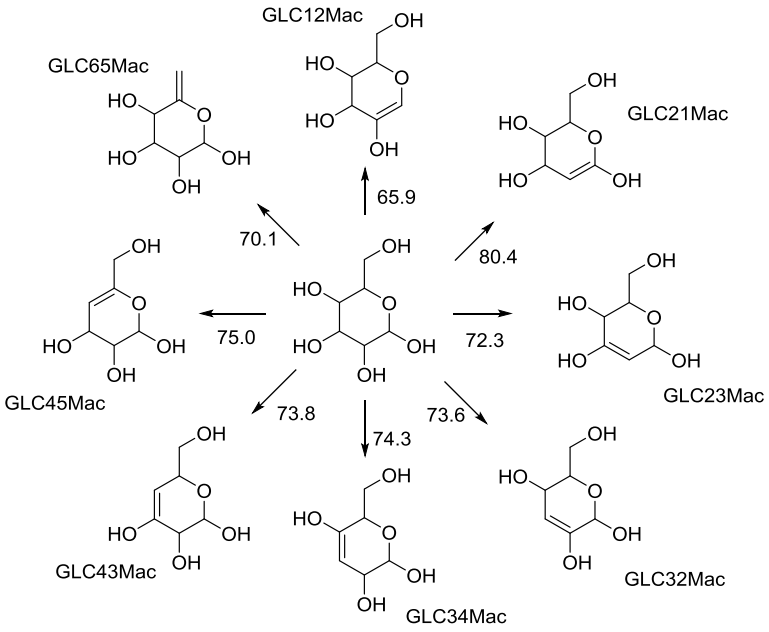

Figure 4.3. All eight possible Maccoll eliminations of β-D-glucopyranose. The numbers near the arrows indicate barrier heights (Gibb's free energy) in kcal/mol calculated at the M06-2X/6-311++G(d,p)//M06-2X/6-311++G(d,p) level of theory at 873.15 K. The reaction codes indicate the reactant (GLC=glucose), the respective carbon sites from which OH and H are lost during dehydration, and the reaction type (Mac=Maccoll).

the C-O bond in the non-reducing end over the reducing end of cellobiose. It is important to note that in the case of the non-reducing end, the reaction corresponds to a Maccoll elimination of the intact reducing end glucose ring by scission of the glycosidic bond.

Table 4.2. Transition state and reaction Gibb's free energies in kcal/mol for Maccoll elimination of cellobiose calculated at 298.15 K and 873.15 K at the M06-2X/6-311++G(d,p)// M06-2X/6-311++G(d,p) level of theory.

Reaction	298.15 K		873.15 K	
	TS ΔG	Rxn ΔG	TS ΔG	Rxn ΔG
CB12Mac	63.3	9.22	63.6	-15.3
CB21Mac	82.9	-1.30	80.6	-24.7
CB23Mac	72.7	-1.11	71.3	-25.8
CB32Mac	72.4	1.80	70.8	-23.6
CB34Mac	64.4	3.83	65.0	-23.5
CB43Mac	68.2	2.25	65.9	-24.1
CB45Mac	71.9	5.98	68.7	-21.8
CB65Mac	69.3	1.23	68.6	-23.1
CB1'2'Mac	66.9	10.4	62.5	-16.4
CB2'1'Mac	82.5	4.03	80.6	-20.5
CB2'3'Mac	75.9	2.14	73.4	-22.6
CB3'2'Mac	75.2	3.28	71.1	-22.2
CB3'4'Mac	74.6	4.67	72.7	-19.9
CB4'3'Mac	73.3	-0.33	70.7	-24.4
CB4'5'Mac	71.7	-0.80	66.8	-26.0
CB6'5'Mac	68.8	-0.09	67.2	-24.5

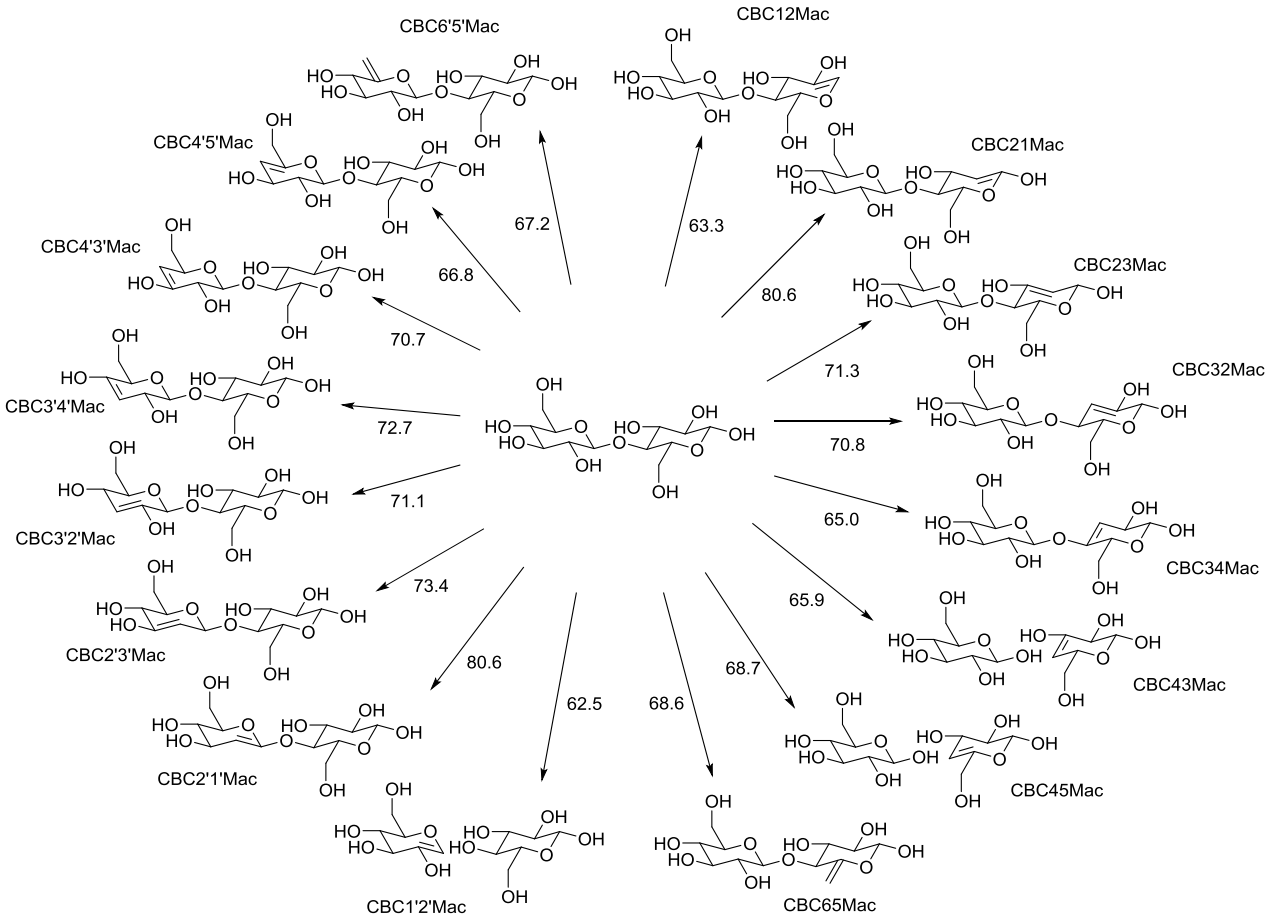

Figure 4.4. All the 16 possible Maccoll eliminations of cellobiose. The numbers by the arrows indicate barrier heights (Gibb's free energy) in kcal/mol calculated at the M06-2X/6-311++G(d,p)//M06-2X/6-311++G(d,p) level of theory at 873.15 K. The reaction codes indicate the reactant (CB=cellobiose), the respective carbon sites from which OH and H are lost during dehydration, and the reaction type (Mac=Maccoll).

In total there are three cases where Maccoll elimination of cellobiose leads to formation of a glucose molecule: CB43Mac, CB45Mac, and CB1'2'Mac. The barriers for these Maccoll elimination reactions are between 62.5 and 68.7 kcal/mol. On the other hand, the bond dissociation energy (BDE) for homolysis and heterolysis of the glycosidic bond is 79.1 kcal/mol and 157.5 kcal/mol, respectively. Hence, Maccoll eliminations are substantially more favorable. These reactions have been used to explain the formation of levoglucosenone in an earlier report that used B3LYP/6-31G(2df,p) level of theory to

calculate activation energies.[50] Cleavage of the aglyconic bond of cellobiose during the Maccoll reactions CB43Mac and CB45Mac leads to intact glucose from the non-reducing end of cellobiose. In contrast, the CB1'2'Mac reaction involves glycosidic bond scission, producing intact glucose from the reducing-end. In our previous work,[30] glucose was demonstrated to be formed exclusively from the non-reducing end upon fast pyrolysis of cellobiose. Based on the above reaction barriers, it would be expected that some glucose from the reducing end (via CB1'2'Mac) would be eliminated in fast pyrolysis experiments if these were the dominating reactions for glucose formation. Therefore, these reactions alone cannot fully explain the process of glucose formation from pyrolysis of cellobiose.

The Maccoll elimination reactions occuring on the reducing and non-reducing ends of cellobiose tend to have lower barriers than Maccoll elimination reactions of glucose (Figure 4.5). The only exceptions are GLC21Mac with a barrier that is 0.2 kcal/mol lower than the barriers of both CB21Mac and CB2'1'Mac, as well as GLC23Mac with a barrier that is 1.2 kcal/mol lower than that of CB2'3'Mac. The small differences in reaction barriers between glucose and cellobiose can be attributed to increased electron delocalization as well as stabilization by an increase in the amount of hydrogen bonding for cellobiose. All these reaction barriers may be lower under certain conditions, *i.e.*, in the presence of water,[38] under acidic conditions,[46,47] or in the presence of alkali metal cations.[47]

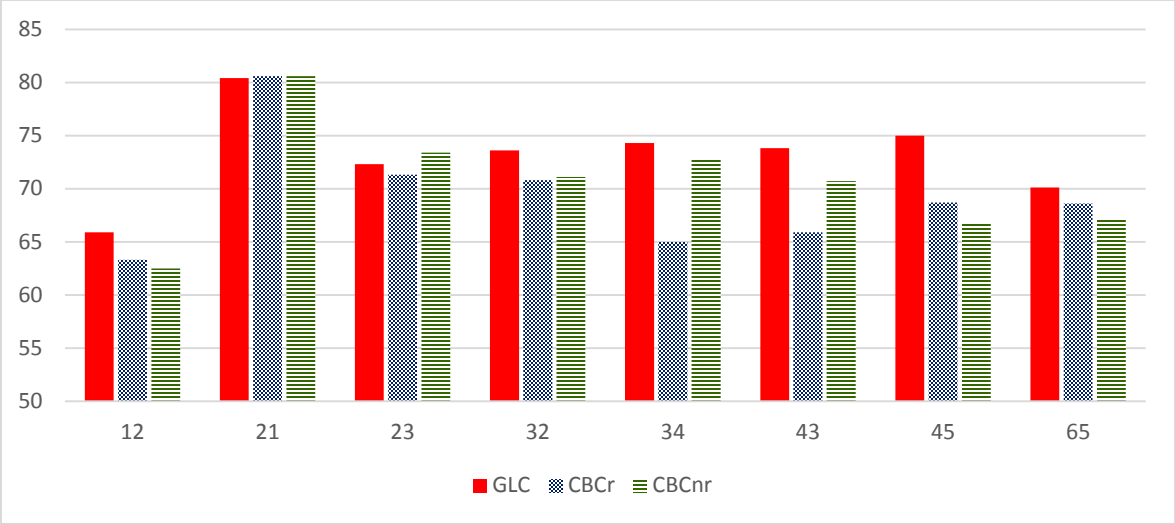

Figure 4.5. Comparison of transition state energies in kcal/mol for Maccoll eliminations of glucose (GLC) and each glucose ring in cellobiose: reducing end (CBr) and non-reducing end (CBnr).

4.3.2 Pinacol Ring Contraction

While a Maccoll elimination reaction includes breaking of a C-H bond, a second dehydration reaction type considered here, termed the Pinacol ring contraction due to its similarity to the Pinacol rearrangement reaction,[39,53] instead breaks an O-H bond. In this mechanism, the hydrogen atom source is the OH group adjacent to the OH group that is eliminated. This reaction forms a carbonyl group while simultaneously contracting the six-membered pyranosyl ring to a five-membered ring (Figure 4.6). The Pinacol reactions of glucose produce six distinct products, including three sets of stereoisomers: 1) GLC12Pin and GLC21Pin, 2) GLC23Pin and GLC32Pin, and 3) GLC34Pin and GLC43Pin. The product whose formation barrier is the lowest is GLC21Pin (see Figure 4.7). At the pyrolysis temperature, the Gibb's free energy barrier for Pinacol rearrangement is comparable to the barrier at room temperature, but the overall reaction is more exergonic by 24-27 kcal/mol at the elevated temperature (Table 4.3). This product, as well as the product from GLC12Pin, are intermediates to the formation of 5-

hydroxymethyl furfural by water losses at C3 and C4. A complete depiction of the Pinacol ring contractions for glucose is shown in Figure 4.7, including the Gibb's free energy barriers for each transition state.

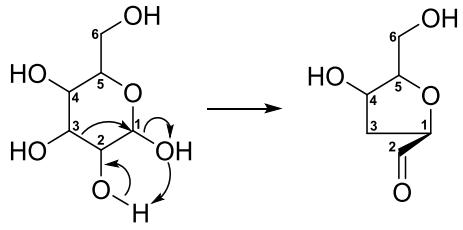

Figure 4.6. Example Pinacol ring contraction mechanism, depicting GLC12Pin. The reaction code indicates the reactant (GLC=glucose), the respective carbon atoms that break a C-O bond and form a C=O bond (C1 and C2 in this case), and the reaction type (Pin=Pinacol rearrangement).

Although the barriers for Pinacol rearrangement are larger than the most favorable Maccoll elimination reaction, the Pinacol rearrangement reaction has been reported to be catalyzed by acids,[53] including formic acid, which is known to be a product of biomass fast pyrolysis.[6] For instance, when an OH group in glucose is protonated, H_2O will spontaneously cleave from the ring, accompanied by a ring contraction to stabilize the cationic charge left on the carbon (see Figure 4.8). This spontaneous ring contraction has been observed by others during molecular orbital geometry optimization of protonated glucose.[74]

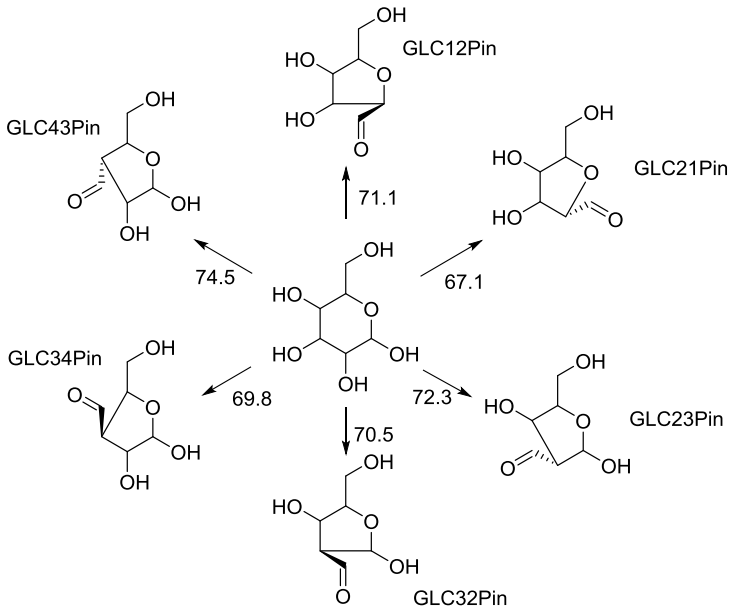

Figure 4.7. Pinacol ring contraction mechanisms for β-ᴅ-glucopyranose. The numbers by the arrows indicate the Gibb's free energy in kcal/mol calculated at the M06-2X/6-311++G(d,p)//M06-2X/6-311++G(d,p) level of theory at 873.15 K. The reaction codes indicate the reactant (GLC=glucose), the respective carbon sites from which a C-O bond is broken and a C=O bond is formed, and the reaction type (Pin=Pinacol rearrangement).

Table 4.3. Transition state and reaction energetics in kcal/mol for Pinacol ring contraction of glucose calculated at the M06-2X/6-311++G(d,p)//M06-2X/6-311++G(d,p) level of theory at 298.15 K and 873.15 K.

Reaction	25 °C		600 °C	
	TS ΔG	Rxn ΔG	TS ΔG	Rxn ΔG
GLC12Pin	72.9	3.85	71.1	-21.6
GLC21Pin	68.7	2.54	67.1	-24.0
GLC23Pin	74.2	-3.40	72.3	-27.6
GLC32Pin	71.6	-5.05	70.5	-30.0
GLC34Pin	72.0	-2.23	69.8	-27.5
GLC43Pin	76.1	-1.99	74.5	-27.7

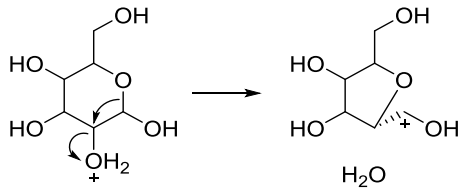

Figure 4.8. Mechanism for water loss and ring contraction of glucose protonated at O2.

In the case of cellobiose, the lowest barriers for Pinacol ring contraction correspond to cleavage of the C-O bond at the anomeric carbon of each glucose ring (Figure 4.9, Table 4.4). For reaction CB12Pin, water is lost from the anomeric carbon of the reducing end with a barrier of 61.5 kcal/mol. For the analogous reaction of C-O cleavage on the non-reducing end (CB1'2'Pin), the products are glucose and the same product as for the GLC12Pin reaction (Figure 4.7), and the barrier is 72.6 kcal/mol. One other Pinacol reaction for cellobiose also produces glucose. While CB1'2'Pin produces glucose from the reducing end, CB43Pin produces glucose from the non-reducing end with a barrier of 76.8 kcal/mol (Figure 4.9). These barriers for glucose formation are larger than those for the Maccoll eliminations that produce glucose, suggesting that Pinacol rearrangements are unlikely pathways towards formation of glucose. As with glucose, the reaction barriers are relatively independent of temperature, while the free energy of reaction decreases by 23-31 kcal/mol between room temperature and the pyrolysis temperature (Table 4.4).

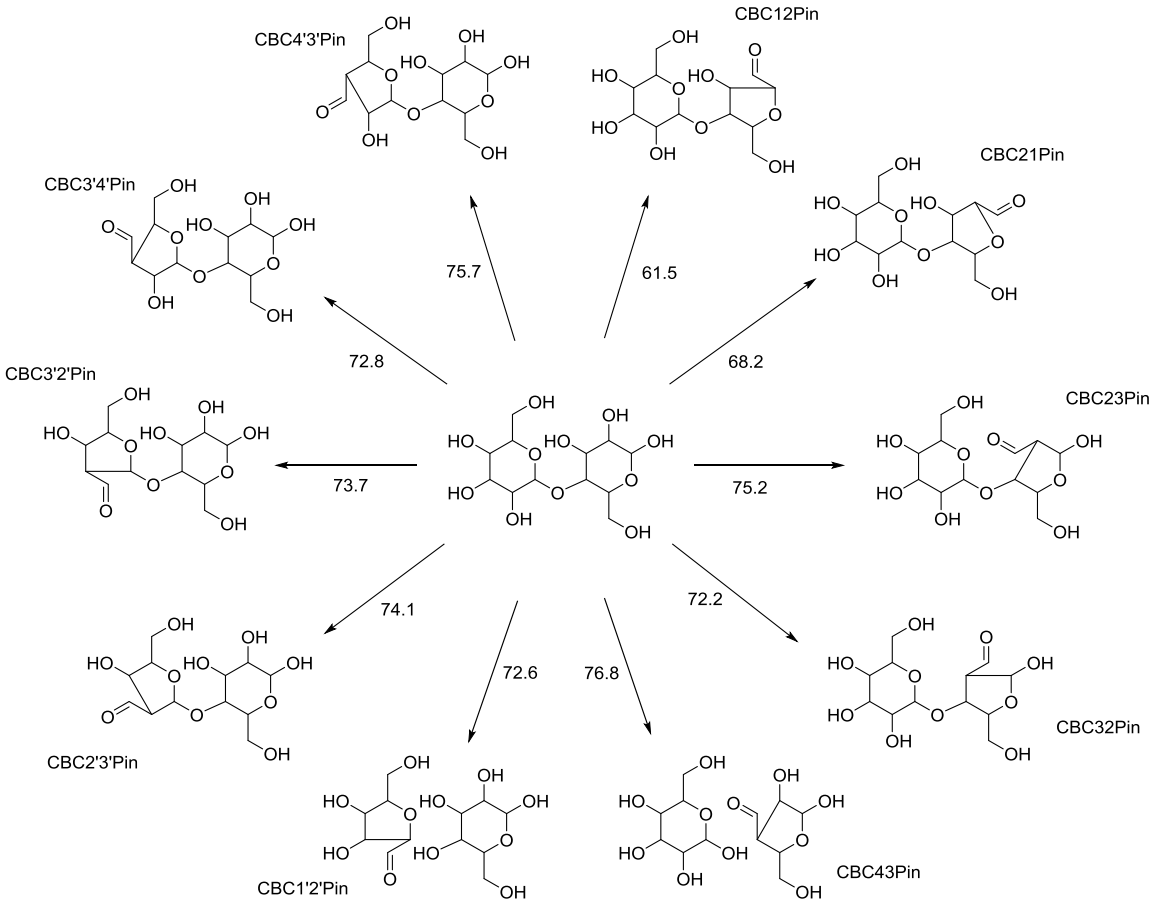

Figure 4.9. Pinacol ring contraction reactions for cellobiose. The numbers by the arrows indicate the Gibb's free energy barriers in kcal/mol calculated at the M06-2X/6-311++G(d,p)//M06-2X/6-311++G(d,p) level of theory at 873.15 K. The reaction codes indicate the reactant (CB=cellobiose), the respective carbon sites from which a C-O bond is broken and a C=O bond is formed, and the reaction type (Pin=Pinacol rearrangement).

Table 4.4. Transition state and reaction free energies in kcal/mol for Pinacol ring contraction of cellobiose calculated at the M06-2X/6-311++G(d,p)// M06-2X/6-311++G(d,p) level of theory at 298.15 K and 873.15 K.

Reaction	25 °C		600 °C	
	TS ΔG	Rxn ΔG	TS ΔG	Rxn ΔG
CB12Pin	62.0	3.97	61.5	-20.6
CB21Pin	70.1	7.12	68.2	-19.6
CB23Pin	77.5	-0.20	75.2	-26.0
CB32Pin	71.5	-2.86	72.2	-26.9
CB43Pin	77.5	2.74	76.8	-28.1
CB1’2’Pin	76.3	8.57	72.6	-22.0
CB2’3’Pin	76.9	-1.47	74.1	-25.1
CB3’2’Pin	78.1	-2.19	73.7	-25.7
CB3’4’Pin	74.9	2.62	71.8	-25.8
CB4’3’Pin	78.1	-2.69	75.7	-25.8

4.3.3 Cyclic Grob Fragmentation

The cyclic Grob fragmentation reaction is another water loss mechanism that applies to 1,3-diols, such as glucose.[15,39] During the reaction, a C-C bond is broken and an alkene and an aldehyde are formed (Figure 4.10). This reaction cannot proceed if the two hydroxyl groups are not in close proximity. With one exception, this is not possible when glucose adopts the lowest-energy $^4C_1$ “equatorial” conformation, where all hydroxyl groups are in the equatorial position. The hydroxyl groups in the $^1C_4$ “axial” conformation are in the axial position, which causes the participating hydroxyl groups to be close enough to react (see Figure 4.11 and Table 4.5). However, the Grob fragmentation wherein the C4 breaks a C-O bond and the C6 forms a carbonyl can proceed even when glucose is in the $^4C_1$ “equatorial” position since the hydroxyl groups

on C4 and C6 are in close enough proximity to interact. This reaction is referred to as GLCeq46Grob to differentiate it from GLCax46Grob, which has “axial” glucose as the reactant. The “axial” conformation is 6.7 kcal/mol higher in free energy than the “equatorial” conformation at 873.15 K and the free energy required to flip the ring from the more stable “equatorial” conformation to the “axial” has been reported to be less than 10 kcal/mol,[38] which means that it is not the rate-determining step of this reaction pathway.

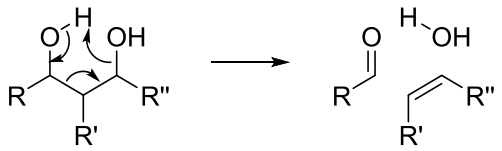

Figure 4.10. Generalized cyclic Grob fragmentation mechanism.

Glucose can undergo Grob fragmentation via eight separate reactions. Five of these reactions result in six-carbon acyclic products, while GLCeq46Grob, GLCax46Grob, and GLC53Grob involve losses of one- or two-carbon fragments. For GLCeq46Grob and GLCax46Grob, a hydroxyl group is lost from the C4 position upon the elimination of a hydrogen atom on C6, which generates formaldehyde and a cyclic alkene, which can further undergo retro-Diels Alder reaction. The barrier for GLCeq46Grob is 14.1 kcal/mol lower than for GLCax46Grob and generates the same products. In reaction GLC53Grob, a water molecule is not formed since hydrogen is transferred from the C3 position to the ring oxygen to form a hydroxyl group. During this reaction, O-C1 and C2-C3 bonds are broken to yield ethenediol, the tautomer of glycolaldehyde. However, this glycolaldehyde-producing reaction is not competitive with the previously proposed reaction pathway for glycolaldehyde formation,[30] which requires only 49.2 kcal/mol of free energy to proceed. The overall lowest barrier among the

studied Grob fragmentations is that for GLC13Grob (62.7 kcal/mol) and the highest barrier is that for GLC24Grob (92.1 kcal/mol), which are similar to the barriers for Maccoll elimination.

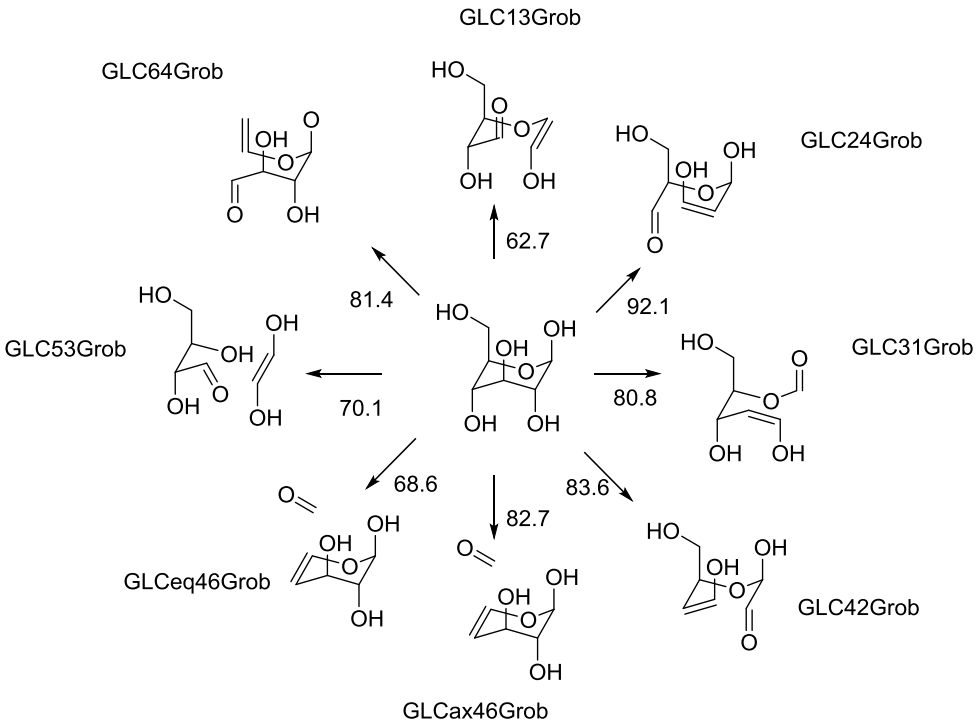

Figure 4.11. The cyclic Grob fragmentation reactions of β-D-glucopyranose with Gibb's free energy barriers in kcal/mol calculated at the M06-2X/6-311++G(d,p)//M06-2X/6-311++G(d,p) level of theory at 873.15 K. The reaction codes indicate the reactant (GLCeq = "equatorial" glucose, GLCax = "axial" glucose), the respective carbon atoms that break a C-O bond and form a C=O bond, and the reaction type (Grob=cylic Grob fragmentation). In the case of GLC53Grob, the C-O bond is not broken but transforms from an ether to a hydroxyl group.

Mayes *et al.* illustrated the importance of Grob fragmentation as it produces 5-hydroxymethylfurfural (5-HMF) from glucose.[37] After isomerization to fructose and dehydration at C2, Grob fragmentation of the anhydrous fructose enol produces a dihydrofuran precursor to 5-HMF. Although conversion from anhydrous fructose to the dihydrofuran can occur in a two-step process of tautomerization to 2,5-anhydro-D-

mannose followed by Maccoll elimination at C3, the Grob fragmentation has an activation energy that is 12.1 kcal/mol lower

Table 4.5. Transition state and reaction free energies in kcal/mol for cyclic Grob fragmentations of glucose calculated at the M06-2X/6-311++G(d,p)//M06-2X/6-311++G(d,p) level of theory at 298.15 K and 873.15 K.

Reaction	25 °C		600 °C	
	TS ΔG	Rxn ΔG	TS ΔG	Rxn ΔG
GLC13Grob	63.7	20.8	62.7	-9.9
GLC24Grob	95.0	19.0	92.1	-12.5
GLC31Grob	78.5	3.8	80.8	-23.6
GLC42Grob	81.0	17.3	83.6	-6.8
GLCax46Grob	82.3	13.9	82.7	-16.3
GLCeq46Grob	83.5	13.7	81.4	-17.7
GLC53Grob	68.7	27.8	68.6	-18.7
GLC64Grob	69.1	7.7	70.1	-22.7

For cyclic Grob fragmentations of cellobiose, 13 separate reactions are reported here (see Figure 4.12 and Table 4.6). The lowest barriers for reactions at the reducing and non-reducing ends are for CB13Grob (barrier 63.4 kcal/mol) and for CB5’3’Grob (barrier 61.8 kcal/mol), respectively. As with glucose, barriers are presented for axial and equatorial starting positions where possible. Six of the reactions lead to an anhydrous cellobiose molecule, four result in breaking of the glycosidic linkage to form glucose, and the remaining three yield a low-molecular weight product (formaldehyde, ethenediol, or erythrose) and a glucoside. As with the other water loss reactions, cyclic Grob fragmentation has reaction barriers that are relatively independent of temperature and

reaction free energies that are much more favorable at higher temperatures, as explained by the increase in entropy as the molecule degrades into two products.

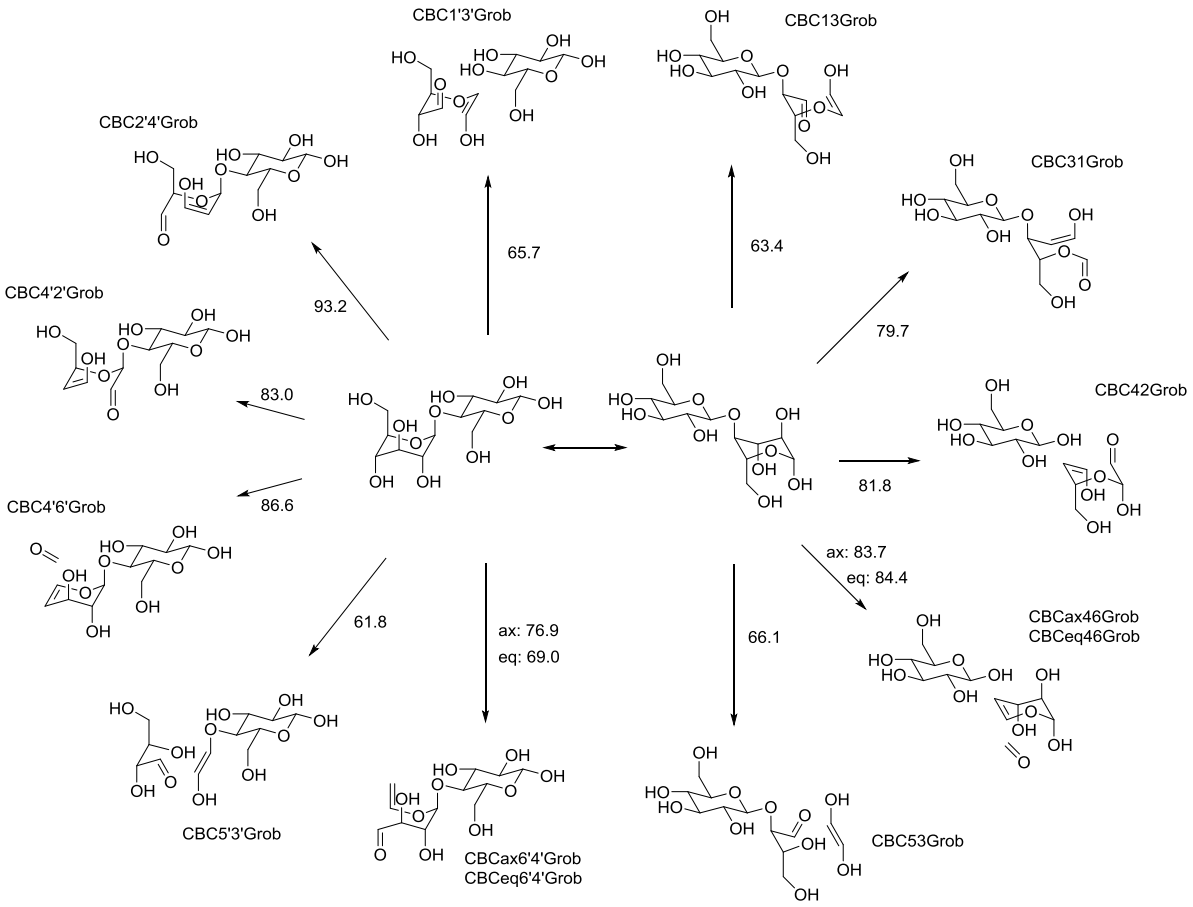

Figure 4.12. The cyclic Grob fragmentation reactions of cellobiose with Gibb's free energy barriers in kcal/mol calculated at the M06-2X/6-311++G(d,p)//M06-2X/6-311++G(d,p) level of theory at 873.15 K. The reaction codes indicate the reactant (CBeq = "equatorial" cellobiose, CBax = "axial" cellobiose), the respective carbon atoms that break a C-O bond and form a C=O bond, and the reaction type (Grob=cylic Grob fragmentation). In the case of CB53Grob and CB5'3'Grob, the C-O bond is not broken, but transforms from an ether to a hydroxyl group.

Table 4.6. Transition state and reaction free energies in kcal/mol for cyclic Grob fragmentation of glucose calculated at the M06-2X/6-311++G(d,p)// M06-2X/6-311++G(d,p) level of theory at 298.15 K and 873.15 K.

Reaction	25 °C		600 °C	
	TS ΔG	Rxn ΔG	TS ΔG	Rxn ΔG
CB13Grob	64.4	22.6	63.4	-2.44
CB31Grob	77.4	0.20	79.7	-26.3
CB42Grob	81.1	22.6	81.8	-5.25
CBax46Grob	83.5	12.6	83.7	-37.1
CBeq46Grob	85.7	13.4	84.4	-37.4
CB53Grob	67.5	30.1	66.1	-3.27
CB1’3’Grob	67.2	29.2	65.7	-4.16
CB2’4’Grob	93.9	19.7	93.2	-8.77
CB4’2’Grob	82.2	21.0	83.0	-6.35
CB4’6’Grob	87.0	10.6	86.6	-36.3
CB5’3’Grob	61.6	28.2	61.8	-4.46
CBax6’4’Grob	75.8	19.8	76.9	-7.28
CBeq6’4’Grob	70.1	10.7	69.0	-18.5

4.3.4 Aldol Condensation Rearrangement

Some Pinacol and Grob reactions yield an aldol product containing a carbonyl group that is in the γ-position relative to a hydroxyl group (see Figure 4.7 and Figure 4.11). These products can undergo aldol rearrangement as depicted in Figure 4.13. For the GLC12Pin and GLC21Pin products, the C3 hydroxyl group in is the γ-position relative to the carbonyl group. After aldol rearrangement, the carbonyl is in the C3 position, and there is a double bond between C1 and C2. This compound corresponds to the GLC13Grob product. The products of GLC23Pin and GLC32Pin have two hydroxyl groups that are in the γ-position relative to the carbonyl group. When these products undergo aldol rearrangement with the C1 hydroxyl group, the product is the GLC24Grob

product. These same products can also undergo aldol rearrangement with the C4 hydroxyl group, resulting in the GLC31Grob product. Finally, the carbonyl and the C3 hydroxyl groups in the products of the GLC34Pin and GLC43Pin reactions can react to yield the GLC42Grob product. This reaction network is shown in Figure 4.14.

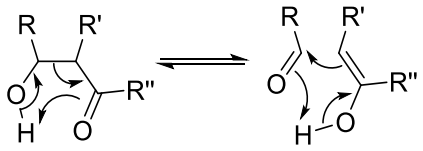

Figure 4.13. Generalized aldol rearrangement mechanism.

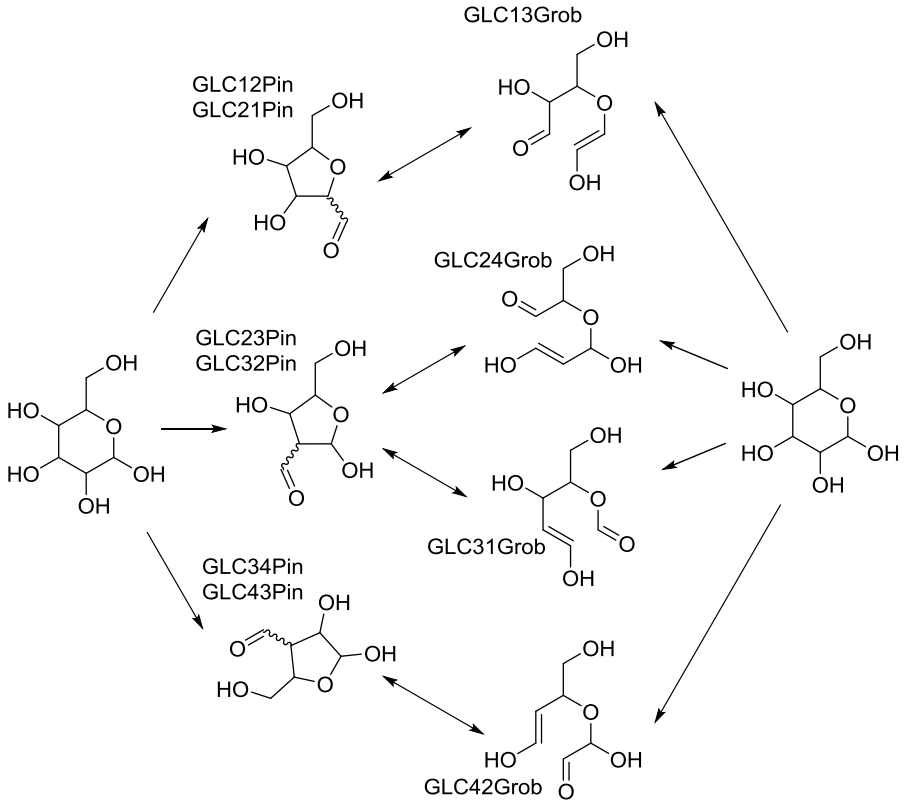

Figure 4.14. Interconversion between Pinacol ring contraction products and cyclic Grob fragmentation products via aldol rearrangement.

The potential energy surface and transition state barriers for the Aldol rearrangement network are shown in Figure 4.15 and Table 4.7. Calculations on the transition states connecting the Pinacol products with the Grob products reveal that

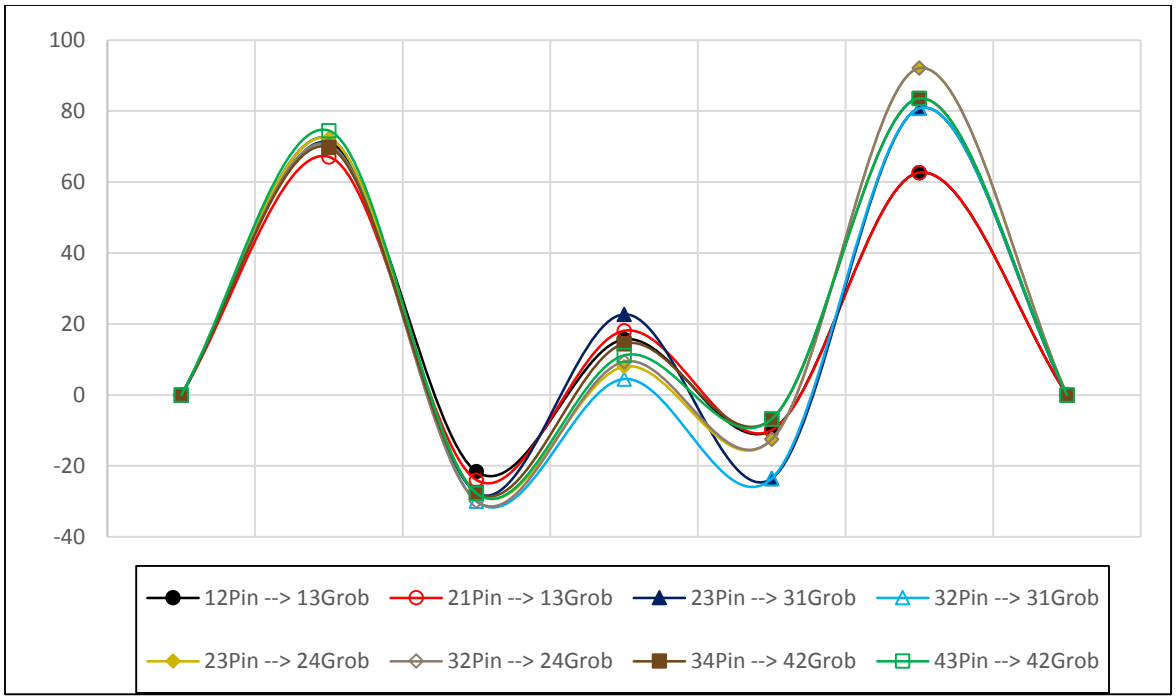

Figure 4.15. Potential energy surface in kcal/mol for the formation and interconversion of Pinacol ring contraction and cyclic Grob fragmentation products of glucose. Calculations were performed at the M06-2X/6-311++G(d,p)//M06-2X/6-311++G(d,p) level of theory at 873.15 K.

Table 4.7. Barrier heights in kcal/mol for transformations between Pinacol products and Grob products via aldol rearrangement. All calculations were carried out at the M06-2X/6-311++G(d,p)//M06-2X/6-311++G(d,p) level of theory at 873.15K.

Reaction	ΔG^{t} Forward	ΔG^{t} Reverse
12Pin → 13Grob	37.3	25.6
21Pin → 13Grob	42.1	28.0
23Pin → 31Grob	50.3	46.3
23Pin → 24Grob	35.6	20.5
32Pin → 31Grob	34.5	28.0
32Pin → 24Grob	39.4	21.9
34Pin → 42Grob	41.9	21.2
43Pin → 42Grob	38.9	17.9

interconversion between these molecules is likely to occur at elevated temperatures. At 600 °C, the largest barrier from a Pinacol product to a Grob product is 50.3 kcal/mol for the reaction from the GLC23Pin product to the GLC31Grob product, while the lowest is 34.5 kcal/mol for the reaction from the GLC32Pin product to the GLC31Grob product.Among the Pinacol and Grob reactions, GLC32Pin produces the molecule that is thermodynamically most stable (-30.0 kcal/mol relative to glucose), with a transition state energy of 70.5 kcal/mol. In contrast, the transition state for GLC13Grob is 9.8 kcal/mol lower in energy, even though the Grob product is thermodynamically less stable (-9.9 kcal/mol relative to glucose). This product can readily convert to the more stable GLC12Pin product (-21.6 kcal/mol relative to glucose) or GLC21Pin product (-24.0 kcal/mol relative to glucose) with barriers of 25.6 kcal/mol and 28.0 kcal/mol, respectively.

4.3.5 Alcohol condensation

The final class of dehydration reactions considered is generalized alcohol condensation wherein an ether linkage replaces two hydroxyl groups (Figure 4.16). The nature of these reactions is such that two separate transition states lead to the same product depending on which oxygen becomes the ether oxygen and which one leaves in the water molecule. Barriers and free energies for alcohol condensation reactions of glucose are shown in Figure 4.17 and Table 4.8.

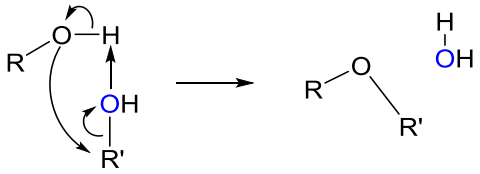

Figure 4.16. Generalized alcohol condensation reaction mechanism.

An example of alcohol condensation is the well-known concerted levoglucosan formation upon attack of the hydroxymethylene group of the glycose ring at the anomeric carbon to form a 5-membered ring, which has been demonstrated for glucose,[38] methyl β-D-glucoside,[40] and methyl cellobiose.[25] The calculated barriers for reactions of this type are among the lowest for pyrolysis reported in literature,[25,38,40] which may help explain the high yield of levoglucosan formation upon glucooligosaccharide pyrolysis.[3]

Figure 4.17 shows alcohol condensation reactions of glucose along with barrier heights. The transition state energy of 50.4 kcal/mol for the levoglucosan-producing GLC16Cond reaction makes it the most kinetically favorable water loss reaction discussed here. Levoglucosan formation through the loss of the oxygen on C1 (reaction GLC16Cond in Figure 4.17) has a barrier that is 30.3 kcal/mol lower than levoglucosan formation via the loss of the C6 oxygen (reaction GLC61Cond in Figure 4.17), which is in agreement with literature.[38] Besides levoglucosan, another bicyclic 5-membered ring product, formed by condensation of the C3 and C6 hydroxyl groups, as well as three other products that contain 4-membered rings can be formed by condensation of 1,3-diols (Figure 4.17). The strain caused by forming these 4-membered rings helps explain the large barriers for many of these reactions, with the exception of GLC13Cond, whose barrier is 62.3 kcal/mol (Figure 4.17). As discussed above for the GLC12Mac reaction, the positive charge on C1 caused by the electron-withdrawing oxygen atoms may explain the 20.3 kcal/mol difference between the barriers for GLC13Cond and GLC31Cond.

Aside from GLC16Cond, the high barriers and high reaction free energies for alcohol condensation reactions suggest that these reactions are a less likely route for lossof water than the other dehydration mechanisms. Therefore, the only alcohol

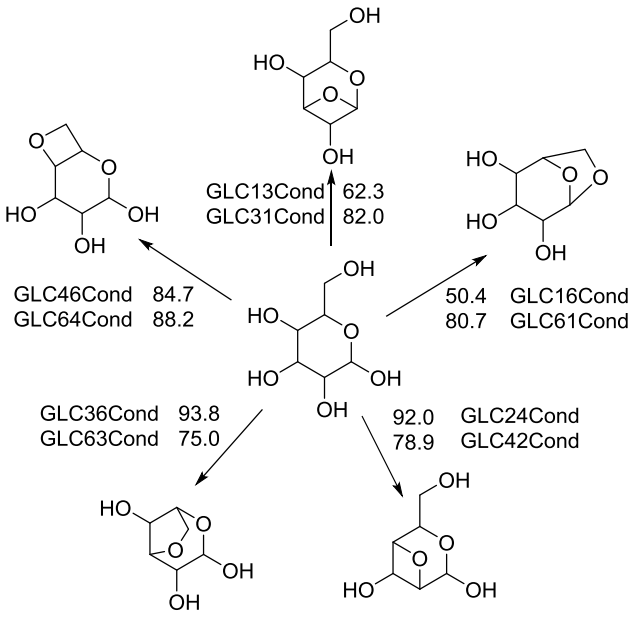

Figure 4.17. Alcohol condensation reactions for β-D-glucopyranose. Each product can be formed in two ways depending on which OH group leaves as water and which OH loses a hydrogen atom. The locations of the lost OH and H are indicated by the reaction numbers (*i.e.* GLC13Cond loses the OH at C1 and the H at C3 whereas GLC31Cond loses the OH at C3 and the H at C1.). Gibb's free energy barriers in kcal/mol were calculated at the M06-2X/6-311++G(d,p)//M06-2X/6-311++G(d,p) level of theory at 873.15 K.

condensation reactions for cellobiose that were calculated are CB16Cond and CB1'6'Cond, which involve cleavage of C-O at the anomeric carbon on the reducing end and non-reducing end, respectively, analogous to GLC16Cond (Figure 4.18). A conformational change must occur when a glucose ring transforms into levoglucosan, which occurs at a much faster rate than the condensation reaction as suggested by the potential energy surface displayed in Figure 4.19. Notably, the products from CB1'6'Cond do not agree with a previous experimental study on selectively ^{13}C-labeled cellobioses because the glucose formed during fast pyrolysis from these molecules was demonstrated to originate exclusively from the non-reducing end.[30] However, the yields of levoglucosans originating from each glucose ring are in equal proportion if cellobiose

undergoes sequential alcohol condensations at the C1 and C6 sites of each glucose, which matches previous experimental results. This finding suggests that there is something prohibitive to 1’6’-condensation of cellobiose relative to other possible reactions, including 1,6-condensation.

Table 4.8. Transition state and reaction free energies in kcal/mol for alcohol condensation reactions of glucose calculated at the M06-2X/6-311++G(d,p)//M06-2X/6-311++G(d,p) level of theory at 298.15 K and 873.15 K.

Reaction	25 °C		600 °C	
	TS ΔG	Rxn ΔG	TS ΔG	Rxn ΔG
GLC13Cond	63.6	20.9	62.3	-0.2
GLC31Cond	83.9	20.9	82.0	-0.2
GLC16Cond	48.1	-1.0	50.4	-17.9
GLC61Cond	76.4	-1.0	80.7	-17.9
GLC24Cond	89.7	17.7	92.0	-2.4
GLC42Cond	80.3	17.7	78.9	-2.4
GLC36Cond	89.0	2.3	93.8	-15.8
GLC63Cond	72.0	2.3	75.0	-15.8
GLC46Cond	84.0	32.1	84.7	12.6
GLC64Cond	89.2	32.1	88.2	12.6

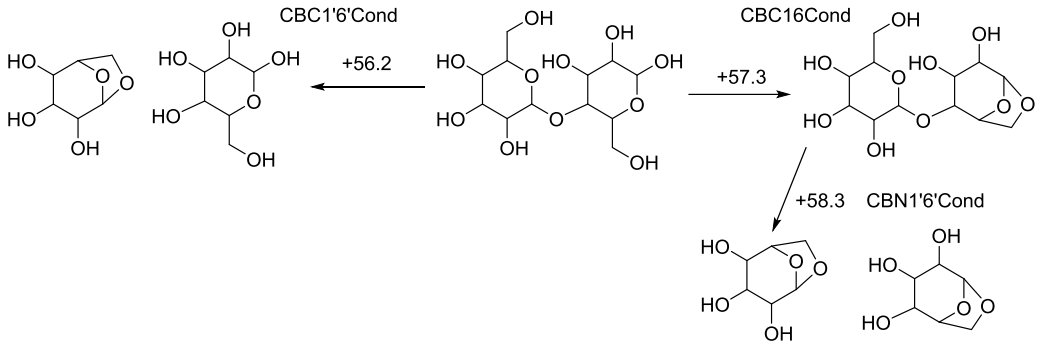

Figure 4.18. Most likely condensation reactions of cellobiose. Reaction codes indicate the reactant (CB=cellobiose, CBN=cellobiosan), the respective carbon sites for C-O cleavage and C-O ether formation, and the reaction type (Cond=alcohol condensation). Numbers indicate the Gibb's free energy in kcal/mol of the transition state relative to the reactants. Calculations were performed at the M06-2X/6-311++G(d,p)//M06-2X/6-311++G(d,p) level of theory at 873.15 K.

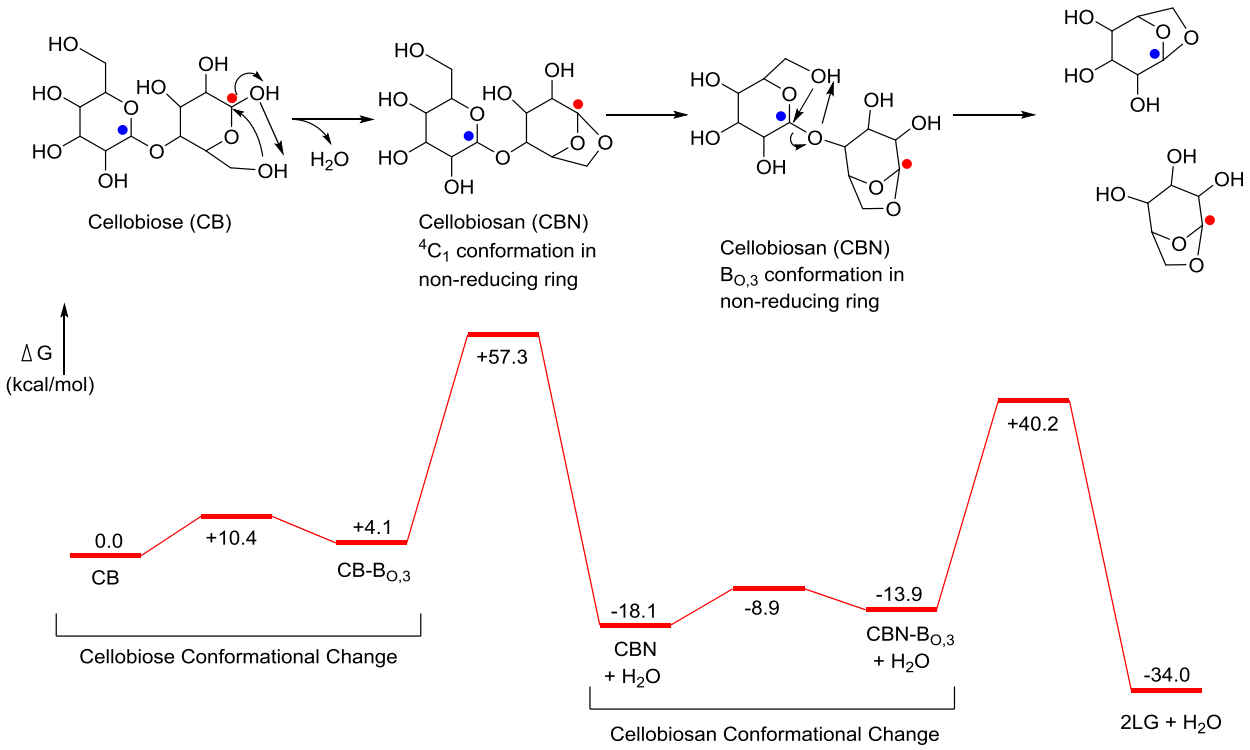

Figure 4.19. Potential energy surface in kcal/mol for levoglucosan formation from cellobiose through a cellobiosan intermediate, including conformational changes. Calculations were performed at the M06-2X/6-311++G(d,p)//M06-2X/6-311++G(d,p) level of theory at 873.15K.

4.3.6 Retro-Diels Alder Reaction

Cyclic alkenes that are formed from Maccoll eliminations and Grob reactions can undergo a wide variety of subsequent reactions. The retro-Diels Alder (rDA) reaction has been suggested to be important to cellulose pyrolysis.[41,75] The transition state structures and reaction free energies were calculated for the rDA reaction of the 1,2-dehydration products of glucose and cellobiose. The generalized rDA mechanism is shown in Figure 4.20. The results for secondary fragmentations of glucose and cellobiose via rDA are shown in Figure 4.21 and Figure 4.22.

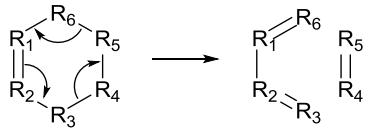

Figure 4.20. Generalized representation of the retro-Diels Alder reaction. Each R group can be either carbon- or oxygen-centered.

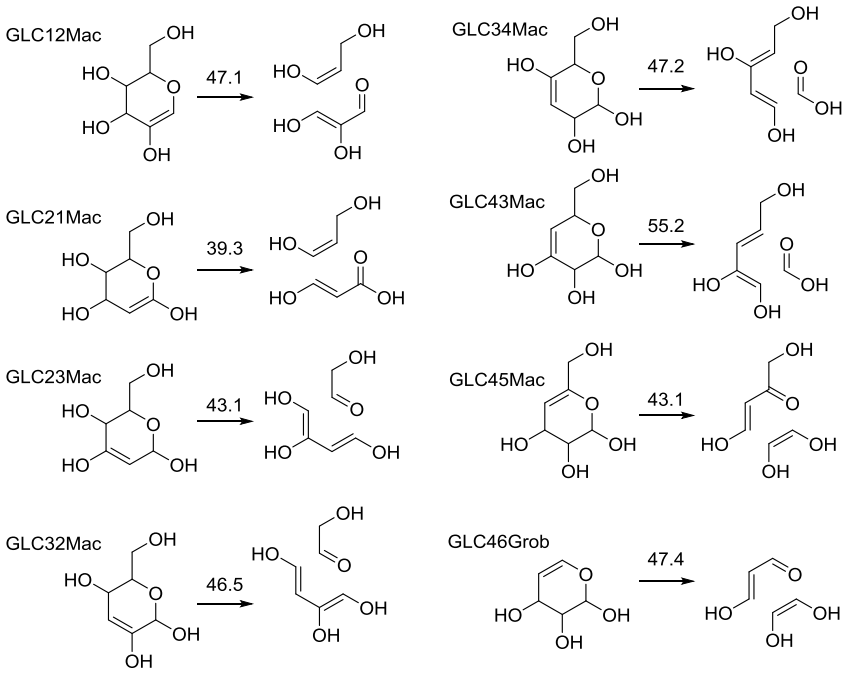

Figure 4.21. The rDA reactions of the cyclic alkene fragments formed upon glucose dehydration. Numbers above the arrows are the Gibb's free energy barriers in kcal/mol calculated at the M06-2X/6-311++G(d,p)//M06-2X/6-311++G(d,p) level of theory at 873.15 K. The labels on the left side of the reactions indicate the dehydration reaction that formed the cyclic alkene.

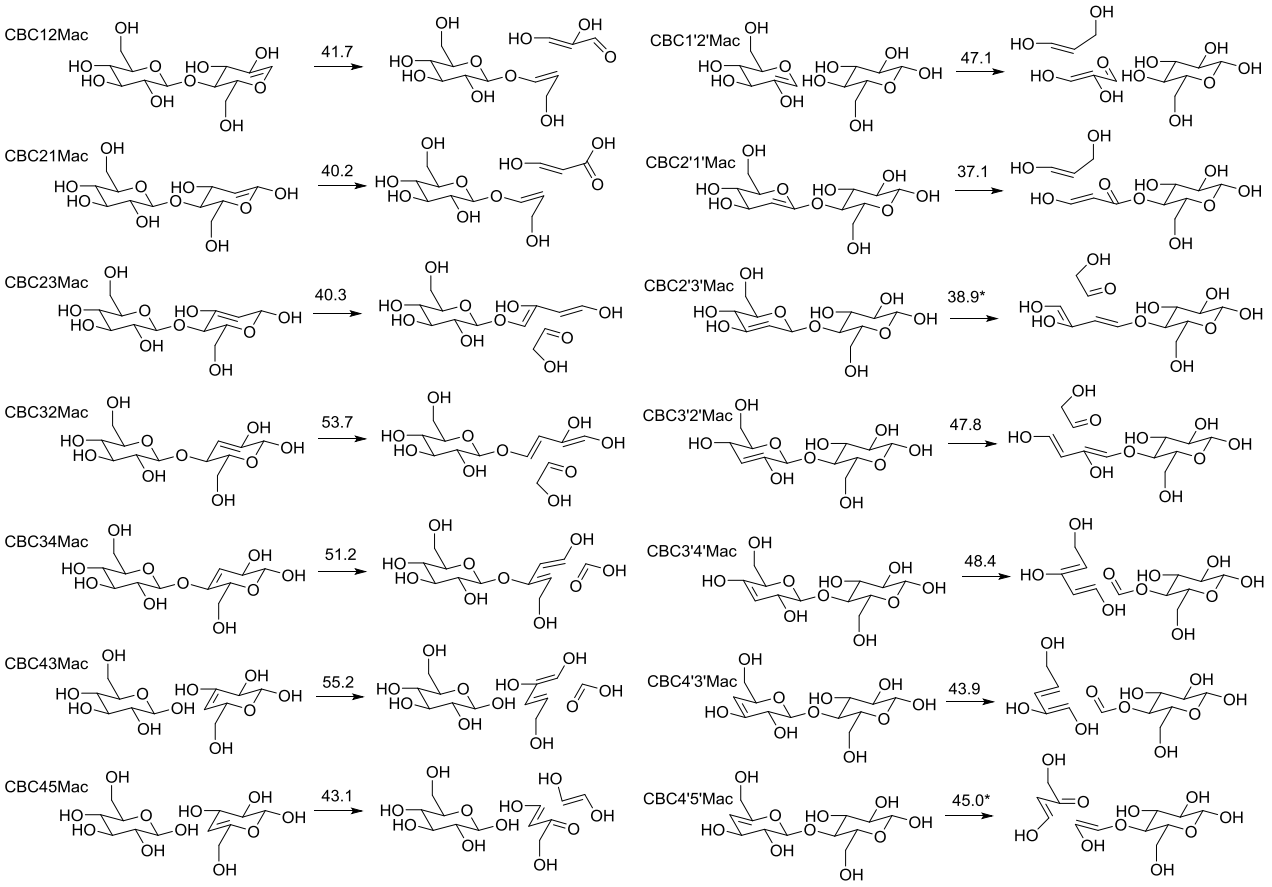

Figure 4.22. The rDA reactions of the cyclic alkene fragments formed upon cellobiose dehydration. Numbers above the arrows are the Gibb's free energy barriers in kcal/mol calculated at the M06-2X/6-311++G(d,p)//M06-2X/6-311++G(d,p) level of theory at 873.15 K. The labels on left side of the reactions indicate the dehydration reaction that formed the cyclic alkene. Two of the rDA transition states (CB2'3'Mac and CB4'5'Mac) were not compatible with a one-step concerted mechanism, but rather a two-step mechanism with a loosely bound zwitterionic intermediate. Reported here are the heights for the rate-limiting barriers.Cyclic alkenes arising from saccharide dehydration are likely to fragment further through a retro-Diels Alder reaction, since the calculated barriers for rDA are so low—between 39.3 and 55.2 kcal/mol (Table 4.9). In general, the reactions of cellobiose have larger barriers than the corresponding reactions of glucose. This is probably due to the additional intramolecular hydrogen bonds that must break during the transition for cellobiose. A comparison of the results obtained for glucose and cellobiose rDA is provided in Table 9.

Table 4.9. Comparison of rDA reaction barriers (Gibb's free energy) in kcal/mol for the cyclic alkene products of the Maccoll eliminations of glucose and both rings of cellobiose. Calculations were performed using the M06-2X/6-311++G(d,p)//M06-2X/6-311++G(d,p) level of theory at 873.15 K.

Alkene Site	Glucose	Cellobiose reducing end	Cellobiose non-reducing end
12Mac	47.1	41.7	47.1
21Mac	39.3	40.2	37.1
23Mac	43.1	40.3	38.9*
32Mac	46.5	53.7	47.8
34Mac	47.2	51.2	48.4
43Mac	55.2	55.2	43.9
45Mac	43.1	43.1	45.0*

*Barrier heights for rate-limiting step in two-step mechanism.

It is clear from the results shown in Table 4.9 that the addition of a second glucose molecule has little impact on the overall barriers for rDA. Thus, larger carbohydrates and perhaps even cellulose may have similar reaction kinetics. The most likely reason for the differences in barriers between glucose and cellobiose is a change in the extent of hydrogen bonding during the transformation. A large fiber of cellulose may be less likely to undergo rDA if it is constrained by a hydrogen bonding network present in its crystalline structure. However, as the fiber liquefies and depolymerizes during pyrolysis, these reactions may again be relevant to the overall product distribution.

4.4 Conclusions

Glucose and cellobiose can lose water via several mechanisms, including Maccoll elimination, Pinacol rearrangement, Grob fragmentation, and alcohol condensation. The dehydration reactions of glucose and cellobiose under pyrolysis conditions have barriers

ranging from 50 kcal/mol up to 94 kcal/mol. For glucose, the lowest barriers for each water loss mechanism are as follows: 65.9 kcal/mol for 1,2-dehydration; 67.1 kcal/mol for Pinacol ring contraction; 62.7 kcal/mol for cyclic Grob fragmentation; and 50.4 for alcohol condensation. Levoglucosan formation via the latter reaction is therefore the most kinetically favored dehydration reaction for glucose. A new reaction network of Aldol rearrangement unlocks the interconversion of Pinacol rearrangement and Grob fragmentation products. The energies for the transition states of these Aldol rearrangements are as low as 4.5 kcal/mol relative to glucose. For cellobiose, the lowest barriers are: 62.5 kcal/mol for Maccoll elimination; 61.5 kcal/mol for Pinacol ring contraction; and 61.8 kcal/mol for cyclic Grob fragmentation. Retro-Diels Alder reactions of the dehydration products of glucose and cellobiose have much lower barriers than the dehydration reactions themselves: 39.3 kcal/mol for anhydrous glucose rDA, and 37.1 kcal/mol for cellobiose rDA. Thus, if the water loss products are formed during pyrolysis, it is likely that they continue to react via this mechanism. It is important to note that the reaction barriers are relatively independent of temperature and the reactions are more exergonic at higher temperatures, as expected. The similarity of reactions for glucose and cellobiose suggests that these reactions should provide insights into the overall pyrolytic processes for oligosaccharides and cellulose.

CHAPTER 5. COMPUTATIONAL RESULTS ON CELLOBIOSE FRAGMENTATION GIVE CLUES TO CELLULOSE DEPOLYMERIZATION DURING FAST PYROLYSIS

5.1 Introduction

Since cellulose serves as a surrogate for biomass in research on alternative energy,[2,3,42] The importance of understanding the mechanisms of depolymerization of cellulose upon fast-pyrolysis for improving the process cannot be understated. During fast pyrolysis, depolymerization of cellulose involves cleavages of either the glycosidic or aglyconic bonds, which can occur through homolysis,[51,75–77] heterolysis,[25,75,78] hydrolysis,[44,51,75] Maccoll elimination,[50,51] 1,6-alcohol condensation to form a levoglucosan end,[25,35,51,75,79,80] or through other minor routes[25] to be discussed below.

Firstly, homolytic cleavage of the glycosidic bond would yield a radical that would induce further cleavages in the opposite manner to how many polymers are formed. For cellulose to produce levoglucosan by homolysis, breaking of two glycosidic bonds would be required to yield two cellulose monoradicals as well as a diradical that can rearrange and combine as levoglucosan.[75,81] The homolytic bond dissociation energies of the glycosidic and aglyconic bonds are prohibitively high for this to be a feasible pathway (101 and 102 kcal/mol, respectively).[75] Maccoll elimination at the anomeric carbon of the non-reducing end of cellobiose to form 1,2-anhydroglucose has been suggested to be the initiating step of levoglucosan formation.[50] This reaction has an activation energy of 59.1 kcal/mol, calculated at the B3LYP/6-31G(2df,p) level of theory.

Two Maccoll elimination reactions that break the glycosidic linkage were found to be less favorable kinetically.[50] Hydrolysis is different from other depolymerization mechanisms proposed for fast pyrolysis in that it is a bimolecular reaction. Hydrolysis has been proposed to be a key step in glucose production during pyrolysis, after which glucose can fragment via numerous reactions.[14,33]

Another proposed mechanism for cellulose depolymerization is the 1,6-alcohol condensation reaction, which is a concerted "hydroxymethylene-assisted glycosidic bond cleavage" (HAGBC) that results in the bicyclic structure characteristic to levoglucosan (see Figure 5.1).[23,35] This cleavage can theoretically occur at any point along the cellulose chain to form cellulosan and cellulose with smaller degrees of polymerization. These smaller anhydro-oligosaccharides (levoglucosan, cellobiosan, cellotriosan, cellulosan, etc.) are thought to correspond to "active cellulose,"[76] which has been proposed to be an intermediate state of cellulose that produces smaller product molecules.[79,14,45,74] Intermolecular interactions of crystalline cellulose may inhibit mid-chain scissions, giving preference to HAGBC reactions near the reducing end of the chain unless the crystallinity is disrupted.[33,63]

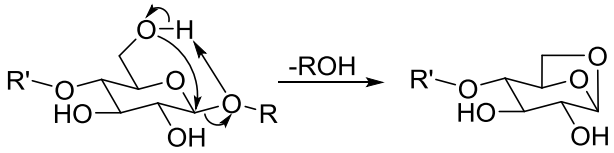

Figure 5.1. Depiction of the "hydroxymethylene-assisted glycosidic bond cleavage" (HAGBC) reaction of a generalized glucosaccharide.

While all of these depolymerization reactions can theoretically occur anywhere along the cellulose chain, a parallel pathway of unraveling cellulose by loss of glycolaldehyde (or isomers) proceeds only at the reducing end.[28,80] Retro-Aldol condensation is the mechanism by which the reducing end unravels, leaving behind

erythrose-cellulosides, ethenediol-cellulosides, and glycolaldehyde-cellulosides, which have been observed experimentally[19,28] and in molecular dynamics simulations.[25] A recent study on ^{13}C-labelled cellobioses provides three important findings for the initial products of cellobiose fast pyrolysis: 1) glucose is formed exclusively from the non-reducing end of cellobiose, 2) levoglucosan production occurs in almost equal proportions from both the reducing and non-reducing ends, and 3) unraveling begins on the reducing end by losses of ethenediol and glycolaldehyde.[28] Hydrolysis and HAGBC reactions of cellobiose have been proposed [14] to explain glucose formation upon pyrolysis of cellobiose with calculated barriers of 34.0 kcal/mol[14] and 54.4 kcal/mol,[23] respectively, but these reactions violate the first finding listed above since they produce glucose from the reducing end. However, it is demonstrated in this chapter that hydrolysis and HAGBC mechanisms may still operate upon the fragments of cellobiose that are formed from the unraveling of the reducing end (*viz.* glucopyranosyl-erythrose, glucopyranosyl-ethenediol, and glucopyranosyl-glycolaldehyde). It will be shown that HAGBC, hydrolysis, and reducing end unraveling can together explain the spectra of the ionized initial products of fast pyrolysis of cellobiose, cellulose, and other compounds discussed in chapters 2 and 3. The large size of cellulose makes DFT investigations of cellulose too computationally expensive to be feasible. Earlier chapters have shown that cellobiose can serve a model for cellulose. In this chapter, calculations on the mechanisms of breaking the glycosidic linkage of cellobiose will be explored to gain insight into the overall depolymerization of cellulose

5.2 Methods

Conformational analysis was performed with the MacroModel program with MCMM torsional sampling and the MMFF94s force field. Geometry optimizations and calculation of energies for minima and transition states were performed with the Gaussian09 program. Thermal corrections for internal energy, enthalpy, and Gibb's free energy were calculated using statistical mechanics, assuming an ideal gas and using the harmonic oscillator approximation. All eigenvalues of the minima are positive, while each transition state possesses exactly one negative eigenvalue.

Gas-phase calculations include three degrees of freedom for translation and three degrees of freedom for rotation per molecule. This leads to large entropy values that may be an overestimate of the entropy that exists in the liquid phase, causing a deviation in Gibb's free energy since it is highly dependent on entropy, especially at elevated temperatures. When two molecules react, the amount of energy required to achieve a transition state includes the entropy that is lost when the total degrees of freedom in rotation and translation are reduced from twelve to six. To overcome this discrepancy, a reactant complex is used as a reference state for the energetics rather than the molecules at infinite separation. The use of this complex is an attempt to accurately describe the constraints imposed on the entropy by intermolecular interactions in the liquid phase. The reactant complexes are determined by a geometry optimization of the reverse pathway in the IRC calculations that follow a transition state optimization. Product complexes are found by using the forward pathway of the IRC.

The global minimum of the cellobiose-water system was found by performing a conformational analysis, followed by DFT geometry optimization. The structure with the

lowest energy according to the MMFF94s force field was re-optimized at the more accurate M06-2X/6-311++G(d,p) level of theory, together with all structures whose MMFF94s energies were within 5 kcal/mol of the lowest MMFF94s energy to ensure that the global minimum was found.

5.3 Results and Discussion

A conformational analysis on the cellobiose and water system, followed by DFT geometry optimization on the ten lowest energy conformations, reveals that all these conformations lie within 5 kcal/mol of each other in Gibb's free energy at 873.15 K (see Table 5.1). For cellobiose, the conformation with the lowest electronic energy is conformation CB_WAT_9 (-23.6 kcal/mol) and it lies 9.6 kcal/mol lower in energy than CB_WAT_5 (-14.0 kcal/mol), the conformation in the cellobiose group with the highest electronic energy. The difference in enthalpy of these two conformations, calculated at 298.15 K, is 9.4 kcal/mol. However, the Gibb's free energy differences between CB_WAT_9 and CB_WAT_5 are merely 6.3 kcal/mol and 0.07 kcal/mol, calculated at 298.15 K and 873.15 K, respectively. In fact, at the elevated temperature, conformation CB_WAT_6 surpasses CB_WAT_9 as the structure with the lowest Gibb's free energy. At higher temperatures, entropic contributions to Gibb's energy become more significant. Conformation CB_WAT_9 has a structure that provides two hydrogen bonds between the external water molecule and hydroxyl groups of cellobiose (see Figure 5.2). Conformation CB_WAT_6, on the other hand, has one hydrogen bond between water and a cellobiose hydroxyl group and one hydrogen bond between water and a ring ether on cellobiose. It is expected that the ether oxygen is less polar than the hydroxyl oxygen atoms in cellobiose so that the hydrogen bond of water and the ether will be weaker than

the hydrogen bond between two hydroxyl groups. Thus, water is less tightly bound to cellobiose in conformation CB_WAT_6 than in CB_WAT_9 (Figure 5.2), leading to a larger entropic contribution to the Gibb's free energy of CB_WAT_6 at elevated temperatures. The same trend was observed in the group of hydrated cellobiosan conformers. The results of the conformational analysis on cellobiosan are shown in Table 5.2. CBN_WAT_5 has the third highest electronic energy of this group of molecules, but it has the lowest Gibb's free energy at 873.15 K because the water is more weakly bound by a hydrogen bond with a cellobiosyl hydroxyl group and a hydrogen bond with the glycosidic ether oxygen. These results suggest that hydrogen bonding has a large impact on the entropy of the bimolecular systems.

Table 5.1. Low energy conformers of cellobiose-water complexes and their electronic energy, enthalpy, and Gibb's free energy (all in kcal/mol) relative to cellobiose and water with no interaction, calculated using the M06-2X/6-311++G(d,p)//M06-2X/6-311++G(d,p) level of theory at the temperatures listed.

System	Electronic Energy	Enthalpy, 298.15 K	Gibb's Energy, 298.15 K	Gibb's Energy, 873.15 K
CB+WAT (no complex)	0.0	0.0	0.0	0.0
CB_WAT_1	-17.5	-15.5	-4.7	15.2
CB_WAT_2	-17.5	-15.5	-3.9	17.8
CB_WAT_3	-21.6	-19.4	-7.1	15.8
CB_WAT_4	-16.8	-14.7	-4.0	15.7
CB_WAT_5	-14.0	-11.9	-2.1	15.9
CB_WAT_6	-15.6	-14.0	-4.6	12.6
CB_WAT_7	-20.7	-18.5	-6.9	14.7
CB_WAT_8	-16.7	-14.7	-3.3	17.8
CB_WAT_9	-23.6	-21.3	-8.4	15.9

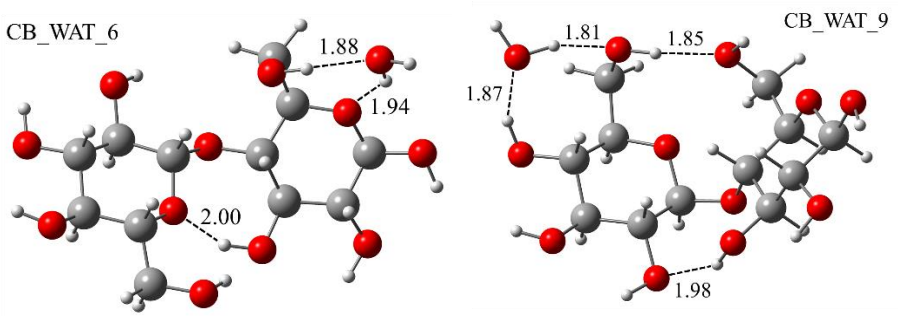

Figure 5.2. Comparison of conformations of cellobiose-water complexes CB_WAT_6 and CB_WAT_9. Distances of hydrogen bonds (dashed lines) displayed in angstroms.

Table 5.2. Low energy conformers of cellobiosan-water complexes and their electronic energy, enthalpy, and Gibb's free energy (all in kcal/mol) relative to cellobiosan and water with no interaction, calculated using the M06-2X/6-311++G(d,p)//M06-2X/6-311++G(d,p) level of theory at the temperatures listed.

System	Electronic Energy	Enthalpy, 298.15 K	Gibb's Energy, 298.15 K	Gibb's Energy, 873.15 K
CBN+WAT (no complex)	0.0	0.0	0.0	0.0
CBN_WAT_1	-17.2	-15.0	-3.7	17.6
CBN_WAT_2	-13.7	-11.6	-0.8	19.3
CBN_WAT_3	-11.9	-9.9	0.07	18.5
CBN_WAT_4	-13.2	-10.8	-0.3	19.1
CBN_WAT_5	-12.1	-10.3	-1.2	15.5
CBN_WAT_6	-12.6	-10.5	-0.5	18.1
CBN_WAT_7	-19.3	-17.0	-4.7	18.1
CBN_WAT_8	-11.2	-9.3	0.7	19.2

Similar conformational analyses were performed for water complexes with open-chain cellobiose, glucopyranosyl-erythrose, glucopyranosyl-ethendiol, and glucopyranosyl-glycolaldehyde since these compounds can also react with water via the

hydrolysis mechanism. Table 5.3 shows the energies for the conformations of water complexes for each of these molecules that has the lowest Gibb's free energy at 873.15 K.

Table 5.3. Lowest Gibb's free energy (in kcal/mol) conformers of water complexes with various molecules, calculated at the M06-2X/6-311++G(d,p)//M06-2X/6-311++G(d,p) level of theory at 873.15 K.

Molecule	Gibb's energy
Cellobiose	12.6
Cellobiosan	15.5
Cellobiose, open-chain	9.7
Glucopyranosyl-erythrose	19.2
Glucopyranosyl-ethendiol	19.1
Glucopyranosyl-glycolaldehdye	19.4

5.3.1 Catalytic Glucose formation via Maccoll Elimination

Maccoll elimination is a means of producing glucose from cellobiose. In this mechanism, a hydrogen transfers from one of three positions (C3, C5 or C2') to the glycosidic oxygen. When transfer occurs from C3 or C5, the result is the cleavage of the aglyconic bond, while transfer from C2' will result in cleavage of the glycosidic bond. In general, the mechanisms that cleave the glycosidic bond of cellobiose produce glucose from the reducing end, contrary to experimental findings as discussed above. Maccoll elimination with hydrogen transfer from C3 has a barrier of 65.9 kcal/mol at 873.15 K (see Table 5.4). The four-membered ring in the transition state structure of the Maccoll elimination mechanism can be altered by the assistance of external alcohol molecules to stabilize the transition state.[33] Figure 5.3 shows a Maccoll elimination reaction along with possible catalysis by water, methanol, formic acid, glucose, or cellobiose self-catalysis

with reaction energies as shown in Table 5.4. Water and methanol are single site catalysts that assist in the transfer of hydrogen by increasing the size of the transition state ring from four-membered to six-membered. The R group does not participate in the reaction, but may affect energetics by steric effects or non-bonding interactions. Water reduces the barrier to 62.1 kcal/mol and methanol reduces the barrier to 61.4 kcal/mol. Other hydroxy-containing compounds present in biomass may also catalyze this reaction. Formic acid and glucose catalysis proceeds by a two-site interaction with cellobiose (see Figure 5.3). It is unclear why glucose does not lower the reaction barrier while formic acid does. It may be an electronic effect caused by reaction of an ether instead of a carbonyl or it may simply be that glucose is too large.

Calculations were not performed on cellobiose self-catalysis, but a possible mechanism is shown in Figure 5.3. An interesting feature of this reaction is that the cellobiose acting as a catalyst undergoes ring-opening while the reactant cellobiose is cleaved into two molecules. This allows the catalyst cellobiose molecule to proceed through the reducing end unraveling pathway.

It is expected that the other two glucose-producing Maccoll elimination reactions have similar trends. If this is the case, the Maccoll elimination reaction that cleaves the glycosidic bond would yield glucose from the reducing end, which is contrary to the experimental results.[28] However, the glucosides that form during the unraveling of the reducing end of cellobiose can also undergo Maccoll elimination. For instance, a Maccoll elimination reaction can lead to cleavage of the glycosidic bond of GER to yield anhydroglucose from the non-reducing end and erythrose from the reducing end.

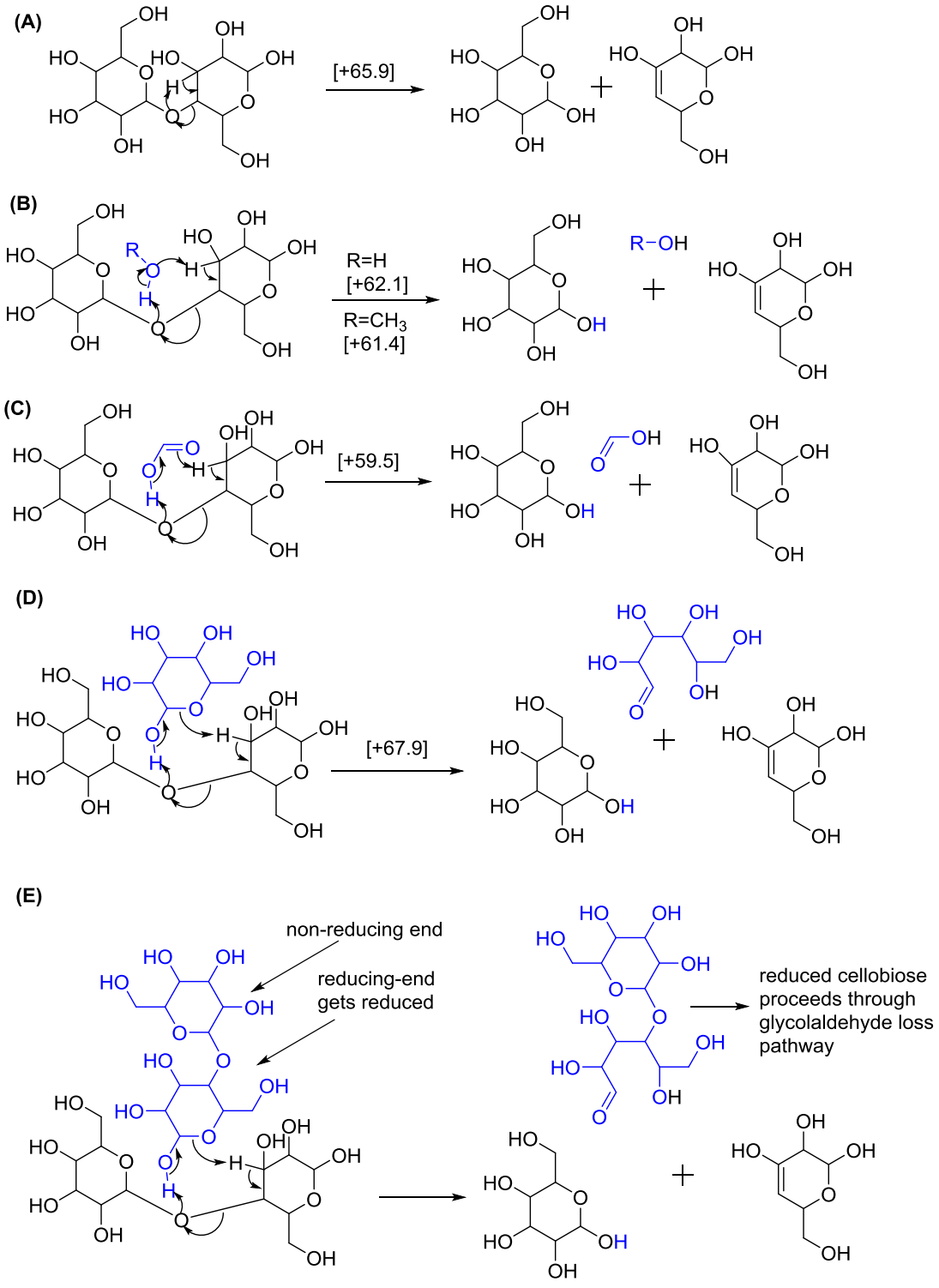

Figure 5.3. Maccoll elimination by hydrogen transfer from C3 to the glycosidic oxygen in isolation (A), with external water or methanol (B), external formic acid (C), external glucose (D), and possible cellobiose self-catalysis (E). Calculations performed at the M06-2X/6-311++G(,dp) level of theory at 873.15 K for reactions in (A)-(D).

Table 5.4**.** Complexation energy and transition state energy for Maccoll elimination of cellobiose by hydrogen transfer from C3 catalyzed by various molecules. Calculations performed at the M06-2X/6-311++G(d,p)//M06-2X/6-311++G(d,p) level of theory at 873.15K.

External molecule	ΔG of reactant complex	$\Delta G^{\ddagger}$ relative to reactant complex
None	N/A	65.9
Water	20.8	62.1
Methanol	19.5	61.4
Formic Acid	15.7	59.5
Glucose	26.6	67.9

5.3.2 Hydrolysis/Alcoholysis

During alcoholysis by ROH, cleavage of the glycosidic or aglyconic bond is possible. In the former case, glucose is formed from the reducing end and an R β-glucoside from the non-reducing-end (Figure 5.4). In the latter case, glucose forms from the non-reducing end and an R β-O4-glucoside from the reducing end (Figure 5.4). Due to the hydrogen atoms on carbons C3 and C5, steric hindrance forces the aglyconic cleavage to proceed only after a conformational change to the $^{1}C_{4}$ position in the reducing end (see Figure 5.4). The barrier for glycosidic bond cleavage of cellobiose by hydrolysis is 51.0 kcal/mol while aglyconic bond cleavage by hydrolysis has a barrier of 77.8 kcal/mol.

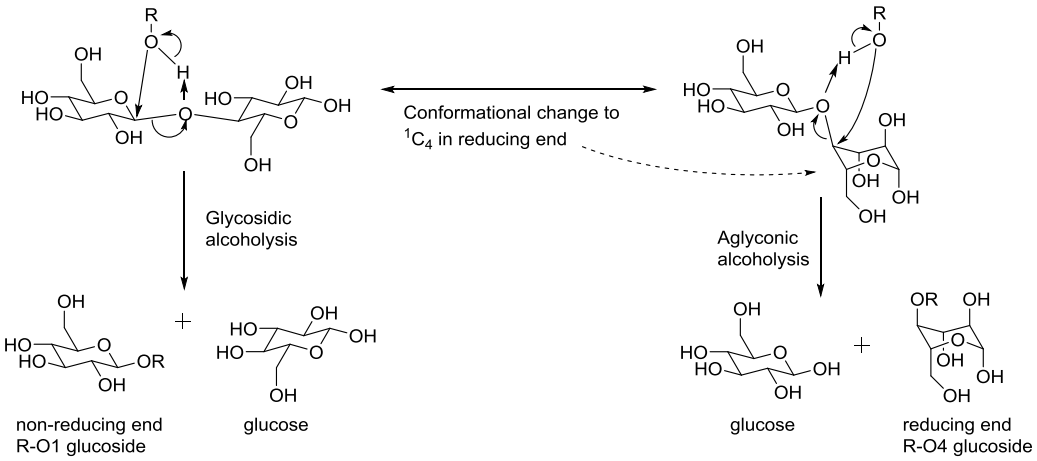

Figure 5.4. Reaction pathways for alcoholysis of cellobiose.

5.3.3 Reducing vs. Non-reducing End Chemistry

While hydrolysis, HAGBC, and Maccoll elimination alone cannot reconcile the results of the carbon-labeled study of Degenstein et al.,[28] the combination of these reactions with the unravelling of the reducing end is in agreement with the experimental findings (see Figure 5.5 and Table 5.5). This network of reactions resolves the issue of glucose production originating exclusively from the non-reducing end of cellobiose. Figure 5.5 shows with dashed arrows the reactions that produce glucose from the reducing end of cellobiose and are thus not feasible. These reactions have barriers ranging from 51.0 to 56.6 kcal/mol at 873.15 K. On the other hand, the barrier initiating the unravelling of the reducing end by tautomerization to open-chain cellobiose is 49.2 kcal/mol. However, in the presence of water, this barrier drops to 39.8 kcal/mol, which corresponds to much faster kinetics than either hydrolysis or HAGBC of cellobiose. In the absence of water, hydrolysis is not possible but the barrier for ring-opening (49.2 kcal/mol) is still lower than the barrier for the "unfeasible" HAGBC reaction (56.2 kcal/mol). Both HAGBC and hydrolysis of open-chain cellobiose (CBOC) result in open-chain glucose (GLOC), which has the same MW as glucopyranose, and is thus also

unfeasible. Alternatively, CBOC can fragment in the manner described by Degenstein et al.[28] to form glucopyranosylerythrose (GER) by loss of ethenediol, followed by loss of glycolaldehyde by retro-aldol condensation to form glucopyranosyl-ethenediol (GED), which can undergo keto-enol tautomerization to glucopyranosyl-glycolaldehyde (GGA). The respective barriers for these reactions are 39.1 kcal/mol, 23.0 kcal/mol, and 32.8 kcal/mol, respectively, relative to cellobiose at 873.15 K, which is more favorable than both HAGBC and hydrolysis reactions of open-chain cellobiose with barriers of 55.9 and 56.6 kcal/mol. Thus, formation of glucose from the reducing end of cellobiose is less favorable than alternative pathways.

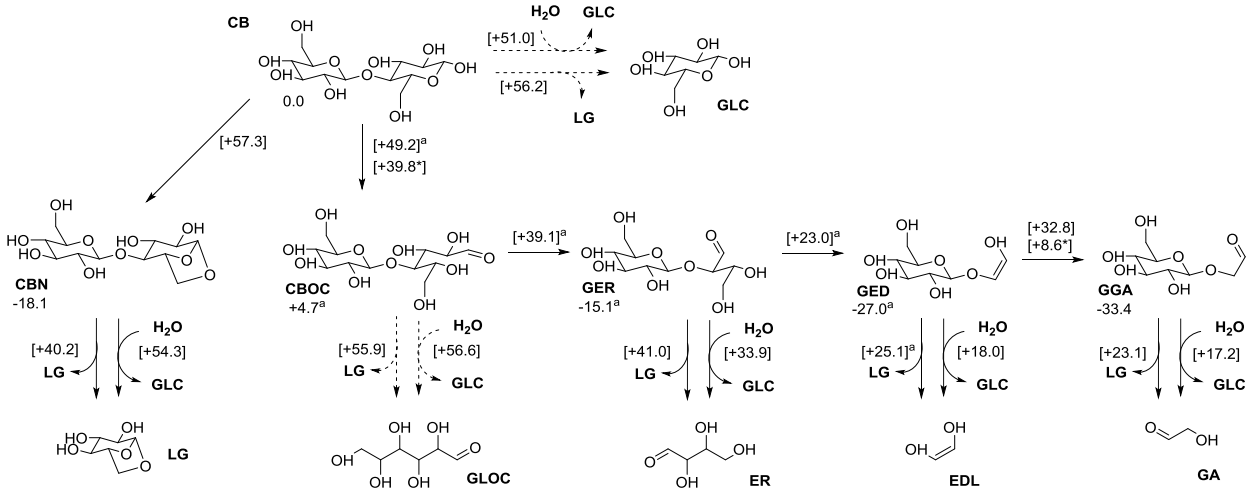

Figure 5.5. Cellobiose fragmentation via hydrolysis, HAGBC, and reducing end unravelling. Reaction free energies and reaction barriers (in square brackets) were calculated at the M06-2X/6-311++G(d,p)//M06-2X/6-311++G(d,p) level of theory at 873.15 K. * Denotes a calculated barrier with an explicit water molecule present, relative to the water complexed reactant. Dashed arrows correspond to reactions that contradict the experimental study of Degenstein et al.[28]

Fast pyrolysis of cellobiose produces a significant amount of glucose originating from the non-reducing end and none originating from the reducing end.[28] This is explained by the ability of each fragment of cellobiose (*viz.* GER, GED, and GGA) to

undergo hydrolysis. GER has a hydrolysis barrier of 33.9 kcal/mol, compared with 41.0 for HAGBC and 23.0 for retro-aldol condensation, which should dominate. GED has a hydrolysis barrier of 18.0, compared with 25.1 for HAGBC and 32.8 for tautomerization. Finally, GGA has a hydrolysis barrier of 17.2, compared with 23.1 for HAGBC. It is reasonable that at pyrolysis temperatures, all these reactions are occurring simultaneously to explain the complex mixture of levoglucosan, glucose, glycolaldehyde, GER, and GGA products and their relative abundances. For example, glucose formation pathways all have barriers lower than for levoglucosan production and the relative abundance of glucose is larger than levoglucosan for cellobiose pyrolysis (see Figure 3.1).

The amount of levoglucosan produced from the reducing and non-reducing ends is almost identical, whereas all the levoglucosan produced from GER, GED, and GGA originate from the non-reducing end. In this proposed scheme, the majority of levoglucosan production will proceed through cellobiosan. Once cellobiosan is formed, it can no longer undergo ring-opening to initiate the reducing end unravelling pathway. This is confirmed by the absence of fragmented reducing ends for cellotriosan during pyrolysis.[19] Therefore, cellobiosan can either evaporate from the surface of the pyroprobe intact or undergo HAGBC, both of which were observed[28] experimentally. In this case, levoglucosan originating from each end of cellobiose will exist in equal quantities. Hydrolysis is ruled out on the basis that it has a barrier 14.3 kcal/mol larger than HAGBC.

Although it is known that water is produced upon pyrolysis of biomass and glucosaccharides,[3,5,32,45] its residence time is unknown at such high temperatures. Many reactions become more likely should water be present during pyrolysis. For example,

tautomerization of the reducing end of cellobiose has a barrier that is 9.4 kcal/mol lower in energy when an external water molecule participates in the reaction. This is due to the transition state increasing in size from the four-membered ring into a more stable six-membered ring. A similar situation was observed for the tautomerization of GED to GGA, which has a barrier that is 24.2 kcal/mol lower in the presence of a water molecule (Figure 5.5). The retro-aldol condensation reactions of CBOC and GER were not considered since the transition state structures already possess the more stable six-membered ring configuration. Further, Seshadri and Westmoreland have shown that water catalyzes many other decomposition reactions of glucose.[33] Furthermore, they report that other hydroxy-containing compounds can be used in place of water as catalysts, where the increasing size of the alcohol corresponds to lower activation energies. Therefore, even if the rate of water evaporation is faster than the rates of reaction, other alcohols will be present to participate as catalysts, as has been demonstrated above in Figure 5.3 for the Maccoll elimination reaction.

5.4 Conclusions

Several mechanisms of cellobiose depolymerization are not in agreement with recent experimental findings.[28] In particular, Maccoll elimination, HAGBC, and hydrolysis have been used in literature[14,17,51] to explain fragmentation of cellobiose and larger glucosaccharides upon fast pyrolysis because the barriers of these reactions are lower than many other possible reactions. However, the unraveling of the reducing end of cellobiose via elimination of glycolaldehyde or isomeric molecules is a more competitive

Table 5.5**.** Reaction barriers for hydrolysis and glycosidic bond cleavage for the intermediates along the "GA loss" pathway. Calculations done with M06-2X/6-311++G(d,p)//M06-2X/6-311++G(d,p) at 873.15 K and energies are reported in kcal/mol.

Molecule	Glycosidic hydrolysis		Aglyconic hydrolysis		HAGBC
	ΔG complex	$\Delta G^{‡}$	ΔG complex	$\Delta G^{‡}$	$\Delta G^{‡}$
CBC	18.7	51.0	26.6	77.8	56.2
CBN	20.2	54.3	23.4	54.4	58.3
CBOC	30.2	51.9	23.8	71.5	51.2
GER	27.8	49.0	23.9	84.0	56.1
GED	31.4	45.0	22.2	81.4	52.1
GGA	20.2	50.6	19.8	86.3	56.5

pathway. As cellulose proceeds through this glycolaldehyde loss pathway, small products may escape into the gas phase for analysis while large ones remain in the pyrolysis zone and undergo further fragmentation by Maccoll, HAGBC, hydrolysis, or retro-Aldol reactions. This will form cellulosides, cellulosan, and cellulose with smaller DP to restart the cycle of decomposition until all products enter the gas phase. This interaction of parallel pathways supports earlier computational claims[14,23,35,36,63] of levoglucosan formation via HAGBC, formation of reducing ends via hydrolysis, and the observation of glucosides and cellulosides in the product distribution of cellulose.

CHAPTER 6. EXPLORING THE MECHANISMS OF FAST PYROLYSIS OF HEMICELLULOSES VIA TANDEM MASS SPECTROMETRY AND QUANTUM CHEMICAL CALCULATIONS: A SYNTHETIC MODEL COMPOUND STUDY

6.1 Introduction

Although numerous studies have been carried out on fast pyrolysis of cellulose and lignin by using model compounds,[5,19,21,23,28] no such mechanistic studies have been published on fast pyrolysis of hemicelluloses.[82–84] This can be attributed to the structural complexity and diversity of hemicelluloses. Hemicelluloses constitute between 20 and 35 wt% of biomass, depending on the feedstock.[4,82] They are defined as alkali-soluble polysaccharides in plant cell walls that have β-(1→4)-linked pyranose backbones, such as xylose or glucose, and possess branched linkages of saccharides, including galactose, glucose, and arabinose. Xylans (glucuronoxylan and glucuronoarabinoxylan) are the most abundant type of hemicelluloses in the secondary cell walls of plants.[85] They possess a backbone of xylopyranoses. In this study, a pyroprobe-mass spectrometry set-up was employed to examine the initial products of fast pyrolysis of unsubstituted xylan model compounds xylobiose and xylotriose. Quantum chemical calculations were performed to explore reaction mechanisms of fast pyrolysis.

6.2 Methods

The same experimental design coupling a pyroprobe with a mass spectrometer as described in chapter 2 was used for fast pyrolysis of the xylan model compounds.

Xylobiose (≥95%, CAS number 6860-47-5) and xylotriose (≥95%, CAS number 47592-59-6) were purchased from Carbosynth. The chemical structures for these compounds are shown in Figure 6.1. Methanol (LC/MS grade ≥99.9%, CAS 67-56-1) and water (LC/MS grade, CAS number 7732-18-5) were purchased from ProteoChem. Ammonium hydroxide (28−30% as NH_3, CAS 1336-21-6) was purchased from Mallinckrodt Chemicals and a compressed nitrogen cylinder (≥99.9%, CAS 7727-37-9) was purchased from Indiana Oxygen. All chemicals were used without further purification. The computational methods employed are the same as described in chapter 3.

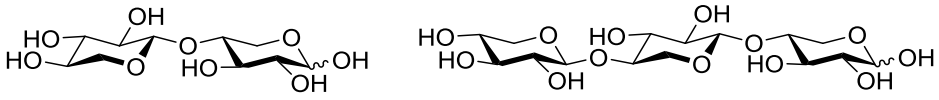

Figure 6.1. Structures of compounds used as model compounds in this study: (a) β-1,4-xylobiose and (b) β-1,4-xylotriose.

6.3 Results and Discussion

The model compounds were loaded on a platinum ribbon on the pyroprobe, which was housed inside the ionization chamber of the mass spectrometer. Initial products of fast pyrolysis evaporating from the surface of the ribbon were quenched in nitrogen atmosphere at 100°C at atmospheric pressure. Atmospheric pressure chemical ionization with ammonium hydroxide as a dopant was used to ionize pyrolysis products. This method ionizes the initial fast pyrolysis products by attaching an ammonium ion to them without fragmentation. Elemental compositions of ionized pyrolysis products were confirmed by high resolution mass analysis. All peaks shown in the mass spectra correspond to ammonium adducts of products generated from pyrolysis.

Ionized products obtained upon fast pyrolysis of xylobiose are shown in Figure 6.2(a). Ions of m/z 300 shown in Figure 6.2(a) are ammonium adducts of xylobiose. The

major product of fast pyrolysis of xylobiose is proposed to be β-D-xylopyranosyl-glyceraldehyde (ions of m/z 240), likely formed by loss of a glycolaldehyde (or isomeric) molecule from xylobiose. Other products observed in significant abundance correspond to ions of m/z 222 (likely formed by loss of a water molecule and a glycolaldehyde or isomeric molecule from xylobiose) and ions of m/z 282 (formed upon loss of a water molecule from xylobiose). Minor products formed upon xylobiose fast pyrolysis include those that correspond to ions of m/z 270 (formed upon loss of a formaldehyde molecule from xylobiose), ions of m/z 210 (likely formed upon loss of a formaldehyde molecule and a glycolaldehyde or isomeric molecule from xylobiose), ions of m/z 168 (xylose) and ions of m/z 150 (anhydroxylose) formed upon cleavage of the glycosidic linkage.

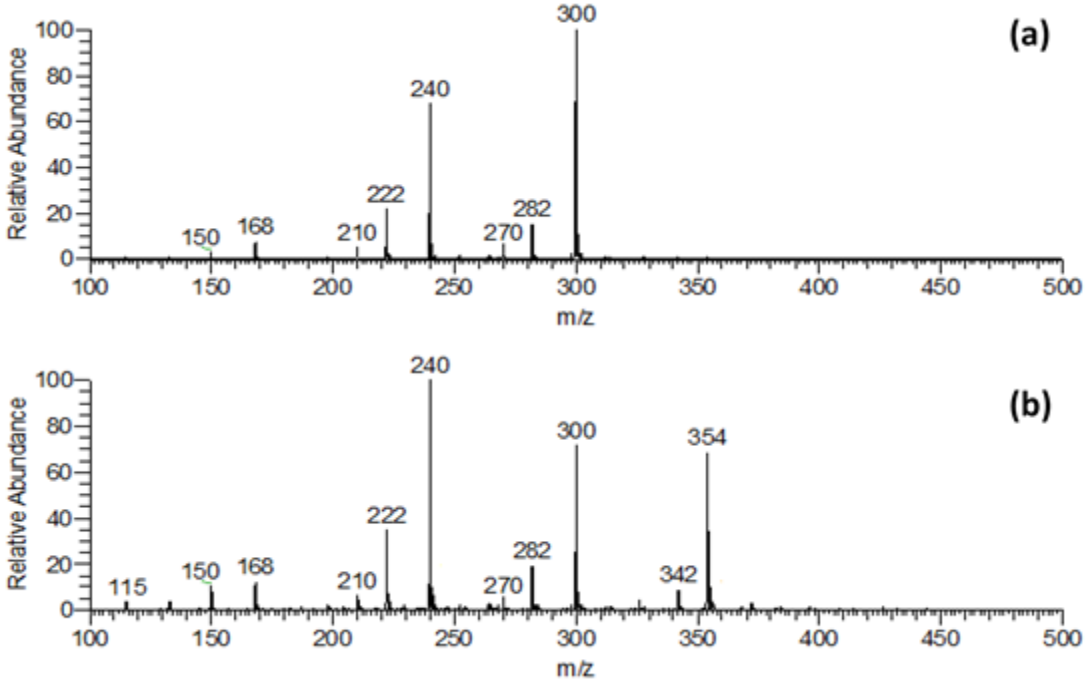

Figure 6.2. Positive ion mode mass spectra showing ionized initial products of fast pyrolysis of (a) β-1,4-xylobiose and (b) β-1,4-xylotriose, ionized by atmospheric pressure chemical ionization with ammonium hydroxide as dopant. All peaks shown in the mass spectra correspond to ammonium adducts of products generated upon pyrolysis.

Pyrolysis mass spectrum of xylotriose is shown in Figure 6.2(b). Xylotriose generated many identical products upon fast pyrolysis as seen for xylobiose. The structures of the ions were examined by using MS^2 experiments (isolating ions and subjecting them to collision-activated dissociation). Major products from fast pyrolysis of xylotriose were found to yield ions of m/z 354 (likely formed upon loss of a glycolaldehyde or isomeric molecule and a water molecule from xylotriose), ions of m/z 300 (xylobiose) and ions of m/z 240 (β-D-xylopyranosyl glyceraldehyde – identical product was proposed for fast pyrolysis of xylobiose). Other products yielded ions of m/z 282, 222, 210, 168, and 150, which were also observed for fast pyrolysis of xylobiose. Products yielding ions of m/z 342 are likely formed by loss of a glycolaldehyde or isomeric molecule and a formaldehyde molecule from xylotriose.

Quantum chemical calculations at 600°C at the M06-2X/6-311++G(d,p)//M06-2X/6-311++G(d,p) level of theory revealed a low-energy pathway (Figure 6.3) for the concerted elimination of an ethenediol molecule (tautomer of glycolaldehyde) from xylobiose, producing β-D-xylopyranosyl-glyceraldehyde (XGRA). The calculated free energy barrier for ring opening of the reducing end of xylobiose to produce open chain xylobiose (XBO) was found to be relatively low at 49.8 kcal/mol. The concerted elimination of ethenediol from open chain xylobiose (XBO) via retro-aldol condensation has a calculated free energy barrier of 42.3 kcal/mol. This reaction was found to be exergonic by 19 kcal/mol. Cellobiose—a model compound for cellulose—follows a similar pathway during fast pyrolysis, with barriers of 49.2 kcal/mol and 39.1 kcal/mol for reducing end ring opening and elimination of ethenediol, respectively.[28] Further fragmentation of β-D-xylopyranosyl glyceraldehyde via loss of formaldehyde to produce

ions of m/z 210 is not a major pathway, which is in agreement with an unfavorably high calculated free energy barrier of 76.6 kcal/mol relative to xylobiose. A Grob fragmentation reaction of XGRA may also explain the loss of formaldehyde to yield an ion with m/z 210. The calculated free energy barrier for elimination of formaldehyde from open-chain xylobiose (XBO) to generate β-D-xylopyranosyl erythrose (ions of m/z 270) was found to be 87.4 kcal/mol, which may explain its relatively low abundance.

Table 6.1. Elemental compositions, proposed structures of fast pyrolysis products as well as m/z values of their ions for xylobiose and xylotriose.

m/z of product ion	Elemental composition	Proposed structure
150	$[C_5H_8O_4+NH_4^+]$	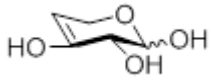 4,3-anhydroxylose
168	$[C_5H_{10}O_5+NH_4^+]$	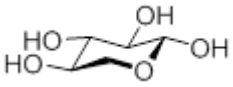 xylose
210	$[C_7H_{12}O_6+NH_4^+]$	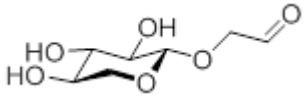 xylopyranosyl-glycolaldehdye (XGA)
222	$[C_8H_{12}O_6+NH_4^+]$	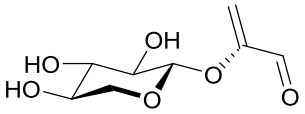 xylopyranosyl-acrylaldehyde (XAL)
240	$[C_8H_{14}O_7+NH_4^+]$	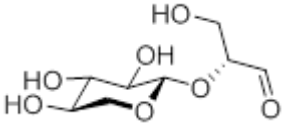 xylopyranosyl-glyceraldehyde (XGRA)

Table 6.1. continued.

270	$[C_9H_{16}O_8+NH_4^+]$	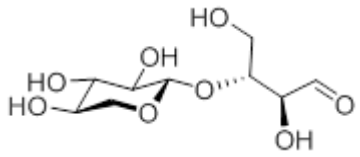 xylopyranosyl-erythrose (XER)
282	$[C_{10}H_{16}O_8+NH_4^+]$	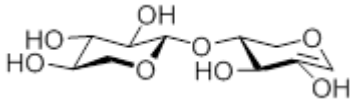 1,2-anhydroxylobiose
300	$[C_{10}H_{18}O_9+NH_4^+]$	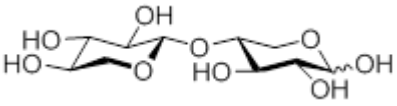 xylobiose (XB)
342	$[C_{12}H_{20}O_{10}+NH_4^+]$	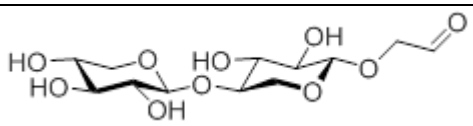 xylobiosyl-glycolaldhyde (XBGA)
354	$[C_{13}H_{20}O_{10}+NH_4^+]$	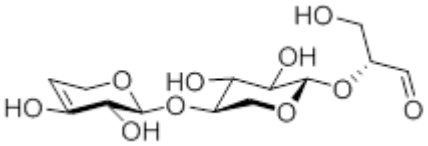

Based on the measured elemental composition, the ion of m/z 282 is an ammonium ion adduct of xylobiose that has lost a water molecule.The proposed structure for this ion (Figure 6.2) is based on quantum chemical calculations of Maccoll elimination of xylobiose, similar to the Maccoll elimination reactions of cellobiose described in chapter 4. Figure 6.4 shows the 14 possible Maccoll elimination reactions of xylobiose with reaction barriers calculated at the M06-2X/6-311++G(d,p) level of theory. Each reaction label indicates the carbon sites for C-O cleavage and C-H cleavage, respectively. For example, in reaction 12Mac, the C-OH bond on C1 and the C-H bond on C2 are broken when water is lost from the molecule. This reaction has the lowest

barrier for production of anhydrous xylobiose, corresponding to ions of m/z 282. The next lowest barrier for anhydrous xylobiose production is 34Mac, which is over 5 kcal/mol higher in energy. Hence, the product from 12Mac is the predicted precursor for the ion with m/z 282 as shown in Table 6.1.

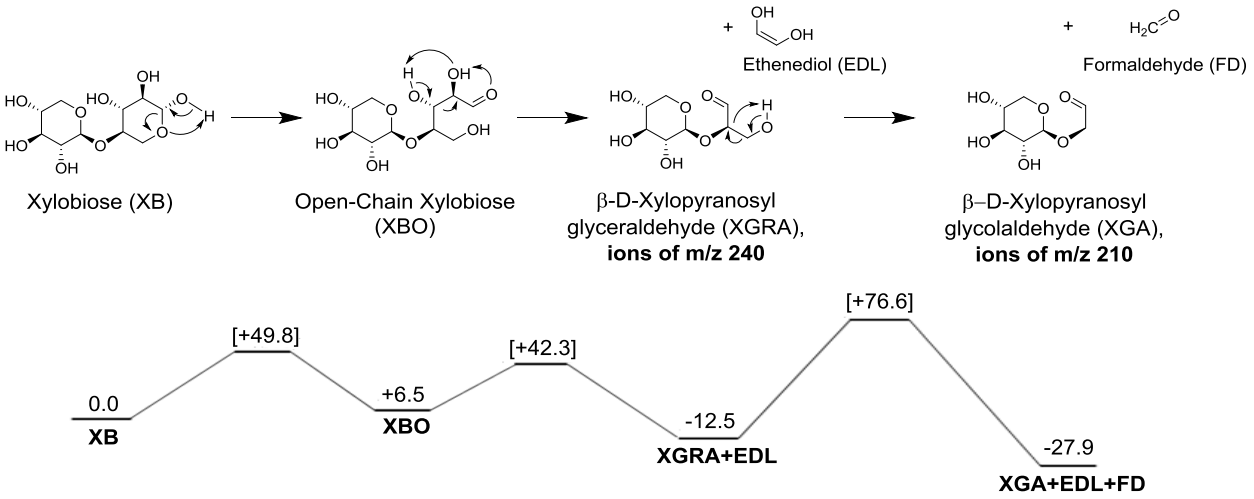

Figure 6.3. Free energies (kcal mol^{-1}) of intermediates and transition states (square brackets) for the formation of β-D-xylopyranosyl-glyceraldehyde (ions of m/z 240) and β-D-xylopyranosyl-glycoaldehyde (ions of m/z 210) from xylobiose at 600°C calculated at the M06-2X/6-311++G(d,p)//M06-2X/6-311++G(d,p) level of theory.

Three of the Maccoll elimination reactions (43Mac, 45Mac, and 1'2'Mac) produce a xylose and an anhydrous xylose by scission of the glycosidic linkage. Cleavages of glycosidic bonds (1'2'Mac) and aglyconic bonds (43Mac and 45Mac) were found to be equally likely based on the energy barriers (Figure 6.4), suggesting that xylose and anhydroxylose are equally likely to be produced from both the reducing and the non-reducing ends. Cleavage of the glycosidic bonds of xylobiose and xylotriose via the HAGBC reaction described in chapter 5 is not possible because of the absence of the hydroxymethylene group. This may explain why the products corresponding to the reducing end unraveling pathway of Figure 6.3 appear to be more dominant for xylobiose

(Figure 6.2) than the analogous products for reducing end unraveling of cellobiose (compare Figure 3.1 and Figure 3.3).

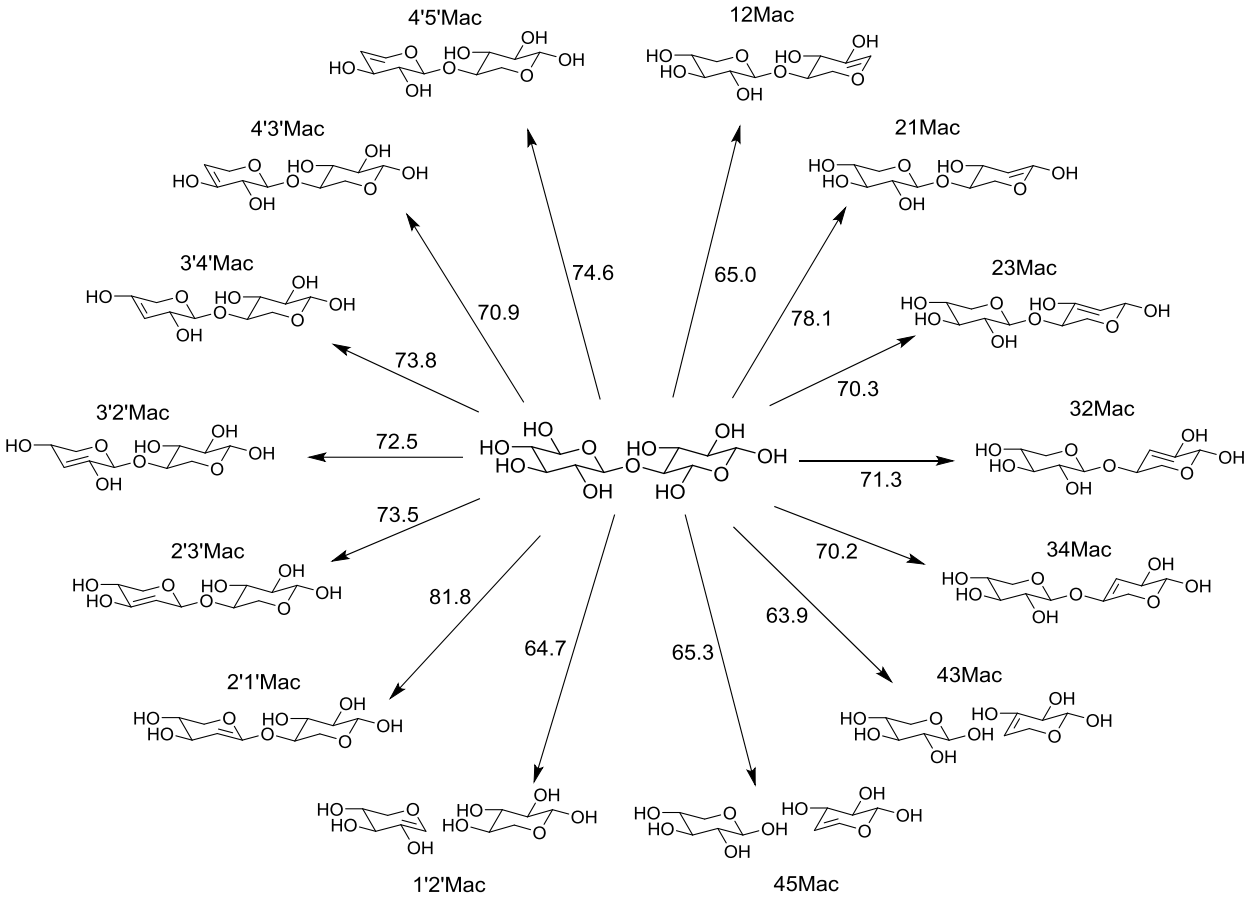

Figure 6.4. Calculated free energy barriers (kcal mol^{-1}) for 1,2-dehydration and cleavage of the glycosidic linkage via Maccoll elimination at 600°C calculated at the M06-2X/6-311++G(d,p)//M06-2X/6-311++G(d,p) level of theory. Reaction codes indicate respective carbon sites that cleave C-O and C-H bonds.

According to the measured elemental composition, the ion with m/z 222 corresponds to an ammonium adduct of xylobiose that has lost ethenediol and water. This can occur by loss of ethenediol from one of the anhydrous xylobiose products shown in Figure 6.4 or by loss of water from xylopyranosylglyceraldehyde (see Figure 6.5). Loss of ethenediol is expected to come from C1 and C2 on the reducing end based on similar

experiments and calculations on cellobiose (see chapter 3). It is possible that water is lost from the non-reducing end prior or subsequent to this loss of ethenediol from the reducing end. If water loss occurs first, the anhydrous xylobiose undergoes ring-opening, tautomerization and retro-aldol condensation analogous to the pathway in Figure 6.3. The barrier heights shown in Figure 6.5 for the reaction of anhydrous xylobiose (yielding ions of m/z 282) to generate anhydrous xylopyranosylglyceraldehyde (yielding ions of m/z 222) correspond to the initial ring-opening reaction, which in all cases is the rate-determining step of the two-step loss of ethenediol. The loss of ethenediol is expected to be much faster than the initial loss of water since the barriers for loss of ethenediol are at least 20 kcal/mol lower in free energy than water loss, which has barriers ranging from 70.9 kcal/mol to 81.8 kcal/mol (Figure 6.5).

Formation of ions with m/z 222 is more likely to occur by losing ethenediol from xylobiose to form XGRA first, followed by water loss. The barrier for XGRA formation is 49.8 kcal/mol (Figure 6.3), which is much lower than those for the dehydration reactions (Figure 6.5). Water loss from XGRA is most likely to occur by breaking the C-O bond at C5 of the fragmented reducing end and forming xylopyranosyl-acrylaldehyde (XAL) (Figure 6.5) with a barrier of 56.1 kcal/mol relative to XGRA. The other water loss pathways are less likely since they require at least 15 kcal/mol more energy.

6.4 Conclusions

Initial products of fast pyrolysis of xylobiose and xylotriose were determined using a fast pyroprobe/tandem mass spectrometry setup. Fast pyrolysis of xylobiose and xylotriose was found to generate many identical products. Ring opening at the reducing end and subsequent elimination of an ethenediol molecule from the reducing end via

retro-aldol condensation was found to be the major pyrolysis pathway. Other pyrolysis pathways include loss of water and formaldehyde molecules. Quantum chemical calculations revealed a feasible low-energy pathway for production of β-D-xylopyranosylglyceraldehyde from xylobiose, which can react further to form β-D-xylopyranosylacrylaldehyde. Other pathways include 1,2-dehydration and cleavage of glycosidic linkages via concerted Maccoll elimination mechanism.

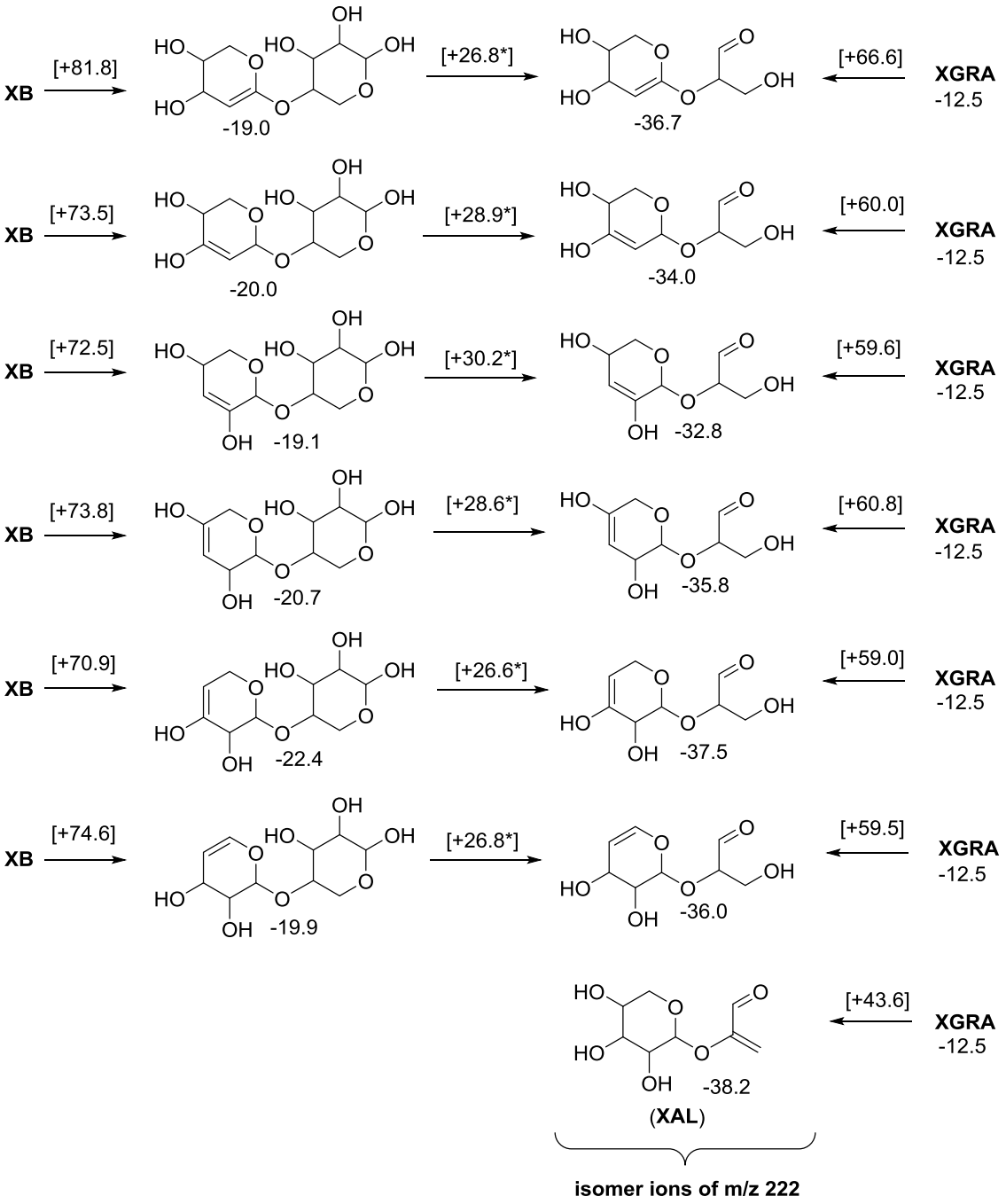

Figure 6.5. Pathways for the formation of product molecules yielding ions with m/z 222 via water loss from xylobiose (XB) followed by loss of ethendiol or loss of water from xylopyranosylglyceraldehyde (XGRA). Reaction free energies and barriers (in brackets) calculated at the M06-2X/6-311++G(d,p)//M06-2X/6-311++G(d,p) level of theory at 600°C relative to xylobiose. Numbers with * indicate the barrier of the rate determining step in the two-step process of ring-opening and loss of ethenediol.

CHAPTER 7. COMPUTATIONAL AND EXPERIMENTAL INVESTIGATION OF ION-MOLECULE REACTIONS TO IDENTIFY PROTONATED SULFONE AND AROMATIC CARBOXYLIC ACID FUNCTIONALITIES

7.1 Introduction

As drug molecules are metabolized, the functionalities of the compounds can be altered in a manner that increases the hydrophilicity of the compound and may lead to toxic drug metabolites.[86,87] Characterization of these metabolites by existing analytical methods (NMR, FT-IR, X-ray crystallography) has proven to be difficult.[88,89,90] Tandem mass spectrometry based on collision-activated dissociation (CAD) can be used to gain elemental composition and structural information of these metabolites. However, this technique often fails to provide unambiguous information for multifunctional drug moieties with same elemental composition and hence only conjectures can be drawn about the elemental connectivity of many analytes. Ion-molecule reactions can be used to differentiate functionalities within an analyte based on its reactivity with the chosen reagent. This technique has already been used in the characterization of organic molecules with functionalities such as epoxide,[91] sulfone,[92] amido,[93,94] carbonyl,[95] polyol,[96] hydroxylamino,[97] N-oxide and sulfoxide[98] groups. In this work, my collaborators demonstrated that gas-phase ion-molecule reactions of trimethoxymethylsilane (TMMS) reagent can be used to identify protonated sulfone and aromatic carboxylic acid functionalities, as present in multifunctional drug moieties. The

experimental work presented here is complemented by a computational investigation of the possible mechanisms by which the analytes react with the reagent in the gas-phase.

7.2 Methods

Most chemicals were purchased from Sigma-Aldrich with purities ≥ 98%. All chemicals were used without further purification. Stock solutions of all the analytes used in this study were prepared at a concentration of 0.1 mM using acetonitrile and are diluted as needed using 50% methanol and 50% water.

Experiments were conducted in a Thermo Scientific LTQ linear quadrupole ion trap (LQIT) equipped with an electrospray ionization (ESI) source. All analytes were analyzed via (+) ESI. In collision-activated dissociation (CAD) experiments, the advanced scan feature of the LTQ tune software interface was used to isolate the ions. The ions were then subjected to CAD by using helium as a collision gas. The isolation parameters were, an isolation width of 2 units, an activation q value of 0.25 and an activation time of 30 ms.

An external manifold for preparing helium/reagent gas mixtures was used as first proposed by Gronert.[99,100] A schematic drawing of the external manifold used in this research was published by Habicht and co-workers.[101] The reagent TMMS was introduced into the trap via the manifold using syringe pumps at a flow rate of 3 µL/h. The manifold surrounding the syringe port was maintained at a temperature of ~125 ^{o}C to ensure evaporation of the neutral reagent (TMMS). A known amount of helium (0.8L/h) was used to dilute the reagent and a small amount of the diluted fraction (~2 mL/min) was drawn into the trap by using Granville-Phillips leak valve and the remaining was removed via exhaust.

Lowest energy conformers for neutral and protonated species were identified using Maestro 7.0 Macro Model.[54] Geometry optimizations and single point energy calculations were completed with Gaussian 09.[37] Geometries and energies used in calculating theoretical proton affinities were performed with the B3LYP/6-31G++(d,p) level of theory.[38,64–67] The optimized structures and energies for the potential energy surfaces of the mechanistic pathways were calculated with M06-2X/6-311++G(d,p).[39] All transition state structures contain exactly one negative frequency.

7.3 Results and Discussion

Gas-phase reactivity of protonated model compounds with different functional groups were studied by my collaborators with TMMS (proton affinity (PA) = 202 kcal/mol) as a reagent in Linear quadrupole ion trap (LQIT). Most of the protonated model compounds react with TMMS to produce a stable adduct. However, when protonated sulfone and aromatic carboxylic acid containing model compounds were allowed to react with TMMS, a characteristic TMMS adduct-MeOH product was formed in addition to the TMMS adduct. Identification and differentiation of these two functionalities is possible by MS^n of the TMMS adduct-MeOH, as discussed below.

7.3.1 Protonated carboxylic acid model compounds

The mass spectra measured after the reaction between TMMS and protonated aromatic carboxylic acids showed the addition product, addition-MeOH product and/or addition-2MeOH product. While the CAD of addition product gives back the protonated analyte, CAD of adduct-MeOH product gives addition-2MeOH as a product. Upon further CAD, adduct-2MeOH product ion showed loss of molecules with MW 44 Da and

MW 90 Da; these losses are characteristic and can be used to identify the presence of an aromatic carboxylic acid functionality.

The mass spectrum of benzoic acid and mass spectrum of benzoic acid fragments after isolation and CAD are shown in Figure 7.1. Figure 7.2A shows the pathway I calculated for the spontaneous proton transfer and formation of adduct-MeOH product (m/z 227) for protonated benzoic acid upon reaction with TMMS. The first step of the reaction is proton transfer from protonated benzoic acid to TMMS. Addition-MeOH elimination product is formed by electrophilic attack of the deprotonated carbonyl group in the benzoic acid at the silicone atom in the protonated TMMS reagent, which involves a four-membered transition state. Both the proton transfer and adduct-MeOH elimination reaction are calculated to be exergonic relative to the reactants. Figure 7.2B depicts the potential energy surface calculated for the formation of adduct-2MeOH (m/z 195) upon CAD of adduct – MeOH elimination product. The highest barrier is calculated to be 28.7 kcal/mol. This second methanol loss is facilitated by proton transfer from the hydroxyl group of the carboxylic acid to a methoxy group bound to silicon atom for simultaneous Si-O bond cleavage to release methanol and formation of a four-membered ring containing silicon and a delocalized charge site. Notably, there is no adduct-3MeOH ion in the mass spectrum, which is explained by the mechanism for MeOH loss outlined above. Each methanol loss requires a hydrogen transfer to one of the methoxy groups of TMMS. Protonated benzoic acid can lose two hydrogen atoms from the carboxylic functionality, but a third hydrogen loss would involve cleavage of a C-H bond on the benzene ring, which is expected to be thermodynamically unfavorable. Figure 7.2C shows the potential energy surface calculated for the characteristic loss of molecules with

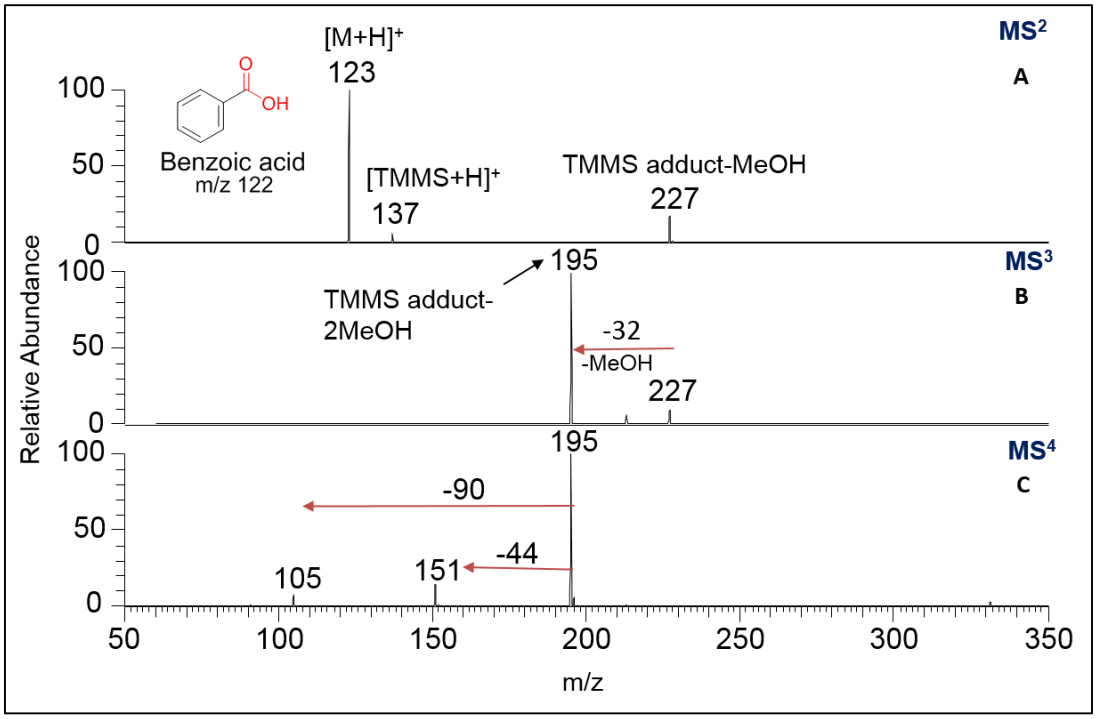

Figure 7.1. The mass spectrum of protonated benzoic acid measured after 300 ms of reaction with TMMS (spectrum A). The most abundant product ion (m/z 227) corresponds to adduct-MeOH. The other product ion (m/z 137) corresponds to proton transfer product. The MS^3 spectrum measured after collision-activated dissociation (CAD) of TMMS adduct-MeOH (spectrum B). The fragment ion (m/z 195) corresponds to TMMS adduct-2MeOH. The MS^4 spectrum measured after CAD of TMMS adduct-2MeOH (spectrum C). The most abundant fragment ion corresponds to CO_2 loss. The other fragment ion corresponds to loss of a molecule with MW of 90.

MW 44 Da and 90 Da upon CAD of adduct-2MeOH (m/z 195). The adduct-2MeOH product can isomerize into two distinct isomers that are conformers by breaking one of the bonds in the four-membered ring. The lower-energy conformer—"extended conformer"—has an energy of 24.8 kcal/mol relative to the original adduct-2MeOH isomer. This lower energy conformer is characterized by a protraction of the silicon and methoxy group away from the benzene ring. This "extended conformer" further fragments into an ion with m/z 105 via loss of a neutral molecules with MW 90 Da by cleavage of the ether bond. This barrierless heterolytic cleavage is endergonic by 35.4

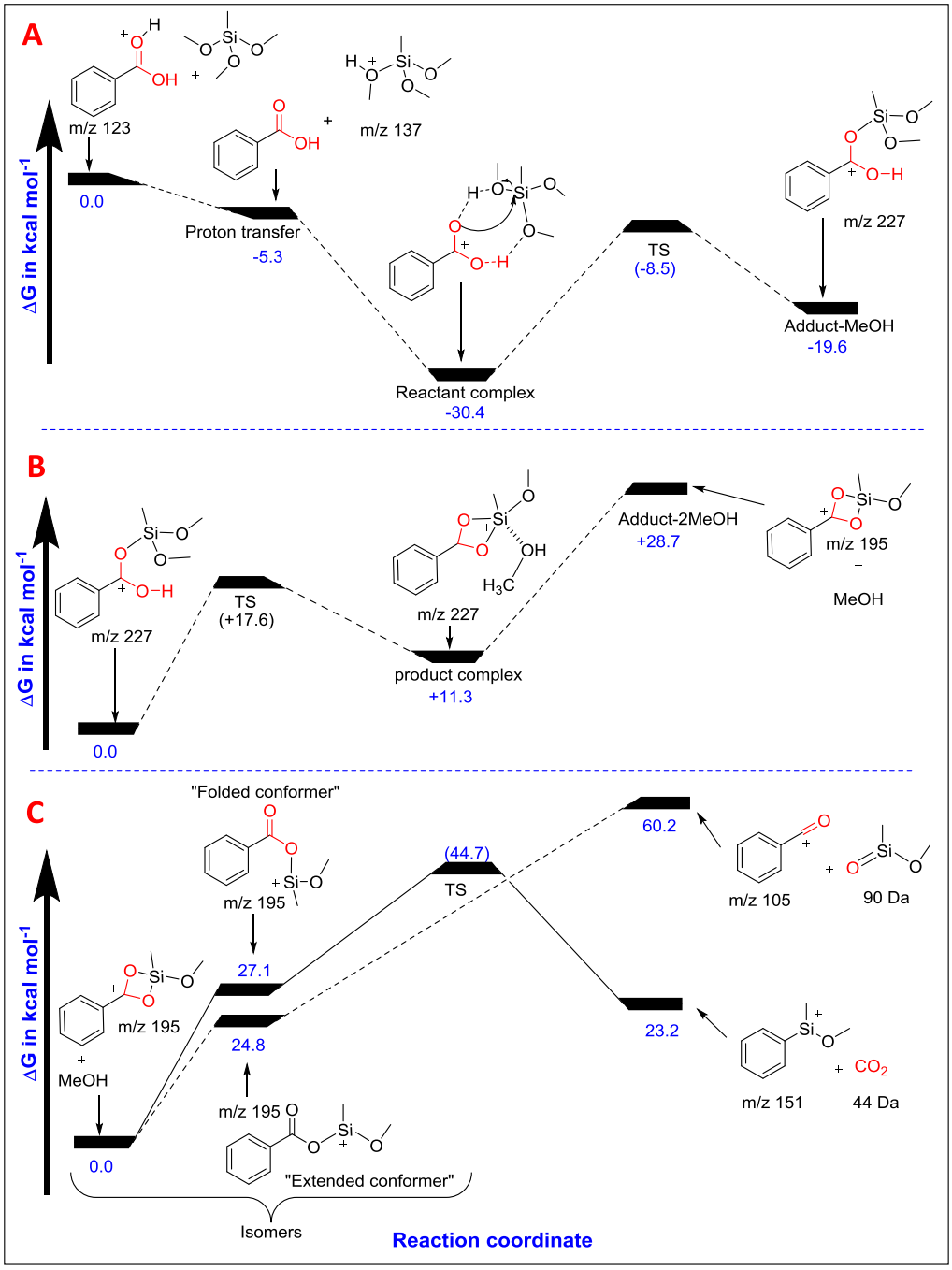

Figure 7.2. Proposed reaction pathways and calculated potential energy surfaces for the formation of different reaction products upon reaction of protonated aromatic benzoic acid with TMMS reagent and upon CAD of the product ions, calculated at the M06-2X/6-311++G(d,p) level of theory. A) Spontaneous proton transfer and formation of TMMS adduct-MeOH upon reaction of protonated benzoic acid with TMMS. B) Formation of adduct-2MeOH upon CAD of adduct-MeOH. C) Characteristic losses of molecules of MW of 44 Da (solid line) and 90 Da (dashed line) upon CAD of adduct-2MeOH.

kcal/mol and endothermic by 48.7 kcal/mol. The higher-energy conformer—"folded conformer"—has an energy of 27.1 kcal/mol relative to the original adduct-2MeOH isomer and is characterized by the silicon and methoxy groups folding towards the benzene ring where the positively charged silicon can interact with the π electrons system of the benzene ring. This conformer can fragment by expulsion of CO_2, shown by the transition state structure for this process in Figure 7.3. This process has a barrier 17.6 kcal/mol relative to the "folded conformer" (m/z 195). The final product is an ion with m/z 151 with an energy that is 3.9 kcal/mol lower than that of the "folded conformer." It is clear that these products can only be seen upon CAD because the overall pathways are endergonic. The formation of the fragment ion with m/z 151 (corresponding to the loss of CO_2) requires less energy than the ion with m/z 105, thus explaining the higher relative abundance of ion of m/z 151 in the MS^4 spectrum (Figure 7.1C).

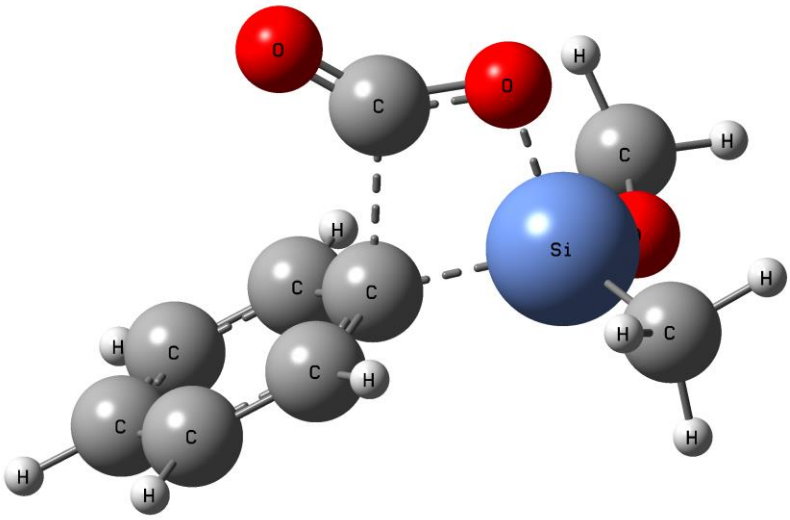

Figure 7.3. Transition state structure for the loss of CO_2 from benzoic acid TMMS adduct-2MeOH calculated at the M06-2X/6-311++G(d,p) level of theory.

The analogous reactivity of carboxylic acid with the TMMS reagent was observed for 3-hydroxybenzoic acid and 4-hydroxybenzoic acid as expected, but 2-hydroxybenzoic acid reacted differently with TMMS. Upon CAD of adduct-2MeOH, loss of CO_2 was still observed, but instead of the characteristic loss of MW 90 Da, a loss of MW 30 Da was observed (see Figure 7.4), corresponding to production of an ion with m/z 181.

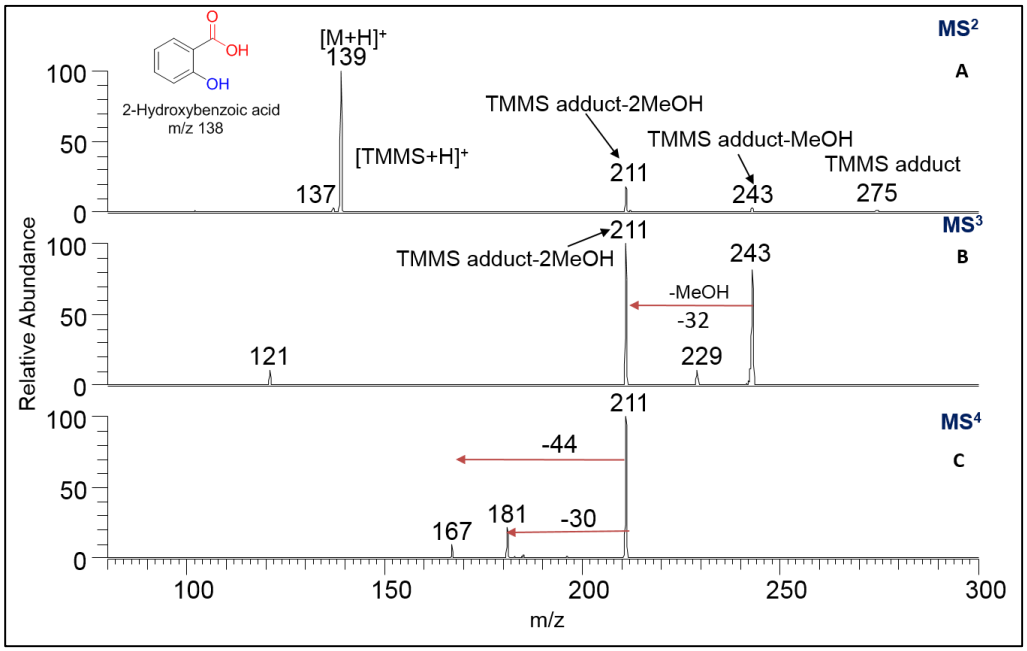

Figure 7.4. The mass spectrum of protonated 2-hydroxybenzoic acid measured after 300 ms of reaction with TMMS (A).Spontaneous formation of TMMS adduct (m/z 275), adduct-MeOH (m/z 243) and adduct-2MeOH (m/z 211) is observed. MS3 spectrum measured after collision activated dissociation (CAD) of TMMS adduct-MeOH (B). The fragment ion (m/z 211) corresponds to TMMS adduct-2MeOH. MS4 spectra measured after CAD of TMMS adduct-2MeOH. The most abundant fragment ion corresponds to the loss of MW 30Da (formaldehyde loss). The other fragment ion corresponds to a neutral loss of MW 44Da (CO2 loss).

The reason for the formation of these products is attributed to the availability of acidic hydrogen in close proximity to the carboxylic acid functionality. The possible mechanism supporting these losses are explored computationally. Figure 7.5A shows the potential energy surface for the exothermic proton transfer and the formation of adduct

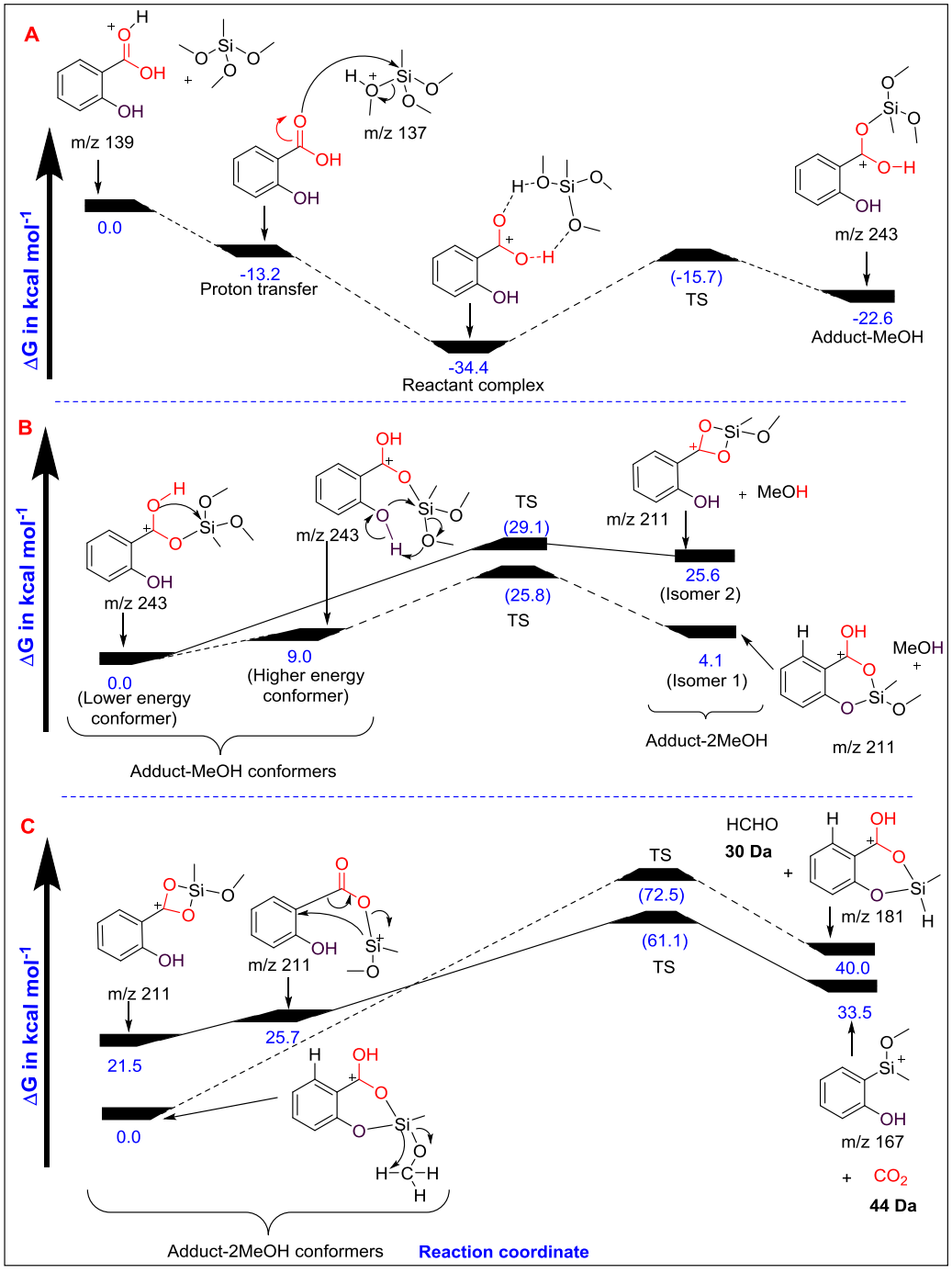

Figure 7.5. Proposed reaction pathway and potential energy surface for the formation of different reaction products and fragments formed upon reaction of 2-hydroxybenzoic acid with TMMS reagent, calculated with the M06-2X/6-311++G(d,p) level of theory for A) spontaneous proton transfer and formation of TMMS adduct-MeOH, B) formation of adduct-2MeOH upon isolation and CAD of adduct-MeOH, and C) characteristic losses of MW of 44 Da (solid line) and 30 Da (dashed line) observed upon CAD of adduct-2MeOH.

-MeOH product formed upon reaction of TMMS with 2-hydroxybenzoic acid. Figure 7.5B shows the potential energy surface for the formation of adduct-2MeOH product (m/z 211) upon CAD of adduct-MeOH (m/z 243). Adduct-MeOH product ion (m/z 243) occurs in two different conformations. Each conformer follows a different pathway for fragmentation to form adduct-2MeOH product. In both pathways, hydrogen from a hydroxyl group is transferred to a methoxy group, which is eliminated as methanol. In the first conformation for the ion m/z 243, the silicon is in close proximity (1.84 A^o) to the phenolic group. Upon CAD, a simultaneous MeOH loss and formation of an adduct -2MeOH product ion (isomer 1) with a six-membered cyclic ring structure was observed as shown in Figure 7.5B (dashed line).This pathway is endergonic by 4.1 kcal/mol and must overcome a barrier of 25.8 kcal/mol relative to adduct-MeOH (lower energy conformer).In the second conformation for ion m/z 243, the silicon is closer to the benzylic hydroxyl group (3.1 A^o) and far away from the phenolic group (4.1 A^o). Upon CAD, a simultaneous methanol loss and formation of an adduct-2MeOH product ion (isomer 2) with a four membered ring structure was observed as shown in Figure 7.5B (solid line). This is similar to the mechanism proposed for benzoic acid and the pathway is endergonic by 25.6 kcal/mol and must overcome a barrier of 29.1 kcal/mol relative to adduct-MeOH (lower energy conformer). Figure 7.5C shows the potential energy surface that shows the energy required for losses of neutral molecules of MW of 30 Da and 44 Da upon CAD of adduct-2MeOH (m/z 211). The formaldehyde loss occurs from adduct-2MeOH isomer 1 and the barrier for this transition is 61.1 kcal/mol. The CO_2 loss occurs from adduct-2MeOH isomer 2 in exactly the same manner as described for benzoic acid and the barrier for this transition is 72.5 kcal/mol. The barrier for CO_2 loss relative to

isomer 2 with m/z 211 is 40.4 kcal/mol while the barrier for formaldehyde loss relative to isomer 1 with m/z 211 is 72.5 kcal/mol (see Figure 7.5C). Although the barrier for CO_2 loss is lower than the barrier for formaldehyde loss, the relative abundance of the product ion corresponding to formaldehyde loss is higher in the MS^4 spectrum. This is due to the relative proportion of isomer 1 to isomer 2 of m/z 211 formed after the initial CAD of adduct-MeOH. Formation of isomer 1 is more energetically favorable than formation of isomer 2. The Gibb's free energy barrier for the reaction producing isomer 1 is 3.3 kcal/mol lower in energy relative to the barrier for the reaction producing isomer 2. Loss of CO_2 is only possible with isomer 2.

7.3.2 Protonated sulfone model compounds

The mass spectra measured after reactions between TMMS and protonated sulfone-containing model compounds showed the dominant adduct-MeOH product. Further isolation and CAD of adduct-MeOH product produced diagnostic product ions of m/z 75, 105 and 123. Observation of these product ions indicates the possible presence of sulfone functionalities in the analyte of interest. The mass spectrum and the CAD spectrum corresponding to dimethyl sulfone is shown in

Figure 7.6.

Based on my calculations, the formation of the adduct-MeOH product is proposed to be initiated by proton transfer from the protonated analyte to the methoxy group in the neutral reagent (TMMS), followed by nucleophilic addition of sulfone to the electron deficient silicon (Figure 7.7A). Figure 7.7B shows the potential energy surface calculated for the spontaneous proton transfer and formation of adduct-MeOH elimination product (m/z 242) for dimethyl sulfone. The adduct-MeOH product is formed by the electrophilic

attack of carbonyl from the dimethyl sulfone to the silicone in the protonated TMMS reagent.

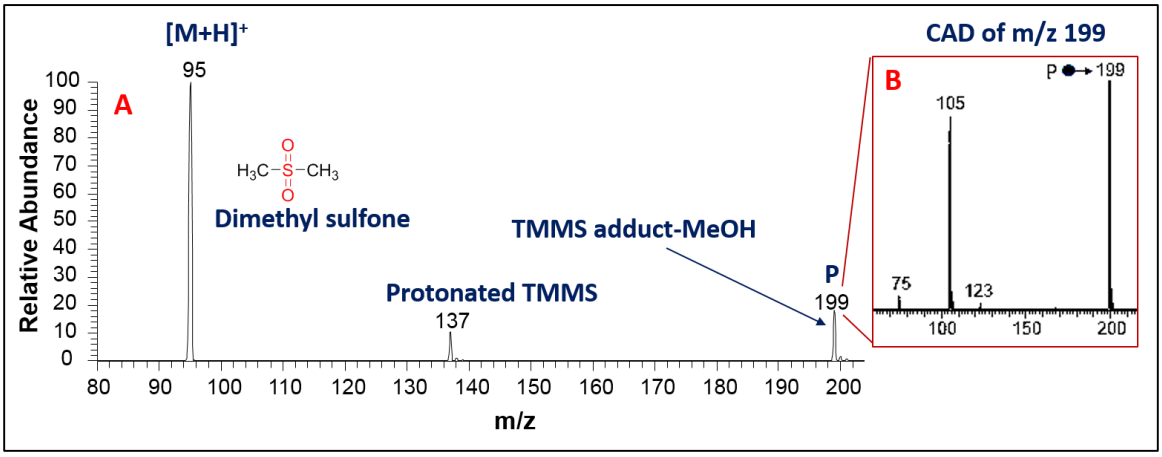

Figure 7.6. The mass spectrum of protonated dimethylsulfone (m/z 95) measured after 300 ms of reaction with TMMS (spectrum A). The most abundant product ion (m/z 199) corresponds to TMMS adduct-MeOH. The other product ion is the protonated TMMS reagent (m/z 137). MS3 spectrum measured after collision activated dissociation (CAD) of TMMS adduct-MeOH (spectrum B). The fragment ions of m/z 75, 105 and 123 are diagnostic to sulfone functionality.

As seen on the potential energy surface, both the proton transfer and adduct-MeOH elimination product (m/z 243) formation are exergonic relative to the reactant and are readily formed. No transition structure was found for the heterocyclic cleavage of the Si-O bond in the adduct-MeOH product. Hence, formation of the most abundant fragment ion m/z 105 is assumed to be a barrierless pathway.

7.4 Conclusions

When protonated aromatic carboxylic acid containing model compounds were allowed to react with TMMS, a characteristic adduct-MeOH product was formed. The mechanism for the formation of the adduct-MeOH product involved transfer of an acidic hydrogen from the analyte to a methoxy group in the TMMS. Isolation and CAD (MS^3)

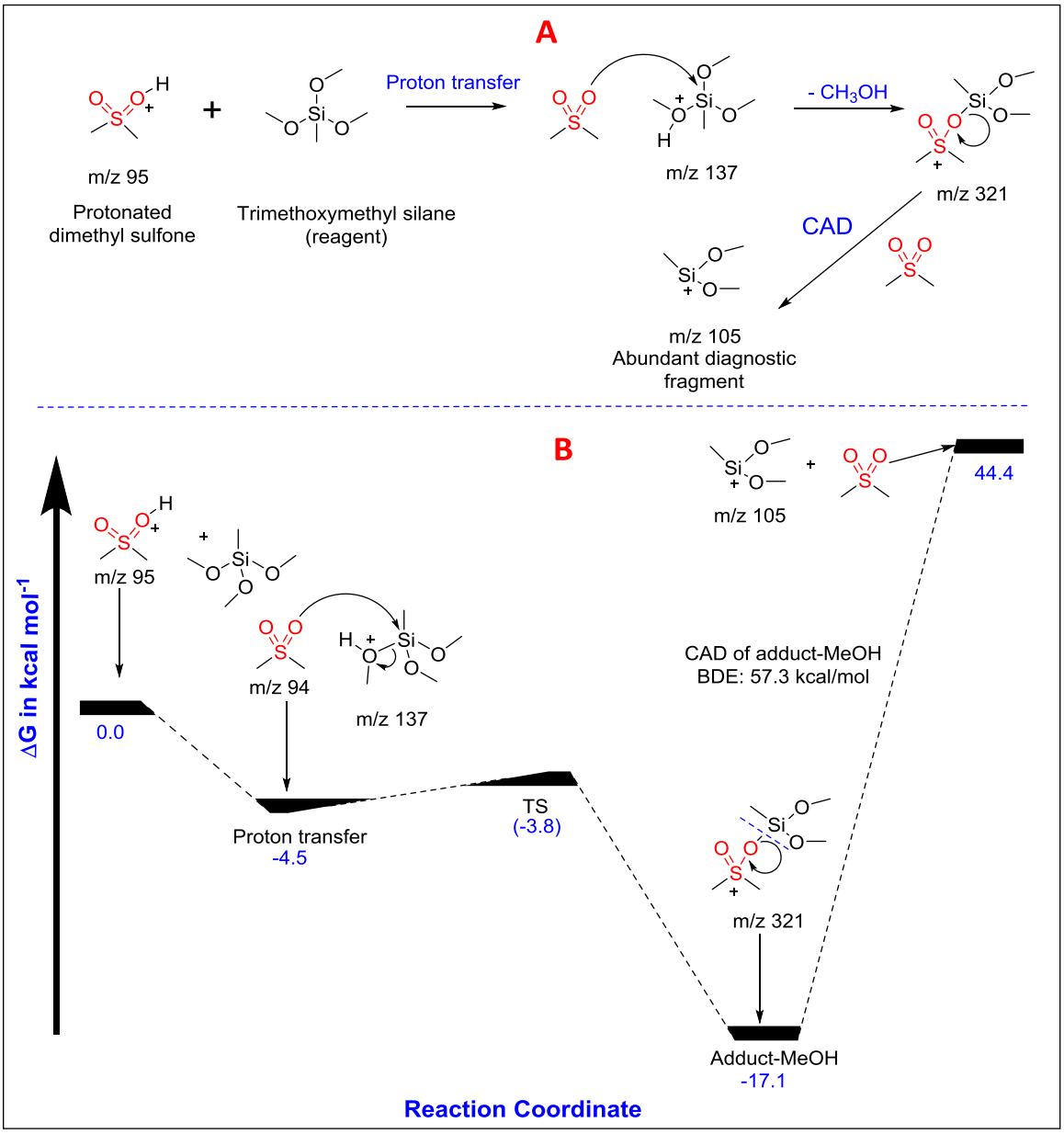

Figure 7.7. Proposed reaction mechanism (A) and calculated potential energy surface (B) (M06-2X/6-311++G(d,p) level of theory) for the spontaneous formation of TMMS adduct-MeOH and endergonic formation of abundant diagnostic fragment ion (m/z 105) upon CAD of the adduct-MeOH of protonated analytes containing sulfone functionality. The pathway for the formation of the fragment ion (m/z 105) is assumed to be a barrierless pathway (Gibbs free energy (ΔG) is reported in kcal/mol).

of the TMMS adduct-MeOH product of aromatic carboxylic acid model compounds produced a second methanol loss. Further CAD of TMMS adduct-2MeOH produced characteristic losses of MW 44 Da and 90 Da. These losses occur by a conformational change in the ion—an extended structure for loss of MW 90 Da and a folded structure for loss of CO_2. Since these conformers can exist in equilibrium and loss of CO_2 has a lower barrier height than loss of MW 90 Da for benzoic acid, the relative abundance of m/z 151 is greater than m/z 105. In the case of 2-hydroxy benzoic acid, loss of MW 90 Da does not occur. The hydroxyl group in the 2-hydroxy benzoic acid is able to bind to the silicon in TMMS to form a thermodynamically stable ion, which does not lose CO_2 or MW 90 Da upon CAD. A similar adduct-MeOH was produced upon reaction of dimethyl sulfone with TMMS. This was initiated by protonation of dimethyl sulfone followed by hydrogen transfer to TMMS

CHAPTER 8. SUMMARY

In addition to the conclusions provided in each chapter, this section will provide future plans on these research topics. A very important theory of cellulose depolymerization has been proposed in Chapter 5. It agrees with the experimental study on pyrolysis of ^{13}C-labeled cellobioses. The next step is to extend the proposed scheme to larger glucosaccharides. Synthesis of ^{13}C-labeled cellotriose is currently underway. Pyrolysis of this isotopically labeled compound will give further information regarding the efficacy of the hypothesized depolymerization. Computational restraints have mitigated the ability to do full geometry optimizations with cellotriose, but by making some compromises to computational accuracy, it may be possible to give a rough idea of the legitimacy of the model for compounds larger than cellobiose. This will be a good complement to the future experimental work.

Now that detailed elementary reaction steps have calculated barriers, it is possible to implement these values into rigorous kinetic models. A semi-batch reactor model developed by Dr. John Degenstein should be able to determine the predicted product distribution of pyrolysis based on these reaction networks. This model incorporates evaporation as a competitive process to the fragmentation reactions by applying Raoult's law between the liquid reaction phase and the gas-phase. It will be insightful to compare the predictions of this model to physical results.

In addition to the work on isolated cellulose, hemicelluloses, and lignins, it will soon become necessary to investigate the interactions between these constituents of biomass by covalent and non-covalent interactions. Covalent bonds between cellulose and other biopolymers may inhibit certain reaction pathways and open up other yet unknown pathways. Further computational and experimental investigations into branched lignins and hemicelluloses are key to bridging the gap between model compounds and native biomass.

REFERENCES

REFERENCES

(1) Service, R. F. Battle for the Barrel. *Science* **2013**, *339* (6126), 1374–1379.

(2) Agrawal, R.; Singh, N. R. Synergistic Routes to Liquid Fuel for a Petroleum-Deprived Future. *AIChE J.* **2009**, *55* (7), 1898–1905.

(3) Venkatakrishnan, V. K.; Degenstein, J. C.; Smeltz, A. D.; Delgass, W. N.; Agrawal, R.; Ribeiro, F. H. High-Pressure Fast-Pyrolysis, Fast-Hydropyrolysis and Catalytic Hydrodeoxygenation of Cellulose: Production of Liquid Fuel from Biomass. *Green Chem.* **2014**, *16* (2), 792–802.

(4) Brown, T. R.; Wright, M. M.; Brown, R. C. Estimating Profitability of Two Biochar Production Scenarios: Slow Pyrolysis vs Fast Pyrolysis. *Biofuels Bioprod. Biorefining* **2011**, *5* (1), 54–68.

(5) Mohan, D.; Pittman, Charles U.; Steele, P. H. Pyrolysis of Wood/Biomass for Bio-Oil: A Critical Review. *Energy Fuels* **2006**, *20* (3), 848–889.

(6) Patwardhan, P. R.; Satrio, J. A.; Brown, R. C.; Shanks, B. H. Product Distribution from Fast Pyrolysis of Glucose-Based Carbohydrates. *J. Anal. Appl. Pyrolysis* **2009**, *86* (2), 323–330.

(7) Mettler, M. S.; Vlachos, D. G.; Dauenhauer, P. J. Top Ten Fundamental Challenges of Biomass Pyrolysis for Biofuels. *Energy Environ. Sci.* **2012**, *5* (7), 7797–7809.

(8) Shafizadeh, F.; Fu, Y. L. Pyrolysis of Cellulose. *Carbohydr. Res.* **1973**, *29* (1), 113–122.

(9) Bradbury, A. G. W.; Sakai, Y.; Shafizadeh, F. A Kinetic Model for Pyrolysis of Cellulose. *J. Appl. Polym. Sci.* **1979**, *23* (11), 3271–3280.

(10) Broido, A.; Nelson, M. A. Char Yield on Pyrolysis of Cellulose. *Combust. Flame* **1975**, *24*, 263–268.

(11) Agrawal, R. K. Kinetics of Reactions Involved in Pyrolysis of Cellulose I. The Three Reaction Model. *Can. J. Chem. Eng.* **1988**, *66* (3), 403–412.

(12) Agrawal, R. K. Kinetics of Reactions Involved in Pvrolvsis of Cellulose II. The Modified Kilzer-Bioid Model. *Can. J. Chem. Eng.* **1988**, *66* (3), 413–418.

(13) Antal, M. J. J.; Varhegyi, G. Cellulose Pyrolysis Kinetics: The Current State of Knowledge. *Ind. Eng. Chem. Res.* **1995**, *34* (3), 703–717.

(14) Várhegyi, G.; Antal Jr., M. J.; Jakab, E.; Szabó, P. Kinetic Modeling of Biomass Pyrolysis. *J. Anal. Appl. Pyrolysis* **1997**, *42* (1), 73–87.

(15) Vinu, R.; Broadbelt, L. J. A Mechanistic Model of Fast Pyrolysis of Glucose-Based Carbohydrates to Predict Bio-Oil Composition. *Energy Environ. Sci.* **2012**, *5* (12), 9808–9826.

(16) Zhou, X.; Nolte, M. W.; Mayes, H. B.; Shanks, B. H.; Broadbelt, L. J. Experimental and Mechanistic Modeling of Fast Pyrolysis of Neat Glucose-Based Carbohydrates. 1. Experiments and Development of a Detailed Mechanistic Model. *Ind. Eng. Chem. Res.* **2014**, *53* (34), 13274–13289.

(17) Zhou, X.; Nolte, M. W.; Shanks, B. H.; Broadbelt, L. J. Experimental and Mechanistic Modeling of Fast Pyrolysis of Neat Glucose-Based Carbohydrates. 2. Validation and Evaluation of the Mechanistic Model. *Ind. Eng. Chem. Res.* **2014**, *53* (34), 13290–13301.

(18) Helle, S.; Bennett, N. M.; Lau, K.; Matsui, J. H.; Duff, S. J. B. A Kinetic Model for Production of Glucose by Hydrolysis of Levoglucosan and Cellobiosan from Pyrolysis Oil. *Carbohydr. Res.* **2007**, *342* (16), 2365–2370.

(19) Becke, A. D. Perspective: Fifty Years of Density-Functional Theory in Chemical Physics. *J. Chem. Phys.* **2014**, *140* (18), 18A301.

(20) Mettler, M. S.; Paulsen, A. D.; Vlachos, D. G.; Dauenhauer, P. J. The Chain Length Effect in Pyrolysis: Bridging the Gap between Glucose and Cellulose. *Green Chem.* **2012**, *14* (5), 1284–1288.

(21) Degenstein, J. C.; Hurt, M.; Murria, P.; Easton, M.; Choudhari, H.; Yang, L.; Riedeman, J.; Carlsen, M. S.; Nash, J. J.; Agrawal, R.; et al. Mass Spectrometric Studies of Fast Pyrolysis of Cellulose. *Eur. J. Mass Spectrom.* **2015**, *21* (3), 321–326.

(22) Shen, D.; Xiao, R.; Gu, S.; Luo, K. The Pyrolytic Behavior of Cellulose in Lignocellulosic Biomass: A Review. *RSC Adv.* **2011**, *1* (9), 1641–1660.

(23) Patwardhan, P. R.; Dalluge, D. L.; Shanks, B. H.; Brown, R. C. Distinguishing Primary and Secondary Reactions of Cellulose Pyrolysis. *Bioresour. Technol.* **2011**, *102* (8), 5265–5269.

(24) Huber, G. W.; Iborra, S.; Corma, A. Synthesis of Transportation Fuels from Biomass: Chemistry, Catalysts, and Engineering. *Chem. Rev.* **2006**, *106* (9), 4044–4098.

(25) Mayes, H. B.; Broadbelt, L. J. Unraveling the Reactions That Unravel Cellulose. *J. Phys. Chem. A* **2012**, *116* (26), 7098–7106.

(26) Mettler, M. S.; Mushrif, S. H.; Paulsen, A. D.; Javadekar, A. D.; Vlachos, D. G.; Dauenhauer, P. J. Revealing Pyrolysis Chemistry for Biofuels Production: Conversion of Cellulose to Furans and Small Oxygenates. *Energy Environ. Sci.* **2012**, *5* (1), 5414–5424.

(27) Agarwal, V.; Dauenhauer, P. J.; Huber, G. W.; Auerbach, S. M. Ab Initio Dynamics of Cellulose Pyrolysis: Nascent Decomposition Pathways at 327 and 600 °C. *J. Am. Chem. Soc.* **2012**, *134* (36), 14958–14972.

(28) Piskorz, J.; Majerski, P.; Radlein, D.; Vladars-Usas, A.; Scott, D. S. Flash Pyrolysis of Cellulose for Production of Anhydro-Oligomers. *J. Anal. Appl. Pyrolysis* **2000**, *56* (2), 145–166.

(29) Hurt, M. R.; Degenstein, J. C.; Gawecki, P.; Borton II, D. J.; Vinueza, N. R.; Yang, L.; Agrawal, R.; Delgass, W. N.; Ribeiro, F. H.; Kenttämaa, H. I. On-Line Mass Spectrometric Methods for the Determination of the Primary Products of Fast Pyrolysis of Carbohydrates and for Their Gas-Phase Manipulation. *Anal. Chem.* **2013**, *85* (22), 10927–10934.

(30) Degenstein, J. C.; Murria, P.; Easton, M.; Sheng, H.; Hurt, M.; Dow, A. R.; Gao, J.; Nash, J. J.; Agrawal, R.; Delgass, W. N.; Ribeiro, F. H.; Kenttämaa, H.I. Fast Pyrolysis of 13C-Labeled Cellobioses: Gaining Insights into the Mechanisms of Fast Pyrolysis of Carbohydrates. *J. Org. Chem.* **2015**, *80* (3), 1909–1914.

(31) Lu, Q.; Yang, X.; Dong, C.; Zhang, Z.; Zhang, X.; Zhu, X. Influence of Pyrolysis Temperature and Time on the Cellulose Fast Pyrolysis Products: Analytical Py-GC/MS Study. *J. Anal. Appl. Pyrolysis* **2011**, *92* (2), 430–438.

(32) Yoneda, Y.; Kawada, T.; Rosenau, T.; Kosma, P. Synthesis of Methyl 4′-O-Methyl-13C12-β-D-Cellobioside from 13C6-D-Glucose. Part 1: Reaction Optimization and Synthesis. *Carbohydr. Res.* **2005**, *340* (15), 2428–2435.

(33) Zheng, S.; Laraia, L.; Connor, C. J. O.; Sorrell, D.; Tan, Y. S.; Xu, Z.; Venkitaraman, A. R.; Wu, W.; Spring, D. R. Synthesis and Biological Profiling of Tellimagrandin I and Analogues Reveals That the Medium Ring Can Significantly Modulate Biological Activity. *Org. Biomol. Chem.* **2012**, *10* (13), 2590–2593.

(34) Gaussian 09, Revision A.02, M. J. Frisch, G. W. Trucks, H. B. Schlegel, G. E. Scuseria, M. A. Robb, J. R. Cheeseman, G. Scalmani, V. Barone, B. Mennucci, G. A. Petersson, H. Nakatsuji, M. Caricato, X. Li, H. P. Hratchian, A. F. Izmaylov, J. Bloino, G. Zheng, J. L. Sonnenberg, M. Hada, M. Ehara, K. Toyota, R. Fukuda, J. Hasegawa, M. Ishida, T. Nakajima, Y. Honda, O. Kitao, H. Nakai, T. Vreven, J. A. Montgomery, Jr., J. E. Peralta, F. Ogliaro, M. Bearpark, J. J. Heyd, E. Brothers, K. N. Kudin, V. N. Staroverov, R. Kobayashi, J. Normand, K. Raghavachari, A. Rendell, J. C. Burant, S. S. Iyengar, J. Tomasi, M. Cossi, N. Rega, J. M. Millam, M. Klene, J. E. Knox, J. B. Cross, V. Bakken, C. Adamo, J. Jaramillo, R. Gomperts, R. E. Stratmann, O. Yazyev, A. J. Austin, R. Cammi, C. Pomelli, J. W. Ochterski, R. L. Martin, K. Morokuma, V. G. Zakrzewski, G. A. Voth, P. Salvador, J. J. Dannenberg, S. Dapprich, A. D. Daniels, O. Farkas, J. B. Foresman, J. V. Ortiz, J. Cioslowski, and D. J. Fox, Gaussian, Inc., Wallingford CT, 2009.

(35) Zhao, Y.; Truhlar, D. G. The M06 Suite of Density Functionals for Main Group Thermochemistry, Thermochemical Kinetics, Noncovalent Interactions, Excited States, and Transition Elements: Two New Functionals and Systematic Testing of Four M06-Class Functionals and 12 Other Functionals. *Theor. Chem. Acc.* **2008**, *120* (1–3), 215–241.

(36) Krishnan, R.; Binkley, J. S.; Seeger, R.; Pople, J. A. Self-consistent Molecular Orbital Methods. XX. A Basis Set for Correlated Wave Functions. *J. Chem. Phys.* **1980**, *72* (1), 650–654.

(37) Mayes, H. B.; Nolte, M. W.; Beckham, G. T.; Shanks, B. H.; Broadbelt, L. J. The Alpha–Bet(a) of Glucose Pyrolysis: Computational and Experimental Investigations of 5-Hydroxymethylfurfural and Levoglucosan Formation Reveal Implications for Cellulose Pyrolysis. *ACS Sustain. Chem. Eng.* **2014**, *2* (6), 1461–1473.

(38) Seshadri, V.; Westmoreland, P. R. Concerted Reactions and Mechanism of Glucose Pyrolysis and Implications for Cellulose Kinetics. *J. Phys. Chem. A* **2012**, *116* (49), 11997–12013.

(39) Paine III, J. B.; Pithawalla, Y. B.; Naworal, J. D. Carbohydrate Pyrolysis Mechanisms from Isotopic Labeling: Part 2. The Pyrolysis of D-Glucose: General Disconnective Analysis and the Formation of C1 and C2 Carbonyl Compounds by Electrocyclic Fragmentation Mechanisms. *J. Anal. Appl. Pyrolysis* **2008**, *82* (1), 10–41.

(40) Hosoya, T.; Nakao, Y.; Sato, H.; Kawamoto, H.; Sakaki, S. Thermal Degradation of Methyl β-D-Glucoside. A Theoretical Study of Plausible Reaction Mechanisms. *J. Org. Chem.* **2009**, *74* (17), 6891–6894.

(41) Zhou, X.; Nolte, M. W.; Mayes, H. B.; Shanks, B. H.; Broadbelt, L. J. Experimental and Mechanistic Modeling of Fast Pyrolysis of Neat Glucose-Based Carbohydrates. 1. Experiments and Development of a Detailed Mechanistic Model. *Ind. Eng. Chem. Res.* **2014**, *53* (34), 13274–13289.

(42) Parsell, T.; Yohe, S.; Degenstein, J.; Jarrell, T.; Klein, I.; Gencer, E.; Hewetson, B.; Hurt, M.; Kim, J. I.; Choudhari, H.; et al. A Synergistic Biorefinery Based on Catalytic Conversion of Lignin prior to Cellulose Starting from Lignocellulosic Biomass. *Green Chem.* **2015**, *17* (3), 1492–1499.

(43) Mettler, M. S.; Paulsen, A. D.; Vlachos, D. G.; Dauenhauer, P. J. Pyrolytic Conversion of Cellulose to Fuels: Levoglucosan Deoxygenation via Elimination and Cyclization within Molten Biomass. *Energy Environ. Sci.* **2012**, *5* (7), 7864–7868.

(44) Liang, X.; Montoya, A.; Haynes, B. S. Local Site Selectivity and Conformational Structures in the Glycosidic Bond Scission of Cellobiose. *J. Phys. Chem. B* **2011**, *115* (36), 10682–10691.

(45) Wang, S.; Guo, X.; Liang, T.; Zhou, Y.; Luo, Z. Mechanism Research on Cellulose Pyrolysis by Py-GC/MS and Subsequent Density Functional Theory Studies. *Bioresour. Technol.* **2012**, *104*, 722–728.

(46) Lin, X.; Qu, Y.; Lv, Y.; Xi, Y.; Phillips, D. L.; Liu, C. The First Dehydration and the Competing Reaction Pathways of Glucose Homogeneously and Heterogeneously Catalyzed by Acids. *Phys. Chem. Chem. Phys.* **2013**, *15* (8), 2967–2982.

(47) Nimlos, M. R.; Blanksby, S. J.; Ellison, G. B.; Evans, R. J. Enhancement of 1,2-Dehydration of Alcohols by Alkali Cations and Protons: A Model for Dehydration of Carbohydrates. *J. Anal. Appl. Pyrolysis* **2003**, *66* (1–2), 3–27.

(48) Matsuoka, S.; Kawamoto, H.; Saka, S. Retro-Aldol-Type Fragmentation of Reducing Sugars Preferentially Occurring in Polyether at High Temperature: Role of the Ether Oxygen as a Base Catalyst. *J. Anal. Appl. Pyrolysis* **2012**, *93*, 24–32.

(49) Zhang, M.; Geng, Z.; Yu, Y. Density Functional Theory (DFT) Study on the Pyrolysis of Cellulose: The Pyran Ring Breaking Mechanism. *Comput. Theor. Chem.* **2015**, *1067*, 13–23.

(50) Assary, R. S.; Curtiss, L. A. Thermochemistry and Reaction Barriers for the Formation of Levoglucosenone from Cellobiose. *ChemCatChem* **2012**, *4* (2), 200–205.

(51) Zhang, Y.; Liu, C.; Chen, X. Unveiling the Initial Pyrolytic Mechanisms of Cellulose by DFT Study. *J. Anal. Appl. Pyrolysis* **2015**, *113*, 621–629.

(52) Maccoll, A. Heterolysis and Pyrolysis of Alkyl Halides in Gas Phase. *Chem. Rev.* **1969**, *69* (1), 33–60.
(53) Collins, C. J. The Pinacol Rearrangement. *Q. Rev. Chem. Soc.* **1960**, *14* (4), 357–377.
(54) *Schrödinger Release 2014-1: MacroModel, Version 10.3, Schrödinger, LLC, New York, NY, 2014.*
(55) Chang, G.; Guida, W. C.; Still, W. C. An Internal-Coordinate Monte Carlo Method for Searching Conformational Space. *J. Am. Chem. Soc.* **1989**, *111* (12), 4379–4386.
(56) Halgren, T. A. MMFF VI. MMFF94s Option for Energy Minimization Studies. *J. Comput. Chem.* **1999**, *20* (7), 720–729.
(57) Jacobson, R. A.; Wunderlich, J. A.; Lipscomb, W. N. The Crystal and Molecular Structure of Cellobiose. *Acta Crystallogr.* **1961**, *14* (6), 598–607.
(58) Nishiyama, Y.; Langan, P.; Chanzy, H. Crystal Structure and Hydrogen-Bonding System in Cellulose 1 Beta from Synchrotron X-Ray and Neutron Fiber Diffraction. *J. Am. Chem. Soc.* **2002**, *124* (31), 9074–9082.
(59) Schnupf, U.; Momany, F. A. Rapidly Calculated DFT Relaxed Iso-Potential Φ/ψ Maps: β-Cellobiose. *Cellulose* **2011**, *18* (4), 859–887.
(60) Dauenhauer, P. J.; Colby, J. L.; Balonek, C. M.; Suszynski, W. J.; Schmidt, L. D. Reactive Boiling of Cellulose for Integrated Catalysis through an Intermediate Liquid. *Green Chem.* **2009**, *11* (10), 1555–1561.
(61) Teixeira, A. R.; Mooney, K. G.; Kruger, J. S.; Williams, C. L.; Suszynski, W. J.; Schmidt, L. D.; Schmidt, D. P.; Dauenhauer, P. J. Aerosol Generation by Reactive Boiling Ejection of Molten Cellulose. *Energy Environ. Sci.* **2011**, *4* (10), 4306–4321.
(62) French, A. D.; Johnson, G. P.; Cramer, C. J.; Csonka, G. I. Conformational Analysis of Cellobiose by Electronic Structure Theories. *Carbohydr. Res.* **2012**, *350*, 68–76.
(63) Hosoya, T.; Sakaki, S. Levoglucosan Formation from Crystalline Cellulose: Importance of a Hydrogen Bonding Network in the Reaction. *ChemSusChem* **2013**, *6* (12), 2356–2368.
(64) Becke, A. D. Density-Functional Thermochemistry. III. The Role of Exact Exchange. *J. Chem. Phys.* **1993**, *98* (7), 5648.
(65) Lee, C.; Yang, W.; Parr, R. G. Development of the Colle-Salvetti Correlation-Energy Formula into a Functional of the Electron Density. *Phys. Rev. B* **1988**, *37* (2), 785–789.
(66) Vosko, S. H.; Wilk, L.; Nusair, M. Accurate Spin-Dependent Electron Liquid Correlation Energies for Local Spin Density Calculations: A Critical Analysis. *Can. J. Phys.* **1980**, *58* (8), 1200–1211.
(67) Stephens, P. J.; Devlin, F. J.; Chabalowski, C. F.; Frisch, M. J. Ab Initio Calculation of Vibrational Absorption and Circular Dichroism Spectra Using Density Functional Force Fields. *J. Phys. Chem.* **1994**, *98* (45), 11623–11627.
(68) Sládkovičová, M.; Mach, P.; Smrčok, L.; Rundlöf, H. DFT and Neutron Diffraction Study of 1,6-Anhydro-β-D-Glucopyranose (Levoglucosan). *Cent. Eur. J. Chem.* **2007**, *5* (1), 55–70.

(69) Lynch, B. J.; Truhlar, D. G. How Well Can Hybrid Density Functional Methods Predict Transition State Geometries and Barrier Heights? *J. Phys. Chem. A* **2001**, *105* (13), 2936–2941.
(70) Zhao, Y.; González-García, N.; Truhlar, D. G. Benchmark Database of Barrier Heights for Heavy Atom Transfer, Nucleophilic Substitution, Association, and Unimolecular Reactions and Its Use to Test Theoretical Methods. *J. Phys. Chem. A* **2005**, *109* (9), 2012–2018.
(71) Strati, G. L.; Willett, J. L.; Momany, F. A. A DFT/ab Initio Study of Hydrogen Bonding and Conformational Preference in Model Cellobiose Analogs Using B3LYP/6-311++G**. *Carbohydr. Res.* **2002**, *337* (20), 1851–1859.
(72) Jarvis, M. W.; Daily, J. W.; Carstensen, H.-H.; Dean, A. M.; Sharma, S.; Dayton, D. C.; Robichaud, D. J.; Nimlos, M. R. Direct Detection of Products from the Pyrolysis of 2-Phenethyl Phenyl Ether. *J. Phys. Chem. A* **2011**, *115* (4), 428–438.
(73) Mayes, H. B.; Broadbelt, L. J.; Beckham, G. T. How Sugars Pucker: Electronic Structure Calculations Map the Kinetic Landscape of Five Biologically Paramount Monosaccharides and Their Implications for Enzymatic Catalysis. *J. Am. Chem. Soc.* **2014**, *136* (3), 1008–1022.
(74) Stubbs, J. M.; Marx, D. Aspects of Glycosidic Bond Formation in Aqueous Solution: Chemical Bonding and the Role of Water. *Chem.- Eur. J.* **2005**, *11* (9), 2651–2659.
(75) Richards, G. N. Glycolaldehyde from Pyrolysis of Cellulose. *J. Anal. Appl. Pyrolysis* **1987**, *10* (3), 251–255.
(76) Zhang, X.; Yang, W.; Dong, C. Levoglucosan Formation Mechanisms during Cellulose Pyrolysis. *J. Anal. Appl. Pyrolysis* **2013**, *104*, 19–27.
(77) Shen, D. K.; Gu, S. The Mechanism for Thermal Decomposition of Cellulose and Its Main Products. *Bioresour. Technol.* **2009**, *100* (24), 6496–6504.
(78) Zhang, X.; Yang, W.; Blasiak, W. Kinetics of Levoglucosan and Formaldehyde Formation during Cellulose Pyrolysis Process. *Fuel* **2012**, *96*, 383–391.
(79) Sullivan, A. L.; Ball, R. Thermal Decomposition and Combustion Chemistry of Cellulosic Biomass. *Atmos. Environ.* **2012**, *47*, 133–141.
(80) Lin, Y.-C.; Cho, J.; Tompsett, G. A.; Westmoreland, P. R.; Huber, G. W. Kinetics and Mechanism of Cellulose Pyrolysis. *J. Phys. Chem. C* **2009**, *113* (46), 20097–20107.
(81) Evans, R. J.; Milne, T. A. Molecular Characterization of the Pyrolysis of Biomass. *Energy Fuels* **1987**, *1* (2), 123–137.
(82) Zhang, X.; Li, J.; Yang, W.; Blasiak, W. Formation Mechanism of Levoglucosan and Formaldehyde during Cellulose Pyrolysis. *Energy Fuels* **2011**, *25* (8), 3739–3746.
(83) Jae, J.; Tompsett, G. A.; Lin, Y.-C.; Carlson, T. R.; Shen, J.; Zhang, T.; Yang, B.; Wyman, C. E.; Conner, W. C.; Huber, G. W. Depolymerization of Lignocellulosic Biomass to Fuel Precursors: Maximizing Carbon Efficiency by Combining Hydrolysis with Pyrolysis. *Energy Environ. Sci.* **2010**, *3* (3), 358–365.
(84) Patwardhan, P. R.; Brown, R. C.; Shanks, B. H. Product Distribution from the Fast Pyrolysis of Hemicellulose. *ChemSusChem* **2011**, *4* (5), 636–643.

(85) Belkacemi, K.; Abatzoglou, N.; Overend, R. P.; Chornet, E. Phenomenological Kinetics of Complex Systems: Mechanistic Considerations in the Solubilization of Hemicelluloses Following Aqueous/steam Treatments. *Ind. Eng. Chem. Res.* **1991**, *30* (11), 2416–2425.

(86) Wang, S.; Ru, B.; Lin, H.; Sun, W.; Yu, C.; Luo, Z. Pyrolysis Mechanism of Hemicellulose Monosaccharides in Different Catalytic Processes. *Chem. Res. Chin. Univ.* **2014**, *30* (5), 848–854.

(87) Bauer, W. D.; Talmadge, K. W.; Keegstra, K.; Albersheim, P. The Structure of Plant Cell Walls II. The Hemicellulose of the Walls of Suspension-Cultured Sycamore Cells. *Plant Physiol.* **1973**, *51* (1), 174–187.

(88) Appendix: Drug Metabolizing Enzymes and Biotransformation Reactions. In *ADME-Enabling Technologies in Drug Design and Development*; Zhang, D., Surapaneni, S., Eds.; John Wiley & Sons, Inc., 2012; pp 545–565.

(89) Zuniga, F. I.; Loi, D.; Ling, K. H. J.; Tang-Liu, D. D.-S. Idiosyncratic Reactions and Metabolism of Sulfur-Containing Drugs. *Expert Opin. Drug Metab. Toxicol.* **2012**, *8* (4), 467–485.

(90) Caslavska, J.; Thormann, W. Stereoselective Determination of Drugs and Metabolites in Body Fluids, Tissues and Microsomal Preparations by Capillary Electrophoresis (2000–2010). *J. Chromatogr. A* **2011**, *1218* (4), 588–601.

(91) Bhave, D. P.; Muse, W. B.; Carroll, K. S. Drug Targets in Mycobacterial Sulfur Metabolism. *Infect. Disord. Drug Targets* **2007**, *7* (2), 140–158.

(92) Dibbern Jr, D. A.; Montanaro, A. Allergies to Sulfonamide Antibiotics and Sulfur-Containing Drugs. *Ann. Allergy. Asthma. Immunol.* **2008**, *100* (2), 91–101.

(93) Eismin, R.; Fu, M.; Yem, S.; Widjaja, F.; Kenttämaa, H. Identification of Epoxide Functionalities in Protonated Monofunctional Analytes by Using Ion/Molecule Reactions and Collision-Activated Dissociation in Different Ion Trap Tandem Mass Spectrometers. *J. Am. Soc. Mass Spectrom.* **2012**, *23* (1), 12–22.

(94) Sheng, H.; Williams, P. E.; Tang, W.; Riedeman, J. S.; Zhang, M.; Kenttämaa, H. I. Identification of the Sulfone Functionality in Protonated Analytes via Ion/Molecule Reactions in a Linear Quadrupole Ion Trap Mass Spectrometer. *J. Org. Chem.* **2014**, *79* (7), 2883–2889.

(95) Campbell, K. M.; Watkins, M. A.; Li, S.; Fiddler, M. N.; Winger, B.; Kenttämaa, H. I. Functional Group Selective Ion/Molecule Reactions: Mass Spectrometric Identification of the Amido Functionality in Protonated Monofunctional Compounds. *J. Org. Chem.* **2007**, *72* (9), 3159–3165.

(96) Fu, M.; Eismin, R. J.; Duan, P.; Li, S.; Kenttämaa, H. I. Ion–molecule Reactions Facilitate the Identification and Differentiation of Primary, Secondary and Tertiary Amino Functionalities in Protonated Monofunctional Analytes in Mass Spectrometry. *Int. J. Mass Spectrom.* **2009**, *282* (3), 77–84.

(97) Somuramasami, J.; Winger, B. E.; Gillespie, T. A.; Kenttämaa, H. I. Identification and Counting of Carbonyl and Hydroxyl Functionalities in Protonated Bifunctional Analytes by Using Solution Derivatization prior to Mass Spectrometric Analysis via Ion-Molecule Reactions. *J. Am. Soc. Mass Spectrom.* **2009**, *21* (5), 773–784.

(98) Watkins, M. A.; Winger, B. E.; Shea, R. C.; Kenttämaa, H. I. Ion−Molecule Reactions for the Characterization of Polyols and Polyol Mixtures by ESI/FT-ICR Mass Spectrometry. *Anal. Chem.* **2005**, *77* (5), 1385–1392.

(99) Sheng, H.; Tang, W.; Yerabolu, R.; Kong, J. Y.; Williams, P. E.; Zhang, M.; Kenttämaa, H. I. Mass Spectrometric Identification of the N-Monosubstituted N-Hydroxylamino Functionality in Protonated Analytes via Ion/molecule Reactions in Tandem Mass Spectrometry. *Rapid Commun. Mass Spectrom.* **2015**, *29* (8), 730–734.

(100) Sheng, H.; Tang, W.; Yerabolu, R.; Max, J.; Kotha, R. R.; Riedeman, J. S.; Nash, J. J.; Zhang, M.; Kenttamaa, H. I. Identification of N-Oxide and Sulfoxide Functionalities in Protonated Drug Metabolites by Using Ion-Molecule Reactions Followed by Collisionally Activated Dissociation in a Linear Quadrupole Ion Trap Mass Spectrometer. *J. Org. Chem.* **2015**.

(101) Oliw, E. H.; Garscha, U.; Nilsson, T.; Cristea, M. Payne Rearrangement during Analysis of Epoxyalcohols of Linoleic and Alpha-Linolenic Acids by Normal Phase Liquid Chromatography with Tandem Mass Spectrometry. *Anal. Biochem.* **2006**, *354* (1), 111–126.

(102) Sforza, S.; Galaverna, G.; Corradini, R.; Dossena, A.; Marchelli, R. ESI-Mass Spectrometry Analysis of Unsubstituted and Disubstituted β-Cyclodextrins: Fragmentation Mode and Identification of the AB, AC, AD Regioisomers. *J. Am. Soc. Mass Spectrom.* **2003**, *14* (2), 124–135.

(103) Eckers, C.; New, A. P.; East, P. B.; Haskins, N. J. The Use of Tandem Mass Spectrometry for the Differentiation of Bile Acid Isomers and for the Identification of Bile Acids in Biological Extracts. *Rapid Commun. Mass Spectrom.* **1990**, *4* (10), 449–453.

(104) Fu, M.; Duan, P.; Li, S.; Habicht, S. C.; Pinkston, D. S.; Vinueza, N. R.; Kenttamaa, H. I. Regioselective Ion-Molecule Reactions for the Mass Spectrometric Differentiation of Protonated Isomeric Aromatic Diamines. *Analyst* **2008**, *133* (4), 452–454.

(105) Bjarnason, A.; Taylor, J. W.; Kinsinger, J. A.; Cody, R. B.; Weil, D. A. Isomer Discrimination of Disubstituted Benzene Derivatives through Gas-Phase iron(I) Ion Reactions in a Fourier-Transform Mass Spectrometer. *Anal. Chem.* **1989**, *61* (17), 1889–1894.

(106) Gronert, S. Quadrupole Ion Trap Studies of Fundamental Organic Reactions. *Mass Spectrom. Rev.* **2005**, *24* (1), 100–120.

(107) Gronert, S. Estimation of Effective Ion Temperatures in a Quadrupole Ion Trap. *J. Am. Soc. Mass Spectrom.* **1998**, *9* (8), 845–848.

(108) Habicht, S. C.; Vinueza, N. R.; Amundson, L. M.; Kenttämaa, H. I. Comparison of Functional Group Selective Ion–Molecule Reactions of Trimethyl Borate in Different Ion Trap Mass Spectrometers. *J. Am. Soc. Mass Spectrom.* **2011**, *22* (3), 520–530.

(109) Watkins, M. A.; Price, J. M.; Winger, B. E.; Kenttamaa, H. I. Ion-Molecule Reactions for Mass Spectrometric Identification of Functional Groups in Protonated Oxygen-Containing Monofunctional Compounds. *Anal. Chem.* **2004**, *76* (4), 964–976.

(110) Tian, Z.; Kass, S. R. Gas-Phase versus Liquid-Phase Structures by Electrospray Ionization Mass Spectrometry. *Angew. Chem. Int. Ed.* **2009**, *48* (7), 1321–1323.

APPENDIX

APPENDIX

This appendix contains the Cartesian coordinates for the geometries of important structures found throughout this thesis.

Cellobiose (CB)		M06-2X/6-311++G(d,p)	
8	0.077485	0.712592	-0.70321
6	-2.64841	-1.13072	0.646615
6	-1.13804	0.549271	-0.04994
6	-2.21011	1.334906	-0.78722
1	-2.5564	-0.79845	1.691398
1	-1.06238	0.908345	0.993123
1	-2.24783	0.974248	-1.82271
6	2.228367	1.325541	0.054472
6	1.204944	0.185366	-0.0106
6	1.783399	-1.02455	-0.73581
6	3.169149	-1.35026	-0.19646
6	4.061943	-0.12443	-0.22543
1	0.916859	-0.12174	1.003228
1	1.873978	-0.76976	-1.80201
1	3.083813	-1.66595	0.852296
1	4.180468	0.24675	-1.25622
6	-3.54226	1.071234	-0.10178
1	-3.49062	1.476708	0.920171
6	-3.827	-0.42286	-0.01214
1	-3.94691	-0.81139	-1.03401
1	2.37026	1.725434	-0.96086
8	-1.98417	2.728903	-0.73604
1	-1.19144	2.927044	-1.24362
8	-4.61879	1.66152	-0.80056
1	-4.43231	2.601468	-0.89383
8	-4.98144	-0.6708	0.756537
1	-5.68876	-0.1227	0.400379
6	-2.71627	-2.64808	0.593962

1	-3.525	-3.00645	1.230884
1	-2.92372	-2.95032	-0.44176
8	-1.46456	-0.8067	-0.06829
8	-1.51015	-3.20721	1.055642
1	-0.79018	-2.79743	0.55289
8	0.94398	-2.1487	-0.57407
1	1.418065	-2.90298	-0.94361
8	3.677716	-2.39269	-1.00025
1	4.54115	-2.64406	-0.65739
8	5.281677	-0.49249	0.323612
1	5.899181	0.2414	0.25631
8	3.476958	0.8827	0.57042
6	1.772315	2.444851	0.973162
1	0.817724	2.841887	0.625175
1	1.635745	2.033256	1.982307
8	2.694465	3.50889	0.977659
1	3.544648	3.144923	1.243246
E(elec)	-1297.870416	au	
ZPVE	0.377474	au	
G correction (873K)	0.108463	au	

Open-chain cellobiose (CBOC)		M06-2X/6-311++G(d,p)	
8	-0.358339	0.949481	0.401284
6	2.429269	-0.884755	-0.848294
6	0.947773	0.781363	-0.055998
6	1.92704	1.285487	0.989557
1	2.549794	-0.317877	-1.783171
1	1.084194	1.327214	-1.00717
1	1.741291	0.737621	1.922142
6	-2.488614	1.309674	-0.591432
6	-1.315475	0.34227	-0.472673
6	-1.619686	-1.097323	0.000855
6	-2.957279	-1.312652	0.744058
6	-2.848067	-0.735267	2.13738
1	-0.883019	0.227576	-1.473353
1	-0.814266	-1.375017	0.689723
1	-3.76933	-0.82292	0.196228
1	-2.654577	0.347594	2.227221
6	3.338273	0.997335	0.499053
1	3.517576	1.59428	-0.408091
6	3.513635	-0.474287	0.141394

1	3.402176	-1.069696	1.059573
1	-2.933926	1.502004	0.396026
8	1.833263	2.681631	1.18764
1	0.988897	2.875573	1.604766
8	4.305773	1.308425	1.479645
1	4.190616	2.230636	1.730818
8	4.770027	-0.699401	-0.452839
1	5.437379	-0.313602	0.124868
6	2.380819	-2.366408	-1.169984
1	3.317991	-2.665567	-1.640008
1	2.267336	-2.924109	-0.230019
8	1.164975	-0.587477	-0.266576
8	1.338	-2.649444	-2.070279
1	0.496497	-2.358416	-1.688569
8	-1.563611	-1.935388	-1.134807
1	-2.009097	-2.760119	-0.900932
8	-3.207057	-2.694862	0.809847
1	-3.164283	-2.95703	1.74034
8	-2.934704	-1.433918	3.112598
1	-4.042159	1.420775	-1.722319
8	-3.437163	0.720092	-1.451804
6	-2.033049	2.645865	-1.157199
1	-1.340925	3.13539	-0.466827
1	-1.535525	2.473174	-2.119741
8	-3.220159	3.407009	-1.332521
1	-3.022529	4.215511	-1.809308
E(elec)	-1297.847934	au	
ZPVE	0.374172	au	
G correction (873K)	0.0934611	au	
β-D-glucopyranosylerythrose (GER)		M06-2X/6-311++G(d,p)	
8	0.933868	-0.35359	0.69923
6	-2.15668	0.961372	-0.51446
6	-0.27714	-0.37343	0.018306
6	-1.13417	-1.46991	0.632088
1	-2.0026	0.75715	-1.58371
1	-0.10742	-0.57294	-1.05407
1	-1.24295	-1.256	1.703134
6	3.247209	-0.17776	0.03098
6	1.90669	0.540097	0.179943
6	1.985695	1.731328	1.126689

1	1.600148	0.919433	-0.80607
1	1.020061	2.016968	1.582532
6	-2.49901	-1.45553	-0.03111
1	-2.37477	-1.70889	-1.09475
6	-3.11748	-0.07131	0.066456
1	-3.28886	0.157724	1.128618
1	3.596244	-0.50949	1.017479
8	-0.57958	-2.74882	0.417607
1	0.240699	-2.81683	0.915744
8	-3.39163	-2.35982	0.582419
1	-2.99408	-3.23645	0.557658
8	-4.32143	-0.00107	-0.66057
1	-4.86696	-0.74764	-0.38944
6	-2.6541	2.382347	-0.34675
1	-3.61081	2.485994	-0.85768
1	-2.8036	2.581529	0.722561
8	-0.90367	0.880326	0.171283
8	-1.76224	3.310661	-0.92161
1	-0.91353	3.207476	-0.4819
8	3.006902	2.310978	1.383291
1	4.366818	1.413492	0.035689
8	4.192228	0.685035	-0.57139
6	3.140474	-1.38064	-0.89203
1	2.442233	-2.11281	-0.48596
1	2.763833	-1.03845	-1.86703
8	4.388351	-2.01472	-1.02518
1	5.024286	-1.33154	-1.26412
E(elec)	-1068.7986478	au	
ZPVE	0.306383	au	
G correction (873K)	0.0618358	au	

β-D-glucopyranosylethenediol (GED)		M06-2X/6-311++G(d,p)	
8	1.565756	-1.32516	0.219848
6	-0.83384	1.277886	-0.254
6	0.404214	-0.72897	-0.26827
6	-0.77253	-1.5476	0.241636
1	-0.8335	1.285545	-1.35393
1	0.416344	-0.71773	-1.37183
1	-0.72069	-1.56297	1.338062
6	2.733062	-0.84061	-0.33999
6	3.643279	-0.25388	0.426582

1	2.856784	-1.01088	-1.40782
1	3.469649	-0.09975	1.483816
6	-2.06237	-0.8825	-0.19985
1	-2.11175	-0.91034	-1.29892
6	-2.08834	0.569989	0.247015
1	-2.09561	0.594994	1.346523
8	-0.77222	-2.85544	-0.28843
1	0.02813	-3.29942	0.009226
8	-3.19916	-1.51537	0.349904
1	-3.16521	-2.44741	0.110405
8	-3.21092	1.242352	-0.27549
1	-3.98685	0.707544	-0.07526
6	-0.70601	2.699951	0.253805
1	-1.54479	3.29234	-0.11071
1	-0.73461	2.685568	1.35146
8	0.319703	0.585041	0.219835
8	0.480338	3.297147	-0.21825
1	1.206452	2.713103	0.024896
8	4.858831	0.192117	0.021788
1	4.972227	0.038363	-0.92111
E(elec)	-839.7298893	au	
ZPVE	0.238092	au	
G correction (873K)	0.0312497	au	

Levoglucosan (LG)		M06-2X/6-311++G(d,p)	
8	-0.4145	0.107133	-1.54266
6	-0.6339	-1.0466	-0.7721
6	0.604516	-1.28379	0.101943
6	0.752736	-0.11066	1.089954
6	0.511578	1.238961	0.373295
6	-0.65708	1.159706	-0.60946
1	0.495037	-2.21069	0.670225
8	1.734745	-1.42791	-0.72162
8	-0.08437	-0.25135	2.220371
1	1.782762	-0.1188	1.459552
8	1.637729	1.591272	-0.41577
1	-0.84892	-1.88172	-1.43771
1	1.79991	-0.62896	-1.26179
1	-0.895	-0.69079	1.941003
1	2.402068	1.693555	0.158048
8	-1.7648	-0.75869	0.051814

6	-1.9502	0.664095	0.032959
1	-2.81507	0.908755	-0.58575
1	-0.75581	2.090814	-1.16498
1	0.299825	2.00092	1.133067
1	-2.10113	1.023004	1.051773
E(elec)	-610.7028323		au
ZPVE	0.175387		au
G correction (873K)	0.0272274		au
(Z)-ethenediol (EDL)		M06-2X/6-311++G(d,p)	
6	0.631355	0.641066	-0.00196
6	-0.6965	0.60802	0.008061
1	1.196763	1.562376	-0.02764
1	-1.2985	1.504857	-0.00125
1	2.122648	-0.50684	0.446057
8	1.315347	-0.55788	-0.06962
1	-0.79854	-1.27805	0.007812
8	-1.41929	-0.53922	0.011926
E(elec)	-229.0105521		au
ZPVE	0.062574		au
G correction (873K)	-0.0387194		au
(E)-ethenediol (EDL)		M06-2X/6-311++G(d,p)	
6	0.527559	0.387872	-0.00333
6	-0.54172	-0.39782	0.02475
1	0.453533	1.473294	-0.04075
1	-0.44849	-1.47577	0.048525
1	2.341949	0.20899	0.603933
8	1.790028	-0.15759	-0.09114
1	-1.8751	0.976899	-0.04422
8	-1.83839	0.017121	0.004142
E(elec)	-229.0020592		au
ZPVE	0.061863		au
G correction (873K)	-0.0399631		au
Glycolaldehyde (GA)		M06-2X/6-311++G(d,p)	
6	0.724135	-0.34761	0.123551
1	0.538733	-1.39905	0.425738
8	1.82504	0.054647	-0.12633
6	-0.51627	0.525276	0.073384
1	-0.55604	1.091056	1.008711
1	-0.41228	1.245124	-0.74497
8	-1.70113	-0.2331	0.00331

1	-1.8089	-0.57552	-0.88694
E(elec)	-229.0150888	au	
ZPVE	0.061539	au	
G correction (873K)	-0.0420198	au	
TS: CB→CBOC		M06-2X/6-311++G(d,p)	
8	0.085896	0.71332	-0.76986
6	-2.58829	-1.16123	0.646261
6	-1.10275	0.532625	-0.06949
6	-2.2015	1.343885	-0.73664
1	-2.45203	-0.85867	1.695345
1	-0.98102	0.864684	0.978479
1	-2.28319	1.018295	-1.78103
6	2.207896	1.420137	-0.10494
6	1.251847	0.223538	-0.12106
6	1.85767	-0.96704	-0.86166
6	3.115339	-1.4439	-0.13823
6	4.272911	-0.45344	-0.13171
1	1.000073	-0.10113	0.898159
1	2.112085	-0.65642	-1.88639
1	2.859369	-1.65952	0.907098
1	4.766049	-0.35223	-1.10718
6	-3.50589	1.061266	-0.00582
1	-3.41328	1.439417	1.023764
6	-3.79048	-0.43445	0.055429
1	-3.95129	-0.79522	-0.97106
1	2.173706	1.88324	-1.09567
8	-1.96777	2.734656	-0.64589
1	-1.22368	2.95843	-1.21274
8	-4.60789	1.670545	-0.6451
1	-4.42829	2.614017	-0.71316
8	-4.91367	-0.70131	0.86235
1	-5.63427	-0.14492	0.547756
6	-2.65878	-2.67735	0.550699
1	-3.42213	-3.05989	1.227922
1	-2.93218	-2.94848	-0.47798
8	-1.43475	-0.81938	-0.10845
8	-1.42236	-3.24541	0.914015
1	-0.74099	-2.81037	0.380398
8	0.928229	-2.02597	-0.88788
1	1.413455	-2.80309	-1.19197

8	3.53134	-2.62524	-0.80186
1	4.16594	-3.09168	-0.24994
8	4.977669	-0.36181	0.955002
1	4.154505	0.725451	1.045
8	3.572811	1.037811	0.114372
6	1.828389	2.454995	0.939216
1	0.774156	2.711649	0.814207
1	1.962769	2.018565	1.939388
8	2.558684	3.648321	0.791943
1	3.496504	3.44935	0.86805
E(elec)	-1297.7840641	au	
ZPVE	0.370820	au	
G correction (873K)	0.1004590	au	

TS: CBOC→(GER+EDL)		M06-2X/6-311++G(d,p)	
8	0.417774	-0.30441	1.086627
6	-2.67818	0.533046	-0.47891
6	-0.67356	-0.49582	0.24082
6	-1.38502	-1.75753	0.69907
1	-2.37433	0.36714	-1.52371
1	-0.34974	-0.61776	-0.80686
1	-1.60791	-1.6457	1.76894
6	1.148555	1.749681	0.008186
6	1.540966	0.372974	0.541714
6	2.169712	-0.49695	-0.5578
6	4.224854	0.029728	-0.03552
6	4.406353	-0.7356	-1.17019
1	2.228031	0.461883	1.3859
1	2.060106	-0.11591	-1.57937
1	4.213491	1.110704	-0.05352
1	4.455422	-0.24719	-2.14405
6	-2.67864	-1.91155	-0.08204
1	-2.42312	-2.09084	-1.13715
6	-3.52044	-0.64713	-0.00633
1	-3.81542	-0.47859	1.039756
1	0.379235	1.631851	-0.7662
8	-0.60172	-2.90252	0.45561
1	0.329001	-2.68754	0.6102
8	-3.46786	-2.97722	0.407609
1	-2.93589	-3.77947	0.37795
8	-4.65518	-0.74845	-0.83637

1	-5.07336	-1.59522	-0.64563
6	-3.37806	1.873839	-0.38679
1	-4.30606	1.826565	-0.95697
1	-3.62448	2.069306	0.665602
8	-1.52092	0.624126	0.349191
8	-2.59386	2.90626	-0.93769
1	-1.78928	3.024503	-0.41528
8	2.14455	-1.76671	-0.361
1	3.222612	-2.17539	-0.76635
8	4.313404	-0.5164	1.192264
1	4.435673	-1.47193	1.091266
8	4.362434	-2.02667	-1.08108
1	2.053121	3.204111	-0.89446
8	2.307278	2.335208	-0.5656
6	0.57368	2.630527	1.100296
1	-0.16816	2.080915	1.681286
1	1.390546	2.968446	1.747538
8	-0.02709	3.733763	0.420397
1	-0.23131	4.43281	1.046363
E(elec)	-1297.7974145	au	
ZPVE	0.369008	au	
G correction (873K)	0.0978314	au	

TS: GER→(GED+GA)		M06-2X/6-311++G(d,p)	
8	-0.86724	-0.15209	-0.77622
6	2.289955	0.957776	0.469967
6	0.334861	-0.24541	-0.07348
6	1.116029	-1.41151	-0.65892
1	2.106818	0.782533	1.540007
1	0.130757	-0.42229	0.997441
1	1.254862	-1.22484	-1.73133
6	-3.57548	-0.28743	-0.08731
6	-1.78383	0.728881	-0.23688
6	-2.32671	1.689288	-1.06317
1	-1.74755	0.879434	0.839064
1	-2.03231	1.713686	-2.11539
6	2.468832	-1.48445	0.024969
1	2.310366	-1.71396	1.089573
6	3.186435	-0.14821	-0.07863
1	3.392554	0.053293	-1.14016
1	-3.57514	-0.72071	-1.09894

8	0.465156	-2.64256	-0.43
1	-0.33509	-2.67566	-0.96314
8	3.3039	-2.45853	-0.5621
1	2.85009	-3.30677	-0.5217
8	4.378938	-0.15445	0.66991
1	4.875019	-0.94068	0.416648
6	2.879249	2.341534	0.286441
1	3.829843	2.396945	0.816146
1	3.061702	2.508513	-0.78331
8	1.045515	0.952554	-0.23348
8	2.032738	3.331727	0.822988
1	1.182442	3.2566	0.379146
8	-3.30679	2.433397	-0.67798
1	-3.99891	1.753902	-0.16827
8	-4.46556	0.565457	0.221684
6	-3.12483	-1.25592	0.997264
1	-2.17533	-1.72994	0.744243
1	-3.03419	-0.70988	1.943337
8	-4.08148	-2.28956	1.083536
1	-4.92451	-1.89501	1.328405
E(elec)	-1068.7339277		au
ZPVE	0.300825		au
G correction (873K)	0.0578254		au

TS: GED→(LG+EDL)		M06-2X/6-311++G(d,p)	
C	0.197031	1.127061	-0.0009
C	0.265256	0.209096	-1.19246
C	1.203924	0.821729	1.124821
O	1.250644	-0.51551	-1.50476
O	-1.9291	-1.14657	-0.91979
C	2.450267	0.181886	0.490772
C	2.117105	-0.98734	-0.42991
C	1.302337	-2.14749	0.208568
O	0.047216	-1.70868	0.509478
H	-0.82328	1.110665	0.387438
H	-0.44477	0.36901	-1.99809
H	1.518615	1.78771	1.528584
H	3.110402	-0.17479	1.287234
H	3.008096	-1.34652	-0.9483
H	1.310951	-2.98076	-0.50951
H	1.876285	-2.46865	1.094517

H	-1.17344	-1.57577	-0.40444
O	0.413501	2.391881	-0.61139
H	1.367563	2.496037	-0.73046
O	0.673267	0.073401	2.16484
H	0.275179	-0.73485	1.725084
O	3.049073	1.234386	-0.26571
H	3.879665	0.945501	-0.6537
C	-2.79074	-0.61784	-0.00901
H	-2.68156	-0.96946	1.016962
C	-3.72106	0.274116	-0.34449
H	-3.84262	0.624857	-1.3611
H	-4.4895	0.4885	1.400123
O	-4.63414	0.828737	0.5125
E(elec)	-839.6478543	au	
ZPVE	0.234247744	au	
G correction (873K)	0.032351279	au	

Glucose (GLC)		M06-2X/6-311++G(d,p)	
O	0.872481	-2.6924	-0.19813
H	1.821512	-2.81419	-0.07933
C	0.563762	-1.42259	0.270477
H	0.544126	-1.40434	1.373644
C	1.552868	-0.37993	-0.2356
H	1.554694	-0.42146	-1.33314
C	1.108857	0.996365	0.215969
H	1.131534	1.036644	1.315367
C	-1.21824	0.117479	0.250728
H	-1.23439	0.118136	1.350787
C	-0.31847	1.255547	-0.23952
H	-0.33712	1.288234	-1.33715
C	-2.64019	0.204808	-0.2714
H	-3.11621	1.116043	0.097213
H	-2.60931	0.23793	-1.3697
O	-0.71569	-1.1235	-0.22537
O	2.819412	-0.72475	0.282471
H	3.434775	-0.01864	0.058958
O	2.018838	1.932648	-0.32171
H	1.730798	2.810606	-0.05094
O	-0.68574	2.511038	0.309754
H	-1.42535	2.87916	-0.17884
O	-3.41601	-0.8753	0.18351

H	-2.93296	-1.68014	-0.03497
E(elec)	-687.13987	au	
ZPVE	0.20044829	au	
G correction (873K)	0.02740347	au	
TS: GLC12Mac		M06-2X/6-311++G(d,p)	
O	-0.11364	-1.65308	1.634143
H	0.070905	-2.22805	2.383068
C	-0.36294	-1.48317	-0.55521
H	-0.48541	-2.5372	-0.77989
C	-1.4939	-0.70277	-0.14837
H	-1.2173	-1.01958	1.025769
C	-1.30528	0.781224	-0.33523
H	-1.35245	1.058491	-1.39941
C	1.175111	0.355394	-0.4877
H	1.422123	0.843654	-1.43261
C	0.064594	1.133577	0.222413
H	0.06285	0.882434	1.288665
C	2.409605	0.204241	0.382088
H	2.736921	1.199301	0.693469
H	2.123316	-0.37922	1.264594
O	0.799009	-1.00993	-0.85215
O	-2.70065	-1.2365	-0.62146
H	-3.38385	-1.01244	0.015684
O	-2.32588	1.437312	0.38157
H	-2.19679	2.384256	0.267379
O	0.27176	2.523172	0.017725
H	0.724975	2.897929	0.77544
O	3.48355	-0.3768	-0.31882
H	3.258354	-1.29399	-0.49826
E(elec)	-687.0189213	au	
ZPVE	0.19143	au	
G correction (873K)	0.01146	au	
TS: GLC21Mac		M06-2X/6-311++G(d,p)	
O	1.063795	-2.45634	-0.92443
H	0.809557	-3.27934	-0.50301
C	0.69208	-1.4049	-0.08253
H	1.647533	-1.38085	1.264857
C	1.60357	-0.28329	-0.19025
H	2.424681	-0.31317	-0.90526
C	1.085164	1.103453	0.105438

H	1.108934	1.27132	1.189217
C	-1.15379	0.058423	0.289164
H	-1.00616	0.040186	1.380189
C	-0.36903	1.216538	-0.32374
H	-0.43313	1.14589	-1.41788
C	-2.63856	0.12287	-0.02347
H	-3.08901	0.982795	0.476535
H	-2.76497	0.234252	-1.11067
O	-0.68987	-1.14234	-0.28657
O	2.50904	-0.69452	1.253116
H	3.332014	-1.16375	1.045009
O	1.907318	2.037316	-0.55461
H	1.524264	2.907069	-0.39734
O	-0.79317	2.491936	0.130648
H	-1.59857	2.748599	-0.32453
O	-3.30653	-1.02242	0.446226
H	-2.79642	-1.78055	0.140179
E(elec)	-687.0005924	au	
ZPVE	0.192440888	au	
G correction (873K)	0.016194055	au	
TS: GLC23Mac		M06-2X/6-311++G(d,p)	
O	-0.72764	2.706638	-0.60666
H	-0.02876	3.344771	-0.43518
C	-0.4303	1.538763	0.076937
H	-0.35958	1.706972	1.159867
C	-1.54288	0.541714	-0.21556
H	-2.31599	0.907388	-0.88721
C	-1.23031	-0.84879	-0.16732
H	-1.90255	-0.47382	1.136663
C	1.143735	-0.1973	0.231301
H	1.04072	-0.11485	1.323072
C	0.199304	-1.28449	-0.28061
H	0.424563	-1.48834	-1.33889
C	2.594975	-0.46077	-0.11878
H	2.921129	-1.39127	0.349412
H	2.682032	-0.56279	-1.20916
O	0.809608	1.045998	-0.38087
O	-2.43428	0.569634	1.317359
H	-3.39321	0.527096	1.189346
O	-2.12364	-1.64803	-0.91874

H	-2.15952	-2.50584	-0.48817
O	0.353661	-2.48914	0.469985
H	1.046465	-3.02216	0.072736
O	3.438906	0.558625	0.364195
H	3.104587	1.388295	0.00945
E(elec)	-687.0114584		au
ZPVE	0.191983427		au
G correction (873K)	0.014237439		au
TS: GLC32Mac		M06-2X/6-311++G(d,p)	
O	-1.06835	-2.47824	0.560538
H	-1.91298	-2.74329	0.184075
C	-0.60196	-1.40624	-0.20355
H	-0.41857	-1.74233	-1.23908
C	-1.5629	-0.23693	-0.23287
H	-1.9722	0.356926	1.005525
C	-1.0303	1.082	-0.28211
H	-1.47763	1.811564	-0.95083
C	1.222573	0.065918	-0.26725
H	1.214847	-0.08267	-1.35654
C	0.424115	1.319738	0.086982
H	0.518537	1.469615	1.168369
C	2.657236	0.122396	0.223373
H	3.179414	0.94162	-0.27024
H	2.651293	0.306523	1.306717
O	0.616205	-1.0349	0.383893
O	-2.65808	-0.52284	-1.07999
H	-3.47504	-0.36598	-0.60258
O	-2.03407	1.568554	1.211125
H	-1.70619	2.019949	2.003437
O	0.973896	2.401278	-0.633
H	0.596783	3.225759	-0.31446
O	3.3372	-1.06944	-0.0869
H	2.814755	-1.79428	0.272875
E(elec)	-687.0050061		au
ZPVE	0.191847555		au
G correction (873K)	0.015571216		au
TS: GLC34Mac		M06-2X/6-311++G(d,p)	
O	-1.11859	-2.62329	-0.00313
H	-2.06971	-2.6581	-0.15526
C	-0.69157	-1.36009	-0.38949

H	-0.64635	-1.2742	-1.48821
C	-1.59153	-0.27015	0.195461
H	-1.52612	-0.37579	1.282207
C	-1.03501	1.064394	-0.23447
H	-1.63215	1.611019	-0.96304
C	1.245341	-0.02356	-0.33561
H	1.499562	-0.18106	-1.39574
C	0.38673	1.231026	-0.22343
H	-0.18558	1.874289	1.040215
C	2.528217	0.066508	0.469492
H	3.107834	0.931326	0.138686
H	2.259741	0.205137	1.524992
O	0.578509	-1.18034	0.159257
O	-2.90814	-0.49258	-0.2654
H	-3.52595	-0.02252	0.300867
O	-1.33265	2.080544	1.204804
H	-1.55118	2.992693	0.964338
O	0.809012	2.248388	-1.12149
H	1.480442	2.780263	-0.69141
O	3.339786	-1.06927	0.285576
H	2.792959	-1.8395	0.473642
E(elec)	-687.0096538	au	
ZPVE	0.191847555	au	
G correction (873K)	0.015571216	au	

TS: GLC43Mac		M06-2X/6-311++G(d,p)	
O	-0.69449	2.724528	0.146863
H	-1.64131	2.86168	0.26635
C	-0.45747	1.376519	0.379331
H	-0.42123	1.164274	1.461326
C	-1.50768	0.495822	-0.28145
H	-1.55965	0.789967	-1.33996
C	-1.13162	-0.95743	-0.17641
H	-0.78219	-1.73824	1.106144
C	1.261616	-0.18784	0.200747
H	1.400156	-0.20263	1.288352
C	0.268342	-1.27679	-0.19487
H	0.61886	-2.02015	-0.91176
C	2.604755	-0.37284	-0.48342
H	3.043908	-1.32199	-0.16919
H	2.445711	-0.39996	-1.57018

O	0.792147	1.086441	-0.1942
O	-2.74334	0.819713	0.349646
H	-3.45787	0.453434	-0.17654
O	-1.90988	-1.77421	-1.04608
H	-2.60193	-2.19292	-0.53234
O	0.241239	-2.26924	1.25876
H	0.189005	-3.21551	1.058612
O	3.499718	0.646663	-0.12229
H	3.055668	1.486252	-0.28594
E(elec)	-687.0105054		au
ZPVE	0.19224453		au
G correction (873K)	0.015641146		au

TS: GLC45Mac		M06-2X/6-311++G(d,p)	
O	-1.00444	2.592337	0.325814
H	-1.96749	2.613609	0.367784
C	-0.61955	1.2666	0.463016
H	-0.60037	0.967844	1.525676
C	-1.53483	0.333454	-0.3242
H	-1.38925	0.545442	-1.39181
C	-1.14471	-1.10092	-0.02379
H	-1.42402	-1.31623	1.011094
C	1.214743	-0.12485	-0.08745
H	1.399756	-0.78987	1.151991
C	0.361451	-1.2629	-0.17064
H	0.685859	-2.14993	-0.70723
C	2.52017	-0.07698	-0.83622
H	2.951781	-1.07851	-0.89284
H	2.346435	0.287706	-1.85808
O	0.669404	1.177426	-0.07285
O	-2.86149	0.600485	0.073211
H	-3.44793	0.013988	-0.41442
O	-1.85996	-1.92751	-0.92409
H	-1.90949	-2.81885	-0.56886
O	0.859356	-1.86264	1.534462
H	1.381766	-2.66905	1.658892
O	3.465922	0.744291	-0.1844
H	3.038929	1.59223	-0.02365
E(elec)	-687.0043322		au
ZPVE	0.190799009		au
G correction (873K)	0.011392478		au

TS: GLC65Mac		M06-2X/6-311++G(d,p)	
O	1.490619	-2.49549	-0.34386
H	2.401009	-2.40265	-0.04111
C	0.802768	-1.3691	0.097196
H	0.542169	-1.45796	1.165443
C	1.623529	-0.10142	-0.11825
H	1.869107	-0.04383	-1.18778
C	0.811832	1.118718	0.269556
H	0.576834	1.074283	1.342309
C	-1.18649	-0.21068	-0.24447
H	-1.94	-0.50141	1.106563
C	-0.50423	1.120884	-0.49574
H	-0.27022	1.258386	-1.56239
C	-2.57198	-0.40979	-0.51923
H	-3.19588	0.461664	-0.681
H	-2.87473	-1.30422	-1.05766
O	-0.37125	-1.29371	-0.66496
O	2.799404	-0.22701	0.65558
H	3.268038	0.613079	0.61412
O	1.606287	2.254713	-0.01263
H	1.099725	3.032733	0.241296
O	-1.26207	2.225918	-0.01986
H	-1.7565	2.609383	-0.7461
O	-3.05879	-0.77753	1.091045
H	-3.2058	-1.72632	1.229316
E(elec)	-687.0164721	au	
ZPVE	0.191646066	au	
G correction (873K)	0.015779939	au	
Product: GLC12Mac		M06-2X/6-311++G(d,p)	
C	-0.48684	-1.71812	0.20057
H	-0.61817	-2.77589	0.380314
C	-1.49885	-0.90601	-0.09339
C	-1.30623	0.568296	-0.30255
H	-1.34214	0.80988	-1.37433
C	1.092969	-0.01948	-0.25568
H	1.044511	-0.09212	-1.35137
C	0.049319	0.978765	0.238219
H	0.006506	0.944435	1.334606
C	2.505307	0.321944	0.177447
H	2.817498	1.256561	-0.29209

H	2.51868	0.448641	1.269881
O	0.818832	-1.30585	0.295445
O	-2.76878	-1.38129	-0.24625
H	-3.36956	-0.67757	0.028155
O	-2.37173	1.226221	0.364325
H	-2.31792	2.163711	0.155888
O	0.289799	2.296162	-0.226
H	0.94333	2.724974	0.331297
O	3.420661	-0.66538	-0.22937
H	3.072936	-1.51394	0.064701
E(elec)	-610.6858885	au	
ZPVE	0.1717666	au	
G correction (873K)	0.009903385	au	
Product: GLC21Mac		M06-2X/6-311++G(d,p)	
O	-0.1163	2.994764	-0.1733
H	0.828995	3.172761	-0.13456
C	-0.30971	1.676522	0.003641
C	-1.49153	1.133574	0.289697
H	-2.3435	1.779668	0.441875
C	-1.6674	-0.35029	0.37041
H	-1.7448	-0.68259	1.416335
C	0.816799	-0.38116	0.282605
H	0.821582	-0.38327	1.379729
C	-0.45652	-1.03997	-0.23676
H	-0.50892	-0.91331	-1.32582
C	2.085879	-1.02041	-0.24315
H	2.151954	-2.04328	0.129958
H	2.044118	-1.04312	-1.3414
O	0.850325	0.983438	-0.16331
O	-2.84925	-0.71527	-0.31954
H	-2.97737	-1.65927	-0.18192
O	-0.52539	-2.40931	0.124785
H	-0.07927	-2.94532	-0.53451
O	3.237899	-0.34886	0.208521
H	3.163863	0.569951	-0.06565
E(elec)	-610.6950492	au	
ZPVE	0.171025504	au	
G correction (873K)	0.007164839	au	
Product: GLC23Mac		M06-2X/6-311++G(d,p)	
O	-0.30199	2.91219	O

H	0.533475	3.380848	H
C	-0.21958	1.729868	C
H	0.05941	1.944383	H
C	-1.54598	1.036964	C
H	-2.42613	1.620123	H
C	-1.64151	-0.25177	C
C	0.814066	-0.40515	C
H	0.77439	-0.456	H
C	-0.42688	-1.08452	C
H	-0.3395	-1.16151	H
C	2.112088	-1.0164	C
H	2.183586	-2.05457	H
H	2.118732	-0.99282	H
O	0.822747	0.943114	O
O	-2.82715	-0.89857	O
H	-2.6471	-1.84291	H
O	-0.64393	-2.37329	O
H	-0.13364	-3.02905	H
O	3.227179	-0.34031	O
H	3.108732	0.592402	H
E(elec)	-610.6932342	au	
ZPVE	0.171997809	au	
G correction (873K)	0.009770934	au	

Product: GLC32Mac		M06-2X/6-311++G(d,p)	
O	-1.79134	-1.98675	0.367288
H	-2.72698	-1.77697	0.280794
C	-1.06676	-0.99508	-0.28858
H	-1.01767	-1.20665	-1.37059
C	-1.68021	0.374237	-0.08367
C	-0.96037	1.440153	0.246121
H	-1.43182	2.408697	0.397231
C	1.040365	0.036106	-0.18628
H	1.001094	0.117012	-1.28205
C	0.535183	1.348458	0.405055
H	0.80604	1.393102	1.469068
C	2.451938	-0.30805	0.244718
H	3.130666	0.47997	-0.08181
H	2.479723	-0.37042	1.340977
O	0.220812	-1.03813	0.250923
O	-3.02468	0.32816	-0.29316

H	-3.41251	1.203507	-0.19937
O	1.209244	2.3783	-0.30606
H	1.055941	3.218636	0.132041
O	2.881608	-1.51374	-0.34332
H	2.229492	-2.18463	-0.11593
E(elec)	-610.6866912	au	
ZPVE	0.17121632	au	
G correction (873K)	0.007167725	au	
Product: GLC34Mac		M06-2X/6-311++G(d,p)	
O	-1.77328	-2.04484	-0.12831
H	-2.71733	-1.85952	-0.18621
C	-1.11632	-0.84543	-0.36838
H	-1.17249	-0.56436	-1.43276
C	-1.67278	0.298325	0.46721
H	-1.73124	-0.04649	1.507516
C	-0.77203	1.492284	0.319411
H	-1.15899	2.484581	0.52547
C	1.08649	-0.0087	-0.38537
H	1.306949	-0.09009	-1.46284
C	0.482353	1.345401	-0.09762
C	2.36861	-0.26076	0.406376
H	3.149258	0.454369	0.135904
H	2.14106	-0.13944	1.472794
O	0.220871	-1.05911	-0.0031
O	-2.98236	0.522667	-0.04151
H	-3.43138	1.174713	0.501335
O	1.288243	2.426801	-0.28942
H	2.138839	2.160107	-0.64707
O	2.878461	-1.53727	0.121532
H	2.161906	-2.16662	0.262609
E(elec)	-610.686253	au	
ZPVE	0.170786077	au	
G correction (873K)	0.005801633	au	
Product: GLC43Mac		M06-2X/6-311++G(d,p)	
O	-0.73775	2.468296	-0.13123
H	-0.16679	3.09628	0.320783
C	-0.45647	1.186462	0.324924
H	-0.57487	1.110542	1.417075
C	-1.42558	0.241752	-0.36161
H	-1.35993	0.417365	-1.44342

C	-1.028	-1.17456	-0.03462
C	1.272821	-0.42276	0.488193
H	1.547193	-0.27822	1.544435
C	0.205976	-1.47363	0.361646
H	0.461396	-2.49799	0.608726
C	2.529613	-0.78221	-0.2901
H	2.947873	-1.71182	0.100165
H	2.253211	-0.93485	-1.34083
O	0.85417	0.838979	-0.03978
O	-2.75485	0.421192	0.091206
H	-3.04599	1.301118	-0.16613
O	-1.99781	-2.10639	-0.18552
H	-2.84911	-1.6503	-0.17984
O	3.520261	0.209868	-0.15456
H	3.124673	1.041986	-0.43256
E(elec)	-610.6993567	au	
ZPVE	0.172198775	au	
G correction (873K)	0.010960984	au	
Product: GLC45Mac		M06-2X/6-311++G(d,p)	
O	-0.64443	2.485899	-0.18817
H	-1.60001	2.613185	-0.15614
C	-0.39091	1.204567	0.270396
H	-0.32515	1.179639	1.369298
C	-1.42915	0.205593	-0.21257
H	-1.35393	0.135647	-1.30579
C	-1.12143	-1.15463	0.379827
H	-1.39774	-1.142	1.442914
C	1.214335	-0.46485	-0.11295
C	0.348144	-1.42904	0.205661
H	0.715151	-2.44079	0.32956
C	2.677966	-0.64789	-0.38817
H	2.967848	-1.67557	-0.1723
H	2.857417	-0.45028	-1.45307
O	0.877158	0.84987	-0.24966
O	-2.69003	0.703177	0.179024
H	-3.35972	0.069526	-0.09707
O	-1.95881	-2.07515	-0.31034
H	-1.9012	-2.93687	0.10948
O	3.47152	0.194797	0.418229
H	3.160416	1.096232	0.287209

E(elec)	-610.6921918	au
ZPVE	0.171550086	au
G correction (873K)	0.007602338	au

Product: GLC65Mac		M06-2X/6-311++G(d,p)	
O	-2.39923	-1.47544	0.273194
H	-3.11703	-0.87217	0.048948
C	-1.22775	-0.90017	-0.19519
H	-1.14067	-1.01001	-1.2877
C	-1.14111	0.573975	0.175886
H	-1.24614	0.656484	1.266294
C	0.206741	1.126956	-0.23785
H	0.313451	1.055337	-1.32988
C	1.073457	-1.16709	0.059421
C	1.29972	0.287848	0.409639
H	1.204719	0.39747	1.499204
C	1.963722	-1.97811	-0.49232
H	2.952224	-1.61938	-0.74229
H	1.705485	-3.00879	-0.69578
O	-0.1753	-1.61913	0.420306
O	-2.20919	1.22164	-0.4802
H	-2.11323	2.16918	-0.33776
O	0.255194	2.475261	0.175188
H	1.127556	2.819019	-0.04321
O	2.53143	0.80867	-0.03896
H	3.24176	0.464415	0.508371

E(elec)	-610.6927462	au
ZPVE	0.171024348	au
G correction (873K)	0.009896273	au

TS: CB12Mac		M06-2X/6-311++G(d,p)	
O	-0.01492	-1.15554	0.130264
C	-2.71663	1.137499	-0.48629
C	-1.29157	-0.77162	-0.30806
C	-2.34549	-1.60208	0.426717
H	-2.79697	0.953203	-1.56905
H	-1.37016	-0.91922	-1.40119
H	-2.19033	-1.4734	1.507035
C	2.239788	-1.36843	-0.66818
C	1.06068	-0.41513	-0.46744
C	1.419265	0.836958	0.383296
C	2.821283	0.738435	0.992544

C	3.20482	-0.60403	1.358589
H	0.755943	-0.06147	-1.46119
H	0.69876	0.89101	1.206002
H	3.690001	0.93656	0.226509
H	3.779701	-0.83497	2.25275
C	-3.73603	-1.08756	0.043722
H	-3.90533	-1.31033	-1.02196
C	-3.86327	0.427519	0.242419
H	-3.79473	0.647335	1.319525
H	1.885819	-2.36772	-0.91845
O	-2.3059	-2.98111	0.070347
H	-1.47976	-3.36529	0.404646
O	-4.75804	-1.69802	0.826507
H	-4.70616	-2.65903	0.694079
O	-5.09325	0.906736	-0.28177
H	-5.80436	0.363232	0.097524
C	-2.61656	2.64023	-0.25031
H	-3.52575	3.128461	-0.60867
H	-2.5221	2.829869	0.831113
O	-1.47704	0.593611	-0.00062
O	-1.5298	3.200944	-0.96892
H	-0.71449	2.711358	-0.74526
O	1.295053	1.999317	-0.43524
H	1.662356	2.751114	0.061571
O	3.011137	1.693276	2.018934
H	3.950659	1.952348	1.964352
O	5.213141	0.611936	0.220324
H	6.061958	1.027246	-0.00853
O	2.932456	-1.61436	0.617556
C	3.256732	-0.85408	-1.73886
H	2.893467	-1.24165	-2.69978
H	3.217104	0.242372	-1.79576
O	4.556119	-1.30888	-1.52394
H	4.984548	-0.65077	-0.89186
E(elec)	-1297.762967	au	
ZPVE	0.370537368	au	
G correction (873K)	0.102379256	au	

TS: CB21Mac		M06-2X/6-311++G(d,p)	
O	-0.15222	0.924158	0.353496
C	2.652258	-1.07055	-0.56631

C	1.114602	0.676978	-0.15661
C	2.124758	1.489972	0.636765
H	2.692121	-0.76878	-1.62324
H	1.154437	0.946525	-1.22709
H	2.023675	1.212444	1.693968
C	-2.41526	1.060674	-0.33423
C	-1.17948	0.165798	-0.27332
C	-1.41548	-1.17936	0.452306
C	-2.83939	-1.35492	0.943286
C	-3.90286	-0.59671	0.377495
H	-0.88	-0.09325	-1.29699
H	-0.71017	-1.24995	1.280765
H	-3.08748	-2.32193	1.373719
H	-3.71028	-0.0566	1.75279
C	3.521872	1.141748	0.150064
H	3.617324	1.468478	-0.89642
C	3.758912	-0.36141	0.205278
H	3.721967	-0.68103	1.256922
H	-2.5584	1.543582	0.64229
O	1.953257	2.879033	0.453979
H	1.094419	3.128552	0.808958
O	4.519886	1.754712	0.939689
H	4.35912	2.704125	0.937143
O	4.995545	-0.69962	-0.37781
H	5.666556	-0.13446	0.020057
C	2.689603	-2.58263	-0.4817
H	3.622851	-2.95072	-0.90824
H	2.649308	-2.87303	0.577613
O	1.396351	-0.69201	-0.00812
O	1.623617	-3.1443	-1.21058
H	0.812047	-2.67376	-0.97201
O	-1.17543	-2.20953	-0.50484
H	-1.38064	-3.06702	-0.11876
O	-2.80748	-0.3524	2.489137
H	-2.97842	-0.77226	3.347001
O	-5.07208	-1.27295	0.092379
H	-5.81221	-0.67683	0.229491
O	-3.55541	0.287424	-0.66214
C	-2.28633	2.118828	-1.41377
H	-1.41388	2.742096	-1.21005

H	-2.14595	1.61969	-2.38185
O	-3.41255	2.963772	-1.4376
H	-4.18359	2.397294	-1.54252
E(elec)	-1297.727936	au	
ZPVE	0.367788848	au	
G correction (873K)	0.094345526	au	
TS: CB23Mac		M06-2X/6-311++G(d,p)	
O	-0.14544	0.748269	0.594677
C	2.671875	-1.02788	-0.67512
C	1.096979	0.607016	0.007441
C	2.123343	1.363872	0.834923
H	2.633239	-0.60605	-1.68975
H	1.087203	0.983106	-1.03069
H	2.088691	0.969884	1.858741
C	-2.33213	1.19854	-0.24306
C	-1.23103	0.146656	-0.14227
C	-1.71295	-1.11078	0.521266
C	-3.10659	-1.4244	0.478184
C	-4.08653	-0.29957	0.178185
H	-0.86135	-0.09523	-1.1503
H	-2.23405	-1.18842	1.955183
H	-3.43245	-2.40708	0.144586
H	-4.32126	0.246175	1.102268
C	3.502519	1.125905	0.24086
H	3.527444	1.572258	-0.76485
C	3.797641	-0.36271	0.108461
H	3.839862	-0.80045	1.116784
H	-2.51924	1.621685	0.754858
O	1.897501	2.75718	0.814258
H	1.05397	2.934224	1.242208
O	4.522873	1.685329	1.04157
H	4.331133	2.621922	1.156205
O	5.006418	-0.57666	-0.58174
H	5.679707	-0.03089	-0.16137
C	2.774197	-2.53595	-0.77801
H	3.712281	-2.80048	-1.26586
H	2.775758	-2.96071	0.235698
O	1.442637	-0.76235	-0.00279
O	1.726102	-3.06333	-1.55814
H	0.880911	-2.80721	-1.16781

O	-0.89397	-2.24622	0.295337
H	-0.03473	-2.03374	0.677976
O	-3.30272	-1.60173	2.214288
H	-3.28405	-2.52873	2.495429
O	-5.21583	-0.86963	-0.38405
H	-5.84228	-0.16938	-0.5898
O	-3.5229	0.606384	-0.74523
C	-1.97085	2.316031	-1.20188
H	-1.04363	2.789938	-0.87503
H	-1.81326	1.884339	-2.19907
O	-2.96412	3.314718	-1.22964
H	-3.78702	2.888599	-1.48768
E(elec)	-1297.745618	au	
ZPVE	0.369026595	au	
G correction (873K)	0.09727671	au	

TS: CB32Mac		M06-2X/6-311++G(d,p)	
O	-0.07249	0.971771	0.589801
C	2.567715	-1.06263	-0.66345
C	1.156742	0.709146	-0.00961
C	2.244112	1.39258	0.803812
H	2.577743	-0.65319	-1.68428
H	1.15867	1.082778	-1.04929
H	2.173224	1.025177	1.835747
C	-2.30736	1.31997	-0.18497
C	-1.16765	0.312819	-0.03221
C	-1.62148	-0.85616	0.820453
C	-2.99927	-1.20534	0.833335
C	-4.01514	-0.21415	0.335125
H	-0.8817	-0.05391	-1.02373
H	-0.99362	-1.06747	1.681497
H	-2.35405	-2.12134	-0.08156
H	-4.37688	0.40969	1.170257
C	3.596577	1.01587	0.222204
H	3.669247	1.438317	-0.79128
C	3.746245	-0.49615	0.120268
H	3.735282	-0.91752	1.136344
H	-2.51336	1.795163	0.785412
O	2.145489	2.79997	0.75259
H	1.329593	3.066265	1.186954
O	4.66022	1.492233	1.020104

H	4.562487	2.446017	1.109071
O	4.935517	-0.83905	-0.55137
H	5.653751	-0.34967	-0.13564
C	2.52978	-2.57435	-0.74501
H	3.447957	-2.93221	-1.2115
H	2.477479	-2.9768	0.276705
O	1.362444	-0.67693	-0.00525
O	1.447641	-3.01016	-1.53056
H	0.627752	-2.64435	-1.1666
O	-1.1397	-2.33658	-0.17885
H	-0.91364	-3.06041	0.423354
O	-3.41	-1.89589	1.989783
H	-4.11908	-2.49206	1.734204
O	-5.07265	-0.92078	-0.2267
H	-5.80777	-0.31858	-0.37551
O	-3.45545	0.635267	-0.6496
C	-1.99105	2.389481	-1.21336
H	-1.1022	2.943742	-0.90787
H	-1.78959	1.900569	-2.17609
O	-3.04604	3.314832	-1.32295
H	-3.83655	2.815638	-1.55173
E(elec)	-1297.745647	au	
ZPVE	0.368601894	au	
G correction (873K)	0.09653768	au	

TS: CB34Mac		M06-2X/6-311++G(d,p)	
O	0.146143	0.916857	-0.46762
C	-2.65719	-1.06385	0.43966
C	-1.09142	0.6816	0.066114
C	-2.12109	1.522639	-0.67326
H	-2.67489	-0.8184	1.512545
H	-1.09838	0.900808	1.14728
H	-2.06061	1.273954	-1.74095
C	2.389179	1.305766	0.110515
C	1.243707	0.319171	0.263391
C	1.497109	-1.07828	-0.18274
C	2.939044	-1.53626	-0.23282
C	3.797282	-0.38021	-0.72029
H	0.755219	-0.89141	1.455741
H	0.936215	-1.4125	-1.05582
H	3.292099	-1.76914	0.778621

H	3.482514	-0.05039	-1.7241
C	-3.50627	1.188785	-0.14844
H	-3.5542	1.471749	0.913938
C	-3.77605	-0.30317	-0.26425
H	-3.77436	-0.57301	-1.33023
H	2.317203	1.817985	-0.86506
O	-1.91937	2.90303	-0.46086
H	-1.027	3.120241	-0.75069
O	-4.52382	1.852789	-0.86957
H	-4.32058	2.794384	-0.86587
O	-5.00096	-0.6552	0.337961
H	-5.6687	-0.04063	0.013511
C	-2.76559	-2.56153	0.275129
H	-3.6878	-2.91599	0.740792
H	-2.76686	-2.81109	-0.79132
O	-1.41266	-0.69569	-0.12367
O	-1.61551	-3.11864	0.913166
H	-1.6529	-4.0777	0.883869
O	0.860543	-1.85805	1.021882
H	-0.03656	-2.21875	0.811737
O	3.026875	-2.66088	-1.07792
H	3.958796	-2.89255	-1.15116
O	5.112773	-0.83594	-0.72864
H	5.688448	-0.1249	-1.02441
O	3.672248	0.678834	0.188632
C	2.381119	2.355348	1.204098
H	1.414883	2.863701	1.201878
H	2.50415	1.84577	2.166989
O	3.375909	3.339359	1.004299
H	4.216874	2.87585	0.948898
E(elec)	-1297.762011	au	
ZPVE	0.371119396	au	
G correction (873K)	0.103624014	au	

TS: CB43Mac		M06-2X/6-311++G(d,p)	
O	-0.14627	-1.05407	-0.18625
C	2.691819	0.867972	0.745727
C	1.145232	-0.877	0.221311
C	2.139284	-1.54193	-0.72821
H	2.801186	0.488818	1.772581
H	1.293272	-1.28486	1.238135

H	1.987572	-1.11285	-1.72818
C	-2.59494	-0.82296	0.949627
C	-1.47762	0.173639	0.733262
C	-1.52146	1.076071	-0.34269
C	-2.74243	1.133342	-1.22088
C	-3.47923	-0.1949	-1.14628
H	-0.79898	0.383101	1.555425
H	-0.72149	0.10345	-0.74125
H	-3.4256	1.913278	-0.8598
H	-2.85975	-1.00194	-1.56914
C	3.549848	-1.24985	-0.25189
H	3.683131	-1.70141	0.742622
C	3.771492	0.250147	-0.13761
H	3.694441	0.684489	-1.14555
H	-2.26	-1.82414	0.664072
O	1.978807	-2.94425	-0.74901
H	1.053001	-3.12479	-0.94389
O	4.529091	-1.75132	-1.14156
H	4.355015	-2.68906	-1.27309
O	5.028298	0.53869	0.432549
H	5.685978	0.026239	-0.04983
C	2.72742	2.386913	0.757044
H	3.646704	2.726538	1.234401
H	2.725718	2.742189	-0.28311
O	1.412274	0.519612	0.238559
O	1.640429	2.91723	1.477852
H	0.829397	2.63718	1.032049
O	-0.83779	2.282025	-0.20512
H	-0.55099	2.554168	-1.0842
O	-2.30289	1.421	-2.5322
H	-3.0782	1.558909	-3.08531
O	-4.66848	-0.04278	-1.83912
H	-5.11825	-0.89093	-1.89451
O	-3.7584	-0.47683	0.210058
C	-3.01846	-0.81391	2.415977
H	-2.19171	-1.16921	3.033444
H	-3.26222	0.215374	2.710705
O	-4.10282	-1.67914	2.627198
H	-4.81206	-1.40107	2.038468
E(elec)	-1297.752143		au

ZPVE	0.368740806	au
G correction (873K)	0.095242439	au

TS: CB45Mac		M06-2X/6-311++G(d,p)	
O	0.179616	0.126594	0.075443
C	-3.20247	1.247174	-0.0421
C	-1.14492	0.084987	-0.27864
C	-1.77994	-1.24011	0.165524
H	-3.27852	1.346268	-1.13551
H	-1.24681	0.180034	-1.37518
H	-1.66847	-1.32154	1.254006
C	2.172736	-1.17095	-0.28126
C	1.792751	-0.02367	-1.02624
C	2.482077	1.303985	-0.8249
C	3.809295	1.101887	-0.11273
C	3.612273	0.1489	1.057611
H	1.228171	-0.12499	-1.9471
H	1.85114	1.930509	-0.18553
H	4.528567	0.631384	-0.7974
H	2.790982	0.489615	1.708236
C	-3.25508	-1.22811	-0.19516
H	-3.3439	-1.17593	-1.2911
C	-3.94045	-0.01189	0.399728
H	-3.89167	-0.08677	1.496187
H	1.02737	-0.84798	0.327741
O	-1.19564	-2.34318	-0.49597
H	-0.46171	-2.71434	0.014513
O	-3.92474	-2.37608	0.285996
H	-3.46034	-3.14598	-0.05898
O	-5.27926	0.081941	-0.03384
H	-5.68599	-0.78007	0.106101
C	-3.74352	2.504502	0.609768
H	-4.78243	2.649932	0.314738
H	-3.69957	2.381269	1.70034
O	-1.83383	1.159482	0.338695
O	-3.01495	3.639219	0.197431
H	-2.08517	3.437174	0.345539
O	2.649228	1.88607	-2.09795
H	3.110363	2.722485	-1.97463
O	4.24535	2.374468	0.298469
H	5.054575	2.263523	0.808367

O	4.817118	0.089783	1.741658
H	4.710101	-0.43861	2.537529
O	3.310175	-1.13634	0.5553
C	1.958212	-2.5587	-0.81979
H	1.250297	-2.52611	-1.64824
H	2.906692	-2.97827	-1.17008
O	1.372216	-3.42021	0.154935
H	1.978236	-3.49361	0.898251
E(elec)	-1297.745374		au
ZPVE	0.368419249		au
G correction (873K)	0.092899033		au

TS: CB65Mac		M06-2X/6-311++G(d,p)	
O	-0.17037	-0.40672	-0.52071
C	2.829676	1.241684	0.454718
C	1.066824	-0.27793	0.080891
C	1.984248	-1.32188	-0.54028
H	2.751377	1.076813	1.539954
H	0.992584	-0.44821	1.170766
H	2.013878	-1.14452	-1.62284
C	-2.14454	-1.18298	0.498692
C	-1.30101	0.051107	0.20866
C	-2.08116	1.042991	-0.63814
C	-3.48556	1.220931	-0.08488
C	-4.17846	-0.12482	0.061098
H	-0.97335	0.568722	1.120657
H	-2.15729	0.629349	-1.65403
H	-3.43011	1.669583	0.916682
H	-4.24323	-0.63469	-0.91357
C	3.373435	-1.15382	0.046291
H	3.325072	-1.37391	1.1239
C	3.858561	0.277972	-0.12909
H	3.962931	0.478427	-1.20537
H	-1.99088	-2.1508	-0.59641
O	1.550322	-2.63242	-0.2446
H	0.694149	-2.79546	-0.6691
O	4.318209	-2.00211	-0.57439
H	3.977472	-2.90167	-0.52953
O	5.083549	0.482605	0.538235
H	5.682113	-0.2192	0.26096
C	3.139391	2.703348	0.189793

H	4.056036	2.984832	0.707653
H	3.286849	2.840017	-0.89002
O	1.566005	1.010149	-0.15751
O	2.099303	3.523341	0.669973
H	1.277201	3.190262	0.288845
O	-1.39128	2.271146	-0.65066
H	-1.94485	2.90336	-1.12142
O	-4.17169	2.066877	-0.98246
H	-5.0619	2.204946	-0.64355
O	-5.43675	0.125066	0.592894
H	-5.91521	-0.70436	0.679173
O	-3.4513	-0.93181	0.961817
C	-1.5231	-2.3289	1.050472
H	-0.45756	-2.3617	1.243868
H	-2.14075	-2.99956	1.638277
O	-1.38008	-3.2129	-0.55222
H	-1.86184	-4.04431	-0.67732
E(elec)	-1297.750925	au	
ZPVE	0.368222257	au	
G correction (873K)	0.098286349	au	
TS: CB1'2'Mac		M06-2X/6-311++G(d,p)	
O	-0.17286	0.407544	0.717767
C	-2.34456	-0.16737	1.653868
C	-2.07854	-0.16706	2.708135
C	-2.62338	1.062653	0.989716
H	-1.43863	1.157921	0.708549
H	-3.43082	0.902027	-0.27779
H	-4.47104	0.638201	-0.03888
C	-2.63723	-1.514	-0.31568
C	-3.56761	-2.08396	-0.32968
C	-2.79773	-0.20575	-1.10229
C	-1.80996	0.151793	-1.4148
C	-1.47825	-2.32659	-0.87975
H	-1.74532	-2.58281	-1.91207
H	-0.60502	-1.67186	-0.89634
H	-2.35571	-1.32014	1.111288
H	-3.06037	2.053597	1.870436
C	-2.86388	2.905528	1.469146
H	-3.38106	2.132048	-0.9582
C	-3.90916	2.05249	-1.75897

H	-3.6396	-0.42918	-2.22012
H	-3.11237	-0.65975	-2.98849
O	-1.23006	-3.5016	-0.16217
H	-0.41975	-3.36237	0.34515
O	5.137579	0.014942	-0.48031
H	5.452222	-0.89554	-0.51423
O	3.750104	-0.03638	-0.56489
H	3.432484	-0.24783	-1.60128
C	3.170702	-1.11503	0.352376
H	3.508051	-0.91517	1.377251
H	1.665598	-1.02381	0.26704
O	1.378028	-1.19008	-0.78212
O	1.869729	1.373373	-0.26322
H	1.53748	1.184405	-1.29648
O	1.203789	0.375018	0.688996
H	1.629859	0.575218	1.691165
O	1.581312	2.814413	0.099143
H	0.51065	3.001269	0.008332
O	1.881576	2.981065	1.142412
H	3.289063	1.230925	-0.18413
O	3.684652	-2.35095	-0.11229
C	3.300823	-3.05572	0.417695
H	1.030125	-2.01069	1.075797
H	0.272408	-1.54317	1.458779
O	2.244749	3.705894	-0.76956
H	3.169889	3.43701	-0.78636
E(elec)	-1297.752788	au	
ZPVE	0.368402892	au	
G correction (873K)	0.090453149	au	

TS: CB2'1'Mac		M06-2X/6-311++G(d,p)	
O	0.089771	0.680166	-0.70567
C	-1.0868	0.59001	0.047213
C	-1.19962	1.953661	1.171034
C	-2.09547	1.527683	-0.42392
H	-1.91722	2.127585	-1.31728
H	-3.54832	1.162863	-0.20762
H	-3.82634	1.427678	0.820467
C	-2.75235	-1.0581	0.556879
C	-2.81831	-0.68178	1.588261
C	-3.76704	-0.34138	-0.33186

C	-3.60721	-0.65066	-1.37361
C	-2.88771	-2.56968	0.558882
H	-3.85236	-2.8549	0.984113
H	-2.83835	-2.93116	-0.47924
H	-1.47452	-0.78445	0.024499
H	-1.80661	2.718876	0.765067
C	-1.27082	3.460786	0.439863
H	-4.32718	1.887961	-1.12849
C	-5.24288	1.618786	-0.99762
H	-5.11431	-0.5441	0.058943
H	-5.41662	-1.40496	-0.24012
O	-1.90005	-3.1736	1.357041
H	-1.03619	-2.85502	1.068145
O	5.286616	-0.62622	0.34782
H	5.506398	-1.53549	0.11377
O	4.069709	-0.33598	-0.25518
H	4.207615	-0.10906	-1.32624
C	3.076714	-1.47971	-0.10149
H	2.953229	-1.67622	0.972337
H	1.739296	-1.0807	-0.69436
O	1.868679	-0.89446	-1.77123
O	2.356603	1.273586	-0.17339
H	2.516791	1.504136	-1.23752
O	1.260433	0.214133	-0.04587
H	1.037162	0.036266	1.013636
O	2.019753	2.552353	0.568284
H	1.128406	2.994941	0.119842
O	1.809413	2.309378	1.619024
H	3.566309	0.800248	0.40114
O	3.631949	-2.6017	-0.75473
C	2.963745	-3.29503	-0.76903
H	0.856147	-2.16659	-0.50083
H	-0.03816	-1.84706	-0.68941
O	3.053652	3.499107	0.458977
H	3.869505	3.054428	0.715154
E(elec)	-1297.730268	au	
ZPVE	0.36958997	au	
G correction (873K)	0.09673415	au	
TS: CB2’3’Mac		M06-2X/6-311++G(d,p)	
O	-0.09695	0.766173	0.703944

C	1.096198	0.581992	0.030399
C	1.004719	0.881463	-1.02359
C	2.187075	1.393611	0.70714
H	1.89191	1.896996	1.625476
H	3.534159	0.956888	0.514861
H	3.251542	2.105988	-0.45949
C	2.629495	-1.07237	-0.63589
C	2.573302	-0.62171	-1.63644
C	3.808993	-0.46947	0.12553
C	3.98167	-1.05256	1.04389
C	2.6741	-2.58223	-0.76917
H	3.569715	-2.87329	-1.32131
H	2.72348	-3.02533	0.235706
H	1.429153	-0.78691	0.080853
H	2.284144	2.77041	-0.38431
C	2.447065	3.604398	0.081286
H	4.412086	1.435324	1.516001
C	5.275122	1.540476	1.107329
H	4.992161	-0.49163	-0.67015
H	5.449608	-1.32513	-0.53571
O	1.570978	-3.07224	-1.49307
H	0.762273	-2.81596	-1.03355
O	-5.29513	-0.53117	-0.30636
H	-5.54302	-1.40565	0.015169
O	-4.07051	-0.21854	0.266684
H	-4.19847	0.118296	1.309739
C	-3.1118	-1.40059	0.224624
H	-2.99153	-1.6959	-0.82686
H	-1.76292	-0.99213	0.786998
O	-1.88545	-0.72388	1.846606
O	-2.31829	1.333144	0.031438
H	-2.4781	1.690074	1.059855
O	-1.25004	0.238015	0.044497
H	-0.99634	-0.04417	-0.98617
O	-1.93146	2.504485	-0.85236
H	-1.00064	2.945061	-0.49216
O	-1.77442	2.132008	-1.87423
H	-3.5326	0.828174	-0.4999
O	-3.69985	-2.44116	0.974186
C	-3.06429	-3.16217	1.034547

H	-0.91499	-2.11781	0.668502
H	-0.01922	-1.84128	0.904407
O	-2.91607	3.508602	-0.82265
H	-3.75231	3.093252	-1.05939
E(elec)	-1297.739277	au	
ZPVE	0.36839583	au	
G correction (873K)	0.094316998	au	

TS: CB3'2'Mac		M06-2X/6-311++G(d,p)	
O	-0.06302	0.811777	0.565561
C	1.11296	0.652667	-0.16016
C	0.911672	0.844045	-1.22812
C	2.180775	1.578448	0.346247
H	2.625549	1.491884	1.760564
H	3.53607	1.1074	0.319068
H	4.290832	1.812942	-0.01641
C	2.711314	-0.99142	-0.7288
C	2.659305	-0.55655	-1.73619
C	3.86721	-0.35982	0.040969
C	3.973454	-0.91004	0.98396
C	2.7932	-2.50263	-0.83705
H	3.694097	-2.77807	-1.38547
H	2.855855	-2.92766	0.175172
H	1.524687	-0.69845	-0.01229
H	2.009038	2.898735	-0.11591
C	1.492043	3.383234	0.531007
H	3.768104	1.374807	2.0789
C	4.030469	0.646095	2.661747
H	5.023249	-0.49017	-0.75471
H	5.79856	-0.22449	-0.25255
O	1.691715	-3.01879	-1.54341
H	0.883589	-2.78204	-1.07238
O	-5.24856	-0.6965	-0.18196
H	-5.44964	-1.5676	0.178898
O	-4.01416	-0.31928	0.328914
H	-4.1137	0.052688	1.363143
C	-3.01541	-1.46802	0.29303
H	-2.92324	-1.79864	-0.7507
H	-1.66507	-0.98823	0.788803
O	-1.75991	-0.68156	1.840752
O	-2.32849	1.2831	-0.04074

H	-2.45976	1.684194	0.975348
O	-1.22282	0.225944	-0.02187
H	-1.00518	-0.09464	-1.04983
O	-2.02005	2.421571	-0.99458
H	-1.08946	2.908423	-0.69965
O	-1.89464	2.005051	-2.00353
H	-3.54671	0.715099	-0.49732
O	-3.5378	-2.50107	1.101012
C	-2.87229	-3.19416	1.164784
H	-0.7735	-2.08264	0.684723
H	0.11914	-1.75125	0.854019
O	-3.0363	3.39457	-0.96852
H	-3.86721	2.940762	-1.14628
E(elec)	-1297.738611	au	
ZPVE	0.367525892	au	
G correction (873K)	0.090027346	au	

TS: CB3’4’Mac		M06-2X/6-311++G(d,p)	
O	0.096651	0.825713	-0.68684
C	-1.11671	0.649502	-0.03529
C	-1.0597	1.006466	1.00652
C	-2.18305	1.400264	-0.81999
H	-2.15134	1.008237	-1.84227
H	-3.52672	1.093814	-0.19521
H	-3.98544	1.955306	0.288945
C	-2.5618	-1.03683	0.770055
C	-2.30072	-0.81849	1.818077
C	-3.77455	-0.2167	0.36463
C	-4.51515	-0.09918	-1.04332
C	-2.74457	-2.53515	0.628486
H	-3.61878	-2.84554	1.204035
H	-2.9249	-2.76256	-0.43048
H	-1.4403	-0.71584	-0.05631
H	-1.9869	2.79258	-0.79034
C	-1.1548	2.985872	-1.23382
H	-4.5659	0.90655	-1.55835
C	-5.42239	1.342311	-1.43173
H	-4.72606	-0.15357	1.423578
H	-5.37454	-0.84733	1.296685
O	-1.64306	-3.25096	1.140244
H	-0.84269	-2.95587	0.690677

O	5.245551	-0.6164	0.384924
H	5.482516	-1.47954	0.026505
O	4.043929	-0.24785	-0.2026
H	4.207737	0.144745	-1.22087
C	3.061761	-1.41031	-0.25577
H	2.903662	-1.76429	0.772183
H	1.740296	-0.93863	-0.83252
O	1.904492	-0.60149	-1.8669
O	2.314221	1.323966	0.076191
H	2.507413	1.736649	-0.92565
O	1.228008	0.252348	-0.02718
H	0.943112	-0.08681	0.977379
O	1.930566	2.450991	1.016863
H	1.011366	2.926144	0.669581
O	1.753037	2.025849	2.014365
H	3.504955	0.766345	0.606978
O	3.653102	-2.41708	-1.04785
C	3.006406	-3.12017	-1.17119
H	0.863646	-2.04688	-0.82099
H	-0.02935	-1.72282	-1.00261
O	2.927932	3.441544	1.054158
H	3.754724	3.003983	1.284327
E(elec)	-1297.742037	au	
ZPVE	0.368763623	au	
G correction (873K)	0.095860373	au	

TS: CB4’3’Mac		M06-2X/6-311++G(d,p)	
O	0.068174	0.761311	-0.75456
C	-1.15178	0.550733	-0.13017
C	-1.12628	0.903085	0.914144
C	-2.23852	1.271577	-0.90883
H	-2.11033	1.017266	-1.97137
H	-3.60055	0.829496	-0.44896
H	-4.12025	0.971098	0.967568
C	-2.5409	-1.18043	0.64525
C	-2.36388	-0.85376	1.676618
C	-3.77538	-0.4781	0.099875
C	-4.57763	-1.10745	-0.28522
C	-2.63293	-2.69492	0.61459
H	-3.48097	-3.01618	1.222254
H	-2.80174	-3.02089	-0.42115

H	-1.4142	-0.83894	-0.14723
H	-2.13871	2.676259	-0.73765
C	-1.38978	2.990428	-1.25347
H	-4.63042	1.199098	-1.34392
C	-4.69811	2.157373	-1.3186
H	-4.54507	0.064843	1.603967
H	-5.51205	0.024298	1.561624
O	-1.48015	-3.28278	1.161998
H	-0.70575	-2.96496	0.681137
O	5.245711	-0.43531	0.469872
H	5.534195	-1.28623	0.119873
O	4.044364	-0.12542	-0.15181
H	4.21738	0.266588	-1.16881
C	3.118823	-1.33277	-0.2223
H	2.951933	-1.68837	0.803734
H	1.793274	-0.92426	-0.83569
O	1.968485	-0.59062	-1.86907
O	2.238268	1.368247	0.065746
H	2.441438	1.77955	-0.93456
O	1.204291	0.248083	-0.05703
H	0.908369	-0.09541	0.942787
O	1.779839	2.486714	0.983014
H	0.851747	2.918541	0.604439
O	1.591653	2.064315	1.979823
H	3.438144	0.867647	0.634906
O	3.776437	-2.31425	-0.99361
C	3.167216	-3.04746	-1.12959
H	0.966306	-2.0722	-0.83578
H	0.080227	-1.79673	-1.10511
O	2.734906	3.517687	1.038098
H	3.572255	3.114846	1.291995
E(elec)	-1297.743289	au	
ZPVE	0.368328234	au	
G correction (873K)	0.094074357	au	

TS: CB4’5’Mac		M06-2X/6-311++G(d,p)	
O	0.096612	0.710456	-0.75429
C	-1.12725	0.537777	-0.14374
C	-1.09107	0.83136	0.919314
C	-2.17843	1.342909	-0.88879
H	-2.2362	0.949288	-1.91202

H	-3.52287	1.163656	-0.18701
H	-3.46454	1.724618	0.750383
C	-2.72449	-1.20671	0.28336
C	-3.12052	-0.88643	1.660385
C	-3.81692	-0.29152	0.154913
C	-4.81604	-0.63333	-0.10671
C	-2.89858	-2.68223	0.050408
H	-3.91173	-2.98278	0.326295
H	-2.7497	-2.91493	-1.01424
H	-1.46413	-0.82948	-0.24203
H	-1.80762	2.696342	-0.87136
C	-2.48288	3.192036	-1.34531
H	-4.50347	1.720104	-1.04215
C	-5.25927	2.006193	-0.52245
H	-4.08381	-0.21156	1.963085
H	-4.84596	-0.68447	2.33017
O	-2.01775	-3.45525	0.841732
H	-1.11681	-3.16051	0.668878
O	5.247375	-0.49514	0.559127
H	5.52522	-1.3681	0.258686
O	4.056634	-0.20139	-0.09268
H	4.247242	0.126106	-1.12909
C	3.112237	-1.39619	-0.10214
H	2.932658	-1.68938	0.941375
H	1.795239	-1.00565	-0.74605
O	1.97953	-0.73235	-1.79561
O	2.273983	1.328085	0.012637
H	2.492579	1.659822	-1.01317
O	1.224856	0.216881	-0.03607
H	0.932265	-0.06215	0.98506
O	1.820562	2.518894	0.835655
H	0.923202	2.949597	0.388058
O	1.583095	2.171803	1.851483
H	3.46093	0.846547	0.627111
O	3.758094	-2.4327	-0.80969
C	3.130633	-3.15541	-0.91665
H	0.950958	-2.13718	-0.68324
H	0.057477	-1.85031	-0.91777
O	2.809514	3.520378	0.861526
H	3.627315	3.102007	1.151479

E(elec)	-1297.731556	au
ZPVE	0.367073561	au
G correction (873K)	0.087703242	au

TS: CB6’5’Mac		M06-2X/6-311++G(d,p)	
O	0.168269	0.744777	-0.6232
C	-1.07157	0.4813	-0.0589
C	-1.03376	0.58144	1.037812
C	-2.07244	1.46651	-0.64869
H	-2.06538	1.337413	-1.73883
H	-3.46378	1.163952	-0.11729
H	-3.47473	1.328947	0.969118
C	-2.72806	-1.1612	0.203146
C	-2.61481	-1.56026	1.77196
C	-3.8191	-0.29173	-0.37919
C	-3.88926	-0.42161	-1.47236
C	-2.93905	-2.56951	0.360547
H	-3.96907	-2.90542	0.321852
H	-2.20614	-3.27249	-0.03143
H	-1.46737	-0.83432	-0.39338
H	-1.76736	2.798494	-0.29184
C	-0.95285	3.052759	-0.73575
H	-4.44196	1.965833	-0.74772
C	-4.19451	2.887545	-0.62169
H	-5.04588	-0.63761	0.225052
H	-5.69576	0.01593	-0.05449
O	-2.667	-2.65389	2.025601
H	-1.79211	-3.01669	2.237629
O	5.359851	-0.63994	0.263926
H	5.584831	-1.51607	-0.06961
O	4.119102	-0.31061	-0.26468
H	4.215675	0.039321	-1.30668
C	3.150068	-1.48069	-0.20064
H	3.055688	-1.7757	0.85365
H	1.789679	-1.06037	-0.72488
O	1.885563	-0.79174	-1.78764
O	2.389994	1.25512	0.048782
H	2.526514	1.641636	-0.97237
O	1.303409	0.176538	0.026718
H	1.042202	-0.1065	1.055969
O	2.042467	2.401424	0.980469

H	1.099718	2.85724	0.675298
O	1.92202	1.997461	1.995015
H	3.614724	0.729551	0.533335
O	3.703346	-2.53033	-0.96509
C	3.039873	-3.22517	-1.03481
H	0.940621	-2.17813	-0.57715
H	0.027893	-1.88928	-0.73356
O	3.02926	3.403025	0.944605
H	3.872006	2.97709	1.135416
E(elec)	-1297.751751	au	
ZPVE	0.369372569	au	
G correction (873K)	0.096849794	au	

Water		M06-2X/6-311++G(d,p)	
O	0	0	0.116592
H	0	0.761649	-0.46637
H	0	-0.76165	-0.46637
E(elec)	-76.420889	au	
ZPVE	0.02162761	au	
G correction (873K)	0.00333169	au	

Product: CB12Mac		M06-2X/6-311++G(d,p)	
O	0.343714	-1.09892	0.15719
C	-2.40707	1.058934	-0.54827
C	-0.93175	-0.77329	-0.29364
C	-1.95517	-1.60505	0.459659
H	-2.46882	0.845247	-1.62536
H	-1.00673	-0.95701	-1.38036
H	-1.82831	-1.40595	1.531666
C	2.587754	-1.0782	-0.69814
C	1.34632	-0.25203	-0.39777
C	1.61997	0.930975	0.543016
C	2.821342	0.690994	1.398015
C	3.525442	-0.4366	1.371542
H	0.984899	0.172283	-1.34178
H	0.756225	1.032393	1.206071
H	4.335412	-0.65217	2.059433
C	-3.34485	-1.17212	0.018727
H	-3.4632	-1.42213	-1.04649
C	-3.53209	0.331359	0.179264
H	-3.48046	0.575647	1.250422
H	2.284144	-2.02616	-1.14579

O	-1.83922	-2.98277	0.17707
H	-0.97218	-3.28131	0.469282
O	-4.35529	-1.80394	0.776985
H	-4.22646	-2.75577	0.70839
O	-4.76001	0.74703	-0.37107
H	-5.44789	0.181957	-0.00304
C	-2.38499	2.560743	-0.33991
H	-3.30358	2.995359	-0.73409
H	-2.33463	2.764773	0.73849
O	-1.16447	0.589202	-0.03659
O	-1.30343	3.146325	-1.0263
H	-0.48417	2.721548	-0.73851
O	1.746931	2.102811	-0.25521
H	2.115706	2.800428	0.297982
O	3.057112	1.751959	2.236689
H	3.871324	1.619534	2.730636
O	3.297614	-1.45563	0.486178
C	3.544886	-0.36327	-1.64837
H	3.036624	-0.16872	-2.59435
H	3.855366	0.599966	-1.22794
O	4.656602	-1.18231	-1.9353
H	5.001509	-1.50466	-1.09653
E(elec)	-1221.409922	au	
ZPVE	0.348281022	au	
G correction (873K)	0.088490969	au	

Product: CB21Mac		M06-2X/6-311++G(d,p)	
O	-0.3821	-0.87374	-0.31634
C	2.560827	1.108963	0.018168
C	0.871085	-0.51046	0.171138
C	1.831218	-1.6581	-0.10937
H	2.471431	1.235824	1.107802
H	0.809723	-0.30293	1.252373
H	1.829262	-1.84021	-1.19169
C	-2.72208	-0.82364	-0.38432
C	-1.48729	-0.15615	0.205902
C	-1.47296	1.341134	-0.1334
C	-2.86508	1.897364	-0.09468
C	-3.93134	1.124455	0.120552
H	-1.51452	-0.26156	1.301294
H	-1.01167	1.460853	-1.11717

H	-3.0117	2.962976	-0.20764
C	3.22582	-1.2557	0.337113
H	3.216247	-1.13562	1.430964
C	3.639549	0.073012	-0.27973
H	3.722431	-0.05438	-1.36875
H	-2.75313	-0.66399	-1.46882
O	1.489242	-2.8278	0.606331
H	0.631463	-3.13177	0.29542
O	4.194019	-2.21606	-0.03335
H	3.92978	-3.06368	0.338746
O	4.859127	0.518313	0.267749
H	5.48686	-0.20918	0.200756
C	2.793615	2.467836	-0.60385
H	3.787006	2.823651	-0.32706
H	2.748683	2.360426	-1.6964
O	1.323979	0.630373	-0.5085
O	1.847878	3.403746	-0.14111
H	0.995975	2.958194	-0.02969
O	-0.62088	2.052465	0.769308
H	-1.1592	2.388452	1.492727
O	-5.17054	1.600938	0.304581
H	-5.79668	0.875175	0.208827
O	-3.89809	-0.22798	0.184365
C	-2.80753	-2.30482	-0.06959
H	-1.97261	-2.81363	-0.54889
H	-2.73097	-2.44382	1.017286
O	-3.98743	-2.87795	-0.58043
H	-4.73505	-2.42658	-0.17855
E(elec)	-1221.427569		au
ZPVE	0.348342807		au
G correction (873K)	0.091215326		au

Product: CB23Mac		M06-2X/6-311++G(d,p)	
O	-0.35972	-0.5713	-0.64209
C	2.577029	1.03417	0.604467
C	0.862839	-0.51171	0.005861
C	1.837287	-1.42314	-0.72132
H	2.483506	0.732992	1.657032
H	0.763892	-0.8137	1.062069
H	1.878657	-1.10833	-1.7719
C	-2.59611	-0.93426	0.10829

C	-1.44997	0.068192	0.033461
C	-1.87646	1.304485	-0.72246
C	-3.15783	1.554787	-0.97731
C	-4.24616	0.634918	-0.51589
H	-1.12756	0.358441	1.042994
H	-3.45184	2.445674	-1.51757
H	-4.633	0.030963	-1.35386
C	3.210018	-1.27388	-0.08843
H	3.155082	-1.62769	0.952211
C	3.643641	0.184567	-0.07915
H	3.753652	0.519936	-1.12118
H	-2.71256	-1.40003	-0.88152
O	1.46873	-2.77946	-0.60468
H	0.64879	-2.91821	-1.0887
O	4.194117	-1.99776	-0.79446
H	3.913097	-2.91773	-0.84118
O	4.848532	0.348937	0.629637
H	5.478838	-0.29223	0.282942
C	2.858116	2.521997	0.536996
H	3.814375	2.719603	1.021028
H	2.930928	2.82303	-0.51656
O	1.327322	0.822657	-0.05869
O	1.876039	3.265458	1.220216
H	1.037268	3.16934	0.75797
O	-0.8979	2.164622	-1.08681
H	-0.03401	1.737383	-0.98642
O	-5.26478	1.400256	0.037289
H	-5.98224	0.81158	0.29062
O	-3.78672	-0.27089	0.478791
C	-2.3531	-2.00974	1.149191
H	-1.42685	-2.54232	0.922397
H	-2.25084	-1.52906	2.131663
O	-3.39098	-2.96047	1.153479
H	-4.21211	-2.47843	1.294128
E(elec)	-1221.426054	au	
ZPVE	0.348103855	au	
G correction (873K)	0.087858397	au	
Product: CB32Mac		M06-2X/6-311++G(d,p)	
O	-0.20599	0.680062	0.576587
C	2.63398	-1.11589	-0.62449

C	1.036637	0.511212	-0.00814
C	2.045719	1.302773	0.809579
H	2.612824	-0.74062	-1.65806
H	1.024945	0.873292	-1.05212
H	2.012227	0.929133	1.840919
C	-2.40686	1.111168	-0.19323
C	-1.29168	0.071986	-0.13334
C	-1.7449	-1.17877	0.559103
C	-3.03017	-1.39724	0.814781
C	-4.09529	-0.39546	0.431311
H	-0.95094	-0.16436	-1.15092
H	-0.99191	-1.89972	0.853634
H	-4.39497	0.183157	1.320907
C	3.429582	1.08196	0.228827
H	3.451517	1.498247	-0.78967
C	3.739932	-0.40376	0.148489
H	3.776954	-0.80704	1.171126
H	-2.50488	1.572238	0.800198
O	1.787365	2.689733	0.758278
H	0.935321	2.854288	1.174344
O	4.436252	1.68158	1.017364
H	4.22105	2.614996	1.114992
O	4.957906	-0.63074	-0.52264
H	5.62229	-0.06593	-0.11342
C	2.801435	-2.62153	-0.64773
H	3.743402	-2.86953	-1.13603
H	2.831659	-2.99058	0.385887
O	1.377446	-0.85763	0.002438
O	1.765911	-3.23642	-1.38107
H	0.932544	-2.96682	-0.98276
O	-3.47571	-2.48503	1.486225
H	-4.39363	-2.63996	1.231054
O	-5.1774	-1.12004	-0.06412
H	-5.91826	-0.52569	-0.21282
O	-3.63584	0.491004	-0.55452
C	-2.14777	2.186698	-1.22797
H	-1.20021	2.682142	-1.00679
H	-2.0732	1.712957	-2.21586
O	-3.15145	3.174928	-1.21088
H	-3.98834	2.731281	-1.37908

E(elec)	-1221.420834	au
ZPVE	0.348042514	au
G correction (873K)	0.086209204	au

Product: CB34Mac		M06-2X/6-311++G(d,p)	
O	-0.21314	-0.96791	-0.45734
C	2.571709	1.205263	0.021609
C	0.987638	-0.51907	0.095257
C	2.027103	-1.60501	-0.1443
H	2.442426	1.338314	1.106514
H	0.846271	-0.3404	1.174066
H	2.090576	-1.7793	-1.22604
C	-2.57064	-1.08931	-0.52962
C	-1.35667	-0.27572	-0.15196
C	-1.42791	0.936481	0.391952
C	-2.765	1.568975	0.655416
C	-3.8179	0.891665	-0.20366
H	-0.54862	1.533408	0.60489
H	-3.06277	1.437747	1.70477
H	-3.62931	1.125167	-1.2631
C	3.367016	-1.11688	0.37392
H	3.293365	-0.99848	1.465611
C	3.723653	0.234264	-0.22733
H	3.860467	0.110823	-1.31166
H	-2.63997	-1.15452	-1.62605
O	1.726784	-2.79675	0.550376
H	0.903424	-3.15443	0.204608
O	4.413549	-2.01052	0.055369
H	4.184117	-2.87581	0.40972
O	4.890345	0.753313	0.368701
H	5.555786	0.056967	0.351465
C	2.783648	2.567197	-0.59354
H	3.79242	2.91287	-0.34715
H	2.684711	2.47477	-1.68135
O	1.385107	0.661247	-0.54483
O	1.794171	3.4211	-0.0498
H	1.679337	4.18522	-0.61687
O	-2.67808	2.943082	0.335817
H	-3.53051	3.339906	0.540673
O	-5.06249	1.346753	0.208356
H	-5.74065	0.984102	-0.3688

O	-3.75744	-0.50634	-0.01466
C	-2.5242	-2.49932	0.049335
H	-1.70195	-3.05334	-0.40239
H	-2.35711	-2.42677	1.132108
O	-3.70779	-3.1999	-0.24479
H	-4.44085	-2.6602	0.068914
E(elec)	-1221.41579		au
ZPVE	0.347179591		au
G correction (873K)	0.081298779		au
Product: CB43Mac		M06-2X/6-311++G(d,p)	
C	1.272587	-0.4223	0.4877
C	0.206119	-1.47361	0.361078
C	-1.02801	-1.17468	-0.03479
C	-1.42602	0.241684	-0.36126
C	-0.45637	1.186682	0.324451
H	0.461606	-2.49802	0.607818
H	-1.361	0.417291	-1.44315
H	-0.57375	1.110552	1.416729
H	1.546069	-0.27713	1.544126
O	-1.99757	-2.10658	-0.18574
H	-2.84898	-1.6507	-0.17898
O	-2.7549	0.421002	0.092444
H	-3.0466	1.300601	-0.16546
O	-0.73799	2.468249	-0.13155
H	-0.16829	3.096751	0.321354
O	0.853988	0.838875	-0.0413
C	2.530018	-0.78208	-0.28947
H	2.947893	-1.71161	0.10139
H	2.254341	-0.93515	-1.34037
O	3.52062	0.209872	-0.15347
H	3.125596	1.041839	-0.4328
E(elec)	-610.6993567		au
ZPVE	0.172199345		au
G correction (873K)	0.011395378		au
Product: CB45Mac		M06-2X/6-311++G(d,p)	
C	1.22805	-0.44936	-0.12714
C	0.36512	-1.42744	0.179333
C	-1.10674	-1.18541	0.358963
C	-1.4743	0.190475	-0.19604
C	-0.43753	1.219402	0.246949

H	0.724837	-2.44479	0.293631
H	-1.37122	-1.20037	1.429551
H	-1.46101	0.144773	-1.29451
H	-0.3631	1.257239	1.344379
O	-1.82502	-2.22541	-0.3065
H	-2.77145	-2.07253	-0.14745
O	-2.77212	0.517313	0.284043
H	-3.02454	1.380482	-0.08252
O	-0.80782	2.456042	-0.28118
H	-0.24335	3.15361	0.088281
O	0.859885	0.875146	-0.2674
C	2.697522	-0.61763	-0.39267
H	2.986246	-1.65793	-0.23089
H	2.906992	-0.35945	-1.44262
O	3.51036	0.167103	0.479688
H	3.261572	1.097125	0.356693
E(elec)	-610.6921918	au	
ZPVE	0.171550086	au	
G correction (873K)	0.008039444	au	
Product: CB65Mac		M06-2X/6-311++G(d,p)	
O	0.167087	-0.96444	0.529263
C	-2.42023	1.211586	-0.57706
C	-1.03891	-0.64619	-0.08239
C	-2.16275	-1.41107	0.596634
H	-2.35884	0.995544	-1.65409
H	-1.00166	-0.90171	-1.15683
H	-2.16807	-1.13642	1.658788
C	2.217052	-1.57122	-0.5516
C	1.307362	-0.43354	-0.12303
C	2.03593	0.552221	0.786738
C	3.394181	0.892465	0.196927
C	4.178768	-0.37073	-0.09216
H	1.002074	0.123679	-1.01943
H	2.182542	0.075653	1.766232
H	3.252354	1.417868	-0.75738
H	4.348565	-0.94731	0.829371
C	-3.4727	-0.98832	-0.04997
H	-3.45303	-1.29297	-1.10731
C	-3.64565	0.523518	0.014984
H	-3.73314	0.809504	1.073445

O	-2.04402	-2.80947	0.430452
H	-1.28943	-3.11055	0.945134
O	-4.58852	-1.56464	0.597135
H	-4.46789	-2.51983	0.600027
O	-4.78108	0.936674	-0.70954
H	-5.52724	0.41222	-0.39997
C	-2.38214	2.714256	-0.3458
H	-3.1485	3.203345	-0.94698
H	-2.59166	2.90758	0.715047
O	-1.2595	0.724596	0.079617
O	-1.12966	3.237355	-0.71888
H	-0.45531	2.726078	-0.24839
O	1.2679	1.728281	0.920747
H	1.80997	2.359352	1.408054
O	4.052968	1.713194	1.136229
H	4.903927	1.970727	0.767641
O	5.371684	0.010534	-0.68332
H	5.907669	-0.7701	-0.85186
O	3.454987	-1.17873	-1.01055
C	1.865192	-2.84824	-0.59468
H	0.868526	-3.1491	-0.30944
H	2.567719	-3.58887	-0.95299
E(elec)	-1221.422204	au	
ZPVE	0.347637337	au	
G correction (873K)	0.08841564	au	
Product: CB1’2’Mac		M06-2X/6-311++G(d,p)	
C	-0.48684	-1.71817	0.20067
H	-0.61803	-2.77599	0.380203
C	-1.49882	-0.90605	-0.09344
C	-1.3062	0.568258	-0.30251
H	-1.34223	0.809749	-1.37431
C	1.09297	-0.0195	-0.25567
H	1.044513	-0.09223	-1.35136
C	0.049325	0.978784	0.238167
H	0.006615	0.944546	1.334563
C	2.505314	0.321976	0.177336
H	2.817362	1.256552	-0.29239
H	2.518727	0.448866	1.269751
O	0.818823	-1.30576	0.295645
O	-2.76877	-1.38122	-0.24649

H	-3.36945	-0.6777	0.028678
O	-2.37166	1.226148	0.364425
H	-2.31753	2.163728	0.156471
O	0.289739	2.296182	-0.22615
H	0.942738	2.725285	0.331544
O	3.420634	-0.66543	-0.22931
H	3.072726	-1.51401	0.064494
E(elec)	-610.6858885	au	
ZPVE	0.171768184	au	
G correction (873K)	0.010343062	au	
Product: CB2’1’Mac		M06-2X/6-311++G(d,p)	
O	-0.00325	0.87496	-1.01548
C	-1.25876	0.704552	-0.55352
C	-2.17136	1.666735	-0.45267
H	-1.90189	2.686713	-0.68731
C	-3.58294	1.354595	-0.04697
H	-3.76777	1.714678	0.975804
C	-2.62348	-0.84006	0.600983
H	-2.41784	-0.40361	1.586949
C	-3.82245	-0.15153	-0.03859
H	-3.91296	-0.48737	-1.08013
C	-2.70869	-2.34839	0.719381
H	-3.52698	-2.61442	1.390629
H	-2.91522	-2.7736	-0.27387
O	-1.49046	-0.59901	-0.24198
O	-4.47045	2.001949	-0.93805
H	-5.36292	1.858339	-0.60692
O	-5.02397	-0.37142	0.677898
H	-5.4149	-1.20759	0.414398
O	-1.53272	-2.88444	1.274918
H	-0.77845	-2.63245	0.725555
O	5.003667	-0.50166	0.66469
H	5.289613	-1.37605	0.376181
C	3.870796	-0.1793	-0.0685
H	4.139959	0.137645	-1.09065
C	2.895251	-1.34651	-0.13721
H	2.643147	-1.63192	0.89338
C	1.630634	-0.92234	-0.86341
H	1.883992	-0.67158	-1.90331
C	2.131904	1.40264	-0.08928

H	2.431142	1.722293	-1.09838
C	1.051737	0.325575	-0.20399
H	0.667085	0.076796	0.791545
C	1.669417	2.611754	0.702788
H	0.814726	3.071216	0.205042
H	1.359423	2.278062	1.702501
O	3.255529	0.88612	0.606559
O	3.555226	-2.39893	-0.80428
H	2.928056	-3.11942	-0.92551
O	0.763856	-2.04401	-0.83937
H	-0.06585	-1.7909	-1.26019
O	2.686048	3.580422	0.779308
H	3.46745	3.144981	1.1365
E(elec)	-1221.417866	au	
ZPVE	0.347892487	au	
G correction (873K)	0.088219922	au	
Product: CB2’3’Mac		M06-2X/6-311++G(d,p)	
O	0.004082	0.91649	-0.56832
C	-1.17197	0.826965	0.166751
H	-0.96354	1.065543	1.223596
C	-2.20352	1.750282	-0.39808
H	-1.91622	2.77557	-0.5929
C	-3.45064	1.337197	-0.61076
C	-2.90712	-0.74459	0.618308
H	-3.00847	-0.28591	1.611122
C	-3.8933	-0.08392	-0.33896
H	-3.90922	-0.63152	-1.29162
C	-3.05968	-2.25054	0.731033
H	-4.03936	-2.49368	1.14845
H	-2.98896	-2.6898	-0.27488
O	-1.60103	-0.52771	0.110711
O	-4.40251	2.150365	-1.11619
H	-5.26209	1.77944	-0.87777
O	-5.20557	-0.00766	0.202545
H	-5.6786	-0.82558	0.033786
O	-2.09837	-2.79959	1.596394
H	-1.22458	-2.57908	1.252327
O	5.14926	-0.73275	0.171613
H	5.323177	-1.61921	-0.16527
C	3.922419	-0.33515	-0.34189

H	4.023019	-0.00323	-1.38939
C	2.887767	-1.44767	-0.25469
H	2.799694	-1.73989	0.800849
C	1.545707	-0.94203	-0.74867
H	1.635129	-0.67168	-1.81112
C	2.292597	1.332514	-0.01564
H	2.423917	1.681352	-1.05073
C	1.151716	0.312652	0.025652
H	0.9391	0.038998	1.068158
C	2.042818	2.525696	0.887756
H	1.143822	3.051017	0.562159
H	1.891425	2.161333	1.913716
O	3.49585	0.742044	0.451835
O	3.363756	-2.52389	-1.03378
H	2.668389	-3.18873	-1.0766
O	0.627384	-2.00661	-0.59718
H	-0.25845	-1.65672	-0.7633
O	3.110171	3.439301	0.826172
H	3.916956	2.943436	1.004058
E(elec)	-1221.420672	au	
ZPVE	0.348077476	au	
G correction (873K)	0.087661136	au	
Product: CB3’2’Mac		M06-2X/6-311++G(d,p)	
O	-0.07919	0.858401	-0.62819
C	-1.29707	0.779331	0.039366
H	-1.16537	1.068521	1.096416
C	-2.27116	1.711591	-0.64035
C	-3.54059	1.361492	-0.81947
H	-4.21638	2.053912	-1.31158
C	-3.07213	-0.69127	0.522244
H	-3.10558	-0.23225	1.519513
C	-4.07926	0.028907	-0.36849
H	-4.29797	-0.59411	-1.24786
C	-3.3111	-2.18239	0.644349
H	-4.3028	-2.34982	1.065252
H	-3.2753	-2.63128	-0.35818
O	-1.76054	-0.54413	-0.02008
O	-1.77929	2.926751	-0.97921
H	-0.83349	2.833081	-1.14748
O	-5.25049	0.155034	0.425996

H	-5.94657	0.561122	-0.09639
O	-2.37512	-2.78433	1.507845
H	-1.49342	-2.63224	1.149939
O	4.997406	-0.88923	0.301565
H	5.167417	-1.77568	-0.0377
C	3.795162	-0.46565	-0.24472
H	3.934937	-0.11421	-1.28139
C	2.741247	-1.56258	-0.21289
H	2.606736	-1.86826	0.833851
C	1.428128	-1.02676	-0.75261
H	1.56708	-0.74406	-1.80669
C	2.183729	1.225753	0.062271
H	2.361369	1.608248	-0.95452
C	1.026649	0.224568	0.022086
H	0.744039	-0.05965	1.044285
C	1.916192	2.389249	0.999785
H	1.019455	2.92775	0.686564
H	1.750023	1.989091	2.009541
O	3.356971	0.603225	0.55635
O	3.229095	-2.63376	-0.98977
H	2.530834	-3.29353	-1.05948
O	0.486458	-2.07397	-0.64998
H	-0.3894	-1.71695	-0.85025
O	2.979866	3.307287	0.982594
H	3.784217	2.814674	1.179789
E(elec)	-1221.418005	au	
ZPVE	0.347525137	au	
G correction (873K)	0.085547103	au	
Product: CB3’4’Mac		M06-2X/6-311++G(d,p)	
O	0.086476	0.824379	0.844219
C	1.322531	0.793721	0.213424
H	1.272927	1.257535	-0.78516
C	2.343647	1.518808	1.070558
H	2.223137	1.167235	2.104283
C	3.718819	1.209277	0.551567
H	4.52289	1.88077	0.827354
C	2.862508	-0.76847	-0.69338
H	2.626611	-0.58895	-1.75455
C	3.954887	0.17978	-0.25778
C	3.177778	-2.25067	-0.51357

H	4.056127	-2.54332	-1.09465
H	3.387979	-2.43517	0.54761
O	1.698044	-0.56248	0.086072
O	2.142539	2.917027	1.001436
H	1.325097	3.124403	1.464373
O	5.192877	-0.01815	-0.78922
H	5.239751	-0.85829	-1.25117
O	2.116924	-3.03994	-0.98798
H	1.299392	-2.75906	-0.55736
O	-4.90933	-0.78577	-0.6357
H	-5.14706	-1.65911	-0.30365
C	-3.77565	-0.38221	0.055156
H	-4.03612	-0.03442	1.069599
C	-2.7479	-1.50344	0.151358
H	-2.50294	-1.82345	-0.87057
C	-1.49482	-0.98729	0.831441
H	-1.74515	-0.6938	1.861457
C	-2.10928	1.276726	-0.03729
H	-2.39711	1.633734	0.962956
C	-0.98609	0.248909	0.097774
H	-0.63512	-0.04589	-0.89926
C	-1.71611	2.462143	-0.89869
H	-0.85653	2.969816	-0.45725
H	-1.43403	2.092431	-1.89438
O	-3.22751	0.683145	-0.67806
O	-3.34996	-2.55342	0.876538
H	-2.6865	-3.23464	1.028688
O	-0.55699	-2.04673	0.850044
H	0.281795	-1.6882	1.16724
O	-2.76239	3.397984	-0.97961
H	-3.54248	2.926221	-1.29101
E(elec)	-1221.416808	au	
ZPVE	0.347892313	au	
G correction (873K)	0.088042985	au	

Product: CB4’3’Mac		M06-2X/6-311++G(d,p)	
O	-0.21298	0.732287	-0.69165
C	-1.40774	0.54304	-0.00995
H	-1.36299	0.97922	1.001606
C	-2.52126	1.187154	-0.81376
H	-2.43425	0.846535	-1.85379

C	-3.85038	0.751533	-0.2421
C	-2.78092	-1.16909	0.889937
H	-2.49934	-1.00148	1.94076
C	-3.97183	-0.32961	0.525008
H	-4.9413	-0.59701	0.929305
C	-2.98566	-2.66181	0.695077
H	-3.84725	-2.98896	1.279734
H	-3.19193	-2.85226	-0.3659
O	-1.65308	-0.83783	0.073809
O	-2.47758	2.60011	-0.74834
H	-1.72355	2.911203	-1.25787
O	-4.9063	1.521996	-0.58959
H	-4.56799	2.386059	-0.85778
O	-1.87477	-3.39573	1.154451
H	-1.08238	-3.07992	0.705262
O	5.010719	-0.41946	0.364073
H	5.290779	-1.2727	0.012794
C	3.78796	-0.12045	-0.21919
H	3.924649	0.267033	-1.24333
C	2.866952	-1.33298	-0.25159
H	2.736659	-1.6842	0.781119
C	1.518723	-0.93474	-0.82098
H	1.656749	-0.60327	-1.86102
C	1.982553	1.365948	0.050752
H	2.149184	1.771816	-0.95851
C	0.952797	0.238533	-0.02745
H	0.693408	-0.1	0.98383
C	1.550036	2.487517	0.976762
H	0.609623	2.915558	0.624524
H	1.393348	2.069339	1.980698
O	3.202911	0.87517	0.581748
O	3.503778	-2.3147	-1.0397
H	2.898347	-3.05616	-1.14437
O	0.695047	-2.08222	-0.78718
H	-0.21283	-1.80059	-0.96193
O	2.501679	3.522281	0.997587
H	3.348213	3.124328	1.227999
E(elec)	-1221.425174		au
ZPVE	0.348057319		au
G correction (873K)	0.089348799		au

Product: CB4’5’Mac		M06-2X/6-311++G(d,p)	
O	0.203654	-0.64544	-0.6774
C	1.388748	-0.44017	-0.01521
H	1.290392	-0.64316	1.061999
C	2.490492	-1.28681	-0.61859
H	2.631556	-0.97136	-1.66076
C	3.78363	-1.0285	0.147837
H	3.724009	-1.58695	1.092213
C	2.976575	1.314462	0.255031
C	3.964209	0.439078	0.427169
H	4.918842	0.790342	0.800983
C	3.014796	2.797246	0.480783
H	3.977796	3.082169	0.902855
H	2.898021	3.303485	-0.48696
O	1.728572	0.943083	-0.16923
O	2.105651	-2.63456	-0.53075
H	2.831079	-3.16468	-0.87645
O	4.814622	-1.58457	-0.65871
H	5.631621	-1.62416	-0.15539
O	2.016977	3.20939	1.389481
H	1.15402	2.974059	1.029657
O	-5.04169	0.371123	0.396416
H	-5.33698	1.237442	0.093283
C	-3.81132	0.128436	-0.19926
H	-3.93845	-0.18745	-1.2489
C	-2.90967	1.355017	-0.14264
H	-2.79426	1.636687	0.913112
C	-1.54949	1.018716	-0.7244
H	-1.67005	0.767426	-1.7882
C	-1.98793	-1.34602	-0.03061
H	-2.14665	-1.66867	-1.07019
C	-0.97622	-0.19987	-0.01085
H	-0.74397	0.068933	1.028468
C	-1.53433	-2.53358	0.797506
H	-0.60331	-2.92953	0.388489
H	-1.35572	-2.19248	1.827484
O	-3.21646	-0.91054	0.533476
O	-3.55407	2.379659	-0.86777
H	-2.9512	3.128132	-0.92689
O	-0.74353	2.174132	-0.5896

H	0.146543	1.946262	-0.88731
O	-2.49204	-3.56451	0.765781
H	-3.3338	-3.17689	1.028381
E(elec)	-1221.418035	au	
ZPVE	0.347975964	au	
G correction (873K)	0.086749744	au	
Product: CB6’5’Mac		M06-2X/6-311++G(d,p)	
O	-0.04252	0.471718	-0.60902
C	-1.24415	0.255179	0.031923
H	-1.19226	0.556554	1.089614
C	-2.31847	1.042496	-0.70185
H	-2.31522	0.724459	-1.75237
C	-3.66965	0.736564	-0.08291
H	-3.66962	1.079146	0.961875
C	-2.76484	-1.47951	0.54086
C	-3.92531	-0.7661	-0.1009
H	-3.97687	-1.08047	-1.1547
C	-2.84006	-2.37441	1.510983
H	-3.80908	-2.65688	1.897223
H	-1.94198	-2.8361	1.900697
O	-1.54504	-1.14003	-0.03016
O	-2.10833	2.431871	-0.58584
H	-1.31608	2.665595	-1.07958
O	-4.72341	1.341829	-0.79896
H	-4.5634	2.29108	-0.82236
O	-5.11357	-1.08615	0.572142
H	-5.80729	-0.52751	0.20542
O	5.262365	-0.35841	0.270683
H	5.556591	-1.23746	0.005112
C	3.985471	-0.18424	-0.24379
H	4.026299	0.097851	-1.30971
C	3.132196	-1.43023	-0.07155
H	3.084693	-1.65566	1.002605
C	1.727942	-1.17597	-0.59042
H	1.780672	-0.97862	-1.67182
C	2.127625	1.235675	0.000426
H	2.211886	1.552892	-1.05012
C	1.144305	0.064333	0.078905
H	0.910179	-0.16428	1.127146
C	1.690509	2.415763	0.848386

H	0.702368	2.756123	0.533942
H	1.631044	2.08744	1.895159
O	3.4017	0.860371	0.49372
O	3.764846	-2.47642	-0.77514
H	3.177149	-3.23964	-0.75877
O	0.994773	-2.35301	-0.34028
H	0.050713	-2.17327	-0.44988
O	2.575197	3.499359	0.703475
H	3.45868	3.172326	0.905208
E(elec)	-1221.424253		au
ZPVE	0.347637337		au
G correction (873K)	0.088275995		au

TS: GLC12Pin		M06-2X/6-311++G(d,p)	
O	-2.20508	-2.51517	0.058274
H	-2.46547	-3.1353	-0.6279
C	-0.76593	-0.96079	-0.34084
H	-0.91729	-1.15132	-1.40608
C	-1.62545	-0.0213	0.336503
H	-1.37882	0.007995	1.416857
C	-0.73765	1.250187	-0.25966
H	-0.78204	1.245032	-1.35749
C	1.346468	-0.10179	-0.25429
H	1.43884	-0.11292	-1.34692
C	0.707108	1.208759	0.20664
H	0.724853	1.26016	1.303789
C	2.678132	-0.40957	0.388141
H	3.367835	0.396486	0.133467
H	2.54868	-0.43307	1.477036
O	0.440811	-1.19048	0.148754
O	-2.87944	0.057296	-0.02343
H	-2.84986	-1.75958	0.031478
O	-1.38061	2.37759	0.24456
H	-2.33203	2.189705	0.169936
O	1.472117	2.250232	-0.35842
H	1.008158	3.077768	-0.19085
O	3.22426	-1.61029	-0.09814
H	2.644552	-2.33136	0.164874
E(elec)	-687.0166155		au
ZPVE	0.194487153		au
G correction (873K)	0.017430426		au

TS: GLC21Pin		M06-2X/6-311++G(d,p)	
O	1.422501	-2.58949	0.09715
H	3.170284	-1.31472	0.006259
C	0.872991	-1.53023	0.427994
H	0.484799	-1.37994	1.449907
C	1.28431	-0.29635	-0.2909
H	1.427144	-0.43211	-1.35715
C	0.90714	1.067415	0.191644
H	1.024632	1.121811	1.28173
C	-1.29935	-0.01104	0.227003
H	-1.28891	-0.1336	1.323403
C	-0.56959	1.279934	-0.14329
H	-0.64714	1.425768	-1.22987
C	-2.74193	-0.04946	-0.25614
H	-3.34576	0.696607	0.268688
H	-2.75665	0.174432	-1.33288
O	-0.60795	-1.0484	-0.41463
O	3.046089	-0.35245	0.133442
H	3.589102	0.148758	-0.48815
O	1.749332	2.004291	-0.44662
H	1.438922	2.883736	-0.20551
O	-0.96152	2.447676	0.552406
H	-1.80623	2.756903	0.215857
O	-3.31584	-1.30528	0.006074
H	-2.67246	-1.95999	-0.29276
E(elec)	-687.0245873	au	
ZPVE	0.195491063	au	
G correction (873K)	0.019030746	au	

TS: GLC23Pin		M06-2X/6-311++G(d,p)	
O	0.866606	2.622151	0.296089
H	0.335761	3.337865	-0.06666
C	0.46254	1.432168	-0.27196
H	0.507856	1.453027	-1.36886
C	1.298087	0.317453	0.289125
H	1.565064	0.400567	1.339383
C	1.222187	-0.98001	-0.29449
H	0.974596	-0.94001	-1.37467
C	-1.31061	-0.15873	-0.25135
H	-1.31469	-0.24313	-1.34625
C	-0.35901	-1.18265	0.34029

H	-0.32135	-1.10634	1.433722
C	-2.7281	-0.30431	0.269931
H	-3.10365	-1.28896	-0.009
H	-2.71282	-0.22978	1.36475
O	-0.86901	1.143294	0.140375
O	3.278554	0.56316	-0.26083
H	3.852529	1.000515	0.375628
O	2.018713	-1.9228	0.109025
H	3.37908	-0.40608	-0.13536
O	-0.65497	-2.47003	-0.07005
H	0.17316	-2.97332	0.040144
O	-3.59	0.655316	-0.29863
H	-3.24537	1.523304	-0.06997
E(elec)	-687.0150602	au	
ZPVE	0.195028804	au	
G correction (873K)	0.017790641	au	

TS: GLC32Pin		M06-2X/6-311++G(d,p)	
O	0.608822	2.741565	-0.00762
H	1.583102	2.768755	0.015361
C	0.296055	1.469948	-0.39502
H	0.285208	1.364456	-1.48865
C	1.500515	0.533738	0.286426
H	1.210631	0.628302	1.350848
C	1.029969	-0.69579	-0.28387
H	1.3322	-0.92805	-1.30272
C	-1.31118	-0.19711	-0.23455
H	-1.41653	-0.26195	-1.32576
C	-0.2344	-1.27852	0.189637
H	-0.25661	-1.37401	1.279723
C	-2.64606	-0.4891	0.429395
H	-2.96331	-1.49921	0.172011
H	-2.51351	-0.41746	1.516948
O	-0.92401	1.090429	0.158062
O	2.703724	0.94746	-0.04621
H	3.183863	-0.71472	0.251311
O	2.838232	-1.6505	0.358004
H	3.323171	-2.19168	-0.27156
O	-0.60967	-2.46728	-0.46041
H	-0.10578	-3.19796	-0.09182
O	-3.63376	0.397355	-0.02997

H	-3.33856	1.292328	0.167333
E(elec)	-687.0191387	au	
ZPVE	0.194610959	au	
G correction (873K)	0.019026007	au	
TS: GLC34Pin		M06-2X/6-311++G(d,p)	
O	-0.60993	2.814724	-0.52653
H	-0.02029	3.518289	-0.23944
C	-0.30964	1.649712	0.155036
H	-0.27796	1.812936	1.242968
C	-1.48145	0.660934	-0.14625
H	-1.64963	0.680235	-1.22776
C	-0.99396	-0.65773	0.298062
H	-1.19839	-0.94437	1.326783
C	1.158284	-0.14225	0.291663
H	1.123958	-0.09953	1.386963
C	0.112029	-1.31914	-0.3436
H	0.188914	-1.05744	-1.41811
C	2.533914	-0.60884	-0.15087
H	2.695596	-1.61156	0.238844
H	2.558338	-0.64184	-1.24623
O	0.902642	1.115977	-0.28555
O	-2.6209	1.034363	0.581493
H	-2.90594	1.896816	0.262604
O	-2.27168	-2.2588	-0.29185
H	-2.89805	-2.57652	0.364111
O	0.35255	-2.54588	0.016587
H	-1.4326	-2.78468	-0.1849
O	3.534028	0.239603	0.366807
H	3.407318	1.111625	-0.01772
E(elec)	-687.0179216	au	
ZPVE	0.194381271	au	
G correction (873K)	0.016681771	au	
TS: GLC43Pin		M06-2X/6-311++G(d,p)	
O	0.92181	-2.78952	-0.225
H	1.877487	-2.89333	-0.15291
C	0.601003	-1.53534	0.277555
H	0.633074	-1.52661	1.378443
C	1.511278	-0.45038	-0.27874
H	1.469039	-0.45622	-1.37392
C	1.093943	1.076412	0.304027

H	1.048278	0.871258	1.393736
C	-1.18816	-0.00253	0.271499
H	-1.18847	0.046358	1.366758
C	-0.194	0.963726	-0.308
H	-0.26042	1.185998	-1.37072
C	-2.60069	0.141708	-0.2627
H	-3.01406	1.098942	0.058971
H	-2.56643	0.116677	-1.36002
O	-0.71929	-1.28012	-0.16053
O	2.809931	-0.61873	0.179443
H	3.249227	0.241127	0.055422
O	1.928209	1.98974	-0.10357
H	0.353155	3.098276	0.048624
O	-0.62542	2.973845	0.117685
H	-1.02324	3.527879	-0.56088
O	-3.42686	-0.86971	0.250559
H	-3.02489	-1.7159	0.02599
E(elec)	-687.0120624	au	
ZPVE	0.194838779	au	
G correction (873K)	0.018299378	au	
Product: GLC12Pin		M06-2X/6-311++G(d,p)	
C	-0.9507530	-0.5411890	-0.6052200
H	-0.9795250	-0.5824230	-1.7063360
C	-2.0863880	-1.3905040	-0.0930420
H	-1.8103000	-2.4083780	0.2370060
C	-0.9923070	0.9412020	-0.1578690
H	-1.3611420	1.5794960	-0.9664070
C	1.2313930	-0.0269310	-0.2947490
H	1.5151810	0.0579410	-1.3535950
C	0.4941510	1.2468870	0.1199990
H	0.5906310	1.4056680	1.2008390
C	2.4416080	-0.3672500	0.5424030
H	3.1780350	0.4330250	0.4501550
H	2.1323000	-0.4441110	1.5931640
O	0.2732210	-1.0685960	-0.1365490
O	-3.2198140	-0.9919090	-0.0547470
O	-1.7118350	1.1603370	1.0335320
H	-2.6323670	0.9149010	0.8865830
O	1.0264450	2.3277360	-0.6103720
H	0.7319620	3.1513220	-0.2137520

O	3.0589070	-1.5563020	0.1032750
H	2.3936110	-2.2508640	0.1221010
E(elec)	-610.6861839	au	
ZPVE	0.17072301	au	
G correction (873K)	0.004220631	au	
Product: GLC21Pin		M06-2X/6-311++G(d,p)	
O	3.133522	-1.1916	0.204757
C	1.988981	-1.55952	0.243241
H	1.693392	-2.51981	0.704528
C	0.879944	-0.71032	-0.32679
H	0.935659	-0.76579	-1.42499
C	1.006212	0.755191	0.097924
H	1.243686	0.81323	1.169037
C	-1.23736	0.012554	0.337931
H	-1.47005	0.097355	1.40397
C	-0.42322	1.227767	-0.10583
H	-0.56515	1.416623	-1.18037
C	-2.50804	-0.21002	-0.45286
H	-3.17932	0.639505	-0.30983
H	-2.25544	-0.28137	-1.52023
O	-0.38075	-1.13516	0.152601
O	1.906633	1.507581	-0.66783
H	2.792146	1.157455	-0.51641
O	-0.79264	2.349459	0.654539
H	-0.29008	3.10686	0.340376
O	-3.18879	-1.36293	-0.01463
H	-2.56786	-2.09677	-0.06327
E(elec)	-610.6872943	au	
ZPVE	0.170265771	au	
G correction (873K)	0.001553707	au	
Product: GLC23Pin		M06-2X/6-311++G(d,p)	
O	0.308817	2.348779	-0.09969
H	0.750242	2.920499	0.535505
C	-0.1265	1.192556	0.561367
H	-0.72413	1.462381	1.439153
C	-0.89358	0.332433	-0.45472
H	-0.56042	0.664596	-1.4466
C	-2.38288	0.541104	-0.4249
H	-2.71589	1.59605	-0.39468
C	1.016317	-0.83606	0.298326

H	1.330687	-1.5986	1.012277
C	-0.40693	-1.0946	-0.18066
H	-0.42727	-1.71354	-1.08466
C	2.034071	-0.71175	-0.8268
H	2.180479	-1.68491	-1.30048
H	1.671306	-0.00621	-1.5875
O	0.946823	0.405247	1.01767
O	-3.18632	-0.35425	-0.45241
O	-1.10769	-1.70622	0.877334
H	-2.03071	-1.78643	0.611767
O	3.283354	-0.30179	-0.32414
H	3.122833	0.469983	0.229397
E(elec)	-610.6993319	au	
ZPVE	0.171619059	au	
G correction (873K)	0.007827638	au	

Product: GLC32Pin		M06-2X/6-311++G(d,p)	
O	-0.45827	-1.9391	0.763734
H	0.139129	-2.68394	0.878875
C	-0.29126	-1.41542	-0.53163
H	-0.48915	-2.17904	-1.28779
C	-2.53147	-0.2897	0.025565
H	-3.083	-1.23668	-0.11762
C	-1.17031	-0.17612	-0.60974
H	-1.30414	0.104644	-1.66203
C	1.116771	0.447305	-0.38012
H	1.403949	1.008886	-1.27403
C	-0.28188	0.873594	0.063185
H	-0.38235	0.774933	1.15098
C	2.180353	0.588303	0.687482
H	2.281633	1.640603	0.961836
H	1.868046	0.020916	1.574604
O	1.013711	-0.94502	-0.74939
O	-3.0175	0.619768	0.644937
O	-0.53985	2.194042	-0.34092
H	-1.38238	2.450829	0.048999
O	3.438378	0.154099	0.221071
H	3.323273	-0.73922	-0.11773
E(elec)	-610.701193	au	
ZPVE	0.17117257	au	
G correction (873K)	0.005866875	au	

Product: GLC34Pin		M06-2X/6-311++G(d,p)	
O	0.990769	1.915338	-1.00356
H	1.714641	2.515682	-0.80495
C	0.357641	1.557042	0.193024
H	0.144752	2.435111	0.807376
C	-0.92885	0.794851	-0.14983
H	-0.91616	0.564222	-1.21938
C	-0.80652	-0.48923	0.670437
H	-1.21196	-0.29671	1.672604
C	0.71174	-0.66186	0.798875
H	1.018075	-1.20622	1.693821
C	-1.58244	-1.64477	0.097853
H	-1.37827	-2.64531	0.526771
C	1.364567	-1.2933	-0.42627
H	1.083764	-2.34821	-0.49363
H	1.024499	-0.78548	-1.3385
O	1.167028	0.684052	0.962778
O	-2.0542	1.574202	0.174898
H	-2.81925	1.179219	-0.25409
O	-2.4148	-1.50906	-0.75991
O	2.766185	-1.24714	-0.3167
H	3.003121	-0.32782	-0.15467
E(elec)	-610.6963895	au	
ZPVE	0.170966316	au	
G correction (873K)	0.005115652	au	

Product: GLC43Pin		M06-2X/6-311++G(d,p)	
O	1.374176	1.968168	-0.28657
H	1.982394	2.390484	0.326213
C	0.344834	1.357033	0.445523
H	-0.06552	2.03448	1.196877
C	-0.7426	0.90524	-0.54314
H	-0.44641	1.205781	-1.55172
C	-1.92716	-1.07536	0.433792
H	-1.75476	-1.10489	1.527443
C	0.582341	-0.93673	0.276225
H	0.542071	-1.79971	0.946561
C	-0.74948	-0.64586	-0.41512
H	-0.84402	-1.12381	-1.39255
C	1.733776	-1.11955	-0.70507
H	1.599655	-2.06109	-1.24262

H	1.738484	-0.29777	-1.43197
O	0.794784	0.203055	1.116649
O	-1.95354	1.519803	-0.16593
H	-2.66975	1.183184	-0.71407
O	-2.99682	-1.35205	-0.03566
O	2.96271	-1.2016	-0.02492
H	3.017124	-0.4343	0.554053
E(elec)	-610.6955333	au	
ZPVE	0.170856903	au	
G correction (873K)	0.003815526	au	
TS: CB12Pin		M06-2X/6-311++G(d,p)	
O	0.002501	-1.08548	-0.32526
C	2.72828	1.16077	0.177625
C	1.228406	-0.65241	0.175352
C	2.292467	-1.63662	-0.29217
H	2.689277	1.152792	1.277062
H	1.192514	-0.60971	1.277598
H	2.258013	-1.67073	-1.3886
C	-2.31912	-1.41525	-0.18409
C	-1.14797	-0.50372	0.269271
C	-1.36449	0.985516	-0.05508
C	-2.8832	1.227905	0.122026
C	-3.48179	0.465321	-1.00318
H	-1.06509	-0.57171	1.363908
H	-1.0212	1.192896	-1.07657
H	-3.1351	0.656582	1.043686
H	-3.87513	0.965351	-1.88283
C	3.655325	-1.13949	0.157608
H	3.687443	-1.16272	1.257382
C	3.890958	0.294748	-0.29402
H	3.928913	0.315228	-1.39286
H	-1.90157	-2.23062	-0.77158
O	2.116025	-2.92248	0.265868
H	1.30789	-3.3008	-0.09192
O	4.700727	-1.92855	-0.37212
H	4.552321	-2.83988	-0.09979
O	5.082514	0.802874	0.258923
H	5.782485	0.170104	0.065808
C	2.779497	2.596943	-0.29503
H	3.727149	3.0423	0.01095

H	2.726247	2.602095	-1.3929
O	1.516188	0.615004	-0.34574
O	1.736211	3.347507	0.275007
H	0.935695	2.801836	0.2857
O	-0.71905	1.833782	0.860241
H	-1.3417	2.572326	0.992156
O	-3.31649	2.490263	0.170539
H	-4.73402	1.889402	0.111016
O	-5.31247	1.039493	-0.08944
H	-6.06352	1.304361	-0.62752
O	-3.21286	-0.77162	-1.16712
C	-3.16546	-2.0161	0.932079
H	-2.48669	-2.56186	1.592011
H	-3.66385	-1.241	1.521621
O	-4.08656	-2.94689	0.421828
H	-4.83139	-2.47322	0.041567
E(elec)	-1297.76531	au	
ZPVE	0.371758791	au	
G correction (873K)	0.1013489	au	

TS: CB21Pin		M06-2X/6-311++G(d,p)	
O	5.407623	-0.64686	-0.16535
H	4.613451	-2.48274	-0.8344
C	4.279651	-0.22865	-0.47027
H	4.13405	0.441892	-1.33473
C	3.121279	-1.0943	-0.12932
H	3.193115	-1.56843	0.84316
C	1.757536	-0.85482	-0.69173
H	1.837225	-0.61279	-1.75907
C	2.298506	1.408703	0.140931
H	2.527356	1.806013	-0.86171
C	1.184172	0.373739	0.035753
H	0.897852	0.060261	1.048834
C	1.930713	2.569171	1.052489
H	1.10183	3.135812	0.621702
H	1.61799	2.164259	2.02626
O	3.401282	0.740794	0.694734
O	3.665662	-2.56723	-1.07035
H	3.302327	-3.38927	-0.71863
O	0.985629	-2.02418	-0.50736
H	0.067779	-1.77635	-0.69336

O	0.052469	0.86379	-0.66744
O	3.022559	3.444139	1.199014
H	3.785356	2.891982	1.408708
C	-1.15549	0.670753	-0.03096
H	-1.11471	1.022846	1.012567
C	-2.25866	1.390373	-0.78675
H	-2.21407	1.069065	-1.83631
C	-3.6085	0.998823	-0.19755
H	-3.66256	1.388605	0.830424
C	-2.615	-1.10557	0.641422
H	-2.60475	-0.70262	1.664243
C	-3.79228	-0.51014	-0.12937
H	-3.80739	-0.91647	-1.14939
C	-2.59519	-2.6199	0.709033
H	-3.50328	-2.97613	1.199345
H	-2.56841	-3.02046	-0.31462
O	-1.42015	-0.72898	-0.03545
O	-2.0443	2.772114	-0.66229
H	-2.81099	3.218472	-1.03741
O	-4.59286	1.614518	-0.99895
H	-5.45335	1.406486	-0.62062
O	-5.03264	-0.72508	0.522855
H	-5.38759	-1.58416	0.284141
O	-1.51296	-3.09206	1.474726
H	-0.69019	-2.77311	1.085652
E(elec)	-1297.752302	au	
ZPVE	0.371932823	au	
G correction (873K)	0.098962284	au	

TS: CB23Pin		M06-2X/6-311++G(d,p)	
O	4.985395	1.110222	-0.19516
H	5.713488	0.736638	0.310714
C	3.797741	0.610018	0.293734
H	3.679518	0.774514	1.373099
C	2.669913	1.200358	-0.4929
H	2.835413	1.230814	-1.56733
C	1.317969	1.197404	-0.0524
H	1.185947	1.188614	1.044443
C	2.464153	-1.3181	0.406087
H	2.334387	-1.21542	1.492165
C	1.317948	-0.58529	-0.28363

H	1.281443	-0.73467	-1.36837
C	2.488889	-2.7931	0.039871
H	1.535151	-3.24182	0.316496
H	2.618446	-2.88309	-1.04633
O	3.719825	-0.78101	0.014569
O	2.825189	3.285364	-0.41877
H	3.357308	3.695798	-1.10712
O	0.460361	1.848398	-0.78186
H	1.889057	3.320048	-0.70542
O	0.165306	-1.04926	0.332505
O	3.503312	-3.4783	0.737197
H	4.343999	-3.08263	0.490433
C	-1.06014	-0.58925	-0.15088
H	-0.95616	-0.26607	-1.19634
C	-2.10987	-1.67924	-0.01332
H	-2.13271	-1.99836	1.037009
C	-3.46448	-1.08963	-0.39278
H	-3.44506	-0.85959	-1.46913
C	-2.58293	1.1553	0.129696
H	-2.44424	1.33456	-0.94771
C	-3.76704	0.212326	0.339757
H	-3.88432	0.008257	1.412277
C	-2.64076	2.498477	0.824133
H	-3.5737	3.010904	0.560823
H	-2.63529	2.326593	1.910426
O	-1.44316	0.490269	0.654156
O	-1.77312	-2.7494	-0.86465
H	-2.52281	-3.35407	-0.87426
O	-4.43261	-2.08651	-0.1346
H	-5.29229	-1.72215	-0.3695
O	-4.98227	0.683394	-0.22177
H	-5.32809	1.40243	0.311917
O	-1.5663	3.309915	0.432127
H	-0.84334	2.748316	0.077505
E(elec)	-1297.739567		au
ZPVE	0.371006309		au
G correction (873K)	0.097451586		au
TS: CB32Pin		M06-2X/6-311++G(d,p)	
O	5.13306	-0.86959	0.004818
H	5.088448	-1.81569	-0.21438

C	3.937764	-0.34382	-0.40295
H	3.938144	-0.10596	-1.47583
C	2.817955	-1.49092	-0.0824
H	2.844268	-1.49298	1.023436
C	1.653382	-0.79205	-0.57016
H	1.420847	-0.85093	-1.63027
C	2.449743	1.395442	-0.02883
H	2.483778	1.700195	-1.08269
C	1.201942	0.413015	0.132145
H	1.034738	0.24328	1.201313
C	2.253624	2.61842	0.854583
H	1.309975	3.100919	0.599396
H	2.223582	2.287487	1.900967
O	3.643087	0.781584	0.360431
O	3.114771	-2.64165	-0.68125
H	1.714205	-3.02915	-0.68184
O	0.6781	-2.81693	-0.56351
H	0.252933	-2.96458	-1.41289
O	0.126826	1.077208	-0.47583
O	3.281721	3.548965	0.635982
H	4.117557	3.122658	0.851427
C	-1.10231	0.780714	0.107513
H	-1.08119	1.033982	1.181761
C	-2.18971	1.576414	-0.59049
H	-2.12908	1.363152	-1.66617
C	-3.54085	1.116602	-0.06157
H	-3.61136	1.398911	1.000079
C	-2.5189	-1.05391	0.567591
H	-2.52464	-0.7622	1.628045
C	-3.69889	-0.39312	-0.14854
H	-3.69958	-0.69308	-1.20523
C	-2.50331	-2.56932	0.483349
H	-3.44075	-2.95605	0.893535
H	-2.44742	-2.85841	-0.57704
O	-1.32132	-0.59691	-0.05207
O	-1.98213	2.940774	-0.32488
H	-2.7533	3.41727	-0.65078
O	-4.52316	1.801025	-0.8085
H	-5.38556	1.52522	-0.48066
O	-4.94605	-0.68218	0.461191

H	-5.24771	-1.5546	0.197883
O	-1.45974	-3.12326	1.231442
H	-0.6318	-3.00661	0.735867
E(elec)	-1297.749652		au
ZPVE	0.370137226		au
G correction (873K)	0.102794477		au
TS: CB43Pin		M06-2X/6-311++G(d,p)	
O	-5.26997	-0.52428	-0.57696
H	-5.4921	-1.43414	-0.34784
C	-4.1188	-0.19241	0.125421
H	-4.35474	0.077031	1.167436
C	-3.09196	-1.3049	0.087456
H	-2.82574	-1.52272	-0.95426
C	-1.69124	-0.94054	0.942406
H	-2.11293	-0.59044	1.909639
C	-2.37004	1.366484	0.082614
H	-2.58223	1.682383	1.113143
C	-1.40656	0.195553	0.084031
H	-0.88847	-0.02722	-0.84934
C	-1.90405	2.556739	-0.74398
H	-1.01972	3.00611	-0.29377
H	-1.65417	2.199194	-1.75303
O	-3.56747	0.920975	-0.53964
O	-3.5721	-2.43139	0.735872
H	-2.77224	-2.94722	0.95655
O	-0.97174	-2.0316	0.983601
H	0.253113	0.73611	1.708317
O	0.170626	1.177859	0.847952
O	-2.90239	3.542702	-0.78317
H	-3.70886	3.125494	-1.10548
C	1.322409	0.830628	0.09315
H	1.145673	1.225914	-0.91705
C	2.610417	1.401936	0.661985
H	2.693148	1.095515	1.716266
C	3.77187	0.786983	-0.11333
H	3.704494	1.118512	-1.16115
C	2.363201	-1.19132	-0.63335
H	2.262648	-0.9029	-1.68986
C	3.720134	-0.73488	-0.09935
H	3.84168	-1.08564	0.934686

C	2.056515	-2.67587	-0.47387
H	2.746268	-3.25706	-1.09454
H	2.2233	-2.94387	0.580185
O	1.355575	-0.5514	0.138089
O	2.586732	2.797387	0.533646
H	3.475505	3.120777	0.719654
O	4.95065	1.288114	0.476743
H	5.700591	0.895137	0.017276
O	4.802983	-1.16069	-0.90768
H	4.969733	-2.09574	-0.76511
O	0.754584	-2.96048	-0.87931
H	0.123762	-2.60335	-0.20402
E(elec)	-1297.740673	au	
ZPVE	0.371805216	au	
G correction (873K)	0.101025434	au	

TS: CB1’2’Pin		M06-2X/6-311++G(d,p)	
O	-0.5242	-0.62098	-1.08844
C	1.488926	-0.17194	-0.22543
H	0.908596	0.05927	0.670888
C	1.845006	-1.5322	-0.52575
H	2.397554	-1.60025	-1.48116
C	3.073556	-1.46617	0.591005
H	2.641894	-1.29932	1.586298
C	3.404052	0.977073	0.179216
H	3.043205	1.286601	1.166835
C	4.093561	-0.38714	0.26047
H	4.544948	-0.62439	-0.71311
C	4.261256	2.05887	-0.43411
H	5.162512	2.146663	0.175048
H	4.550544	1.751634	-1.44635
O	2.236728	0.806348	-0.71077
O	0.9691	-2.46739	-0.23439
H	-0.16255	-1.54007	-0.81512
O	3.677405	-2.71796	0.523194
H	2.960481	-3.37146	0.526273
O	5.079317	-0.28008	1.260913
H	5.448291	-1.15805	1.408031
O	3.61978	3.309074	-0.42844
H	2.891163	3.283264	-1.05429
O	-5.25696	1.079562	1.017934

H	-5.34705	2.039117	1.038963
C	-4.19168	0.787666	0.176409
H	-4.4792	0.917085	-0.88151
C	-2.98175	1.666546	0.478673
H	-2.71954	1.524862	1.535935
C	-1.82271	1.234727	-0.39655
H	-2.08839	1.407709	-1.44838
C	-2.84026	-1.03977	-0.44859
H	-3.14781	-0.91809	-1.49769
C	-1.55276	-0.24711	-0.20014
H	-1.24649	-0.42025	0.844038
C	-2.69781	-2.51744	-0.13185
H	-1.94066	-2.96952	-0.77502
H	-2.37136	-2.62363	0.911262
O	-3.86272	-0.5542	0.413565
O	-3.367	3.001208	0.230021
H	-2.59378	3.561341	0.351588
O	-0.69682	2.03021	-0.04755
H	-0.06482	1.998394	-0.77182
O	-3.90901	-3.19676	-0.36306
H	-4.58893	-2.74186	0.145254
E(elec)	-1297.739485	au	
ZPVE	0.370378949	au	
G correction (873K)	0.093243735	au	

TS: CB2’3’Pin		M06-2X/6-311++G(d,p)	
O	0.068565	0.653345	-0.62158
C	-1.10785	0.466185	0.068247
H	-1.02851	0.795095	1.114046
C	-2.23239	1.154227	-0.64876
H	-2.19515	1.142073	-1.73469
C	-3.50452	1.258298	-0.01235
H	-3.41899	1.291224	1.0934
C	-2.72712	-1.22217	0.579481
H	-2.75991	-0.93123	1.637144
C	-3.75859	-0.43666	-0.20883
H	-3.72209	-0.68727	-1.27616
C	-2.88431	-2.7275	0.470503
H	-3.86866	-3.00402	0.848888
H	-2.82365	-3.01629	-0.58735
O	-1.43947	-0.91962	0.031187

O	-1.88917	3.178849	-0.60575
H	-1.4764	3.57878	-1.37855
O	-4.45408	1.944446	-0.56585
H	-2.85799	3.308768	-0.69314
O	-5.03172	-0.57834	0.306426
H	-5.52432	0.20841	0.005316
O	-1.92703	-3.40613	1.24983
H	-1.04807	-3.17791	0.929566
O	5.315947	-0.47	0.330035
H	5.592542	-1.33052	-0.0059
C	4.077915	-0.19131	-0.22922
H	4.185659	0.166806	-1.26741
C	3.160282	-1.40633	-0.19994
H	3.061623	-1.72634	0.846406
C	1.7921	-1.03265	-0.74059
H	1.895276	-0.73991	-1.79607
C	2.277933	1.298179	0.04347
H	2.416885	1.669084	-0.98325
C	1.249189	0.166899	0.028342
H	1.012717	-0.13811	1.056048
C	1.863286	2.450181	0.940182
H	0.914219	2.863987	0.594488
H	1.731739	2.066201	1.961443
O	3.510662	0.825343	0.558374
O	3.775899	-2.40939	-0.97674
H	3.172839	-3.15785	-1.03571
O	0.978476	-2.18156	-0.63212
H	0.067466	-1.92557	-0.82709
O	2.813456	3.485669	0.903601
H	3.664906	3.099601	1.135981
E(elec)	-1297.740362	au	
ZPVE	0.371265639	au	
G correction (873K)	0.096543708	au	

TS: CB3’2’Pin		M06-2X/6-311++G(d,p)	
O	-0.10189	0.324841	0.67803
C	1.052668	0.211964	-0.03438
H	0.90897	0.423234	-1.10125
C	2.032017	1.415803	0.655504
H	2.054049	1.014234	1.688466
C	3.182113	1.018552	-0.1142

H	3.296797	1.480353	-1.09286
C	2.820065	-1.2909	-0.44895
H	2.742479	-1.14766	-1.53477
C	3.87587	-0.25864	0.093429
H	4.055987	-0.47035	1.152062
C	3.244534	-2.7199	-0.15986
H	4.253348	-2.87465	-0.54122
H	3.243753	-2.8697	0.927546
O	1.583083	-1.07396	0.177665
O	1.589204	2.624295	0.468362
H	3.255547	3.136294	0.653108
O	4.21044	2.837779	0.638454
H	4.669528	3.440137	0.046933
O	5.027566	-0.42273	-0.69342
H	5.722021	0.146652	-0.34909
O	2.404999	-3.63686	-0.81556
H	1.502885	-3.50873	-0.50591
O	-5.3773	-0.20991	-0.55382
H	-5.75683	-1.05231	-0.27886
C	-4.15909	-0.07944	0.099997
H	-4.30856	0.185222	1.160899
C	-3.33959	-1.3651	0.014094
H	-3.21099	-1.6127	-1.04839
C	-1.98327	-1.13301	0.648179
H	-2.12317	-0.91066	1.715805
C	-2.23731	1.287039	0.069697
H	-2.40563	1.550729	1.123939
C	-1.32442	0.067427	-0.01173
H	-1.12147	-0.16934	-1.06371
C	-1.68392	2.49356	-0.66466
H	-0.74048	2.803032	-0.20739
H	-1.49545	2.208247	-1.7106
O	-3.47525	0.958093	-0.55116
O	-4.07672	-2.3685	0.67858
H	-3.53826	-3.16571	0.71409
O	-1.21106	-2.30808	0.495081
H	-0.3334	-2.12471	0.852505
O	-2.58703	3.572635	-0.59357
H	-3.43755	3.253291	-0.91311
E(elec)	-1297.736137		au

ZPVE	0.369731606	au
G correction (873K)	0.091587442	au

TS: CB3'4'Pin		M06-2X/6-311++G(d,p)	
O	0.143114	0.707381	-0.59494
C	-1.02441	0.531172	0.116183
H	-0.90865	0.861503	1.160724
C	-2.1212	1.409593	-0.55731
H	-2.06103	1.243679	-1.6373
C	-3.40541	0.912246	-0.01489
H	-3.78272	1.387735	0.887151
C	-2.65733	-1.03301	0.688476
H	-2.6756	-0.6411	1.711683
C	-3.90385	-0.41082	-0.29274
H	-3.55357	-0.79424	-1.27272
C	-2.92236	-2.52809	0.721323
H	-3.92543	-2.68727	1.111814
H	-2.87418	-2.91805	-0.30271
O	-1.40402	-0.81679	0.07892
O	-1.93977	2.756593	-0.20922
H	-1.18409	3.098542	-0.69665
O	-5.0551	1.757011	-1.04495
H	-5.47342	2.528118	-0.65186
O	-5.11376	-0.67984	0.086516
H	-5.52799	0.953975	-0.70561
O	-2.00303	-3.17293	1.571962
H	-1.12048	-3.08534	1.197677
O	5.396749	-0.51425	0.181308
H	5.64508	-1.37895	-0.16566
C	4.143899	-0.21284	-0.33076
H	4.218726	0.147812	-1.37091
C	3.205994	-1.41056	-0.26882
H	3.13766	-1.72769	0.780832
C	1.827112	-1.01198	-0.762
H	1.897813	-0.72293	-1.82105
C	2.381816	1.308944	0.018658
H	2.489158	1.696123	-1.00583
C	1.331522	0.197235	0.023558
H	1.113463	-0.10686	1.055609
C	2.022595	2.448895	0.954077
H	1.065773	2.884075	0.659663

H	1.925651	2.045641	1.971541
O	3.62436	0.810223	0.481591
O	3.775246	-2.42581	-1.06473
H	3.15443	-3.16095	-1.10458
O	0.998693	-2.14633	-0.61975
H	0.085651	-1.88543	-0.79612
O	2.983145	3.472881	0.899622
H	3.838444	3.071766	1.089099
E(elec)	-1297.742802	au	
ZPVE	0.370669393	au	
G correction (873K)	0.09523133	au	

TS: CB4'3'Pin		M06-2X/6-311++G(d,p)	
O	0.154381	0.700819	-0.71015
C	-1.03192	0.581653	-0.01916
H	-0.93131	0.931699	1.019709
C	-2.12474	1.353795	-0.73716
H	-2.19466	1.030408	-1.78149
C	-3.64005	1.138914	0.018958
H	-3.37056	1.395471	1.064736
C	-2.6281	-1.08929	0.604278
H	-2.60958	-0.75734	1.648428
C	-3.59058	-0.27161	-0.20611
H	-3.86366	-0.63299	-1.1949
C	-2.80265	-2.59491	0.536894
H	-3.74746	-2.8735	1.005984
H	-2.82668	-2.90144	-0.5179
O	-1.37315	-0.80733	-0.01752
O	-1.93597	2.71499	-0.62225
H	-2.79799	3.118643	-0.82741
O	-4.55355	1.8577	-0.56225
H	-5.69334	0.432594	0.079319
O	-5.58603	-0.49102	0.414395
H	-6.19539	-1.04076	-0.08799
O	-1.77582	-3.24048	1.242845
H	-0.9261	-2.98008	0.866534
O	5.342587	-0.51588	0.450333
H	5.620049	-1.38092	0.127423
C	4.138627	-0.2152	-0.17142
H	4.304133	0.114586	-1.21142
C	3.18978	-1.40781	-0.16156

H	3.040402	-1.70848	0.884571
C	1.856824	-1.00594	-0.76364
H	2.010406	-0.7328	-1.81773
C	2.36694	1.324531	-0.01466
H	2.558678	1.65731	-1.04542
C	1.314857	0.215693	-0.03154
H	1.058953	-0.06555	0.99841
C	1.945243	2.516016	0.825159
H	1.037968	2.955671	0.407077
H	1.735512	2.166502	1.846421
O	3.565667	0.832536	0.566634
O	3.812123	-2.43848	-0.89702
H	3.190652	-3.16957	-0.9758
O	1.003588	-2.13213	-0.67765
H	0.124132	-1.85389	-0.96171
O	2.939774	3.510296	0.82412
H	3.761611	3.091086	1.100985
E(elec)	-1297.738527	au	
ZPVE	0.371371997	au	
G correction (873K)	0.097201755	au	
Product: CB12Pin		M06-2X/6-311++G(d,p)	
O	0.329594	-1.09059	0.390204
C	-2.45902	1.087553	-0.05824
C	-0.87767	-0.65475	-0.14751
C	-1.9222	-1.7275	0.125146
H	-2.34541	1.211626	-1.14574
H	-0.77072	-0.48392	-1.23305
H	-1.96495	-1.88612	1.21033
C	2.704403	-1.06001	0.573351
C	1.474276	-0.3805	-0.04002
C	1.577375	1.073377	0.458176
C	3.855571	1.48619	-0.66723
C	3.094257	1.228174	0.630303
H	1.515648	-0.38946	-1.14019
H	1.10417	1.118576	1.441093
H	4.947772	1.323623	-0.58807
H	3.361228	2.009621	1.347786
C	-3.26998	-1.23716	-0.3718
H	-3.21836	-1.13144	-1.46606
C	-3.6076	0.123474	0.221187

H	-3.72461	0.01265	1.309136
H	2.396494	-1.70708	1.39695
O	-1.63995	-2.93142	-0.55709
H	-0.82183	-3.2939	-0.20422
O	-4.31331	-2.12316	-0.02196
H	-4.09576	-2.99252	-0.37357
O	-4.78097	0.644282	-0.35894
H	-5.45723	-0.03953	-0.3047
C	-2.62478	2.454933	0.568862
H	-3.58669	2.870917	0.266524
H	-2.62075	2.335439	1.661381
O	-1.2612	0.535834	0.488458
O	-1.61672	3.338243	0.141705
H	-0.76705	2.874865	0.146048
O	0.969103	2.056231	-0.3358
H	1.471782	2.155204	-1.15486
O	3.349259	1.794153	-1.71479
O	3.525031	-0.01798	1.145076
C	3.537253	-1.84737	-0.42068
H	2.940783	-2.6663	-0.83052
H	3.830387	-1.19354	-1.25626
O	4.664777	-2.41686	0.19811
H	5.108794	-1.71719	0.688891
E(elec)	-1221.42	au	
ZPVE	0.347547	au	
G correction (873K)	0.087258	au	

Product: CB21Pin		M06-2X/6-311++G(d,p)	
O	4.648744	-2.63275	-0.9874
C	4.264207	-1.50165	-1.04934
H	4.573023	-0.81508	-1.86486
C	3.307041	-0.87843	-0.05466
H	3.312814	-1.45735	0.874534
C	1.885834	-0.80138	-0.61459
H	1.917487	-0.55811	-1.68786
C	2.565371	1.354506	0.077609
H	2.597229	1.889199	-0.87896
C	1.352456	0.436754	0.108464
H	1.091753	0.163559	1.140773
C	2.646761	2.345112	1.218182
H	1.802852	3.036578	1.160213

H	2.592706	1.797753	2.169454
O	3.695491	0.472822	0.166322
O	1.190065	-1.99802	-0.39617
H	0.284457	-1.82748	-0.68687
O	0.247737	1.038871	-0.53982
O	3.824585	3.113617	1.141628
H	4.566089	2.500014	1.121428
C	-0.97265	0.759756	0.043725
H	-0.9791	1.064161	1.103435
C	-2.08343	1.464441	-0.71551
H	-1.99446	1.187986	-1.7749
C	-3.43074	0.989138	-0.18312
H	-3.53222	1.337717	0.856041
C	-2.36527	-1.09277	0.613191
H	-2.39636	-0.71301	1.644549
C	-3.5488	-0.52841	-0.17164
H	-3.51701	-0.90024	-1.20429
C	-2.27438	-2.60559	0.658323
H	-3.19235	-3.01207	1.087867
H	-2.17138	-2.98822	-0.36759
O	-1.1766	-0.6443	-0.02935
O	-1.9397	2.849063	-0.53217
H	-2.71768	3.271427	-0.91195
O	-4.41834	1.590936	-0.99126
H	-5.27896	1.326391	-0.65009
O	-4.79685	-0.81629	0.435948
H	-5.09801	-1.69006	0.176851
O	-1.22029	-3.03796	1.482236
H	-0.37804	-2.74997	1.108855
E(elec)	-1221.41	au	
ZPVE	0.346834	au	
G correction (873K)	0.081875	au	
Product: CB23Pin		M06-2X/6-311++G(d,p)	
O	4.256732	1.349251	0.855144
H	4.948946	1.153587	1.493381
C	3.135354	0.56157	1.150601
H	2.885725	0.639074	2.214298
C	1.992484	1.015851	0.219151
H	2.409618	1.68415	-0.53606
C	0.927093	1.776316	0.970663

H	0.506861	1.265818	1.854589
C	2.773328	-1.16343	-0.3574
H	2.518518	-2.222	-0.29627
C	1.519003	-0.29849	-0.44359
H	1.200881	-0.12622	-1.47701
C	3.755999	-0.91427	-1.49638
H	3.343475	-1.30803	-2.42795
H	3.929269	0.163166	-1.61913
O	3.363303	-0.80365	0.893444
O	0.56597	2.882649	0.664444
O	0.48434	-0.94303	0.281999
O	4.967813	-1.59057	-1.26137
H	5.258056	-1.34651	-0.37628
C	-0.78171	-0.79326	-0.25591
H	-0.78006	-1.0387	-1.33165
C	-1.74878	-1.70474	0.479988
H	-1.66163	-1.49334	1.554575
C	-3.16468	-1.39406	0.018483
H	-3.249	-1.66087	-1.04627
C	-2.43671	0.895246	-0.60337
H	-2.48424	0.64722	-1.67387
C	-3.4893	0.083244	0.154649
H	-3.46534	0.357566	1.218003
C	-2.59672	2.396058	-0.43334
H	-3.5969	2.683916	-0.76904
H	-2.50049	2.640295	0.633243
O	-1.15818	0.557782	-0.08205
O	-1.41309	-3.03812	0.191524
H	-2.11847	-3.59158	0.543483
O	-4.03218	-2.20107	0.786253
H	-4.93289	-2.01086	0.503894
O	-4.79409	0.242417	-0.37958
H	-5.18296	1.060389	-0.06166
O	-1.67882	3.119133	-1.2099
H	-0.83595	3.144453	-0.74092
E(elec)	-1221.42	au	
ZPVE	0.347345	au	
G correction (873K)	0.084495	au	
Product: CB32Pin		M06-2X/6-311++G(d,p)	
O	-3.5062	1.688281	0.797116

H	-4.45075	1.787573	0.948616
C	-3.30077	1.236382	-0.52123
H	-3.75499	1.914488	-1.24579
C	-0.99929	2.183585	-0.10246
H	-0.8393	2.147255	0.989313
C	-1.7928	1.050789	-0.69185
H	-1.55713	0.956853	-1.75376
C	-2.90876	-1.04096	-0.30996
H	-2.7499	-1.71814	-1.15312
C	-1.60172	-0.30287	0.005246
H	-1.49724	-0.15271	1.089618
C	-3.4806	-1.80228	0.86902
H	-2.78013	-2.58481	1.170322
H	-3.61582	-1.10507	1.707117
O	-3.8497	-0.03637	-0.72788
O	-0.56316	3.094868	-0.76046
O	-0.51925	-1.06443	-0.47698
O	-4.69405	-2.43411	0.530209
H	-5.26724	-1.76344	0.145602
C	0.690621	-0.82196	0.148291
H	0.59102	-0.92578	1.24251
C	1.704045	-1.82437	-0.37921
H	1.700047	-1.76027	-1.4756
C	3.083599	-1.46371	0.141014
H	3.088171	-1.58604	1.234942
C	2.338587	0.889912	0.405948
H	2.309579	0.775824	1.499533
C	3.431502	-0.01955	-0.16612
H	3.485827	0.114069	-1.25499
C	2.570303	2.35423	0.074462
H	3.611914	2.598201	0.306356
H	2.411701	2.494462	-1.00171
O	1.088448	0.503528	-0.16068
O	1.324989	-3.10501	0.059966
H	2.042809	-3.70688	-0.16424
O	3.994165	-2.36736	-0.44833
H	4.875171	-2.13807	-0.13475
O	4.697804	0.201363	0.435288
H	5.120252	0.968814	0.043663
O	1.760878	3.216253	0.834795

H	0.996259	3.472391	0.302985
E(elec)	-1221.43	au	
ZPVE	0.34784	au	
G correction (873K)	0.088979	au	
Product: CB43Pin		M06-2X/6-311++G(d,p)	
O	1.373351	1.968567	-0.28703
H	1.981425	2.391391	0.325564
C	0.344474	1.35704	0.445444
H	-0.06593	2.03442	1.196819
C	-0.74302	0.904499	-0.54294
H	-0.4472	1.20486	-1.55168
C	-1.92679	-1.07725	0.433522
H	-1.7535	-1.11227	1.52689
C	0.582871	-0.9367	0.27662
H	0.543121	-1.79946	0.947256
C	-0.749	-0.64673	-0.41466
H	-0.84289	-1.1245	-1.39225
C	1.734158	-1.11953	-0.70493
H	1.600403	-2.06161	-1.24163
H	1.738142	-0.29836	-1.43253
O	0.795298	0.203384	1.116548
O	-1.954	1.51864	-0.16548
H	-2.67065	1.180097	-0.71191
O	-2.99757	-1.34909	-0.03621
O	2.963401	-1.20021	-0.02517
H	3.017024	-0.43289	0.553862
E(elec)	-610.696	au	
ZPVE	0.170857	au	
G correction (873K)	0.001281	au	
Product: CB1’2’Pin		M06-2X/6-311++G(d,p)	
C	-0.95077	-0.54078	-0.6054
H	-0.97947	-0.58152	-1.70653
C	-2.08649	-1.39022	-0.09365
H	-1.81065	-2.40842	0.23563
C	-0.99226	0.941249	-0.15725
H	-1.36185	1.579925	-0.96514
C	1.23143	-0.02686	-0.29478
H	1.515386	0.058082	-1.35358
C	0.494278	1.247079	0.119868
H	0.591175	1.406254	1.200608

C	2.441477	-0.36739	0.54251
H	3.178124	0.432677	0.450186
H	2.132099	-0.44404	1.593267
O	0.273178	-1.06851	-0.13692
O	-3.21984	-0.9914	-0.05503
O	-1.71101	1.159344	1.034793
H	-2.63172	0.914425	0.888116
O	1.026222	2.327687	-0.61112
H	0.732327	3.151429	-0.2144
O	3.058445	-1.55668	0.103581
H	2.392667	-2.25081	0.121616
E(elec)	-610.686	au	
ZPVE	0.170728	au	
G correction (873K)	0.001582	au	
Product: CB2'3'Pin		M06-2X/6-311++G(d,p)	
O	-0.31226	0.487343	-0.47312
C	-1.42705	0.439751	0.375845
H	-1.25354	1.09047	1.241725
C	-2.67076	0.814803	-0.4426
H	-2.39534	0.696579	-1.49821
C	-3.09379	2.250981	-0.27872
H	-2.28032	3.000394	-0.33111
C	-2.81948	-1.4421	0.245697
H	-3.27659	-2.0984	0.986723
C	-3.71161	-0.24057	-0.04645
H	-4.41704	-0.4416	-0.85945
C	-2.4401	-2.23935	-0.99774
H	-3.36086	-2.60231	-1.46283
H	-1.92818	-1.58887	-1.72024
O	-1.65725	-0.85867	0.874629
O	-4.23449	2.596655	-0.12313
O	-4.38103	0.088272	1.147349
H	-4.88256	0.896937	0.994565
O	-1.66407	-3.3693	-0.69091
H	-0.75213	-3.09791	-0.5227
O	5.057401	-0.11167	0.32191
H	5.353146	-1.0295	0.315581
C	3.771154	-0.09366	-0.19699
H	3.789016	-0.15963	-1.29834
C	2.915649	-1.21688	0.370566

H	2.903846	-1.10648	1.463924
C	1.495541	-1.10748	-0.16229
H	1.516853	-1.22435	-1.25391
C	1.916692	1.347846	-0.35065
H	1.954925	1.3014	-1.44925
C	0.945401	0.278093	0.159163
H	0.841199	0.384149	1.249383
C	1.516717	2.747728	0.079086
H	0.537181	2.990734	-0.3348
H	1.456649	2.773516	1.176442
O	3.210011	1.136235	0.188595
O	3.520715	-2.43377	-0.00383
H	2.953004	-3.15357	0.292191
O	0.731664	-2.17339	0.379251
H	-0.02695	-1.81698	0.868793
O	2.425837	3.703856	-0.40372
H	3.305235	3.425873	-0.12425
E(elec)	-1221.43	au	
ZPVE	0.347889	au	
G correction (873K)	0.089719	au	
Product: CB3'2'Pin		M06-2X/6-311++G(d,p)	
O	0.453606	0.677168	-0.15549
C	1.456658	0.425448	-1.10484
H	1.125712	0.743764	-2.09816
C	2.592856	2.444323	0.000832
H	1.928208	3.158631	-0.51992
C	2.736283	1.068426	-0.59721
H	3.449608	1.128706	-1.42865
C	2.767376	-1.29772	-0.196
H	3.585574	-1.79257	-0.72284
C	3.247513	0.028433	0.402885
H	2.76059	0.202404	1.370507
C	2.182035	-2.22534	0.855488
H	2.961466	-2.40282	1.602735
H	1.346914	-1.71597	1.353878
O	1.773686	-0.94508	-1.19298
O	3.197942	2.770748	0.986406
O	4.6438	0.014443	0.553428
H	4.887733	0.794423	1.063474
O	1.79265	-3.47359	0.337072

H	0.882435	-3.40783	0.028375
O	-4.8709	-0.37701	0.397255
H	-5.07893	-1.31076	0.517731
C	-3.50058	-0.23901	0.561371
H	-3.22991	-0.23413	1.630882
C	-2.73168	-1.33027	-0.16458
H	-3.00874	-1.28043	-1.22622
C	-1.23347	-1.10261	-0.03347
H	-0.958	-1.17916	1.029218
C	-1.79531	1.331509	0.178683
H	-1.56241	1.348609	1.253804
C	-0.87989	0.309197	-0.50616
H	-1.00923	0.372583	-1.59694
C	-1.63557	2.730137	-0.39161
H	-0.61436	3.076378	-0.232
H	-1.83582	2.691332	-1.47185
O	-3.15759	0.995459	-0.01425
O	-3.12004	-2.56368	0.398297
H	-2.61593	-3.26192	-0.0326
O	-0.61174	-2.14029	-0.77086
H	0.25218	-1.83092	-1.09605
O	-2.4918	3.638563	0.25271
H	-3.38132	3.270579	0.209471
E(elec)	-1221.43	au	
ZPVE	0.347975	au	
G correction (873K)	0.089949	au	
Product: CB3’4’Pin		M06-2X/6-311++G(d,p)	
O	0.02579	0.642741	-0.69505
C	-1.16304	0.623327	-0.01509
H	-1.0605	1.017875	1.006734
C	-2.26526	1.404693	-0.73709
H	-2.2313	1.216022	-1.81306
C	-3.57846	0.86461	-0.17918
H	-4.13437	1.517528	0.510527
C	-2.858	-0.24343	0.756502
H	-2.69882	0.221509	1.727761
C	-4.4969	0.058971	-1.00709
H	-3.99122	-0.47596	-1.85886
C	-3.80887	-1.4606	0.940319
H	-4.77061	-1.12839	1.317457

H	-3.9352	-1.97176	-0.01794
O	-1.74374	-0.63586	0.0863
O	-2.05538	2.770215	-0.4384
H	-1.28235	3.054527	-0.93901
O	-5.65281	-0.1798	-0.72834
O	-3.20616	-2.2917	1.902312
H	-2.39075	-2.65483	1.541605
O	5.177153	-0.7627	0.324595
H	5.39638	-1.66147	0.050169
C	3.953133	-0.44279	-0.24332
H	4.070721	-0.16966	-1.30614
C	2.956625	-1.58702	-0.11522
H	2.854784	-1.81892	0.95368
C	1.616741	-1.16287	-0.67605
H	1.727525	-0.96855	-1.75168
C	2.264401	1.183298	-0.06149
H	2.414714	1.48411	-1.1093
C	1.162782	0.127157	-0.00026
H	0.90564	-0.0847	1.045643
C	1.937647	2.409085	0.773866
H	1.011704	2.867329	0.421897
H	1.797531	2.091501	1.816517
O	3.47057	0.664436	0.472247
O	3.497391	-2.68611	-0.81501
H	2.843125	-3.39256	-0.8166
O	0.726854	-2.24404	-0.47088
H	-0.15771	-1.97147	-0.74087
O	2.951032	3.376735	0.666899
H	3.780372	2.949948	0.908553
E(elec)	-1221.42	au	
ZPVE	0.346372	au	
G correction (873K)	0.077728	au	

Product: CB4’3’Pin		M06-2X/6-311++G(d,p)	
O	-0.30505	0.780173	-0.05121
C	-1.34331	0.656498	0.879131
H	-1.06295	1.061901	1.854602
C	-2.58646	1.311613	0.295095
H	-2.33795	2.234539	-0.2349
C	-4.53917	0.245977	-0.9838
H	-4.94205	-0.64779	-1.49922

C	-2.64528	-1.1054	0.060523
H	-3.47226	-1.58714	0.588994
C	-3.07282	0.201351	-0.6459
H	-2.52688	0.278668	-1.59662
C	-2.01963	-2.09414	-0.915
H	-2.76078	-2.3132	-1.6918
H	-1.16024	-1.61188	-1.39934
O	-1.70691	-0.69502	1.07273
O	-3.45601	1.533779	1.375531
H	-4.29853	1.836309	1.018098
O	-5.25792	1.178351	-0.73674
O	-1.66556	-3.31363	-0.3177
H	-0.78346	-3.22342	0.062615
O	5.020997	-0.39759	-0.21213
H	5.2152	-1.342	-0.21862
C	3.664578	-0.25793	-0.46778
H	3.454728	-0.36186	-1.54628
C	2.835649	-1.25942	0.320135
H	3.05514	-1.10617	1.385429
C	1.352006	-1.02447	0.080384
H	1.137816	-1.19882	-0.98477
C	1.969103	1.363928	-0.34404
H	1.793508	1.267503	-1.42599
C	1.002926	0.430609	0.395292
H	1.086385	0.601634	1.478696
C	1.799383	2.81723	0.061829
H	0.789719	3.149576	-0.17879
H	1.951329	2.897102	1.147285
O	3.314188	1.034406	-0.04466
O	3.230844	-2.54902	-0.09268
H	2.699902	-3.19287	0.387496
O	0.664146	-1.98042	0.870406
H	-0.19124	-1.61194	1.153059
O	2.695216	3.642555	-0.64041
H	3.579274	3.285986	-0.50042
E(elec)	-1221.43	au	
ZPVE	0.347916	au	
G correction (873K)	0.090756	au	
“Axial” Glucose		M06-2X/6-311++G(d,p)	
C	-1.33718	-1.00884	0.02193

C	-0.03047	-1.27628	-0.72084
C	0.725768	0.998803	-0.46375
C	-0.51545	1.361902	0.355126
C	-1.1559	0.132292	1.034496
H	-0.20449	-1.96582	-1.55041
H	-1.62198	-1.92361	0.553245
H	0.89136	1.817227	-1.169
H	-0.23207	2.068073	1.140488
H	-2.14299	0.45348	1.382107
O	0.477226	-0.11758	-1.32192
O	0.864425	-1.82196	0.223187
H	1.768053	-1.65935	-0.08993
O	-2.28882	-0.67112	-0.97547
H	-3.16256	-0.64885	-0.57577
O	-0.43788	-0.3008	2.169711
H	0.193272	-0.97512	1.887051
O	-1.46357	2.018856	-0.46093
H	-1.76147	1.384337	-1.12524
C	1.999076	0.8229	0.387361
H	2.41399	1.817341	0.585811
H	1.788361	0.355591	1.346808
O	2.958854	-0.00677	-0.24874
H	3.073699	0.287055	-1.15776
E(elec)	-687.1395596	au	
ZPVE	0.202795956	au	
G correction (873K)	0.03768798	au	

TS: GLC13Grob		M06-2X/6-311++G(d,p)	
O	-1.24815	1.735894	0.645373
C	1.057221	-1.34997	-0.59347
C	1.516933	-0.86499	0.686859
C	0.979184	0.763959	0.814072
C	-0.35385	0.821051	0.038764
C	-1.08062	-0.51772	-0.06438
H	1.696698	-1.70567	-1.39254
O	-0.18558	-1.35452	-0.8834
H	2.599992	-0.83992	0.781234
H	0.758946	0.711451	1.898628
H	-0.11866	1.141692	-0.98564
H	-1.21824	-0.99125	0.907621
C	-2.40017	-0.44313	-0.81943

H	-2.26458	0.148871	-1.73373
H	-2.7072	-1.45101	-1.10532
O	2.189307	0.57124	-1.79427
H	3.016864	0.759525	-2.23976
O	0.850155	-1.49904	1.76423
H	1.198675	-2.38825	1.874162
O	1.853744	1.650798	0.441859
H	2.155158	1.173711	-0.96609
O	-3.40525	0.081865	0.008836
H	-3.10551	0.945315	0.320025
H	-0.75817	2.550451	0.805835
E(elec)	-687.1395596		au
ZPVE	0.202795956		au
G correction (873K)	0.03768798		au
TS: GLC24Grob		M06-2X/6-311++G(d,p)	
C	-0.99051	-0.37085	0.907958
C	-0.05943	-1.37704	0.255002
C	0.894651	0.366181	-1.07826
C	-0.38813	1.194696	-0.99009
C	-1.06926	1.044844	0.675225
H	-0.57116	-2.31989	0.065947
H	-1.15183	-0.67268	1.945515
H	1.230266	0.423727	-2.11903
H	-0.19942	2.282453	-1.01997
H	-2.00407	1.42596	0.286097
O	0.560482	-1.00935	-0.92359
O	0.892518	-1.52306	1.306832
H	1.774932	-1.44465	0.909005
O	-2.731	-1.23429	-0.31708
H	-3.63904	-0.96124	-0.15906
O	-0.77202	1.773286	1.831759
H	0.021012	1.423038	2.247491
O	-1.35769	0.69352	-1.66706
H	-2.37331	-0.63776	-1.01668
C	2.02925	0.816126	-0.15911
H	2.456806	1.745281	-0.55061
H	1.673956	1.01729	0.85299
O	3.02777	-0.18253	-0.00908
H	3.321974	-0.46606	-0.88029
E(elec)	-686.980287		au

ZPVE	0.193505886	au
G correction (873K)	0.014623608	au

TS: GLC31Grob		M06-2X/6-311++G(d,p)	
C	-1.68448	-0.49892	0.6238
C	-0.7486	-1.3596	-0.75466
C	0.617301	0.667125	-0.89053
C	0.03415	1.29736	0.413573
C	-0.6597	0.256788	1.255617
H	-1.65664	-1.68644	-1.27716
H	-2.17554	-1.25712	1.229644
H	0.64047	1.520215	-1.57488
H	0.833658	1.772538	0.979565
H	-0.55082	0.279324	2.328139
O	-0.31669	-0.21721	-1.47157
O	0.075773	-2.21695	-0.33624
H	0.712032	-1.69412	0.844739
O	-2.58416	0.190807	-0.23152
H	-3.30643	0.511013	0.317016
O	0.899068	-1.06923	1.644768
H	1.732452	-0.60279	1.488088
O	-0.87482	2.326651	0.065481
H	-1.56458	1.915401	-0.4735
C	2.038643	0.055593	-0.83071
H	1.970481	-1.02587	-0.75725
H	2.557135	0.287812	-1.76407
O	2.80372	0.500297	0.28556
H	3.200736	1.355008	0.105262

E(elec)	-687.0107623	au
ZPVE	0.195330727	au
G correction (873K)	0.027016637	au

TS: GLC42Grob		M06-2X/6-311++G(d,p)	
C	-1.42112	-0.96633	-0.31131
C	-0.15654	-0.6943	-1.18381
C	0.716493	1.12379	0.180626
C	-0.4245	0.881707	1.130043
C	-0.87172	-0.45245	1.345606
H	-0.46971	-0.79354	-2.22702
H	-1.47663	-2.04057	-0.06038
H	0.802719	2.19856	0.005084
H	-0.81245	1.708759	1.704021

H	-1.75111	-0.53906	1.97847
O	0.350863	0.612753	-1.10733
O	0.837495	-1.64157	-0.86157
H	1.694978	-1.29489	-1.15067
O	-2.51251	-0.40912	-0.68603
H	-2.33442	0.951983	-0.44972
O	0.081555	-1.42035	1.701315
H	0.430562	-1.86012	0.911419
O	-1.92612	1.867611	-0.12311
H	-1.42919	2.165599	-0.89205
C	2.100108	0.599902	0.652569
H	2.550795	1.366435	1.291818
H	2.010372	-0.31527	1.228739
O	2.935421	0.295712	-0.44713
H	2.994068	1.057975	-1.03121
E(elec)	-687.0060854	au	
ZPVE	0.194411308	au	
G correction (873K)	0.026848873	au	
TS: axGLC46Grob		M06-2X/6-311++G(d,p)	
C	-1.47841	-1.14716	-0.14808
C	-1.90217	0.308827	-0.32157
C	-0.83532	1.181845	0.389747
C	0.505383	0.544541	0.329369
C	0.80973	-0.58899	-0.52015
H	-2.22185	-1.84883	-0.53022
O	-0.32152	-1.36429	-0.91204
H	-2.86286	0.501796	0.157702
H	-0.76029	2.113992	-0.18378
H	1.211677	0.762581	1.122089
H	1.309344	-0.25468	-1.43329
C	2.06296	-1.33612	0.210952
H	1.668299	-1.79227	1.141967
H	2.316625	-2.15334	-0.48619
O	-1.23443	-1.31943	1.225921
H	-0.90421	-2.20994	1.387107
O	-2.02431	0.617546	-1.6821
H	-1.35238	0.129787	-2.17315
O	-1.18505	1.518433	1.707651
H	-1.26854	0.6952	2.202817
O	2.127293	1.766494	-0.72046

O	2.970199	-0.38302	0.377956
H	2.679832	0.996638	-0.33765
H	2.553838	2.595425	-0.48452
E(elec)	-687.0019474	au	
ZPVE	0.193521466	au	
G correction (873K)	0.021322469	au	
TS: eqGLC46Grob		M06-2X/6-311++G(d,p)	
O	2.457058	-1.84777	0.242917
H	2.283992	-2.70368	0.647013
C	1.363921	-1.01962	0.441176
H	1.173506	-0.84778	1.513634
C	1.677275	0.290113	-0.26973
H	1.816402	0.058641	-1.33308
C	0.502039	1.253357	-0.10817
H	0.469993	1.531517	0.963242
C	-0.95217	-0.82732	0.041336
H	-1.30393	-0.90364	1.079085
C	-0.78687	0.572829	-0.30983
H	-1.59483	1.069992	-0.83532
C	-2.29759	-1.29232	-0.73896
H	-2.06344	-1.32806	-1.818
H	-2.45636	-2.32662	-0.39049
O	0.225314	-1.58883	-0.16025
O	2.797533	0.951185	0.26437
H	3.565479	0.38087	0.153756
O	0.615713	2.387561	-0.92034
H	1.467842	2.795529	-0.73188
O	-2.2507	1.207207	1.435476
H	-2.73628	2.014958	1.622501
O	-3.19832	-0.38718	-0.37041
H	-2.83483	0.618559	0.860465
E(elec)	-686.9976	au	
ZPVE	0.192134499	au	
G correction (873K)	0.014825373	au	
TS: GLC53Grob		M06-2X/6-311++G(d,p)	
C	-1.74152	-0.58025	-0.81149
C	-1.84586	0.662266	-0.14779
C	-0.61796	0.572636	1.245354
C	0.772316	0.737938	0.612736
C	1.029042	-0.43503	-0.374

H	-1.2807	-0.64882	-1.79231
O	0.069924	-1.46383	-0.17738
H	-2.73264	0.76232	0.47387
H	-0.96317	1.492763	1.738553
H	1.458586	0.631996	1.459673
H	0.921691	-0.04063	-1.39513
C	2.414947	-1.03954	-0.22475
H	2.506698	-1.43621	0.794801
H	2.514223	-1.87204	-0.93123
O	-2.46501	-1.5768	-0.35598
H	-2.11254	-2.41639	-0.68115
O	-1.51724	1.783573	-0.93039
H	-2.29675	2.123559	-1.3769
O	-0.77864	-0.55554	1.858641
H	-0.27206	-1.32347	0.843044
O	1.031841	2.003916	0.067861
H	0.323438	2.220689	-0.54734
O	3.362681	-0.0226	-0.47727
H	4.238996	-0.35164	-0.27001
E(elec)	-687.0237903	au	
ZPVE	0.194204547	au	
G correction (873K)	0.020586699	au	

TS: GLC64Grob		M06-2X/6-311++G(d,p)	
O	2.303079	-1.97615	-0.41683
H	3.153433	-1.52162	-0.42996
C	1.402667	-1.12882	0.211896
H	1.536446	-1.16007	1.306771
C	1.563397	0.306932	-0.2716
H	1.455575	0.307971	-1.36463
C	0.505074	1.215178	0.321924
H	0.575999	1.229102	1.418194
C	-0.88533	-0.97563	0.605659
H	-0.63029	-0.73506	1.638945
C	-0.89364	0.770665	-0.0948
H	-0.90836	0.417678	-1.14197
C	-2.17918	-1.46111	0.411731
H	-2.35418	-2.25936	-0.29925
H	-2.92024	-1.31431	1.182308
O	0.122705	-1.62111	-0.11131
O	2.868125	0.704008	0.098431

H	2.959876	1.641424	-0.10336
O	0.749746	2.508696	-0.1953
H	-0.00939	3.057213	0.036017
O	-1.87278	1.491188	0.307818
H	-2.92336	0.70064	-0.26836
O	-3.39126	-0.17054	-0.62179
H	-3.25041	-0.21565	-1.57174
E(elec)	-687.0237903	au	
ZPVE	0.194033634	au	
G correction (873K)	0.023021272	au	
Product: GLC13Grob		M06-2X/6-311++G(d,p)	
O	-2.45136	0.36348	0.274056
C	1.757617	0.540966	-0.5323
C	2.833406	0.242237	0.192627
C	-0.66734	1.899748	0.483367
C	-1.16877	0.670896	-0.26752
C	-0.29025	-0.56652	-0.06421
H	1.574147	1.528635	-0.93527
O	0.879824	-0.47596	-0.87279
H	3.574176	0.983695	0.459375
H	-0.47085	1.73491	1.561397
H	-1.23041	0.897801	-1.33798
H	-0.00902	-0.65216	0.995261
C	-1.00811	-1.85039	-0.48191
H	-1.52493	-1.68838	-1.43662
H	-0.2475	-2.61663	-0.63851
O	3.113975	-0.99592	0.652212
H	2.471808	-1.60645	0.267494
O	-0.57008	2.984755	-0.01848
O	-1.87919	-2.328	0.513011
H	-2.5521	-1.6538	0.652888
H	-3.07001	1.063931	0.047577
E(elec)	-610.6540629	au	
ZPVE	0.168281543	au	
G correction (873K)	-0.009258166	au	
Product: GLC24Grob		M06-2X/6-311++G(d,p)	
C	-1.16427	-0.98669	0.278511
C	-0.04601	-1.20892	-0.70141
C	1.057663	0.943925	-0.28934
C	0.011393	1.991738	0.071573

C	-2.33012	-0.46863	-0.0967
H	-0.41852	-1.64339	-1.63355
H	-0.98807	-1.31489	1.298931
H	1.778816	1.53773	-0.87801
H	0.336727	2.697113	0.864778
H	-2.51536	-0.1392	-1.1132
O	0.61146	-0.0384	-1.18421
O	0.859145	-2.07858	-0.07591
H	1.726355	-1.96088	-0.48043
O	-3.3988	-0.24319	0.695827
H	-3.2101	-0.55099	1.588112
O	-1.01907	2.138273	-0.47528
C	1.829069	0.43252	0.929566
H	2.102125	1.288962	1.558204
H	1.221757	-0.25009	1.521251
O	2.978122	-0.29927	0.546634
H	3.573002	0.281306	0.064187
E(elec)	-610.6558466	au	
ZPVE	0.167664285	au	
G correction (873K)	-0.011576885	au	
Product: GLC31Grob		M06-2X/6-311++G(d,p)	
C	1.958688	-0.30739	1.094525
C	0.314453	1.897904	-0.54979
C	-0.95032	-0.18233	-0.60939
C	-0.07742	-1.29848	-0.02028
C	0.749456	-0.84709	1.162185
H	0.9979	2.460808	-1.19841
H	2.51363	-0.02181	1.981448
H	-1.45719	-0.61874	-1.47525
H	-0.77419	-2.06598	0.325664
H	0.328596	-0.97478	2.151832
O	-0.10749	0.821725	-1.21545
O	0.004682	2.230328	0.555893
O	2.567333	-0.03065	-0.10551
H	3.496478	0.166498	0.029092
O	0.68544	-1.9001	-1.04392
H	1.385448	-1.28553	-1.29038
C	-2.02029	0.343737	0.350957
H	-1.60675	0.569531	1.330693
H	-2.45937	1.264069	-0.04754

O	-2.99642	-0.66564	0.545065
H	-3.50027	-0.7775	-0.265
E(elec)	-610.6851383	au	
ZPVE	0.169822449	au	
G correction (873K)	6.95918E-05	au	
Product: GLC42Grob		M06-2X/6-311++G(d,p)	
C	-2.00487	-0.53007	0.271979
C	-0.64697	-1.2456	0.382232
C	0.758262	0.042296	-1.11959
C	-0.11326	1.270232	-1.13748
C	-0.42564	2.107028	-0.13557
H	-0.85331	-2.31025	0.533875
H	-2.20896	0.240765	1.039707
H	1.054068	-0.14969	-2.15222
H	-0.52095	1.548138	-2.10155
H	-0.99381	3.005568	-0.35471
O	0.106667	-1.19601	-0.78842
O	0.027082	-0.69953	1.492089
H	0.922283	-1.07814	1.508151
O	-2.80553	-0.84412	-0.55794
O	-0.1557	2.010814	1.175951
H	0.062396	1.092001	1.418023
C	2.063787	0.235386	-0.29677
H	2.830043	0.633314	-0.96876
H	1.940314	0.953575	0.511443
O	2.512255	-0.96379	0.317558
H	2.501869	-1.66975	-0.3367
E(elec)	-610.6660901	au	
ZPVE	0.17075832	au	
G correction (873K)	0.007802327	au	
Product: axGLC46Grob		M06-2X/6-311++G(d,p)	
C	-1.29645	-0.83837	0.772728
C	-1.75539	0.493191	0.180667
C	-0.55186	1.24078	-0.40916
C	0.275257	0.272469	-1.2158
C	0.151141	-1.04641	-1.07694
H	-2.14161	-1.41397	1.15384
O	-0.71476	-1.66607	-0.21816
H	-2.20497	1.096443	0.970522
H	-0.94697	2.022585	-1.06119

H	0.994535	0.651162	-1.93129
H	0.72069	-1.76919	-1.64742
C	3.015919	0.29195	0.245974
H	2.878854	1.339209	-0.07493
H	2.395855	-0.03478	1.102134
O	-0.36124	-0.55246	1.78088
H	-0.07357	-1.37674	2.185392
O	-2.753	0.257847	-0.78414
H	-2.37223	-0.25537	-1.50548
O	0.207993	1.911464	0.583277
H	0.400518	1.266937	1.274544
O	3.785648	-0.45178	-0.29323
E(elec)	-610.665431	au	
ZPVE	0.167842845	au	
G correction (873K)	-0.008117667	au	

Product: eqGLC46Grob		M06-2X/6-311++G(d,p)	
O	2.665774	-0.95177	-0.91305
H	3.142106	-1.75811	-0.69363
C	1.756438	-0.66351	0.091029
H	2.249323	-0.55294	1.068153
C	1.040027	0.618247	-0.29358
H	0.474327	0.417098	-1.21385
C	0.066833	1.000197	0.807927
H	0.644996	1.418835	1.643493
C	-0.29934	-1.44953	0.892861
H	-0.85486	-2.34462	1.140611
C	-0.68878	-0.22334	1.236801
H	-1.5931	-0.0958	1.817414
C	-3.06322	0.125073	-0.76172
H	-3.22129	0.971738	-0.07202
H	-2.1863	0.213267	-1.42876
O	0.829615	-1.7375	0.187792
O	1.939974	1.687432	-0.46553
H	2.577076	1.439193	-1.14331
O	-0.86332	1.968478	0.35029
H	-0.36187	2.743795	0.076287
O	-3.78982	-0.82855	-0.78879
E(elec)	-610.6641447	au	
ZPVE	0.16702915	au	
G correction (873K)	-0.011643855	au	

Product: GLC53Grob		M06-2X/6-311++G(d,p)	
C	0.049178	0.63703	1.482375
C	0.802115	0.920512	0.201537
C	1.334893	-0.36042	-0.50112
O	0.656554	-1.56025	-0.16253
H	-0.75077	1.36225	1.730993
H	1.691959	1.479244	0.526958
H	1.182027	-0.19705	-1.57047
C	2.821806	-0.56882	-0.23475
H	2.973276	-0.72707	0.843729
H	3.135229	-1.47219	-0.76679
O	0.318601	-0.27374	2.225019
H	0.671996	-1.64314	0.801889
O	0.104087	1.793277	-0.64779
H	-0.85555	1.690922	-0.57981
O	3.516437	0.576738	-0.68742
H	4.46096	0.419806	-0.63392
E(elec)	-458.069163	au	
ZPVE	0.130769636	au	
G correction (873K)	-0.01133237	au	

Product: GLC64Grob		M06-2X/6-311++G(d,p)	
O	-1.45631	-1.96138	-0.46681
H	-0.8919	-2.74171	-0.40355
C	-0.79567	-0.91779	0.185591
H	-0.84469	-1.06361	1.276593
C	0.656738	-0.83534	-0.25451
H	0.680663	-0.62724	-1.33294
C	1.47892	0.226389	0.499955
H	1.232028	0.171426	1.569787
C	-2.70303	0.434051	0.255015
H	-3.13621	-0.44741	0.716952
C	1.196768	1.638735	0.013047
H	0.184982	2.038002	0.165727
C	-3.36043	1.569464	0.078536
H	-2.89885	2.415573	-0.41439
H	-4.38294	1.652306	0.416006
O	-1.40656	0.288782	-0.16325
O	1.18606	-2.11341	0.017617
H	2.147341	-2.04679	-0.0352
O	2.83826	-0.08045	0.320424

H	3.241771	0.668448	-0.1429
O	2.067041	2.277449	-0.51822
E(elec)	-610.6744719	au	
ZPVE	0.167406158	au	
G correction (873K)	-0.009236991	au	

TS: CB13Grob		M06-2X/6-311++G(d,p)	
O	-0.29358	0.927224	0.449352
C	2.405626	-1.2631	-0.2627
C	0.923932	0.544097	-0.09301
C	1.97877	1.512544	0.404125
H	2.336182	-1.17847	-1.35751
H	0.871638	0.57413	-1.19612
H	1.972713	1.488137	1.501803
C	3.328766	1.04317	-0.11225
H	3.329848	1.137229	-1.20858
C	3.578931	-0.42336	0.235539
H	3.645057	-0.51744	1.32915
O	1.737508	2.816856	-0.08012
H	0.797084	3.006718	0.048577
O	4.397363	1.793971	0.43356
H	4.238099	2.722654	0.236857
O	4.762091	-0.88257	-0.37884
H	5.457754	-0.25193	-0.16481
C	2.431634	-2.73323	0.104498
H	3.345967	-3.18674	-0.2814
H	2.436903	-2.8143	1.201107
O	1.220575	-0.75081	0.333786
O	1.338874	-3.40766	-0.46353
H	0.506908	-2.943	-0.25474
C	-4.00315	-0.58707	0.093118
C	-3.20164	-1.17339	1.131115
C	-1.58649	-1.16368	0.527199
C	-1.40628	0.255157	-0.10861
C	-2.54595	1.266561	0.065391
H	-4.78543	-1.09763	-0.45441
O	-3.81162	0.618666	-0.28338
H	-3.44134	-2.21105	1.349305
H	-1.10861	-1.15305	1.520606
H	-1.25614	0.089595	-1.18374
H	-2.59105	1.611465	1.097599

C	-2.48714	2.436962	-0.90792
H	-2.36994	2.044777	-1.92472
H	-3.4416	2.971641	-0.84614
O	-3.00845	-1.61752	-1.94278
H	-3.24509	-2.30148	-2.57203
O	-3.08486	-0.34347	2.269859
H	-3.90015	-0.38769	2.777124
O	-1.30631	-2.17887	-0.23811
H	-2.22419	-1.98395	-1.38297
O	-1.40869	3.279896	-0.54599
H	-1.41989	4.046638	-1.12438
E(elec)	-1221.385879	au	
ZPVE	0.34608644	au	
G correction (873K)	0.08497923	au	
TS: CB31Grob		M06-2X/6-311++G(d,p)	
O	-0.18538	-1.03965	-0.54641
C	2.456074	1.100044	0.505545
C	1.017552	-0.75659	0.097662
C	2.132117	-1.59601	-0.50333
H	2.370077	0.983834	1.595431
H	0.934447	-0.96727	1.178177
H	2.178412	-1.39368	-1.58124
C	3.436094	-1.17723	0.157334
H	3.371387	-1.41074	1.230902
C	3.664167	0.318812	-0.00321
H	3.792158	0.526398	-1.076
O	1.956424	-2.97158	-0.24424
H	1.168031	-3.27248	-0.70587
O	4.549165	-1.83129	-0.41323
H	4.403796	-2.78085	-0.34816
O	4.792131	0.743248	0.724494
H	5.530535	0.179286	0.470058
C	2.508721	2.577257	0.136858
H	3.284556	3.068594	0.724061
H	2.772563	2.661685	-0.92568
O	1.279412	0.60116	-0.12101
O	1.283086	3.212101	0.405177
H	0.633965	2.856195	-0.21768
C	-3.25248	1.246674	-0.87982
C	-1.65853	1.715821	-0.1766

C	-1.41115	0.652389	0.740428
C	-1.35185	-0.77316	0.249977
C	-2.54875	-1.09011	-0.69929
H	-3.22872	1.972238	-1.70255
O	-2.86788	0.014076	-1.50405
H	-1.76374	2.694444	0.285955
H	-1.12055	0.867317	1.756253
H	-1.34952	-1.46105	1.097803
H	-2.1231	-1.8244	-1.38729
C	-3.80409	-1.71618	-0.05571
H	-4.55678	-0.94737	0.112132
H	-4.2078	-2.44508	-0.76306
O	-4.23173	1.277631	-0.06982
H	-3.79653	0.791447	1.154683
O	-0.88606	1.852068	-1.33747
H	-0.53569	0.992052	-1.59899
O	-3.17393	0.422245	1.918963
H	-3.3396	-0.52531	2.013735
O	-3.43929	-2.35948	1.1659
H	-4.15279	-2.93988	1.441656
E(elec)	-1297.742701	au	
ZPVE	0.371616031	au	
G correction (873K)	0.107801843	au	

TS: CB42Grob		M06-2X/6-311++G(d,p)	
C	2.202896	1.751903	-0.53547
C	3.135316	1.320464	0.630975
C	2.576569	-1.0407	0.493296
C	1.78805	-0.7231	-0.73897
C	2.213926	0.321485	-1.60999
H	3.045871	2.091966	1.400518
H	2.735256	2.416087	-1.23505
H	1.960425	-1.67517	1.131126
H	0.922018	-1.33403	-0.95494
H	1.518084	0.542622	-2.41595
O	2.737178	0.148065	1.271383
O	4.469032	1.228781	0.168255
H	4.95564	0.644045	0.769537
O	1.021895	2.148349	-0.17859
H	0.447628	1.126737	0.32854
O	3.521785	0.281434	-2.11803

H	4.13896	0.697866	-1.49396
O	0.081891	0.092299	0.537733
C	3.939232	-1.74069	0.215111
H	3.763808	-2.81984	0.165309
H	4.370514	-1.41947	-0.7295
O	4.891987	-1.42311	1.210471
H	4.517	-1.59764	2.079497
C	-1.14542	-0.06024	-0.05199
H	-1.10134	0.101686	-1.14639
C	-1.70429	-1.44987	0.23193
H	-1.71922	-1.58711	1.32046
C	-3.11383	-1.55848	-0.31747
H	-3.07527	-1.452	-1.41246
C	-3.32244	0.894654	-0.07926
H	-3.24944	1.021746	-1.17017
C	-3.99131	-0.44578	0.227611
H	-4.08807	-0.56587	1.31503
C	-4.04124	2.092374	0.512196
H	-5.04404	2.175442	0.086548
H	-4.12617	1.948668	1.598875
O	-2.02813	0.905175	0.501192
O	-0.85606	-2.40451	-0.37964
H	-1.31638	-3.25089	-0.36234
O	-3.59881	-2.84246	0.021633
H	-4.50466	-2.90633	-0.29869
O	-5.25031	-0.59324	-0.41158
H	-5.92271	-0.1132	0.077253
O	-3.36705	3.287154	0.206912
H	-2.44004	3.158906	0.440962
E(elec)	-1297.73401	au	
ZPVE	0.370019595	au	
G correction (873K)	0.102472586	au	

TS: axCB46Grob		M06-2X/6-311++G(d,p)	
C	4.163625	0.336243	0.58594
C	3.082467	1.024848	1.416544
C	1.78857	1.016149	0.566582
C	1.719477	-0.18074	-0.3043
C	2.611037	-1.30836	-0.17214
H	5.145618	0.375239	1.06055
O	3.844543	-1.02655	0.481136

H	3.344613	2.063503	1.622706
H	0.936067	0.931239	1.252592
H	1.126837	-0.11097	-1.20911
H	2.131525	-2.12562	0.371635
C	2.626039	-1.98552	-1.66971
H	3.154854	-1.28094	-2.34148
H	3.262333	-2.87587	-1.53233
O	4.149045	0.97288	-0.66834
H	4.780721	0.546525	-1.25758
O	2.918787	0.366191	2.641154
H	3.052114	-0.58005	2.508578
O	1.615649	2.200537	-0.18149
H	2.3823	2.293961	-0.7616
O	-0.12961	-1.60731	0.013255
O	1.347423	-2.19534	-1.94885
H	0.355925	-1.99738	-0.81161
C	-1.32667	-1.02989	-0.35463
H	-1.56998	-1.26278	-1.4023
C	-2.45857	-1.48729	0.557275
H	-2.1563	-1.27942	1.593652
C	-3.72076	-0.706	0.236054
H	-4.0312	-0.95054	-0.79107
C	-2.29542	1.141854	-0.60669
H	-2.56153	0.905639	-1.64734
C	-3.47023	0.787548	0.308529
H	-3.21983	1.054453	1.344342
C	-1.91016	2.60748	-0.51583
H	-2.77838	3.216877	-0.7801
H	-1.63182	2.832077	0.524585
O	-1.15907	0.384185	-0.2143
O	-2.66078	-2.86304	0.353482
H	-3.47522	-3.10118	0.808726
O	-4.71507	-1.12077	1.151306
H	-5.51961	-0.63227	0.949147
O	-4.68174	1.410646	-0.09321
H	-4.71205	2.31101	0.237154
O	-0.88179	2.948881	-1.40628
H	-0.05253	2.605951	-1.04794
E(elec)	-1297.730055		au
ZPVE	0.370016349		au

G correction (873K)	0.101443149	au	
TS: eqCB46Grob		M06-2X/6-311++G(d,p)	
O	0.155019	-1.6312	-0.04582
C	2.410822	1.011544	0.690036
C	1.388726	-1.10633	0.249204
C	2.396602	-1.41946	-0.85068
H	2.793845	0.628728	1.647183
H	1.759085	-1.47867	1.216372
H	1.974153	-1.0608	-1.80037
C	-2.56102	-1.331	0.494348
C	-1.6869	-0.19126	0.688958
C	-1.83897	1.024861	-0.11857
C	-3.26883	1.223538	-0.61385
C	-3.85951	-0.11494	-1.03678
H	-0.97127	-0.21186	1.505156
H	-1.20919	0.782907	-1.00012
H	-3.88638	1.597148	0.21258
H	-3.26675	-0.57345	-1.84528
C	3.700003	-0.69059	-0.57445
H	4.12671	-1.08197	0.361298
C	3.465845	0.796436	-0.39838
H	3.100359	1.211927	-1.34754
H	-2.10675	-2.03239	-0.21687
O	2.603862	-2.80934	-0.88056
H	3.354639	-2.97124	-1.46135
O	4.572459	-0.96455	-1.65297
H	5.402234	-0.50879	-1.47859
O	4.726156	1.355627	-0.05704
H	4.725212	2.298846	-0.23346
C	2.043253	2.474853	0.853815
H	2.943261	3.04206	1.104443
H	1.655607	2.844415	-0.10768
O	1.224708	0.317507	0.330356
O	1.125468	2.689374	1.892428
H	0.276571	2.328802	1.606841
O	-1.34611	2.160602	0.542899
H	-1.4714	2.919916	-0.03837
O	-3.19402	2.156096	-1.66321
H	-4.08756	2.329835	-1.9779
O	-5.16024	0.140426	-1.43582

H	-5.58224	-0.68394	-1.69682
O	-3.86418	-0.96314	0.089118
C	-2.40985	-2.19773	1.867927
H	-2.89034	-1.62648	2.680484
H	-3.02255	-3.09131	1.665753
O	-1.09823	-2.38333	1.993768
H	-0.25752	-2.0878	0.789423
E(elec)	-1297.725084	au	
ZPVE	0.369236903	au	
G correction (873K)	0.09758905	au	
TS: CB53Grob		M06-2X/6-311++G(d,p)	
C	3.318451	-1.55042	-0.74022
C	2.036178	-1.85285	-0.20713
C	1.739218	-0.63982	1.053523
C	1.461366	0.751074	0.437043
C	2.694586	1.263965	-0.33539
H	3.422831	-1.0596	-1.70313
O	3.833985	0.501557	0.00422
H	2.073659	-2.72916	0.441955
H	0.81465	-1.10548	1.438337
H	1.283807	1.398293	1.305306
H	2.480827	1.139887	-1.40631
C	2.977453	2.732512	-0.06086
H	3.178668	2.847606	1.011852
H	3.875966	3.025705	-0.61591
O	4.364849	-2.02449	-0.13437
H	5.161546	-1.55085	-0.41309
O	1.038909	-1.94694	-1.18387
H	0.416983	-1.21074	-1.09813
O	2.759734	-0.58691	1.866155
H	3.606939	0.094645	0.965207
O	0.330787	0.841989	-0.42772
O	1.844544	3.471904	-0.46736
H	1.878813	4.350203	-0.08536
C	-0.89147	0.584423	0.168801
H	-0.81644	0.621108	1.266962
C	-1.96742	1.551	-0.29755
H	-1.96667	1.563244	-1.39572
C	-3.31892	1.060448	0.210463
H	-3.31049	1.112934	1.31018

C	-2.43641	-1.25701	0.291801
H	-2.38799	-1.24553	1.390598
C	-3.59506	-0.38173	-0.18439
H	-3.66937	-0.44112	-1.27862
C	-2.49883	-2.69393	-0.2031
H	-3.35556	-3.19895	0.249287
H	-2.6336	-2.68266	-1.29407
O	-1.23924	-0.72565	-0.24918
O	-1.67878	2.819385	0.232796
H	-2.43216	3.387304	0.03954
O	-4.29549	1.941428	-0.30419
H	-5.15351	1.648133	0.019764
O	-4.82904	-0.72682	0.425381
H	-5.21005	-1.49034	-0.01415
O	-1.35255	-3.41931	0.160917
H	-0.59553	-3.04965	-0.31471
E(elec)	-1297.754955	au	
ZPVE	0.370248951	au	
G correction (873K)	0.098373725	au	

TS: CB1’3’Grob		M06-2X/6-311++G(d,p)	
O	-4.09976	1.310563	-1.07865
C	-1.47922	-0.88046	1.079037
C	-1.66652	0.403443	1.693989
C	-2.16517	1.45104	0.397403
C	-3.01846	0.573385	-0.54069
C	-3.61598	-0.66924	0.118353
H	-0.52948	-1.40919	1.016737
O	-2.44557	-1.48045	0.490885
H	-0.75613	0.838202	2.101337
H	-2.82968	2.060792	1.036777
H	-2.35592	0.226121	-1.34642
H	-4.18741	-0.42753	1.013631
C	-4.44532	-1.52258	-0.83165
H	-3.91793	-1.62423	-1.78912
H	-4.56983	-2.51753	-0.40017
O	0.152754	0.105956	-0.83977
O	-2.77725	0.458313	2.564424
H	-2.55544	0.013764	3.387879
O	-1.18703	2.079635	-0.18315
H	-0.3197	1.014295	-0.66005

O	-5.72656	-0.97226	-0.9896
H	-5.62102	-0.06975	-1.31455
H	-3.74646	2.13148	-1.43961
O	5.430096	-0.40654	0.476167
H	5.759424	-1.30912	0.399085
C	4.223565	-0.35426	-0.21248
H	4.394293	-0.36647	-1.30296
C	3.315494	-1.52205	0.161021
H	3.176013	-1.50631	1.250522
C	1.983411	-1.33861	-0.53121
H	2.140237	-1.36941	-1.61784
C	2.393201	1.104323	-0.5406
H	2.57617	1.086669	-1.62525
C	1.380349	0.012809	-0.17386
H	1.251098	0.053501	0.923957
C	1.975085	2.503493	-0.12561
H	1.066748	2.803264	-0.64712
H	1.760837	2.500589	0.952437
O	3.613341	0.850741	0.156082
O	3.973491	-2.70401	-0.24416
H	3.366069	-3.4405	-0.12151
O	1.131084	-2.41471	-0.14945
H	0.423324	-2.45814	-0.80054
O	2.984112	3.434954	-0.44302
H	3.802433	3.104178	-0.05761
E(elec)	-1297.756138	au	
ZPVE	0.371151777	au	
G correction (873K)	0.09893446	au	
TS: CB2’4’Grob		M06-2X/6-311++G(d,p)	
O	-5.22024	0.59894	-0.29259
C	-1.78893	1.215742	0.465396
C	-3.98075	0.348533	0.276462
C	-3.48575	-0.97158	-0.28984
H	-1.8378	1.180248	1.564153
H	-4.04635	0.292529	1.375048
H	-3.45138	-0.86927	-1.3832
C	-2.08982	-1.27115	0.231435
H	-2.14482	-1.42825	1.318683
C	-1.1729	-0.09105	-0.04509
H	-1.03094	-0.01112	-1.13084

O	-4.30897	-2.04897	0.095752
H	-5.19553	-1.88859	-0.24306
O	-1.54763	-2.40828	-0.40194
H	-2.15377	-3.14332	-0.25996
O	0.069493	-0.24501	0.614791
C	-0.98239	2.430312	0.039679
H	-1.47224	3.331689	0.421468
H	0.021985	2.373968	0.462382
O	-3.0908	1.385767	-0.0821
O	-0.83737	2.484779	-1.36641
H	-1.71893	2.533859	-1.75113
C	1.122242	-0.86191	-0.15684
C	1.664492	0.27336	-0.99908
C	3.002421	0.809502	-0.9711
C	3.948282	-0.13761	0.065347
C	3.046743	-0.54909	1.234991
H	0.701535	-1.65786	-0.7688
O	2.011081	-1.4093	0.728974
H	0.897839	0.974795	-1.34422
H	3.539694	0.562367	-1.88791
H	4.702385	0.601248	0.393956
H	3.625065	-1.21346	1.879111
C	2.481529	0.600932	2.05753
H	3.309477	1.115053	2.550127
H	1.982762	1.337062	1.41057
O	2.644885	-1.39806	-2.3844
H	2.434422	-2.27051	-2.72866
O	2.91006	2.190394	-0.73524
H	3.518238	2.663441	-1.3088
O	1.607554	0.157049	3.070018
H	0.905616	-0.33631	2.630945
O	4.387627	-1.16086	-0.63102
H	3.414863	-1.48661	-1.67938
H	-5.59871	1.391429	0.099377
E(elec)	-1297.711876	au	
ZPVE	0.368400374	au	
G correction (873K)	0.098407739	au	

TS: CB4’2’Grob		M06-2X/6-311++G(d,p)	
C	2.435926	1.504088	-0.66842
C	1.377847	0.362759	-0.84631

C	2.640438	-1.29582	0.470232
C	3.661373	-0.22465	0.730053
C	3.197005	1.09801	0.936183
H	1.065857	0.397471	-1.8944
H	1.925571	2.415892	-0.30128
H	3.174687	-2.19929	0.161647
H	4.691006	-0.50586	0.888508
H	3.957502	1.860623	1.087791
O	1.869456	-0.94765	-0.68791
O	0.281865	0.633181	-0.00612
O	3.278939	1.672847	-1.61204
H	4.110631	0.532405	-1.57597
O	2.142962	1.192129	1.855867
H	1.354676	1.567203	1.443042
O	4.541728	-0.36404	-1.25276
H	4.013892	-1.03201	-1.70339
C	1.719714	-1.68827	1.632996
H	2.316351	-1.95845	2.510359
H	1.06921	-0.86108	1.895767
O	0.883782	-2.75471	1.214446
H	1.357944	-3.58848	1.269528
O	-5.08462	-0.34604	-0.04062
H	-5.31009	-1.27956	-0.12521
C	-3.72972	-0.27901	0.253151
H	-3.5513	-0.46461	1.326278
C	-2.91902	-1.25776	-0.57949
H	-3.09862	-1.02247	-1.63792
C	-1.43662	-1.10212	-0.27851
H	-1.25706	-1.36901	0.77306
C	-1.97128	1.284184	0.277351
H	-1.8279	1.119874	1.356901
C	-1.02956	0.354045	-0.49429
H	-1.0781	0.585769	-1.56697
C	-1.74311	2.751397	-0.04117
H	-0.72694	3.038722	0.231196
H	-1.8704	2.89714	-1.12255
O	-3.32119	1.025991	-0.06948
O	-3.37565	-2.556	-0.27366
H	-2.77373	-3.17721	-0.69843
O	-0.76163	-2.00192	-1.12851

H	0.085988	-2.21977	-0.71873
O	-2.62225	3.568019	0.691951
H	-3.51445	3.247114	0.520819
E(elec)	-1297.733039	au	
ZPVE	0.370319587	au	
G correction (873K)	0.10335586	au	
TS: CB5’3’Grob		M06-2X/6-311++G(d,p)	
C	-0.73958	-1.13106	-0.82099
C	-1.81126	-1.98359	-0.42432
C	-2.48789	-1.37296	1.099979
C	-3.53646	-0.2968	0.772104
C	-2.87798	0.867533	0.016222
H	-0.8311	-0.40814	-1.63324
O	-1.58323	1.051093	0.538803
H	-1.44594	-2.94346	-0.05947
H	-2.95681	-2.30734	1.433531
H	-3.8348	0.066276	1.762627
H	-2.83712	0.592413	-1.05463
C	-3.69998	2.148069	0.117867
H	-3.8309	2.399175	1.179265
H	-3.14449	2.96155	-0.35323
O	0.358928	-1.21734	-0.18059
O	-2.84928	-2.06501	-1.3672
H	-2.70506	-2.80145	-1.96716
O	-1.52412	-0.90745	1.868726
H	-1.4076	0.178756	1.345614
O	-4.72057	-0.76599	0.163326
H	-4.47615	-1.18766	-0.66806
O	-4.93914	2.047042	-0.55307
H	-5.36239	1.22607	-0.27702
O	5.006433	1.630386	0.188949
H	4.887878	2.586493	0.231242
C	3.765772	1.053762	0.411011
H	3.525743	1.031336	1.487068
C	2.660953	1.766523	-0.35199
H	2.923024	1.740822	-1.41945
C	1.3288	1.053977	-0.14931
H	1.065217	1.087321	0.918436
C	2.702012	-1.03674	0.180294
H	2.48415	-1.05651	1.258152

C	1.517204	-0.40499	-0.55097
H	1.636121	-0.48143	-1.63693
C	3.024958	-2.44149	-0.30018
H	2.18228	-3.10493	-0.09951
H	3.202227	-2.40672	-1.38446
O	3.86021	-0.26675	-0.07402
O	2.602244	3.090076	0.117182
H	1.81519	3.497174	-0.26371
O	0.362403	1.703372	-0.92095
H	-0.49462	1.613776	-0.40211
O	4.135155	-2.9609	0.383122
H	4.853528	-2.32517	0.290437
E(elec)	-1297.763601	au	
ZPVE	0.368782086	au	
G correction (873K)	0.100126306	au	

TS: axCB6'4'Grob		M06-2X/6-311++G(d,p)	
O	5.272743	0.53076	-0.5121
C	1.753608	1.01967	-0.82011
C	3.958133	0.188396	-0.79907
C	3.582455	-0.95774	0.122683
H	1.642255	0.676987	-1.86013
H	3.845589	-0.11684	-1.85232
H	3.746395	-0.61633	1.153977
C	2.117304	-1.32554	-0.05228
H	1.965232	-1.71885	-1.06785
C	1.252233	-0.08332	0.118744
H	1.346357	0.276423	1.151624
O	4.336036	-2.11951	-0.15097
H	5.266853	-1.91137	-0.0222
O	1.745162	-2.29467	0.90515
H	2.353544	-3.03632	0.816146
O	-0.1017	-0.31811	-0.20961
C	0.987954	2.315778	-0.6595
H	1.466092	3.085315	-1.27333
H	-0.0404	2.177805	-0.98793
O	3.124303	1.297382	-0.54621
O	0.919697	2.727092	0.699702
H	1.807149	2.945974	0.999531
C	-0.90247	-0.82906	0.850645
C	-1.52147	0.329863	1.63972

C	-2.48179	1.221512	0.826734
C	-3.00705	0.571715	-0.45079
C	-3.15341	-1.24435	0.138264
H	-0.26544	-1.42909	1.506839
O	-1.84172	-1.70996	0.322099
H	-0.68934	0.956945	1.989035
H	-3.34317	1.438633	1.468957
H	-2.19907	0.338816	-1.16013
H	-3.68596	-1.03475	1.064905
C	-3.87052	-1.91845	-0.84506
H	-3.38548	-2.69636	-1.4197
H	-4.9474	-1.94647	-0.7626
O	-2.25049	-0.17676	2.746745
H	-1.69486	-0.78746	3.239696
O	-1.8749	2.420552	0.390468
H	-1.13368	2.658863	0.96011
O	-4.06311	-0.77252	-2.5168
H	-4.88738	-1.0029	-2.95395
O	-4.11608	0.995379	-0.9217
H	-4.21314	0.144782	-1.95421
H	5.556397	1.228147	-1.1105
E(elec)	-1297.742884	au	
ZPVE	0.369764445	au	
G correction (873K)	0.103422068	au	

TS: eqCB6’4’Grob		M06-2X/6-311++G(d,p)	
O	0.243675	0.281459	-0.74431
C	-2.58674	-0.89892	0.994296
C	-0.91922	0.411163	-0.01464
C	-1.87521	1.29264	-0.80503
H	-2.58625	-0.17946	1.815025
H	-0.72493	0.878184	0.966613
H	-1.94291	0.887039	-1.82288
C	2.33683	1.12026	0.04359
C	1.401954	-0.09401	-0.01649
C	2.087433	-1.24817	-0.7309
C	3.462274	-1.49458	-0.12798
C	4.272429	-0.21109	-0.10219
H	1.13109	-0.42177	0.995221
H	2.214444	-0.96684	-1.78739
H	3.346179	-1.8301	0.911642

H	4.432696	0.163314	-1.12604
C	-3.26484	1.304343	-0.18935
H	-3.22972	1.752356	0.813753
C	-3.87624	-0.08953	-0.0963
H	-3.61651	-0.71053	-0.97246
H	2.515585	1.474829	-0.98237
O	-1.32696	2.591951	-0.81136
H	-1.98474	3.178681	-1.20044
O	-4.06563	2.100448	-1.04092
H	-4.97903	1.995771	-0.74898
O	-5.07294	-0.15872	0.356278
H	-5.19711	-1.58922	0.329891
C	-3.09324	-2.15999	1.309266
H	-2.62342	-3.04593	0.899803
H	-3.69686	-2.28204	2.195551
O	-1.44667	-0.8874	0.193474
O	-4.87191	-2.58623	0.367372
H	-4.73769	-2.88439	-0.53669
O	1.29111	-2.4028	-0.62108
H	1.795183	-3.12728	-1.00673
O	4.080605	-2.48998	-0.91539
H	4.943776	-2.68078	-0.53503
O	5.478101	-0.49928	0.523925
H	6.047243	0.275073	0.491083
O	3.577748	0.761049	0.646514
C	1.77794	2.266251	0.867379
H	0.861919	2.637523	0.404308
H	1.550089	1.897461	1.878049
O	2.690124	3.339836	0.918361
H	3.522767	2.985126	1.245255
E(elec)	-1297.750538	au	
ZPVE	0.369676709	au	
G correction (873K)	0.098536275	au	

TS: GLC12Pin→GLC13Grob		M06-2X/6-311++G(d,p)	
O	-0.7021	2.360735	-0.07763
C	-1.17891	0.08183	0.301831
C	-0.16527	1.07105	-0.26583
C	1.128344	0.903383	0.522125
C	1.647705	-1.40869	-0.45855
C	0.79257	-1.11856	0.584951

H	0.038696	0.863035	-1.32547
H	0.983316	1.055227	1.603721
H	1.23395	-1.74713	-1.41343
H	1.136514	-1.18987	1.613019
H	-1.43742	0.392545	1.322666
O	2.269535	1.16334	0.037075
H	2.876977	-0.01973	-0.15021
O	2.894491	-1.08653	-0.40158
O	-0.56218	-1.21516	0.347267
C	-2.4399	-0.0517	-0.52158
H	-2.9431	0.914915	-0.56592
H	-2.16578	-0.3554	-1.54104
O	-3.33502	-0.96983	0.062096
H	-2.87036	-1.80692	0.158917
H	-0.07785	3.008963	-0.41775
TS: GLC21Pin→GLC13Grob		M06-2X/6-311++G(d,p)	
O	-3.02209	-1.03322	0.195974
C	-1.90492	-1.39497	-0.3485
H	-1.92105	-1.85264	-1.33938
C	-0.71928	-1.01026	0.242063
H	-0.72579	-0.82752	1.315573
C	-1.12637	0.836318	-0.25283
H	-1.20263	0.802114	-1.35414
C	1.235253	0.054087	-0.32823
H	1.532356	0.272747	-1.35739
C	0.307342	1.167415	0.17537
H	0.323377	1.24252	1.270456
C	2.465181	-0.13311	0.534316
H	3.035289	0.797965	0.554738
H	2.150051	-0.37229	1.560337
O	0.497514	-1.19243	-0.35615
O	-2.13948	1.198772	0.423977
H	-2.86598	0.012645	0.465046
O	0.745441	2.366525	-0.41892
H	0.234301	3.096289	-0.05631
O	3.3076	-1.13362	0.015186
H	2.784891	-1.93703	-0.07274
TS: GLC23Pin→GLC31Grob		M06-2X/6-311++G(d,p)	
O	1.13386	2.193543	-0.08371
H	2.08307	1.894172	-0.11148

C	0.503101	1.165082	-0.49432
H	1.056659	0.42683	-1.06579
C	0.813061	-0.91995	1.040598
H	0.436217	-1.18536	2.021584
C	2.088174	-0.38371	1.01032
H	2.546635	-0.28399	2.007476
C	-1.20517	-0.36137	-0.44395
H	-1.54268	-0.48627	-1.474
C	-0.05327	-1.34875	-0.11476
H	-0.56719	-2.28262	0.150965
C	-2.36229	-0.44287	0.530361
H	-2.7985	-1.44059	0.45785
H	-1.98382	-0.3023	1.550186
O	-0.74913	1.05431	-0.32426
O	2.764409	0.049568	0.013182
O	0.672779	-1.5566	-1.32215
H	1.603424	-1.67283	-1.09145
O	-3.38209	0.474008	0.218027
H	-3.05416	1.363715	0.376515
TS: GLC23Pin→GLC24Grob		M06-2X/6-311++G(d,p)	
O	-0.9316	2.079366	0.059523
H	-1.26109	2.607181	-0.6734
C	0.034538	1.180227	-0.44003
H	0.688237	1.673622	-1.16354
C	0.824068	0.706641	0.7683
H	0.384987	0.975849	1.722596
C	2.202685	0.605282	0.720537
H	2.800983	0.709896	1.629625
C	-0.80643	-0.98694	-0.30889
H	-1.07402	-1.80414	-0.98409
C	0.526831	-1.34328	0.337939
H	0.493467	-1.73606	1.363737
C	-1.93229	-0.77049	0.700955
H	-2.16951	-1.72639	1.174133
H	-1.62263	-0.06977	1.485469
O	-0.5886	0.133442	-1.14311
O	2.808029	0.221574	-0.34262
O	1.477868	-1.70785	-0.41727
H	2.249345	-0.7102	-0.64138
O	-3.10335	-0.32395	0.065443

H	-2.88496	0.510698	-0.36172
TS: GLC32Pin→GLC31Grob		M06-2X/6-311++G(d,p)	
O	1.795358	-1.70088	0.545727
H	2.61679	-1.00297	-0.02197
C	0.788649	-0.98085	0.797714
H	0.590156	-0.693	1.836363
C	1.96027	0.577194	-0.85019
H	1.611951	0.702706	-1.88471
C	1.124319	0.942006	0.199253
H	1.558696	1.2138	1.154882
C	-1.16861	0.04386	0.240711
H	-1.47403	0.127009	1.291172
C	-0.30567	1.292886	-0.09653
H	-0.41466	1.502899	-1.17124
C	-2.38616	-0.11501	-0.64024
H	-2.99821	0.784983	-0.55682
H	-2.05633	-0.21976	-1.68261
O	-0.35394	-1.11044	0.06188
O	3.025246	-0.0981	-0.66877
O	-0.83946	2.345272	0.678974
H	-0.40945	3.167667	0.431662
O	-3.18426	-1.20393	-0.24331
H	-2.64525	-1.99921	-0.29711
TS: GLC32Pin→GLC24Grob		M06-2X/6-311++G(d,p)	
O	-0.55319	2.138749	-0.80869
H	0.099054	2.819295	-0.99886
C	-0.25638	1.568549	0.434942
H	-0.2538	2.329583	1.220702
C	-2.36135	0.194439	-0.06797
H	-2.70259	0.867043	-0.8558
C	-1.2204	0.453483	0.668905
H	-1.11056	-0.08242	1.605332
C	1.045405	-0.43556	0.320956
H	1.107964	-0.8913	1.314639
C	-0.2321	-0.90683	-0.36095
H	-0.32248	-0.51919	-1.38953
C	2.27461	-0.80501	-0.49311
H	2.347028	-1.89103	-0.57116
H	2.170105	-0.38191	-1.50099
O	1.042999	0.993165	0.439416

O	-2.9291	-0.9581	0.036528
O	-0.77196	-2.02295	-0.07803
H	-2.0914	-1.66904	0.078895
O	3.450353	-0.34957	0.134425
H	3.345097	0.594193	0.290921
TS: GLC34Pin→GLC42Grob		M06-2X/6-311++G(d,p)	
O	0.994249	2.084604	-0.73099
H	1.681391	2.65499	-0.37472
C	0.297505	1.499649	0.333444
H	-0.03266	2.246934	1.059634
C	-0.9398	0.855171	-0.33651
H	-0.69668	0.588082	-1.37719
C	-0.69259	-0.80302	0.672347
H	-1.1644	-0.38591	1.557525
C	0.801171	-0.79464	0.734405
H	1.186876	-1.3531	1.590342
C	-1.54892	-1.44465	-0.20268
H	-1.20109	-2.11677	-0.99075
C	1.51895	-1.26469	-0.52392
H	1.329405	-2.33008	-0.67856
H	1.151812	-0.71333	-1.39938
O	1.12227	0.577968	1.017707
O	-2.12934	1.216728	-0.07602
H	-2.77518	-0.01379	-0.09005
O	-2.79249	-1.10281	-0.2291
O	2.909613	-1.11046	-0.38391
H	3.068223	-0.19216	-0.14091
TS: GLC43Pin→GLC42Grob		M06-2X/6-311++G(d,p)	
O	1.166708	2.02036	-0.12202
H	1.670022	2.510878	0.533487
C	0.173252	1.267835	0.531045
H	-0.31186	1.842791	1.322947
C	-0.86222	0.952335	-0.57052
H	-0.41138	0.974576	-1.57317
C	-1.74296	-1.25249	0.438869
H	-1.62166	-1.52208	1.492805
C	0.716661	-1.03336	0.27249
H	0.892118	-1.86761	0.956578
C	-0.6399	-1.07623	-0.37055
H	-0.75611	-1.2003	-1.44172

C	1.852213	-0.97323	-0.74312
H	1.911607	-1.93278	-1.26223
H	1.654077	-0.1901	-1.4862
O	0.718499	0.123526	1.133694
O	-2.07766	1.267265	-0.45139
H	-2.78808	0.093452	-0.33032
O	-2.92466	-0.90597	0.055261
O	3.08892	-0.7632	-0.11111
H	3.00448	0.046195	0.40294
TS: GLC13Cond		M06-2X/6-311++G(d,p)	
C	1.634165	-0.28506	-0.23988
C	0.715339	0.595157	-1.05668
C	-1.29062	-0.46554	-0.21866
C	-0.42717	-1.25151	0.774703
C	0.866833	-0.46755	1.065357
H	1.103616	1.342298	-1.74624
H	2.552161	0.270426	-0.05134
H	-1.78913	-1.15441	-0.90371
H	-0.98936	-1.28951	1.710913
H	1.462022	-1.04965	1.788035
O	-0.51388	0.400314	-1.15674
O	1.96693	2.583182	0.17601
H	1.87901	3.495318	0.455622
O	1.861022	-1.42907	-1.07053
H	2.796975	-1.5234	-1.26212
O	0.561604	0.815652	1.418332
H	1.456687	2.016121	0.831084
O	-0.23856	-2.58981	0.363963
H	0.511277	-2.6208	-0.24082
C	-2.28841	0.487835	0.42347
H	-2.86425	-0.09095	1.154661
H	-1.72713	1.256439	0.954605
O	-3.12236	1.117331	-0.52283
H	-3.77084	0.487285	-0.84636
TS: GLC31Cond		M06-2X/6-311++G(d,p)	
C	-0.79798	0.100313	1.474732
C	-1.82126	-0.09498	0.354022
C	-0.97623	0.332145	-0.82416
C	0.36013	-0.33884	-0.99254
C	1.078963	-0.7542	0.302438

H	-1.21078	0.010255	2.484879
O	0.20131	-0.92095	1.398696
H	-2.63902	0.609999	0.510531
H	-1.4802	0.512326	-1.76627
H	1.033556	0.257327	-1.60933
H	1.502956	-1.7414	0.098465
C	2.254742	0.156355	0.644751
H	1.922983	1.188243	0.765625
H	2.67641	-0.19912	1.590489
O	-0.33463	1.314428	1.127396
H	-0.72366	2.370092	-0.02587
O	-2.28302	-1.39899	0.048406
H	-3.24225	-1.43044	0.043812
O	-0.95142	2.523754	-0.9804
H	-0.16881	2.890603	-1.40287
O	-0.01881	-1.46191	-1.78675
H	-0.584	-2.0315	-1.24661
O	3.182782	0.018476	-0.42641
H	3.952796	0.560415	-0.24579
TS: GLC16Cond		M06-2X/6-311++G(d,p)	
C	0.502459	1.229415	0.341458
C	-0.22454	1.02783	-0.96384
C	-0.17427	-1.34114	-0.81422
C	1.143112	-1.18341	-0.07738
C	1.116285	-0.05483	0.96554
H	-0.41581	1.900146	-1.5794
H	-0.25201	1.600465	1.039122
H	-0.05383	-2.04664	-1.63622
H	1.352805	-2.12599	0.440595
H	2.157152	0.194872	1.201817
O	-0.44226	-0.07032	-1.52011
O	-2.39612	1.383503	-0.31773
H	-2.9322	2.01837	0.161398
O	1.4605	2.227035	0.026687
H	1.609773	2.770034	0.804274
O	0.485788	-0.42625	2.142989
H	-0.48716	-0.55233	1.875412
O	2.097044	-0.90394	-1.08978
H	2.940495	-0.68854	-0.68263
C	-1.41969	-1.64424	0.035731

H	-2.24832	-1.81531	-0.66914
H	-1.21514	-2.61036	0.528647
O	-1.68667	-0.63292	0.922609
H	-2.26217	0.536527	0.275084
TS: GLC61Cond		M06-2X/6-311++G(d,p)	
C	-1.10989	-1.20907	0.004496
C	0.319601	-1.14901	-0.54281
C	0.483422	1.156301	-0.41005
C	-0.88985	1.286482	0.283271
C	-1.32627	-0.02759	0.963181
H	0.485744	-1.94652	-1.27865
H	-1.22731	-2.14904	0.554719
H	0.638888	2.042467	-1.02945
H	-0.8527	2.071451	1.043432
H	-2.39401	0.075253	1.182748
O	0.466952	0.062217	-1.31073
O	1.221344	-1.14484	0.480981
H	2.613042	-0.83165	-0.0411
O	-1.99411	-1.14532	-1.10535
H	-2.8759	-1.39472	-0.81608
O	-0.65397	-0.24025	2.186895
H	0.121398	-0.78732	1.981596
O	-1.82588	1.692192	-0.6861
H	-1.91033	0.967696	-1.32168
C	1.633331	1.034164	0.563741
H	2.472724	1.698449	0.417693
H	1.436747	0.777225	1.595347
O	3.253239	-0.1062	-0.33766
H	3.089091	-0.01339	-1.2838
TS: GLC24Cond		M06-2X/6-311++G(d,p)	
C	1.276532	0.136231	0.700535
C	0.270109	1.234861	0.379162
C	-0.84271	-0.2175	-1.1503
C	0.295318	-1.21016	-0.87817
C	0.756292	-1.28139	0.59938
H	0.750394	2.212876	0.357752
H	1.839659	0.372017	1.600971
H	-0.97668	-0.16473	-2.23328
H	0.035653	-2.19729	-1.28372
H	1.583057	-1.98975	0.595522

O	-0.40608	1.103158	-0.81632
O	-0.62372	1.134884	1.487723
H	-1.51475	1.318693	1.141525
O	2.890515	1.032418	-0.26609
H	3.711536	0.578777	-0.04732
O	-0.02922	-1.58767	1.723232
H	-0.55305	-0.80871	1.95281
O	1.467806	-0.68512	-1.34682
H	2.4966	0.524649	-1.02231
C	-2.18695	-0.56586	-0.47474
H	-2.7733	-1.19185	-1.15521
H	-2.0428	-1.132	0.444668
O	-2.92275	0.592254	-0.10012
H	-2.98032	1.180759	-0.85953
TS: GLC42Cond		M06-2X/6-311++G(d,p)	
C	-1.49717	-0.69285	-0.84717
C	-1.70177	0.556327	0.016816
C	-0.74659	0.531383	1.215359
C	0.570152	0.625491	0.495825
C	0.865616	-0.18045	-0.70457
H	-2.18373	-0.6951	-1.69525
O	-0.21602	-0.72033	-1.42418
H	-2.75608	0.608454	0.3213
H	-0.92499	1.437685	1.792975
H	1.457633	0.87724	1.06547
H	1.446661	0.465602	-1.37317
C	1.785703	-1.35206	-0.28483
H	1.260717	-1.98393	0.440283
H	1.974866	-1.92989	-1.19427
O	-1.70578	-1.83919	-0.03404
H	-1.67291	-2.62606	-0.58562
O	-1.2179	1.64042	-0.648
H	0.081367	2.571999	-0.50185
O	-0.61784	-0.55339	2.109695
H	-0.92767	-1.34112	1.640764
O	1.033858	2.730727	-0.2603
H	1.070498	3.51128	0.298701
O	2.966814	-0.79835	0.250798
H	3.572902	-1.50236	0.49025
TS: GLC36Cond		M06-2X/6-311++G(d,p)	

C	-0.84751	1.143518	-0.31867
C	-0.30435	1.056843	1.11301
C	0.203196	-1.32581	0.848819
C	-0.46466	-1.36026	-0.51899
C	-0.25201	0.017105	-1.16261
H	-0.97397	1.627016	1.762334
H	-0.62486	2.119585	-0.74408
H	-0.06147	-2.20819	1.430557
H	-0.00753	-2.12562	-1.13805
H	-0.3969	0.065347	-2.23481
O	-0.33483	-0.24206	1.629323
O	0.983182	1.620901	1.102047
H	1.332846	1.596982	1.997914
O	-2.253	0.983477	-0.17796
H	-2.66715	1.027657	-1.04528
O	1.33333	1.288297	-1.64796
H	1.451375	1.974178	-0.97959
O	-1.84774	-1.63869	-0.48266
H	-2.26713	-1.05404	0.160507
C	1.707935	-1.25015	0.527289
H	2.221547	-0.62742	1.270711
H	2.117512	-2.26727	0.603874
O	1.842429	-0.79108	-0.77359
H	1.83314	0.41745	-1.2108
TS: GLC63Cond		M06-2X/6-311++G(d,p)	
C	-1.42127	-0.37416	0.807121
C	-1.13574	-1.28248	-0.38995
C	0.46062	0.345846	-1.27754
C	0.195272	1.361412	-0.08703
C	-0.14915	0.436081	1.117934
H	-2.06346	-1.69185	-0.78813
H	-1.65284	-1.01449	1.662664
H	0.513578	0.995884	-2.15977
H	1.123739	1.893722	0.127751
H	-0.33931	1.118817	1.96545
O	-0.63202	-0.50937	-1.48643
O	-0.29177	-2.32349	-0.04163
H	0.314185	-1.94913	0.633708
O	-2.54236	0.442874	0.46904
H	-2.94503	0.771452	1.276876

O	0.876693	-0.43871	1.339088
H	2.253123	-0.02858	1.150197
O	-0.75932	2.29899	-0.4399
H	-1.62137	1.856394	-0.43738
C	1.75135	-0.29632	-1.13425
H	1.827249	-1.35538	-0.92149
H	2.630436	0.211932	-1.49913
O	3.130984	0.160858	0.639609
H	3.495475	0.999812	0.933202
TS: GLC46Cond		M06-2X/6-311++G(d,p)	
O	-2.25454	1.55751	0.712266
C	-0.79446	-1.14026	0.261981
C	-0.93022	0.253594	-0.30399
C	0.168894	1.181023	0.103764
C	1.478649	0.472014	-0.27576
C	1.538588	-0.90775	0.370474
H	-1.24522	0.338454	-1.33841
H	0.167965	1.317656	1.191504
H	1.523769	0.326984	-1.36324
H	1.480768	-0.81872	1.46797
H	-0.88543	-1.08362	1.355538
O	0.051373	2.410193	-0.56272
H	0.859519	2.908036	-0.39713
O	2.515511	1.314206	0.170731
H	3.355352	0.904548	-0.06193
O	2.738488	-1.4807	-0.02826
H	2.797858	-2.37064	0.332148
O	0.466854	-1.69134	-0.09913
C	-2.0597	-1.76907	-0.29609
H	-1.89499	-2.09232	-1.33716
H	-2.40037	-2.63383	0.285108
O	-2.8725	-0.66	-0.18527
H	-2.86859	0.800903	0.548109
H	-2.46252	2.266261	0.094261
TS: GLC64Cond		M06-2X/6-311++G(d,p)	
O	2.312014	-2.07136	-0.0706
H	3.151279	-1.65403	0.156833
C	1.310898	-1.18751	0.296758
H	1.136764	-1.21908	1.385485
C	1.668135	0.250051	-0.11342

H	1.84993	0.246248	-1.19708
C	0.553829	1.250146	0.187405
H	0.340249	1.25808	1.266359
C	-0.86757	-0.68901	-0.0996
H	-1.02354	-0.60257	0.989918
C	-0.6761	0.751549	-0.55741
H	-0.45906	0.798201	-1.63977
C	-2.20018	-1.00206	-0.66502
H	-2.53759	-0.49373	-1.55715
H	-2.68268	-1.93579	-0.3983
O	0.136629	-1.62748	-0.36664
O	2.858563	0.556898	0.584143
H	3.050793	1.489423	0.437558
O	1.031901	2.515456	-0.22532
H	0.322193	3.156156	-0.12029
O	-1.92371	1.213283	-0.24331
H	-3.16163	0.51518	0.745486
O	-3.68047	-0.29847	0.934867
H	-4.60026	-0.10375	0.733593
Product: GLC13Cond, GLC31Cond		M06-2X/6-311++G(d,p)	
C	-1.85632	-0.41195	-0.41556
C	-0.81595	-1.47798	0.003915
C	0.868222	0.184223	-0.20649
C	-0.10841	1.010701	0.679267
C	-1.39597	0.225129	0.896539
H	-0.98276	-2.54012	-0.16404
H	-2.87812	-0.79068	-0.35096
H	0.901878	0.668783	-1.18834
H	0.343577	1.176973	1.661234
H	-2.10869	0.740849	1.538849
O	0.46157	-1.17682	-0.4258
O	-1.63172	0.363729	-1.56315
H	-1.78151	-0.16092	-2.3538
O	-1.01615	-1.08671	1.369111
O	-0.34993	2.287485	0.134888
H	-0.77711	2.156422	-0.7205
C	2.259435	0.175301	0.400151
H	2.530816	1.21197	0.642596
H	2.235781	-0.40485	1.325308
O	3.227118	-0.43137	-0.42593

H	3.282928	0.058587	-1.25021
Product: GLC24Cond, GLC42Cond		M06-2X/6-311++G(d,p)	
C	1.704939	-0.31	-0.33745
C	1.026934	1.022023	-0.63214
C	-0.97657	-0.34793	-0.60013
C	0.032261	-1.44009	-0.29668
C	1.006581	-1.02267	0.838744
H	1.156883	1.283383	-1.69003
H	2.790255	-0.23866	-0.39606
H	-1.25205	-0.40412	-1.66042
H	-0.39915	-2.44172	-0.31782
H	1.591408	-1.88669	1.149688
O	-0.36746	0.93109	-0.34591
O	1.567843	1.981029	0.216033
H	1.194752	2.839855	-0.00376
O	0.590624	-0.34914	1.977421
H	0.307461	0.53827	1.728594
O	1.128736	-1.28106	-1.23075
C	-2.22906	-0.4004	0.254979
H	-2.76754	-1.32736	0.04691
H	-1.95192	-0.38947	1.315724
O	-3.10228	0.660969	-0.0615
H	-2.60027	1.477762	0.020836
Product: GLC36Cond, GLC63Cond		M06-2X/6-311++G(d,p)	
C	-0.24853	-1.18313	0.632428
C	0.66604	-1.17485	-0.60591
C	0.220061	1.20166	-0.85431
C	-1.01592	1.15963	0.04938
C	-0.42318	0.254688	1.145692
H	0.442769	-2.04727	-1.21816
H	0.237527	-1.79196	1.402649
H	0.149786	1.920859	-1.66819
H	-1.19385	2.152531	0.47008
H	-0.97134	0.287634	2.089456
O	0.399487	-0.07343	-1.45885
O	2.012975	-1.26523	-0.24353
H	2.148112	-0.77693	0.576049
O	-1.47316	-1.77608	0.231707
H	-2.09316	-1.76526	0.967022
O	0.889357	0.792669	1.355701

O	-2.20677	0.755192	-0.54969
H	-2.08931	-0.14026	-0.8901
C	1.27726	1.545839	0.181024
H	2.28482	1.259628	-0.11758
H	1.255148	2.613062	0.416295
Product: GLC46Cond, GLC64Cond		M06-2X/6-311++G(d,p)	
O	2.144845	-1.79113	-0.36168
H	2.958533	-1.30746	-0.17928
C	1.112442	-1.08797	0.240481
H	1.188414	-1.14253	1.339646
C	1.178398	0.405084	-0.17228
H	1.230109	0.432921	-1.26895
C	-0.02741	1.270673	0.251735
H	-0.07726	1.336647	1.345953
C	-1.111	-0.91664	0.323751
H	-1.01967	-0.80892	1.413919
C	-1.16778	0.457321	-0.29465
H	-1.08456	0.401686	-1.38838
C	-2.60821	-0.92747	0.002945
H	-2.83653	-1.26773	-1.01098
H	-3.3006	-1.34609	0.730963
O	-0.08536	-1.72431	-0.16697
O	2.383559	0.882562	0.386864
H	2.475963	1.808452	0.139073
O	0.206577	2.544467	-0.3182
H	-0.48381	3.151406	-0.03933
O	-2.56328	0.530367	0.060672
TS: CB16Cond		M06-2X/6-311++G(d,p)	
C	-2.90766	1.066768	0.13731
C	-3.61402	0.354918	-0.97016
C	-1.41294	0.83724	-0.09235
O	-3.17804	-0.70935	-1.46988
O	-5.49694	0.388475	0.572901
C	-1.1741	-0.6746	0.025617
C	-2.24902	-1.52891	-0.67518
C	-3.18186	-2.28093	0.311354
O	-3.8411	-1.40067	1.086134
H	-3.17611	0.603683	1.089405
H	-4.40123	0.848293	-1.53182
H	-1.11123	1.179166	-1.09196

H	-1.19572	-0.91452	1.096173
H	-1.78028	-2.17097	-1.41846
H	-3.82749	-2.93672	-0.30446
H	-2.49755	-2.95053	0.870249
H	-4.97515	-0.46285	0.828205
O	-3.20245	2.436923	0.097188
H	-4.05317	2.552248	0.539253
O	-0.68233	1.52207	0.898329
H	-1.13999	2.353383	1.078267
H	-6.43434	0.206102	0.657717
O	0.054556	-1.10343	-0.5447
C	1.216812	-0.63195	0.06039
H	1.065073	-0.52143	1.146106
C	2.33451	-1.62349	-0.23489
H	2.421052	-1.7179	-1.32516
C	3.635955	-1.08557	0.334673
H	3.543413	-1.0466	1.430552
C	2.694148	1.194524	0.122192
H	2.528213	1.239825	1.209053
C	3.91054	0.323979	-0.16875
H	4.070526	0.284706	-1.25591
O	1.554254	0.608447	-0.50647
O	2.107075	-2.87872	0.370746
H	1.315185	-3.26301	-0.01668
O	4.740211	-1.88889	-0.02763
H	4.564405	-2.78689	0.271585
O	5.027772	0.882043	0.483055
H	5.747146	0.244648	0.418806
O	1.628722	3.333716	-0.0511
H	0.888115	2.715102	-0.08258
C	2.782151	2.606429	-0.41409
H	2.895744	2.562392	-1.50562
H	3.652459	3.106422	0.011925
TS: CB1’6’Cond		M06-2X/6-311++G(d,p)	
O	-0.44562	-1.20499	0.014059
O	1.685387	1.644023	-1.71224
O	4.231549	2.012891	-0.4721
O	5.511105	-0.51696	0.327483
O	2.47583	-1.64796	-0.71074
O	1.384037	-0.68996	1.55896

C	1.737326	-0.65178	-1.00552
C	2.156448	0.769624	-0.72066
C	3.693952	0.732925	-0.70466
C	4.137938	-0.18609	0.434718
C	3.347682	-1.51029	0.463485
C	2.352092	-1.6321	1.661336
O	-5.2666	1.372	0.21393
O	-5.18886	-1.37067	-0.47944
O	-2.59231	-2.21853	-1.34932
O	-3.02339	1.370947	0.638383
O	-0.49752	2.393712	-0.08188
C	-4.18654	0.562312	0.557636
C	-4.06548	-0.51563	-0.52385
C	-2.7999	-1.32312	-0.2794
C	-1.58122	-0.39076	-0.13684
C	-1.83774	0.640442	0.976974
C	-0.75656	1.698397	1.144206
H	0.8838	2.05326	-1.33744
H	3.791122	2.610722	-1.08968
H	0.23041	-1.00067	0.80316
H	1.007148	-0.85087	-1.78156
H	1.830816	1.058325	0.275989
H	4.063464	0.321845	-1.65782
H	3.935457	0.35211	1.371295
H	4.03781	-2.35025	0.384413
H	2.986635	-1.52367	2.56412
H	1.978107	-2.67525	1.661805
H	-5.96417	-0.80679	-0.58131
H	-1.70669	-2.57461	-1.19949
H	-1.35877	2.662734	-0.4251
H	-4.34678	0.07265	1.535782
H	-3.98364	-0.00779	-1.49763
H	-2.92105	-1.87676	0.668278
H	-1.49513	0.174995	-1.07872
H	-1.96761	0.124063	1.942496
H	0.173255	1.235403	1.476167
H	-1.08664	2.412913	1.909817
H	-5.46251	1.952707	0.956739
H	5.998189	0.315382	0.317218
Product: CB16Cond (CBN)		M06-2X/6-311++G(d,p)	

C	0.970799	-0.72402	0.130334
C	2.071106	-1.53251	-0.53948
C	3.414468	-1.08858	0.018309
C	3.596031	0.4175	-0.11639
C	2.408893	1.126009	0.524944
O	1.215027	0.648044	-0.0942
O	1.949227	-2.9137	-0.27871
O	4.490425	-1.70033	-0.66034
O	4.769587	0.844893	0.532729
C	2.398996	2.630552	0.342739
O	1.284967	3.210151	0.981358
H	1.142789	-3.23135	-0.69607
H	4.374792	-2.65472	-0.60565
H	0.478857	2.848775	0.593169
H	2.033232	-1.32559	-1.61672
H	3.44836	-1.34615	1.087729
H	3.626252	0.669047	-1.18681
H	2.379841	0.89675	1.599631
H	5.492799	0.291839	0.217724
H	3.295746	3.052714	0.79587
H	2.411338	2.858445	-0.73208
H	0.955362	-0.91552	1.216655
C	-4.17841	-0.21719	-0.00067
C	-3.36788	1.032796	-0.37797
C	-1.96072	0.609944	-0.7827
C	-1.39898	-0.46004	0.156548
C	-2.4707	-1.54877	0.392223
O	-3.55542	-1.37234	-0.51519
O	-4.01633	1.677609	-1.4521
O	-1.1717	1.781644	-0.84349
O	-0.24277	-1.05779	-0.44683
C	-3.20567	-1.3773	1.722251
O	-4.17367	-0.38002	1.411141
H	-3.45539	2.406614	-1.73637
H	-0.2708	1.515627	-1.06914
H	-3.31604	1.690909	0.49698
H	-2.03601	0.149671	-1.77459
H	-1.10234	0.005047	1.104315
H	-2.044	-2.53798	0.237837
H	-3.70841	-2.3035	2.010977

H	-2.57068	-1.02911	2.538264
H	-5.19819	-0.15713	-0.37749
TS: CBN1'6'Cond		M06-2X/6-311++G(d,p)	
O	3.217284	-2.00115	1.529137
O	1.320214	0.047766	2.204837
O	2.899114	-0.54098	-1.37971
O	4.677458	0.562008	-0.54091
C	3.913174	-0.62974	-0.41618
C	3.291049	-0.6871	0.995615
C	1.853769	-0.19472	0.912384
C	1.752569	1.078602	0.072707
C	2.510476	0.834589	-1.26511
C	3.888105	1.489297	-1.29201
H	4.090589	-2.28183	1.813717
H	1.478111	-0.75078	2.720821
H	4.533129	-1.50241	-0.62946
H	3.867665	-0.03221	1.65855
H	1.27245	-0.97897	0.40963
H	2.234382	1.89061	0.629598
H	1.867402	1.076982	-2.10897
H	3.921848	2.465597	-0.80793
H	4.275811	1.559973	-2.31104
H	-4.89796	1.960852	0.187824
O	-4.77622	1.167061	-0.34337
C	-3.75865	0.397418	0.246793
O	-4.62099	-1.713	-0.54575
C	-3.53279	-0.8174	-0.64215
H	-3.4158	-0.44661	-1.66687
C	-2.26223	-1.59562	-0.27518
H	-2.50598	-2.61665	0.01275
H	-1.60991	-1.91645	-2.27018
C	-1.16684	-1.46203	-1.36549
O	-0.871	-0.15065	-1.50531
H	-0.01399	0.748645	-0.77075
H	-0.31502	-2.10083	-1.06834
O	-1.58999	-1.03425	0.903129
C	-1.47075	0.217906	0.990688
H	-2.11095	1.493165	-0.60771
C	-2.45565	1.174682	0.376455
O	-2.65805	2.253892	1.26055

H	-1.95394	2.895753	1.119326
O	0.421073	1.452037	-0.14427
H	-0.76365	0.549185	1.748654
H	-4.06978	0.054145	1.244279
H	-5.40901	-1.24537	-0.84158
C	2.782151	2.606429	-0.41409
H	2.895744	2.562392	-1.50562
H	3.652459	3.106422	0.011925
TS: rDA of GLC12Mac product		M06-2X/6-311++G(d,p)	
C	-0.30116	-1.59545	0.593598
H	-0.78398	-2.52559	0.272601
C	0.954407	-1.26087	0.097472
C	1.392703	0.035857	0.41251
H	1.181837	0.407958	1.407683
C	-1.15052	1.009394	0.058874
H	-1.61045	1.537478	0.886172
C	0.132782	1.36801	-0.34194
H	0.414179	1.18587	-1.3786
C	-2.03221	0.253278	-0.87686
H	-2.40311	0.921503	-1.66146
H	-1.41875	-0.51648	-1.38342
O	-0.92003	-0.7333	1.290023
O	1.591997	-2.02769	-0.82704
H	2.480162	-1.67302	-0.95092
O	2.602741	0.408884	-0.14308
H	3.12353	0.886738	0.506751
O	0.674167	2.51983	0.213511
H	1.51056	2.699838	-0.22369
O	-3.15435	-0.30273	-0.2466
H	-2.82627	-0.70547	0.568459
TS: rDA of GLC21Mac product		M06-2X/6-311++G(d,p)	
O	1.947295	1.987455	-0.14263
H	2.685753	1.686693	0.397724
C	0.835925	1.32752	0.269148
C	-0.37638	1.633723	-0.3119
H	-0.47534	2.324766	-1.1352
C	-1.44874	0.814835	0.118972
H	-1.49692	0.606159	1.188068
C	0.178404	-1.32747	0.192155
H	0.29978	-1.8507	1.134685

C	-1.11277	-0.99636	-0.24073
H	-1.28489	-0.95299	-1.31528
C	1.300373	-1.38888	-0.78793
H	1.184309	-2.27858	-1.41649
H	1.22379	-0.51347	-1.45825
O	0.95135	0.369187	1.094195
O	-2.65779	1.039978	-0.47327
H	-3.29573	0.43726	-0.07462
O	-2.21103	-1.49049	0.492705
H	-2.34074	-2.42005	0.290184
O	2.558069	-1.47723	-0.17228
H	2.535922	-0.85056	0.561053
TS: rDA of GLC23Mac product		M06-2X/6-311++G(d,p)	
O	0.338807	1.919482	1.169504
H	-0.45514	2.455453	1.06083
C	1.043013	1.957641	0.033096
H	1.046248	2.901983	-0.50289
C	1.894971	0.959339	-0.33237
H	2.606282	1.151069	-1.12386
C	1.622784	-0.383	-0.03317
C	-0.93243	-0.20031	-0.5587
H	-0.80868	-1.03439	-1.28076
C	0.441277	-0.82064	0.61829
H	0.166065	-0.32641	1.541
C	-2.1316	-0.39092	0.37961
H	-2.18156	-1.38382	0.837289
H	-2.05241	0.358501	1.178935
O	-0.81004	0.983139	-1.01456
O	2.370326	-1.29219	-0.64969
H	2.019863	-2.16493	-0.40719
O	0.386007	-2.22127	0.672828
H	-0.48513	-2.52447	0.397008
O	-3.32116	-0.22954	-0.35808
H	-3.19512	0.557239	-0.9009
TS: rDA of GLC32Mac product		M06-2X/6-311++G(d,p)	
O	-2.24699	-1.18271	-1.22992
H	-2.41987	-1.80833	-0.51063
C	-1.59238	-0.15053	-0.73889
H	-1.38172	0.633753	-1.44364
C	-1.43352	-0.0067	0.639793

C	-0.50254	0.850795	1.196772
H	-0.25382	0.710423	2.246183
C	1.368062	0.214976	-0.4939
H	1.886935	0.992547	-1.07737
C	0.368397	1.646352	0.44474
H	1.120638	2.217159	0.98543
C	2.196805	-0.45849	0.590018
H	2.796266	0.260447	1.153196
H	1.515589	-0.98231	1.274747
O	0.53971	-0.52208	-1.10741
O	-2.06959	-0.98916	1.37972
H	-1.50676	-1.2773	2.103701
O	-0.07864	2.270215	-0.7226
H	-0.75461	2.91157	-0.47936
O	3.102096	-1.36875	-0.00167
H	2.595656	-1.89648	-0.62853
TS: rDA of GLC34Mac product		M06-2X/6-311++G(d,p)	
O	-1.94577	1.480599	0.445757
H	-2.82189	1.124096	0.2607
C	-1.16122	0.452697	0.955146
H	-1.71491	-0.23866	1.598763
C	-1.16679	-0.73415	-0.61901
H	-1.04263	0.132765	-1.25279
C	-0.11112	-1.6195	-0.38989
H	-0.36808	-2.64727	-0.14705
C	1.518912	0.137294	0.050424
H	2.327585	0.360942	0.746029
C	1.169652	-1.20848	-0.0523
C	1.37571	1.190453	-1.01692
H	2.315099	1.17876	-1.58223
H	0.585434	0.949299	-1.73166
O	0.019401	0.769213	1.261512
O	-2.46103	-1.24772	-0.6216
H	-2.81976	-1.22532	-1.5126
O	1.938412	-2.1702	0.567159
H	2.855547	-1.88904	0.582144
O	1.243779	2.48234	-0.49382
H	0.574286	2.430684	0.201834
TS: rDA of GLC43Mac product		M06-2X/6-311++G(d,p)	
O	-0.01011	2.428679	0.122228

H	-0.87658	2.833967	0.011342
C	-0.18162	1.216638	0.802481
H	-1.03121	1.265132	1.503609
C	-1.03567	0.250645	-0.56092
H	-0.30188	0.502871	-1.30963
C	-1.11916	-1.0875	-0.09667
C	1.276702	-1.30966	0.29612
H	1.967732	-1.68245	1.049802
C	-0.00783	-1.79829	0.365727
C	2.009344	-0.70876	-0.87255
H	2.557326	-1.54757	-1.32123
H	1.336569	-0.3358	-1.64891
O	0.884345	0.65212	1.176214
O	-2.28582	0.867089	-0.73771
H	-2.39668	1.131318	-1.65428
O	2.961252	0.239612	-0.48895
H	2.503011	0.832305	0.12729
O	-2.32341	-1.55148	0.249195
H	-2.98409	-0.89837	-0.02594
H	-0.23488	-2.56803	1.095044
TS: rDA of GLC45Mac product		M06-2X/6-311++G(d,p)	
O	0.577776	1.444142	-1.05095
H	1.50298	1.483545	-0.73949
C	-0.28769	1.478495	-0.04476
H	-0.11721	2.118217	0.811477
C	-1.49627	0.819054	-0.29122
H	-1.7284	0.639804	-1.33841
C	-1.26786	-1.03259	0.158677
H	-1.3802	-0.79074	1.21429
C	1.056837	-0.79381	0.352824
C	0.012586	-1.47323	-0.25065
H	0.13691	-2.11787	-1.10995
C	2.499474	-0.87341	-0.12759
H	3.072389	-1.57289	0.491526
H	2.556209	-1.19501	-1.16711
O	0.817896	0.095167	1.229248
O	-2.59073	1.074823	0.542696
H	-3.05328	1.858694	0.235765
O	-2.35434	-1.62287	-0.42202
H	-3.14535	-1.25788	-0.01164

O	3.068396	0.429439	-0.05198
H	2.901424	0.72145	0.85393
TS: rDA of GLC46Grob product		M06-2X/6-311++G(d,p)	
O	1.663908	-1.15202	0.963536
H	2.541696	-0.97662	0.60432
C	0.793421	-1.24802	-0.05177
H	1.093195	-1.72814	-0.9743
C	-0.53967	-1.02137	0.272384
H	-0.78843	-0.96173	1.32814
C	-0.9317	0.862252	-0.1326
H	-0.90014	0.599499	-1.18858
C	1.351555	1.420258	-0.20281
H	2.233066	1.957839	0.170885
C	0.104276	1.688729	0.340929
H	-0.04567	2.362431	1.172751
O	1.505936	0.489593	-1.05054
O	-1.53637	-1.53437	-0.56928
H	-1.71205	-2.45003	-0.33826
O	-2.1739	1.019407	0.396279
H	-2.76551	0.40473	-0.0517
Formaldehyde		M06-2X/6-311++G(d,p)	
C	3.015919	0.29195	0.245974
H	2.878854	1.339209	-0.07493
H	2.395855	-0.03478	1.102134
O	3.785648	-0.45178	-0.29323
TS: rDA of CB12Mac product		M06-2X/6-311++G(d,p)	
O	-0.26567	-0.68584	-0.53606
C	2.634799	1.082263	0.572474
C	0.97445	-0.52377	0.074424
C	1.959501	-1.42418	-0.65534
H	2.586736	0.814166	1.637959
H	0.91281	-0.80163	1.140498
H	1.961415	-1.13361	-1.71371
C	-2.01666	-0.77449	1.082557
C	-1.32253	-0.04621	0.122787
C	-2.44354	0.172308	-1.53196
C	-3.76054	0.473443	-1.12265
C	-4.37981	-0.40523	-0.25533
H	-1.17806	1.023908	0.253059
H	-2.20362	-0.8583	-1.75737

H	-5.34655	-0.1373	0.19611
C	3.340361	-1.21852	-0.06328
H	3.322617	-1.54259	0.988188
C	3.717805	0.252025	-0.11033
H	3.788436	0.557494	-1.16459
H	-1.7468	-1.81167	1.249402
O	1.637827	-2.7891	-0.49815
H	0.776963	-2.9464	-0.89869
O	4.331245	-1.93264	-0.77218
H	4.06721	-2.85841	-0.79966
O	4.934372	0.486973	0.560583
H	5.577809	-0.1445	0.220707
C	2.874988	2.573078	0.440612
H	3.808223	2.832099	0.939584
H	2.962289	2.823148	-0.62484
O	1.373534	0.821718	-0.04371
O	1.841607	3.312042	1.053448
H	1.017296	3.028359	0.647118
O	-1.77847	1.059953	-2.29847
H	-2.2516	1.902246	-2.27942
O	-4.2204	1.719426	-1.47272
H	-4.96117	1.976737	-0.91693
O	-3.75006	-1.43811	0.137841
C	-2.7754	-0.07328	2.160643
H	-2.07653	0.333614	2.898506
H	-3.29681	0.790883	1.709808
O	-3.66169	-0.91717	2.846042
H	-4.07957	-1.47102	2.173626

TS: rDA of CB21Mac product		M06-2X/6-311++G(d,p)	
O	-0.22421	-1.06905	-0.28333
C	2.568764	1.120272	0.113906
C	1.014826	-0.64357	0.185812
C	2.045185	-1.66626	-0.27823
H	2.551391	1.134962	1.214299
H	1.002301	-0.57099	1.286127
H	1.987009	-1.72247	-1.37283
C	-2.51472	-1.35729	-0.01864
C	-1.36638	-0.70446	0.439265

C	-1.56555	1.199511	0.181886
C	-2.91368	1.628909	0.25366
C	-3.82264	0.97124	-0.55351
H	-1.21255	-0.63591	1.516228
H	-1.10479	1.082508	-0.79617
H	-3.2474	2.347381	0.991179
C	3.430036	-1.20448	0.134358
H	3.482946	-1.20119	1.2337
C	3.697043	0.209891	-0.35853
H	3.713271	0.202061	-1.45794
H	-2.42677	-2.00148	-0.8859
O	1.834631	-2.93245	0.310241
H	0.991783	-3.273	-0.00474
O	4.442253	-2.03623	-0.39414
H	4.264	-2.93857	-0.10982
O	4.912958	0.699171	0.158166
H	5.590792	0.041037	-0.0296
C	2.668755	2.54521	-0.38456
H	3.647282	2.948823	-0.12227
H	2.569739	2.539461	-1.47851
O	1.329294	0.605161	-0.37483
O	1.687357	3.358402	0.215944
H	0.8615	2.858743	0.246429
O	-0.67579	1.772731	1.065597
H	-1.15676	2.14669	1.811125
O	-5.12882	1.321692	-0.46214
H	-5.61739	0.819751	-1.12379
O	-3.48614	-0.0131	-1.26784
C	-3.69302	-1.54665	0.868512
H	-3.44612	-2.27347	1.649391
H	-3.90766	-0.59064	1.380955
O	-4.81345	-2.04034	0.182136
H	-4.85904	-1.55558	-0.64998
TS: rDA of CB23Mac product		M06-2X/6-311++G(d,p)	
O	0.446051	0.598198	-0.51495
C	-2.5988	-1.03207	0.382014
C	-0.77813	0.479405	0.135552
C	-1.68126	1.604746	-0.34306
H	-2.48232	-1.00444	1.474304
H	-0.64276	0.521776	1.22792

H	-1.75376	1.542246	-1.43679
C	3.076271	0.833284	-0.53538
C	1.49688	-0.15377	0.034555
C	1.691924	-1.4316	-0.54797
C	2.839868	-2.19687	-0.30691
C	3.806856	-1.78271	0.563648
H	1.601359	-0.05774	1.108531
H	3.096025	-2.94421	-1.0454
H	4.820352	-2.16074	0.476284
C	-3.05735	1.416079	0.269979
H	-2.96873	1.510296	1.362867
C	-3.60082	0.032368	-0.05386
H	-3.74261	-0.03575	-1.14289
H	2.664882	1.042932	-1.53833
O	-1.20764	2.866692	0.068796
H	-0.38386	3.054708	-0.39221
O	-3.9876	2.355275	-0.22333
H	-3.64225	3.237604	-0.05138
O	-4.8111	-0.20847	0.623336
H	-5.39248	0.540446	0.451885
C	-2.99341	-2.43186	-0.04489
H	-3.94718	-2.68749	0.41615
H	-3.11682	-2.44668	-1.13615
O	-1.3356	-0.76464	-0.23274
O	-2.04649	-3.38483	0.377801
H	-1.19713	-3.15233	-0.0109
O	0.948992	-1.81013	-1.58984
H	0.160643	-1.2477	-1.63557
O	3.509861	-1.12451	1.691413
H	4.286353	-0.62902	1.975961
O	4.178121	0.199113	-0.46809
C	2.934612	2.007249	0.435272
H	1.92751	2.427352	0.433832
H	3.174559	1.648618	1.445856
O	3.811883	3.041445	0.04342
H	4.666477	2.629348	-0.12421
TS: rDA of CB32Mac product		M06-2X/6-311++G(d,p)	
O	-0.27451	0.462061	0.820025
C	2.605977	-1.17689	-0.50294
C	0.92064	0.356399	0.115338

C	1.915415	1.315353	0.750569
H	2.462679	-0.91482	-1.56148
H	0.761484	0.6197	-0.94536
H	2.011732	1.052804	1.811865
C	-2.7786	1.319988	0.143561
C	-1.36172	-0.16122	0.224286
C	-2.0468	-1.08773	1.005724
C	-3.30648	-1.58063	0.703356
C	-3.97048	-1.17709	-0.44353
H	-1.28732	-0.26794	-0.85151
H	-1.70779	-1.21368	2.02997
H	-5.05326	-1.25062	-0.49198
C	3.257288	1.155837	0.060397
H	3.147818	1.463612	-0.99061
C	3.70065	-0.29744	0.093062
H	3.860816	-0.58855	1.14166
H	-2.54504	1.676277	1.156923
O	1.520085	2.659989	0.586682
H	0.70817	2.806567	1.082467
O	4.266025	1.921063	0.685003
H	3.972361	2.83795	0.708292
O	4.874004	-0.48672	-0.66324
H	5.510681	0.178212	-0.37928
C	2.90635	-2.65822	-0.39204
H	3.813561	-2.88553	-0.95107
H	3.071702	-2.90526	0.665064
O	1.387434	-0.96525	0.210602
O	1.860344	-3.42821	-0.93956
H	1.047536	-3.15713	-0.5007
O	-4.03472	-2.12868	1.739686
H	-4.47427	-2.9261	1.437173
O	-3.29736	-1.07784	-1.60646
H	-3.78263	-0.48256	-2.18911
O	-3.94756	0.871373	-0.07499
C	-2.12885	2.127021	-0.97421
H	-1.06142	2.277036	-0.80251
H	-2.27448	1.595358	-1.92413
O	-2.70415	3.417803	-1.01875
H	-3.65936	3.307597	-1.05914
TS: rDA of CB34Mac product		M06-2X/6-311++G(d,p)	

O	-0.08733	-0.8456	-0.68048
C	2.699864	1.159761	0.269509
C	1.107559	-0.54512	-0.02679
C	2.144348	-1.55011	-0.50451
H	2.590328	1.077627	1.361123
H	0.97564	-0.62076	1.066208
H	2.208442	-1.4751	-1.59767
C	-1.822	-0.65873	0.953343
C	-1.2042	-0.17298	-0.19807
C	-1.87543	0.63634	-1.09477
C	-3.21968	0.954449	-0.88865
C	-4.10067	-0.76873	-0.66607
H	-1.44286	0.783522	-2.07902
H	-3.54868	1.20575	0.115931
H	-4.15928	-1.02635	-1.72471
C	3.483243	-1.19592	0.110888
H	3.408552	-1.31545	1.202476
C	3.840592	0.250361	-0.1888
H	3.968328	0.35996	-1.27586
H	-1.40139	-1.58497	1.337909
O	1.829809	-2.86531	-0.09935
H	0.998538	-3.11626	-0.51468
O	4.528434	-2.00282	-0.39186
H	4.282142	-2.92391	-0.25762
O	5.018004	0.624257	0.490895
H	5.676425	-0.0576	0.317893
C	2.948739	2.607697	-0.07908
H	3.972302	2.861934	0.213901
H	2.841484	2.722739	-1.16473
O	1.497144	0.756064	-0.37355
O	1.998861	3.390125	0.620361
H	2.070681	4.301025	0.329192
O	-3.87265	1.634308	-1.88338
H	-4.81542	1.60213	-1.68122
O	-5.33489	-0.27706	-0.25203
H	-5.26501	-0.10121	0.697962
O	-3.42385	-1.50548	0.115443
C	-2.4585	0.232529	2.008611
H	-1.87743	0.08312	2.926584
H	-2.36299	1.282751	1.733766

O	-3.83105	-0.0078	2.278171
H	-3.96283	-0.96174	2.224884
TS: rDA of CB12Mac product		M06-2X/6-311++G(d,p)	
O	-0.26567	-0.68584	-0.53606
C	2.634799	1.082263	0.572474
C	0.97445	-0.52377	0.074424
C	1.959501	-1.42418	-0.65534
H	2.586736	0.814166	1.637959
H	0.91281	-0.80163	1.140498
H	1.961415	-1.13361	-1.71371
C	-2.01666	-0.77449	1.082557
C	-1.32253	-0.04621	0.122787
C	-2.44354	0.172308	-1.53196
C	-3.76054	0.473443	-1.12265
C	-4.37981	-0.40523	-0.25533
H	-1.17806	1.023908	0.253059
H	-2.20362	-0.8583	-1.75737
H	-5.34655	-0.1373	0.19611
C	3.340361	-1.21852	-0.06328
H	3.322617	-1.54259	0.988188
C	3.717805	0.252025	-0.11033
H	3.788436	0.557494	-1.16459
H	-1.7468	-1.81167	1.249402
O	1.637827	-2.7891	-0.49815
H	0.776963	-2.9464	-0.89869
O	4.331245	-1.93264	-0.77218
H	4.06721	-2.85841	-0.79966
O	4.934372	0.486973	0.560583
H	5.577809	-0.1445	0.220707
C	2.874988	2.573078	0.440612
H	3.808223	2.832099	0.939584
H	2.962289	2.823148	-0.62484
O	1.373534	0.821718	-0.04371
O	1.841607	3.312042	1.053448
H	1.017296	3.028359	0.647118
O	-1.77847	1.059953	-2.29847
H	-2.2516	1.902246	-2.27942
O	-4.2204	1.719426	-1.47272
H	-4.96117	1.976737	-0.91693
O	-3.75006	-1.43811	0.137841

C	-2.7754	-0.07328	2.160643
H	-2.07653	0.333614	2.898506
H	-3.29681	0.790883	1.709808
O	-3.66169	-0.91717	2.846042
H	-4.07957	-1.47102	2.173626
TS: rDA of CB2'1'Mac product		M06-2X/6-311++G(d,p)	
O	0.048438	0.754211	0.58804
C	1.246328	0.667941	-0.06289
C	2.230138	1.578461	0.253831
H	2.11254	2.335493	1.014716
C	3.469183	1.338434	-0.398
H	3.402169	1.058042	-1.44961
C	3.16865	-1.3131	0.019013
H	3.09089	-2.01132	-0.80694
C	4.16998	-0.33282	0.022527
H	4.565094	-0.05055	0.998302
C	2.505154	-1.65134	1.312447
H	3.278811	-1.99966	2.006152
H	2.117352	-0.7114	1.751526
O	1.482017	-0.3049	-0.842
O	4.481674	2.204571	-0.10048
H	5.238142	1.978897	-0.65339
O	5.140064	-0.34972	-0.99763
H	5.749297	-1.07737	-0.84968
O	1.55094	-2.66585	1.244882
H	0.802841	-2.4093	0.68294
O	-5.13875	-0.57123	-0.46467
H	-5.30106	-1.5202	-0.51618
C	-3.87888	-0.40263	0.092557
H	-3.9128	-0.52884	1.188235
C	-2.86217	-1.3624	-0.50549
H	-2.83759	-1.18462	-1.58971
C	-1.48418	-1.09247	0.079041
H	-1.51091	-1.28775	1.159658
C	-2.24942	1.269929	0.380544
H	-2.3161	1.160108	1.473041
C	-1.12073	0.371985	-0.13781
H	-0.9668	0.558777	-1.20904
C	-2.03611	2.732819	0.035197
H	-1.11136	3.087634	0.489979

H	-1.95285	2.825456	-1.05644
O	-3.48427	0.909289	-0.21626
O	-3.29828	-2.67289	-0.22233
H	-2.61278	-3.28357	-0.51443
O	-0.56914	-2.00353	-0.51255
H	0.124989	-1.49179	-0.96721
O	-3.0875	3.52277	0.534917
H	-3.90907	3.14134	0.20679
TS: rDA of CB2'3'Mac product		M06-2X/6-311++G(d,p)	
O	-0.37205	0.987921	0.573584
C	-1.14535	0.859551	1.618598
H	-0.64151	0.632095	2.557024
C	-2.48689	1.184203	1.632346
H	-2.95825	1.331603	2.594487
C	-3.30024	1.055178	0.522858
C	-2.53328	-1.17363	-0.35925
H	-3.55365	-1.61532	-0.30476
C	-2.86932	0.3944	-0.72084
H	-1.96605	0.846342	-1.12877
C	-1.81444	-1.71294	-1.61239
H	-2.4228	-1.65306	-2.52182
H	-0.90979	-1.10416	-1.76916
O	-1.82213	-1.38779	0.741509
O	-4.57725	1.32707	0.641747
H	-4.99144	1.131504	-0.22032
O	-3.93563	0.476016	-1.64796
H	-4.07022	-0.38605	-2.05524
O	-1.48845	-3.0641	-1.41856
H	-1.27639	-3.14441	-0.47895
O	4.757083	-0.5784	-0.45919
H	4.926361	-1.51545	-0.30692
C	3.380539	-0.41187	-0.48885
H	2.966434	-0.72095	-1.46356
C	2.688206	-1.18257	0.626225
H	3.109018	-0.84198	1.583177
C	1.195517	-0.89346	0.597925
H	0.796721	-1.21735	-0.37467
C	1.78855	1.330085	-0.39363
H	1.383251	1.025276	-1.37092
C	1.015732	0.617778	0.714126

H	1.36412	0.958389	1.696671
C	1.753775	2.843785	-0.28126
H	0.726966	3.200172	-0.37209
H	2.141324	3.129359	0.7065
O	3.154047	0.966731	-0.30097
O	2.950577	-2.54971	0.423246
H	2.368448	-3.04456	1.011821
O	0.58102	-1.59601	1.636518
H	-0.37241	-1.68352	1.366246
O	2.498128	3.438025	-1.31424
H	3.380199	3.050943	-1.28942
TS: rDA of CB3'2'Mac product		M06-2X/6-311++G(d,p)	
O	0.056149	0.799672	0.097157
C	1.225229	0.496347	-0.5801
H	1.021884	0.314292	-1.6454
C	2.182102	1.643909	-0.41551
C	3.089966	1.760206	0.603721
H	3.687798	2.665602	0.630409
C	3.110548	-0.86118	-0.52041
H	3.880283	-0.14257	-0.27313
C	3.413579	0.764101	1.529184
H	2.77059	-0.06666	1.77823
C	3.445024	-2.29712	-0.73272
H	3.48193	-2.86033	0.211228
H	2.655792	-2.76416	-1.34226
O	1.811573	-0.68514	-0.05999
O	1.975945	2.720667	-1.20874
H	1.361488	2.510901	-1.91783
O	4.417777	1.0535	2.381074
H	4.564332	0.320036	2.983382
O	4.719663	-2.45085	-1.31873
H	4.755255	-1.87892	-2.09148
O	-5.07366	-1.02573	0.244954
H	-5.15713	-1.95398	0.49179
C	-3.76936	-0.64391	0.526588
H	-3.64054	-0.44919	1.604993
C	-2.76454	-1.68777	0.06641
H	-2.91159	-1.83583	-1.01237
C	-1.34478	-1.2023	0.310319
H	-1.18338	-1.09869	1.393564

C	-2.279	1.117066	0.095684
H	-2.1937	1.306986	1.175774
C	-1.15275	0.171381	-0.3294
H	-1.14951	0.061536	-1.42351
C	-2.24359	2.440207	-0.64803
H	-1.3129	2.961472	-0.42157
H	-2.28732	2.23465	-1.72767
O	-3.54145	0.540536	-0.19293
O	-3.03381	-2.87691	0.775099
H	-2.34171	-3.50992	0.555581
O	-0.50158	-2.20062	-0.22374
H	0.417897	-1.96293	-0.03983
O	-3.30303	3.272467	-0.24748
H	-4.11466	2.761225	-0.33768
TS: rDA of CB3'4'Mac product		M06-2X/6-311++G(d,p)	
O	0.197265	0.464005	0.433302
C	1.300033	0.642588	-0.45362
H	1.238542	1.61413	-0.95951
C	2.473739	1.189198	1.01008
H	2.144731	0.313831	1.554439
C	3.728825	1.217759	0.406139
H	4.171669	2.192597	0.221488
C	3.621075	-1.08499	-0.41658
H	3.843031	-1.6516	-1.32081
C	4.250958	0.147477	-0.31122
C	3.137696	-1.96561	0.705846
H	3.974098	-2.63906	0.931786
H	2.948301	-1.40238	1.622963
O	1.740999	-0.35584	-1.06073
O	1.996542	2.376103	1.507566
H	1.09348	2.22125	1.803952
O	5.225197	0.503103	-1.21801
H	5.672731	-0.2846	-1.53379
O	2.066608	-2.78857	0.348357
H	1.343939	-2.2423	0.000694
O	-5.09626	-0.55862	-0.34163
H	-5.71161	0.124404	-0.06013
C	-3.84027	-0.29537	0.185831
H	-3.88113	-0.17991	1.281127
C	-2.94258	-1.46214	-0.18913

H	-2.95002	-1.54613	-1.28405
C	-1.5222	-1.20461	0.28647
H	-1.52004	-1.18566	1.386715
C	-2.04779	1.236168	0.116611
H	-2.1045	1.353885	1.20983
C	-1.02804	0.142916	-0.21295
H	-0.88058	0.080479	-1.29808
C	-1.69562	2.572365	-0.50955
H	-0.72895	2.912904	-0.13447
H	-1.62368	2.443721	-1.59797
O	-3.33344	0.89017	-0.3888
O	-3.36478	-2.66321	0.418422
H	-4.24836	-2.86933	0.097899
O	-0.65267	-2.20589	-0.18751
H	-0.98369	-3.05785	0.119227
O	-2.64322	3.558224	-0.17261
H	-3.50285	3.23123	-0.45568
TS: rDA of CB4'3'Mac product		M06-2X/6-311++G(d,p)	
O	0.27357	0.769034	0.295396
C	1.413814	0.70889	-0.61145
H	1.417091	1.649687	-1.19979
C	2.593402	1.059755	0.549882
H	2.320396	0.459966	1.41367
C	3.87888	0.690423	-0.00131
C	3.349096	-1.68963	-0.18108
H	3.57194	-2.57039	-0.78208
C	4.178274	-0.61968	-0.38659
H	5.006121	-0.72581	-1.07775
C	2.360155	-2.0404	0.906715
H	2.953228	-2.12924	1.829769
H	1.600389	-1.27797	1.064779
O	1.540777	-0.37109	-1.28743
O	2.580594	2.432549	0.834528
H	1.665599	2.699053	0.978327
O	4.687573	1.654917	-0.36829
H	4.298213	2.502033	-0.08638
O	1.763542	-3.28048	0.65327
H	0.892904	-3.10727	0.255619
O	-4.92939	-0.72916	-0.19855
H	-5.57971	-0.16055	0.222727

C	-3.66223	-0.40343	0.266807
H	-3.62815	-0.40992	1.368466
C	-2.69917	-1.44698	-0.28386
H	-2.79621	-1.45007	-1.37791
C	-1.2667	-1.09236	0.085705
H	-1.16667	-1.19301	1.177834
C	-2.04238	1.302947	0.259809
H	-2.02051	1.290646	1.360249
C	-0.96306	0.366442	-0.27723
H	-0.92354	0.458499	-1.37134
C	-1.86733	2.728071	-0.2297
H	-0.9087	3.117608	0.114025
H	-1.87267	2.725889	-1.32785
O	-3.32181	0.887156	-0.1975
O	-2.99401	-2.70905	0.264589
H	-3.8835	-2.94767	-0.01345
O	-0.38026	-1.98356	-0.55287
H	0.335424	-1.45053	-0.98081
O	-2.87085	3.57376	0.282509
H	-3.71602	3.182127	0.040397
TS: rDA of CB4’5’Mac product		M06-2X/6-311++G(d,p)	
O	-0.49404	-1.41006	0.069202
C	-1.44905	-1.61123	-0.77179
H	-1.22754	-1.60616	-1.83722
C	-2.7661	-1.72999	-0.31019
H	-2.86836	-2.06538	0.723173
C	-3.34282	0.003742	-0.07918
H	-3.15904	0.45683	-1.05027
C	-1.86018	1.736342	0.826558
C	-2.69185	0.639166	1.023255
H	-2.85217	0.260216	2.027761
C	-1.2299	2.409781	2.042185
H	-1.89137	3.227087	2.361375
H	-1.1265	1.707658	2.870752
O	-1.57279	2.262972	-0.28749
O	-3.60894	-2.32405	-1.22811
H	-4.49234	-1.96634	-1.06478
O	-4.70162	-0.30698	0.031594
H	-4.96996	-0.1644	0.944713
O	0.053176	2.89751	1.720893

H	-0.02234	3.25557	0.825735
O	4.430921	0.856595	-0.5512
H	4.426775	1.739627	-0.93808
C	3.127576	0.573553	-0.16934
H	2.849569	1.124896	0.744159
C	2.125799	0.889942	-1.27361
H	2.418781	0.331114	-2.17335
C	0.740526	0.458642	-0.81404
H	0.502137	1.016053	0.100558
C	1.858161	-1.26843	0.600344
H	1.594354	-0.71132	1.511271
C	0.794068	-1.01973	-0.46366
H	0.990419	-1.62514	-1.35587
C	2.056888	-2.7352	0.9359
H	1.136896	-3.14751	1.353801
H	2.299899	-3.27727	0.011538
O	3.098858	-0.81335	0.089411
O	2.180586	2.278134	-1.50178
H	1.471813	2.508594	-2.11241
O	-0.23064	0.696107	-1.79391
H	-0.86705	1.350798	-1.39537
O	3.064167	-2.89321	1.901716
H	3.849864	-2.44383	1.57129
TS: CB43Mac Water catalysis		M06-2X/6-311++G(d,p)	
O	0.024513	0.978372	0.502108
C	2.726546	-1.03754	-0.62923
C	1.253969	0.740186	-0.05702
C	2.352935	1.474553	0.710392
H	2.723776	-0.68525	-1.67118
H	1.270454	1.065593	-1.1134
H	2.308087	1.148709	1.759757
C	-2.35107	1.303057	-0.35638
C	-1.38268	0.154925	-0.58908
C	-1.74454	-1.1131	-0.12115
C	-3.20794	-1.40948	0.097201
C	-3.9534	-0.15552	0.517838
H	-0.7142	0.216271	-1.44537
H	-1.22051	-0.9668	1.192542
H	-3.65552	-1.75684	-0.84507
H	-3.61391	0.173955	1.513341

C	3.707538	1.111182	0.130955
H	3.754759	1.478541	-0.9051
C	3.894496	-0.39853	0.113287
H	3.900205	-0.76154	1.151966
H	-2.16639	1.732523	0.63571
O	2.211333	2.874492	0.610369
H	1.337276	3.108344	0.939712
O	4.770556	1.658395	0.885602
H	4.638331	2.610637	0.938468
O	5.089379	-0.75218	-0.54381
H	5.79436	-0.21401	-0.16788
C	2.736708	-2.55189	-0.62689
H	3.660395	-2.90894	-1.08323
H	2.708615	-2.89793	0.416985
O	1.508367	-0.65379	0.00472
O	1.657269	-3.06098	-1.36984
H	0.845552	-2.61785	-1.08111
O	-1.05353	-2.20687	-0.68902
H	-1.35023	-2.99774	-0.22422
O	-3.29481	-2.43014	1.076452
H	-4.2143	-2.70744	1.141938
O	-5.30474	-0.46578	0.51699
H	-5.80239	0.277942	0.868426
O	-3.70251	0.864961	-0.42392
C	-2.1866	2.388957	-1.40325
H	-1.17064	2.783689	-1.34162
H	-2.33702	1.94982	-2.39849
O	-3.07204	3.456973	-1.17554
H	-3.9621	3.091299	-1.16409
O	-0.55891	-0.64433	2.152273
H	-0.15649	0.180318	1.550651
H	0.146985	-1.29719	2.240029
TS: CB43Mac Methanol catalysis		M06-2X/6-311++G(d,p)	
O	0.020459	0.974644	0.516922
C	2.72044	-0.86394	-0.88717
C	1.244611	0.819894	-0.07588
C	2.345348	1.443335	0.780603
H	2.717787	-0.38593	-1.87813
H	1.25689	1.287635	-1.07849
H	2.306101	0.971443	1.773783

C	-2.33537	1.401575	-0.36452
C	-1.37017	0.263253	-0.65225
C	-1.75667	-1.02954	-0.28162
C	-3.22329	-1.32827	-0.10652
C	-3.96755	-0.09597	0.376074
H	-0.6891	0.373629	-1.4936
H	-1.29474	-0.95304	1.070599
H	-3.66011	-1.6232	-1.07119
H	-3.64621	0.165286	1.397554
C	3.698034	1.169056	0.150666
H	3.73828	1.674027	-0.826
C	3.889175	-0.32366	-0.07104
H	3.899645	-0.82196	0.910537
H	-2.17009	1.760993	0.658343
O	2.199247	2.842748	0.880622
H	1.311653	3.024315	1.207412
O	4.763096	1.61448	0.967655
H	4.625148	2.549428	1.151843
O	5.08232	-0.58316	-0.77411
H	5.787245	-0.09608	-0.33364
C	2.733577	-2.3688	-1.06605
H	3.64256	-2.6641	-1.59087
H	2.741628	-2.83686	-0.06989
O	1.503231	-0.56725	-0.20994
O	1.631297	-2.79463	-1.82687
H	0.826711	-2.40541	-1.45204
O	-1.0597	-2.08912	-0.90597
H	-1.34088	-2.90453	-0.47645
O	-3.33166	-2.40111	0.817747
H	-4.25346	-2.6769	0.851373
O	-5.32183	-0.39276	0.328803
H	-5.8203	0.339022	0.703528
O	-3.68934	0.980903	-0.49107
C	-2.14249	2.553304	-1.33282
H	-1.127	2.938711	-1.22336
H	-2.27212	2.181556	-2.35801
O	-3.02961	3.608655	-1.05555
H	-3.92029	3.245226	-1.08329
O	-0.69508	-0.70254	2.068929
H	-0.18795	0.089371	1.550222

C	0.148021	-1.7984	2.444556
H	0.73709	-1.50796	3.314473
H	-0.49598	-2.63663	2.707945
H	0.806056	-2.06609	1.61571
TS: CB43Mac Formic acid catalysis		M06-2X/6-311++G(d,p)	
O	0.065402	1.10727	0.175817
C	2.71394	-0.97696	-0.96858
C	1.343707	0.833379	-0.31081
C	2.423585	1.419718	0.599955
H	2.803323	-0.53676	-1.97274
H	1.421314	1.275924	-1.31643
H	2.293702	1.000461	1.605321
C	-2.31563	1.325257	-0.60966
C	-1.34532	0.162929	-0.76784
C	-1.68106	-1.07803	-0.19299
C	-3.17278	-1.36237	-0.05808
C	-3.94481	-0.09752	0.271462
H	-0.69969	0.155539	-1.644
H	-1.2598	-1.04893	1.088213
H	-3.54542	-1.72813	-1.02474
H	-3.65295	0.28478	1.263206
C	3.783348	1.015185	0.05638
H	3.916974	1.477245	-0.93362
C	3.871849	-0.49504	-0.10251
H	3.789577	-0.95517	0.893238
H	-2.1649	1.787638	0.374267
O	2.392032	2.830926	0.62763
H	1.623495	3.118528	1.12962
O	4.828149	1.412268	0.919047
H	4.748805	2.360961	1.064068
O	5.077936	-0.8661	-0.72826
H	5.795126	-0.43431	-0.25144
C	2.618523	-2.48336	-1.10013
H	3.542756	-2.8632	-1.53645
H	2.502545	-2.91353	-0.09552
O	1.486138	-0.55857	-0.373
O	1.555915	-2.84634	-1.94509
H	0.734171	-2.50267	-1.56428
O	-1.00788	-2.1902	-0.74376
H	-1.07178	-2.90469	-0.09884

O	-3.33788	-2.34853	0.935122
H	-4.25237	-2.64649	0.910213
O	-5.29145	-0.41619	0.220205
H	-5.80996	0.327323	0.540209
O	-3.65715	0.879363	-0.70992
C	-2.11608	2.373526	-1.68956
H	-1.10386	2.773721	-1.61193
H	-2.23713	1.897169	-2.67164
O	-3.0086	3.446337	-1.52687
H	-3.89978	3.083506	-1.54482
H	-0.00682	0.888074	1.21191
O	-0.02676	0.668065	2.590075
O	-0.87907	-1.37611	2.26348
C	-0.3335	-0.48276	2.963208
H	-0.11632	-0.75835	4.00525
H	0.806056	-2.06609	1.61571
TS: CB43Mac Glucose catalysis		M06-2X/6-311++G(d,p)	
O	-1.05919	1.473277	-0.71952
C	-2.88405	-0.79158	1.351656
C	-2.16259	1.064242	-0.04695
C	-3.33909	0.823475	-0.99216
H	-3.18521	-0.15168	2.195016
H	-2.47415	1.797874	0.724571
H	-3.01442	0.103421	-1.75731
C	0.595582	3.344956	-0.23276
C	0.330325	2.11788	0.613102
C	1.373502	1.276218	0.98624
C	2.756618	1.901062	1.009044
C	2.887153	2.999389	-0.03616
H	-0.51216	2.155672	1.299224
H	1.720349	0.157337	-0.10719
H	2.916051	2.352463	1.997197
H	2.844692	2.559023	-1.04672
C	-4.50969	0.246691	-0.22171
H	-4.82197	0.970026	0.546724
C	-4.09403	-1.04723	0.459605
H	-3.80988	-1.76815	-0.322
H	0.607504	3.061775	-1.2919
O	-3.77033	2.029046	-1.58624
H	-3.00753	2.425829	-2.02139

O	-5.6028	-0.06101	-1.06528
H	-5.81311	0.730289	-1.57252
O	-5.13004	-1.56579	1.261639
H	-5.93132	-1.57082	0.726358
C	-2.25128	-2.07789	1.85806
H	-2.91511	-2.57366	2.567128
H	-2.08848	-2.73723	0.995
O	-1.85219	-0.16892	0.608516
O	-1.00618	-1.81634	2.496156
H	-0.71267	-0.92244	2.256033
O	1.0843	0.492236	2.123845
H	1.544245	-0.35906	2.06789
O	3.750915	0.91173	0.775612
H	4.612817	1.326453	0.891084
O	4.1094	3.62163	0.190724
H	4.265623	4.272311	-0.49972
O	1.849409	3.933812	0.106791
C	-0.45344	4.418705	-0.01021
H	-1.4275	4.027087	-0.30493
H	-0.47905	4.6714	1.058322
O	-0.19564	5.558246	-0.79585
H	0.689867	5.86183	-0.57331
H	-0.5172	0.391335	-1.52628
O	-0.09178	-0.45135	-1.95848
O	1.842622	-0.7594	-0.71978
C	0.412408	-1.20481	-0.97111
C	2.817236	-1.74009	-0.21778
C	2.110553	-2.83346	0.566897
H	2.861092	-3.58997	0.816701
C	1.001352	-3.53192	-0.24006
H	0.158614	-3.73182	0.437361
C	0.467846	-2.6629	-1.37091
H	1.119202	-2.75194	-2.25015
C	3.678916	-2.24453	-1.36746
H	3.177766	-3.04048	-1.92547
H	3.891403	-1.40546	-2.03772
O	1.626297	-2.21229	1.742661
H	0.738746	-2.50924	2.003981
O	1.525908	-4.74511	-0.7431
H	0.826055	-5.19027	-1.23242

O	-0.83133	-3.11396	-1.68081
H	-1.20803	-2.49027	-2.31369
H	3.457328	-1.17448	0.456784
O	4.856354	-2.73338	-0.7515
H	5.303235	-3.33366	-1.35128
H	-0.08666	-1.05229	-0.01256
TS: GED→GGA		M06-2X/6-311++G(d,p)	
O	-1.58947	-1.35474	-0.16576
C	0.804876	1.2641	0.263052
C	-0.42676	-0.75108	0.301847
C	0.745175	-1.56082	-0.23182
H	0.832189	1.26719	1.362506
H	-0.42081	-0.73859	1.405578
H	0.669769	-1.57668	-1.32701
C	-2.77451	-0.82578	0.338049
C	-3.52561	0.119611	-0.41246
H	-2.74044	-0.55113	1.397875
H	-3.20703	0.847504	-1.16047
C	2.04136	-0.89093	0.179811
H	2.116674	-0.91639	1.277368
C	2.047959	0.559887	-0.27133
H	2.025059	0.582669	-1.37076
O	0.7596	-2.86787	0.297884
H	-0.05933	-3.30413	0.041304
O	3.168207	-1.51791	-0.39606
H	3.145512	-2.45009	-0.15546
O	3.179905	1.240253	0.219078
H	3.952598	0.704769	0.007891
C	0.674811	2.688735	-0.2342
H	1.540766	3.264253	0.091361
H	0.650223	2.678415	-1.33196
O	-0.36207	0.57098	-0.1833
O	-0.47561	3.309346	0.296323
H	-1.22301	2.737278	0.09789
O	-4.75055	-0.01965	-0.11479
H	-4.24607	-1.05068	0.439066
TS:CB Hydrolysis		M06-2X/6-311++G(d,p)	
O	-0.63532	0.833817	0.395638
C	4.02147	-1.02648	0.241163
C	1.821111	-0.47591	-0.43708

C	2.157835	0.979444	-0.3057
H	4.65939	-1.83359	-0.11199
H	0.853878	-0.81308	-0.82277
H	2.28752	1.213269	0.763262
C	-3.01714	1.036825	0.611727
C	-1.83762	0.49659	-0.20912
C	-2.0012	-1.01407	-0.35377
C	-3.37196	-1.35428	-0.90268
C	-4.44081	-0.73825	-0.01473
H	-1.90382	0.930459	-1.22239
H	-1.8915	-1.47812	0.638122
H	-3.48614	-0.92103	-1.90524
H	-4.37208	-1.15468	1.003884
C	3.515175	1.123537	-1.0026
H	3.436113	0.722814	-2.02332
C	4.562613	0.327241	-0.23884
H	4.825748	0.920779	0.648365
H	-2.95263	0.636364	1.635331
O	1.218989	1.777677	-0.91915
H	0.326958	1.534815	-0.42568
O	3.921832	2.464063	-1.03222
H	3.165828	2.981715	-1.33894
O	5.708773	0.080974	-1.02028
H	6.057494	0.930744	-1.31079
C	3.826639	-1.10109	1.756905
H	4.82367	-1.11073	2.205104
H	3.312018	-0.19706	2.104633
O	2.713988	-1.36117	-0.35795
O	3.152062	-2.25776	2.14842
H	2.2121	-2.12977	1.947177
O	-0.9862	-1.51231	-1.21558
H	-1.19723	-2.43634	-1.39339
O	-3.47302	-2.76406	-0.94667
H	-4.34538	-2.99013	-1.28448
O	-5.67108	-1.03337	-0.5936
H	-6.37289	-0.68257	-0.03798
O	-4.27178	0.656633	0.035887
C	-3.02164	2.54954	0.668211
H	-2.09741	2.889819	1.132795
H	-3.0662	2.939147	-0.35762

O	-4.09853	3.037624	1.441196
H	-4.90096	2.659989	1.068509
O	0.731897	-0.78031	1.629679
H	0.03254	-0.12072	1.155603
H	0.813304	-0.44516	2.527801
TS:CBN Hydrolysis		M06-2X/6-311++G(d,p)	
O	-0.69885	0.429236	0.475217
O	0.934644	-2.0217	0.219857
O	3.409031	-2.59652	-0.87568
O	2.73408	0.8269	1.251323
O	3.121001	3.102994	-0.18924
C	1.768304	0.063896	1.042318
C	1.815995	-0.98146	-0.01989
C	3.236265	-1.5598	0.051088
C	4.270189	-0.48912	-0.25351
C	3.917606	0.874299	0.35038
C	3.63478	1.931701	-0.72037
O	-4.49934	-2.33112	0.194008
O	-1.72226	-1.98218	-0.53418
O	-4.01062	0.736967	1.211999
O	-4.78119	1.102312	-0.87566
C	-4.73154	0.138583	0.169072
C	-3.98646	-1.11736	-0.337
C	-2.54517	-1.03117	0.13281
C	-1.95575	0.354875	-0.09423
C	-2.95695	1.396981	0.491587
C	-3.78829	2.089529	-0.58196
H	0.015949	-1.76778	-0.01408
H	2.672284	-3.20964	-0.76284
H	-0.04632	1.304678	-0.06168
H	0.929351	0.132809	1.734029
H	1.652988	-0.47168	-0.98247
H	3.403672	-1.92915	1.07354
H	4.29368	-0.37583	-1.34615
H	4.69848	1.201794	1.033213
H	2.955946	1.504478	-1.4681
H	4.600626	2.12429	-1.20142
H	-5.32892	-2.54573	-0.23942
H	-2.11182	-2.85143	-0.38786
H	-5.73898	-0.09515	0.518792

H	-4.02338	-1.12695	-1.43198
H	-2.53406	-1.22744	1.210237
H	-1.89787	0.507074	-1.1889
H	-2.43607	2.063921	1.175293
H	-3.23096	2.318422	-1.49074
H	-4.26919	2.992673	-0.19794
O	0.724444	2.049927	-0.5583
H	2.145117	2.962305	-0.17807
H	0.329508	2.417071	-1.35179
O	5.544629	-0.85178	0.227887
H	5.801482	-1.67479	-0.20131
TS:CBOC Hydrolysis		M06-2X/6-311++G(d,p)	
O	-0.84956	0.719575	1.05592
C	2.276558	-0.47616	-1.3106
C	1.702935	1.201433	0.338264
C	2.947755	0.993262	1.162601
H	2.715906	-0.06706	-2.22272
H	0.959998	1.945695	0.623447
H	2.66676	0.37359	2.015672
C	-2.61667	1.482764	-0.32975
C	-1.5123	0.440384	-0.133
C	-2.0058	-1.02051	-0.15691
C	-3.36532	-1.26448	0.512472
C	-3.25303	-0.96469	1.991377
H	-0.85251	0.520143	-1.01797
H	-1.26279	-1.61013	0.397335
H	-4.1139	-0.61243	0.047919
H	-3.01429	0.069648	2.27969
C	3.997343	0.279759	0.329511
H	4.373105	0.969168	-0.4405
C	3.369678	-0.92584	-0.35084
H	2.941774	-1.58649	0.411555
H	-3.26392	1.49512	0.560224
O	3.449023	2.262273	1.53118
H	3.090174	2.52159	2.384329
O	5.055443	-0.1928	1.127812
H	5.554651	0.558629	1.461267
O	4.315464	-1.59027	-1.15511
H	5.049262	-1.8465	-0.58601
C	1.262598	-1.54961	-1.65863

H	1.850813	-2.42837	-1.95213
H	0.697673	-1.79018	-0.75289
O	1.49539	0.664268	-0.76666
O	0.451044	-1.10843	-2.71025
H	-0.47923	-1.2236	-2.45326
O	-2.0512	-1.49254	-1.49713
H	-2.55096	-2.31848	-1.49152
O	-3.73514	-2.60889	0.306463
H	-3.71424	-3.04328	1.170939
O	-3.38192	-1.84317	2.807821
H	-3.88951	1.960927	-1.69104
O	-3.37396	1.173939	-1.48159
C	-2.00631	2.866383	-0.46156
H	-1.48849	3.125353	0.465518
H	-1.30015	2.861083	-1.30295
O	-3.08602	3.759081	-0.72201
H	-2.74193	4.618945	-0.96883
O	0.871106	-0.90239	1.483668
H	-0.00767	-0.18621	1.338841
H	0.717443	-1.40843	2.284475
TS:GER Hydrolysis		M06-2X/6-311++G(d,p)	
O	1.759296	1.108217	-0.70305
O	-0.12963	-1.8488	-0.59633
O	-2.71421	-2.70844	0.061417
O	-1.91145	1.127596	-1.02809
O	-2.4094	2.993081	0.875216
C	-0.92317	0.378579	-0.83385
C	-1.06854	-0.93706	-0.12753
C	-2.46062	-1.45489	-0.51042
C	-3.53668	-0.50056	-0.02241
C	-3.15346	0.966697	-0.24091
C	-2.93116	1.720316	1.071732
O	5.167438	0.71931	-1.28194
O	4.423204	-0.95367	0.77317
O	1.929199	-1.94118	1.10781
C	3.988839	0.933056	-1.43832
C	2.860629	0.292441	-0.63573
C	3.358692	-0.01558	0.791841
C	2.293099	-0.67176	1.649404
H	0.660707	-1.88063	-0.01032

H	-1.99097	-3.29554	-0.18966
H	0.981267	1.505038	0.226205
H	0.015491	0.630019	-1.34596
H	-1.01358	-0.77568	0.9575
H	-2.51362	-1.51319	-1.60708
H	-3.64547	-0.66899	1.058648
H	-3.8934	1.463704	-0.864
H	-2.28662	1.116197	1.723382
H	-3.91191	1.802581	1.550073
H	2.75677	-2.38351	0.873729
H	3.630923	1.655229	-2.196
H	2.685638	-0.69243	-1.11869
H	3.66687	0.923971	1.271929
H	1.386336	-0.07016	1.682615
H	2.681156	-0.80781	2.663268
O	0.058892	1.75935	0.838137
H	-1.45084	2.877168	0.735181
H	0.317395	1.87833	1.755364
H	5.097972	-0.61441	0.168627
O	-4.76275	-0.72766	-0.67717
H	-5.02462	-1.63977	-0.51112
TS:GED Hydrolysis		M06-2X/6-311++G(d,p)	
O	-2.38994	-0.7407	-1.14057
C	1.93273	1.101898	0.559707
C	-0.1684	0.021805	0.429153
C	0.433808	-1.02762	-0.45747
H	2.385183	1.603342	1.412102
H	-1.19486	-0.05763	0.79553
H	0.666413	-0.57164	-1.43184
C	-3.36297	-0.77925	-0.2166
C	-3.75847	0.261962	0.528453
H	-3.8503	-1.74898	-0.07386
H	-3.34255	1.256209	0.411217
C	1.747523	-1.40889	0.232839
H	1.530922	-1.71001	1.267729
C	2.678723	-0.20401	0.253909
H	3.108346	-0.11952	-0.75462
O	-0.38158	-2.1351	-0.56376
H	-1.28158	-1.76786	-0.88931
O	2.396356	-2.4425	-0.45497

H	1.747448	-3.14148	-0.60664
O	3.700871	-0.34937	1.2113
H	4.182978	-1.15939	1.012323
C	1.829541	2.041827	-0.64416
H	2.835116	2.429218	-0.8283
H	1.524952	1.470898	-1.52983
O	0.548908	0.868486	1.021429
O	0.975377	3.117032	-0.4048
H	0.06472	2.791578	-0.48194
O	-4.76231	0.227462	1.471333
H	-5.14478	-0.65422	1.48911
O	-1.14343	1.357109	-1.20652
H	-1.79335	0.4966	-1.25476
H	-0.98757	1.617173	-2.11952
TS:GGA Hydrolysis		M06-2X/6-311++G(d,p)	
O	-2.23053	-0.05633	-0.05845
C	2.320112	0.867998	0.394963
C	0.185079	-0.00676	0.999492
C	0.294739	-0.98847	-0.11079
H	3.069042	1.231969	1.094889
H	-0.65241	-0.01454	1.69297
H	0.253663	-0.41176	-1.05306
C	-3.45292	0.106305	0.572883
C	-4.613	-0.32324	-0.31178
H	-3.64402	1.156877	0.848726
H	-4.30836	-0.64792	-1.32973
C	1.698461	-1.58744	0.045344
H	1.805659	-1.98648	1.064314
C	2.740757	-0.49649	-0.17127
H	2.846392	-0.38289	-1.2593
O	-0.67637	-1.95964	-0.0363
H	-1.53429	-1.38493	-0.09907
O	1.921722	-2.5947	-0.90082
H	1.158355	-3.18627	-0.88093
O	3.978904	-0.83136	0.411329
H	4.29217	-1.64592	0.00387
C	2.035194	1.907461	-0.69054
H	3.002733	2.124445	-1.15498
H	1.378025	1.475118	-1.45277
O	1.113704	0.788461	1.264393

O	1.496093	3.076902	-0.16644
H	0.531506	2.94508	-0.16194
O	-5.76285	-0.32001	0.033183
H	-3.53996	-0.47537	1.50599
O	-0.9579	1.980793	-0.70987
H	-1.56972	1.17372	-0.486
H	-1.40166	2.479703	-1.39899
TS:CBOC HAGBC		M06-2X/6-311++G(d,p)	
O	0.911716	-0.10895	0.704862
O	-2.65446	2.283228	0.817062
O	-4.68152	0.945558	-0.68261
O	-4.69869	-1.91342	-0.25878
O	-1.81814	-1.03761	1.403717
O	-0.66714	-0.85844	-0.99421
C	-1.6092	0.185636	1.204466
C	-2.45493	1.010806	0.270573
C	-3.79248	0.283191	0.17864
C	-3.55063	-1.10412	-0.39104
C	-2.39814	-1.83368	0.312583
C	-1.17822	-2.06499	-0.61331
H	-1.86888	2.806695	0.584014
H	-4.7758	1.853122	-0.37293
H	0.330964	-0.4106	-0.13142
H	-0.96327	0.671207	1.930637
H	-2.00551	1.035332	-0.72275
H	-4.22629	0.192326	1.184668
H	-3.27951	-0.97552	-1.44618
H	-2.76411	-2.73478	0.80084
H	-1.56637	-2.66255	-1.45499
H	-0.46058	-2.69621	-0.06099
H	-5.41677	-1.48239	-0.73464
C	1.892598	1.617036	-0.7945
C	1.954082	0.799679	0.511572
C	3.278779	0.050581	0.679335
C	3.596765	-1.01943	-0.38125
C	2.527485	-2.09193	-0.47794
H	1.924337	1.540373	1.322925
H	3.234636	-0.46678	1.646337
H	3.701885	-0.53872	-1.36063
H	1.591705	-1.83688	-0.99829

H	2.218071	1.011724	-1.65264
O	4.336307	0.998545	0.679441
H	5.16587	0.506779	0.706194
O	4.839924	-1.58974	-0.03761
H	4.657359	-2.48191	0.290587
O	2.729094	-3.18996	-0.02368
H	3.544066	2.51656	-0.28495
O	2.697349	2.779845	-0.67035
C	0.498101	2.11391	-1.1132
H	0.560053	2.78292	-1.97705
H	-0.1512	1.275546	-1.35683
O	-0.07089	2.808693	-0.00019
H	0.57566	3.471535	0.271271
TS:GER HAGBC		M06-2X/6-311++G(d,p)	
O	-1.55597	2.371689	-1.47043
O	-4.44889	-0.02893	-0.33696
C	-2.51985	1.929429	-0.89863
C	-2.4267	1.035483	0.325058
C	-3.10865	-0.30495	0.018535
C	-3.05616	-1.23912	1.218494
H	-3.54361	2.148484	-1.24912
H	-3.01711	1.525075	1.114535
H	-2.57875	-0.78592	-0.81805
H	-2.02151	-1.47889	1.469099
H	3.848334	0.881787	2.198247
O	3.782638	0.057784	1.704071
C	3.082083	0.312723	0.51304
O	4.139676	-1.47617	-0.7218
C	2.908675	-1.01851	-0.20495
H	2.500897	-1.7251	0.527736
C	1.922815	-0.93561	-1.37954
H	2.424183	-1.18334	-2.31331
H	0.94753	-2.77667	-1.00255
C	0.615526	-1.72933	-1.12376
O	-0.01147	-1.2327	-0.03175
H	-0.73822	-0.01771	0.360131
H	0.020508	-1.68379	-2.05435
O	1.417471	0.426445	-1.58657
C	1.080271	1.098686	-0.57904
H	1.115512	0.17368	1.355054

C	1.698713	0.891269	0.776457
O	1.816004	2.134116	1.422018
H	0.963638	2.335052	1.825721
O	-1.11231	0.858371	0.750328
H	0.477208	1.979317	-0.79472
H	3.653577	0.997699	-0.12963
H	4.745149	-1.5804	0.019794
H	-4.92973	-0.8617	-0.26183
H	-3.54621	-0.75945	2.06996
O	-3.8099	-2.41093	0.925185
H	-3.23976	-3.02592	0.456524
TS:GED HAGBC		M06-2X/6-311++G(d,p)	
O	4.934965	-0.4489	0.385156
C	3.645637	-0.29672	-0.0814
C	3.096383	0.9162	-0.14223
H	3.147866	-1.17446	-0.48525
H	3.637651	1.780908	0.229437
H	-3.45193	1.965131	-0.41598
O	-3.34141	1.029521	-0.61476
C	-2.30427	0.527754	0.189434
O	-3.23334	-1.69436	0.32734
C	-2.13697	-0.94518	-0.15243
H	-2.05766	-1.01519	-1.24352
C	-0.86564	-1.55336	0.455759
H	-1.11516	-2.36693	1.134243
H	-0.30412	-2.64478	-1.28106
C	0.18545	-1.89762	-0.63188
O	0.506076	-0.75163	-1.27216
H	1.424784	0.297285	-0.99334
H	1.030678	-2.40383	-0.13051
O	-0.13643	-0.59245	1.285318
C	0.017375	0.579801	0.841411
H	-0.69341	1.159474	-1.09952
C	-0.98758	1.255549	-0.05442
O	-1.13079	2.596904	0.353107
H	-0.46813	3.127535	-0.10091
O	1.87738	1.183235	-0.6636
H	0.735949	1.176431	1.395491
H	-2.56732	0.617707	1.253608
H	-4.02746	-1.35024	-0.09489

H	4.994308	-1.26621	0.883567
TS:GGA HAGBC		M06-2X/6-311++G(d,p)	
O	4.968217	-0.53962	0.468316
C	3.807777	-0.33056	0.251959
C	3.291622	0.794761	-0.62713
H	3.011117	-0.97142	0.692975
H	3.822572	1.711236	-0.35416
H	-3.22277	2.194525	-0.47423
O	-3.19361	1.255845	-0.68744
C	-2.26745	0.637381	0.167697
O	-3.39249	-1.4977	0.192439
C	-2.21251	-0.83685	-0.2122
H	-2.08431	-0.88247	-1.29986
C	-1.03144	-1.57747	0.429878
H	-1.3843	-2.38678	1.066464
H	-0.47288	-2.6949	-1.2828
C	0.041521	-1.98267	-0.61255
O	0.478009	-0.86784	-1.23987
H	1.410877	0.133661	-0.85891
H	0.823253	-2.55332	-0.07786
O	-0.26912	-0.71	1.344638
C	-0.01182	0.466953	0.987163
H	-0.51621	1.114667	-0.99231
C	-0.87357	1.241902	0.029702
O	-0.90898	2.588717	0.435307
H	-0.16079	3.042732	0.032795
O	1.912236	0.975201	-0.49195
H	0.709765	0.989559	1.608458
H	-2.59561	0.722491	1.213993
H	-4.13079	-1.08838	-0.27101
H	3.571127	0.550909	-1.66218
XB		M06-2X/6-311++G(d,p)	
O	-0.01462	0.759279	-0.39931
C	-2.48251	-1.69414	0.398575
C	-1.1666	0.258896	0.177294
C	-2.33952	1.053237	-0.38267
H	-2.45523	-1.62309	1.493617
H	-1.12653	0.352407	1.275396
H	-2.32702	0.946884	-1.47507
C	2.093725	1.725995	0.047977

C	1.230362	0.477334	0.241333
C	1.92389	-0.72978	-0.38316
C	3.354049	-0.80096	0.125543
C	4.074618	0.51587	-0.12163
H	1.065733	0.291161	1.309964
H	1.939948	-0.58326	-1.47388
H	3.339955	-0.97305	1.210601
H	4.085991	0.734749	-1.20399
C	-3.63532	0.492201	0.171125
H	-3.63903	0.630742	1.262995
C	-3.72875	-0.9939	-0.12725
H	-3.78585	-1.12508	-1.21633
H	2.119307	1.970239	-1.02397
O	-2.27358	2.408802	0.000713
H	-1.47982	2.792337	-0.38512
O	-4.7671	1.112141	-0.40036
H	-4.69418	2.060796	-0.25262
O	-4.84232	-1.57387	0.508566
H	-5.61523	-1.04874	0.274363
O	-1.31354	-1.10963	-0.16907
O	1.332142	-1.96699	-0.0591
H	0.386005	-1.92151	-0.25969
O	4.088192	-1.81259	-0.5298
H	3.581776	-2.62954	-0.46551
O	5.364235	0.495882	0.390832
H	5.741033	-0.36302	0.16801
O	3.394724	1.541589	0.554636
H	-2.48349	-2.74543	0.116113
H	1.657911	2.567923	0.585416
XBO		M06-2X/6-311++G(d,p)	
O	-0.28957	0.771993	0.229675
C	2.233264	-1.10625	-1.43503
C	0.959449	0.519255	-0.32227
C	1.990622	0.674967	0.786983
H	2.453746	-0.41358	-2.25866
H	1.165637	1.23714	-1.13615
H	1.735092	-0.02972	1.589191
C	-2.15208	2.083981	-0.3044
C	-1.37301	0.834514	-0.70191
C	-2.14118	-0.49193	-0.6817

C	-3.13671	-0.6468	0.485398
C	-2.41665	-0.68946	1.814324
H	-0.98953	0.949452	-1.72129
H	-1.38982	-1.28707	-0.59226
H	-3.82804	0.205183	0.467645
H	-1.87298	0.21642	2.127507
C	3.363392	0.343583	0.233598
H	3.614453	1.083433	-0.54188
C	3.351669	-1.03578	-0.40234
H	3.164406	-1.77825	0.38506
H	-2.36735	2.040828	0.77263
O	2.043374	2.001342	1.269235
H	1.184569	2.219167	1.643638
O	4.354356	0.341477	1.239515
H	4.338715	1.199352	1.675937
O	4.566312	-1.30125	-1.0637
H	5.278632	-1.1305	-0.43838
O	0.985194	-0.79033	-0.83436
O	-2.83219	-0.60549	-1.90008
H	-3.42846	-1.35825	-1.81568
O	-3.86769	-1.83054	0.283453
H	-3.61826	-2.44687	0.986149
O	-2.42417	-1.6827	2.494334
H	-3.75378	3.010894	-0.9036
O	-3.33634	2.161712	-1.06315
H	-1.49963	2.948618	-0.47483
H	2.145794	-2.11254	-1.84023
XGRA		M06-2X/6-311++G(d,p)	
O	1.069389	0.6136	-0.34554
C	-1.50688	-1.68357	0.51549
C	-0.12707	0.195788	0.22321
C	-1.24621	1.012352	-0.40564
H	-1.50983	-1.55203	1.605899
H	-0.10432	0.353498	1.316303
H	-1.20967	0.854921	-1.49137
C	3.332434	1.040402	0.34726
C	2.233032	-0.00646	0.180624
C	2.655213	-1.12734	-0.76104
H	2.024225	-0.45497	1.161894
H	1.828039	-1.65489	-1.26578

C	-2.57696	0.524809	0.136447
H	-2.60812	0.723927	1.218452
C	-2.71442	-0.97204	-0.0827
H	-2.74669	-1.16195	-1.16422
H	3.613529	1.431886	-0.63797
O	-1.13884	2.381635	-0.0829
H	-0.31406	2.715808	-0.44925
O	-3.66859	1.151024	-0.50312
H	-3.56642	2.103283	-0.4034
O	-3.86595	-1.47656	0.55072
H	-4.61252	-0.94126	0.261325
O	-0.30468	-1.17536	-0.0485
O	3.808421	-1.41081	-0.95539
H	4.817808	-0.17863	0.478229
O	4.436869	0.509063	1.036206
H	-1.53855	-2.74829	0.291957
H	2.938739	1.864332	0.944183
XGA		M06-2X/6-311++G(d,p)	
O	1.544062	1.21667	-0.12666
C	-0.48077	-1.67573	0.30284
C	0.456112	0.480125	0.322525
C	-0.80207	1.114907	-0.25001
H	-0.53266	-1.69814	1.399582
H	0.421924	0.487426	1.426813
H	-0.70935	1.118499	-1.34377
C	2.787	0.737234	0.345354
C	3.304293	-0.44239	-0.46264
H	2.73893	0.454485	1.403006
H	2.828563	-0.58577	-1.44959
C	-2.00309	0.282427	0.158228
H	-2.09979	0.321529	1.25387
C	-1.80328	-1.16534	-0.25718
H	-1.77162	-1.20901	-1.35437
O	-1.00628	2.418358	0.25051
H	-0.26351	2.966677	-0.02113
O	-3.19303	0.738905	-0.44938
H	-3.30516	1.668319	-0.22451
O	-2.82946	-1.98612	0.248544
H	-3.6688	-1.58735	-0.00415
O	0.588062	-0.84638	-0.1328

O	4.194193	-1.14126	-0.06785
H	-0.27184	-2.68101	-0.05803
H	3.503714	1.555565	0.238608
XAL		M06-2X/6-311++G(d,p)	
O	1.409369	0.930434	-0.3967
C	-0.86013	-1.70343	0.374325
C	0.278354	0.336375	0.174034
C	-0.94248	1.054932	-0.37915
H	-0.84141	-1.6412	1.470491
H	0.324383	0.43323	1.271428
H	-0.92016	0.965206	-1.473
C	3.292533	1.043547	1.038751
C	2.61235	0.439065	0.074172
C	3.117467	-0.78191	-0.63251
H	2.490859	-1.11482	-1.47693
C	-2.19083	0.383934	0.163833
H	-2.2105	0.513322	1.256573
C	-2.16111	-1.10361	-0.14591
H	-2.20709	-1.22951	-1.23617
H	4.249096	0.635648	1.339479
O	-0.98376	2.406632	0.023232
H	-0.21762	2.856244	-0.34657
O	-3.36682	0.915207	-0.40851
H	-3.37075	1.865505	-0.25374
O	-3.22499	-1.77756	0.482914
H	-4.03888	-1.32217	0.242754
O	0.254456	-1.02148	-0.1858
O	4.127619	-1.34864	-0.31512
H	-0.77339	-2.74802	0.081814
H	2.911473	1.936336	1.518448
TS:XB→XBO		M06-2X/6-311++G(d,p)	
O	-0.00377	0.735285	0.152514
C	-2.49578	-1.62923	-0.78962
C	-1.17607	-0.00459	0.262324
C	-2.32104	0.998276	0.314769
H	-2.49817	-2.25879	0.111095
H	-1.17611	-0.61451	1.183678
H	-2.28207	1.594576	-0.60552
C	1.433268	-0.95231	1.105496
C	1.184344	-0.0043	-0.07178

C	2.317937	1.003546	-0.20209
C	3.606351	0.275894	-0.5683
C	4.126219	-0.64926	0.525633
H	1.091686	-0.55556	-1.01296
H	2.45204	1.525043	0.75949
H	3.431871	-0.33057	-1.46571
H	4.570752	-0.10305	1.368775
C	-3.63374	0.242828	0.38296
H	-3.66375	-0.32834	1.323455
C	-3.72843	-0.73257	-0.77795
H	-3.76361	-0.15503	-1.71144
H	1.195036	-0.429	2.035795
O	-2.24171	1.819364	1.459499
H	-1.43495	2.340559	1.394647
O	-4.74788	1.106881	0.305892
H	-4.66034	1.768159	1.00044
O	-4.85957	-1.56305	-0.65731
H	-5.62418	-0.99206	-0.52814
O	-1.311	-0.84897	-0.85389
O	1.982206	1.916205	-1.2155
H	2.79411	2.380408	-1.44939
O	4.573503	1.280048	-0.82706
H	5.34084	0.878252	-1.24491
O	4.638713	-1.79037	0.167496
H	3.404046	-2.15608	0.627934
O	2.797564	-1.37131	1.187687
H	-2.50009	-2.27434	-1.66628
H	0.819978	-1.85202	1.035677
TS:XBO→XGRA		M06-2X/6-311++G(d,p)	
O	0.127717	0.328188	1.072654
C	-2.85779	1.562509	-0.4118
C	-0.96207	0.306852	0.207275
C	-1.80635	-0.90199	0.590458
H	-2.62401	1.469767	-1.48224
H	-0.638	0.203624	-0.84371
H	-2.01884	-0.83005	1.665897
C	1.207616	2.260025	0.05413
C	1.352092	0.835392	0.575438
C	1.897669	-0.10666	-0.51067
C	3.978427	0.052073	0.144419

C	4.102564	-0.70415	-1.00425
H	2.009949	0.822832	1.444678
H	1.915442	0.306633	-1.52631
H	4.150154	1.119246	0.165453
H	4.292567	-0.20579	-1.95566
C	-3.10536	-0.88419	-0.19299
H	-2.86759	-1.00795	-1.26075
C	-3.81175	0.444704	-0.01099
H	-4.0804	0.560356	1.047726
H	0.522309	2.285793	-0.80155
O	-1.14761	-2.10658	0.278054
H	-0.20064	-2.009	0.453277
O	-3.98782	-1.90656	0.222641
H	-3.51507	-2.74388	0.16747
O	-4.95383	0.535999	-0.83168
H	-5.46578	-0.26864	-0.69688
O	-1.67391	1.512626	0.370111
O	1.656849	-1.36105	-0.3596
H	2.668747	-1.93248	-0.71816
O	3.895066	-0.53077	1.355003
H	3.848004	-1.48967	1.228085
O	3.839202	-1.97076	-0.9654
H	2.458155	3.593154	-0.64677
O	2.507005	2.688988	-0.32892
H	0.785846	2.881605	0.848357
H	-3.3125	2.536458	-0.23809
TS:XGRA→XED		M06-2X/6-311++G(d,p)	
O	1.019806	0.624555	-0.22333
C	-1.60184	-1.74058	0.214599
C	-0.198	0.136428	0.262062
C	-1.29407	1.065873	-0.23757
H	-1.62049	-1.79558	1.311389
H	-0.18376	0.116919	1.36553
H	-1.24156	1.091506	-1.33366
C	3.757156	1.144785	-0.21692
C	2.134462	-0.00369	0.306788
C	2.664052	-1.09716	-0.34386
H	2.320426	0.151455	1.366034
H	2.215822	-1.43428	-1.28075
C	-2.63966	0.514326	0.196989

H	-2.6847	0.529626	1.296665
C	-2.79222	-0.92225	-0.27159
H	-2.80987	-0.92748	-1.36993
H	3.574343	1.213001	-1.2982
O	-1.17642	2.360403	0.311909
H	-0.35645	2.752167	-0.00366
O	-3.71267	1.256443	-0.34215
H	-3.59934	2.176298	-0.08145
O	-3.96005	-1.50816	0.252233
H	-4.69489	-0.91966	0.049069
O	-0.38651	-1.1604	-0.23928
O	3.785256	-1.61552	0.031183
H	4.437712	-0.76594	0.235552
O	4.778731	0.544254	0.222198
H	-1.64085	-2.75165	-0.18619
H	3.319093	1.964622	0.364396
TS:XGRA→XAL		M06-2X/6-311++G(d,p)	
O	1.028856	0.67607	-0.64885
C	-1.39808	-1.73745	0.311744
C	-0.09256	0.185666	0.011907
C	-1.28778	1.015434	-0.43367
H	-1.27752	-1.68817	1.402689
H	0.048915	0.264	1.103698
H	-1.37399	0.927934	-1.52435
C	3.249079	1.135262	0.379306
C	2.246177	0.176338	-0.1821
C	2.852661	-0.93001	-0.86119
H	2.754613	-0.27925	1.245349
H	2.209473	-1.52787	-1.52404
C	-2.5387	0.466715	0.223552
H	-2.44406	0.588301	1.313487
C	-2.67991	-1.01361	-0.08532
H	-2.83868	-1.12671	-1.16635
H	4.105798	1.394668	-0.24508
O	-1.16199	2.366609	-0.04001
H	-0.39043	2.732561	-0.4829
O	-3.70823	1.113121	-0.23497
H	-3.60057	2.05877	-0.08981
O	-3.743	-1.58604	0.640495
H	-4.52295	-1.04313	0.484577

O	-0.27906	-1.16235	-0.34503
O	4.03123	-1.25537	-0.65129
H	4.342093	-0.39032	0.941919
O	3.770795	0.232513	1.464698
H	-1.44092	-2.78344	0.013199
H	2.813979	2.006294	0.861895
TS:XB12Mac		M06-2X/6-311++G(d,p)	
O	-0.14408	0.673333	-0.25522
C	2.501943	-1.70647	-0.34525
C	1.132974	0.189803	-0.51358
C	2.113218	1.058728	0.262449
H	2.733869	-1.67235	-1.41845
H	1.348093	0.247809	-1.59579
H	1.848325	0.998563	1.325877
C	-2.19775	1.149674	-1.311
C	-1.18668	0.060834	-1.00072
C	-1.85092	-1.06717	-0.20377
C	-3.02395	-0.51686	0.583436
C	-3.06547	0.898828	0.816923
H	-0.80504	-0.36065	-1.93647
H	-1.11539	-1.48445	0.488815
H	-4.053	-0.41483	-0.06593
H	-3.42075	1.343031	1.738663
C	3.517725	0.522692	0.055207
H	3.77762	0.623668	-1.00964
C	3.574093	-0.94844	0.428191
H	3.375597	-1.03969	1.504705
H	-1.75922	1.972531	-1.86919
O	2.103007	2.39504	-0.1921
H	1.235395	2.76858	-0.00938
O	4.464401	1.20302	0.851577
H	4.3976	2.143182	0.655009
O	4.821582	-1.5114	0.097343
H	5.503083	-0.95619	0.490709
O	1.220716	-1.14778	-0.09021
O	-2.26387	-2.03782	-1.14637
H	-2.80529	-2.68788	-0.68801
O	-3.37885	-1.3004	1.688435
H	-4.33474	-1.17384	1.780011
O	-5.19957	0.391349	0.334537

H	-6.11126	0.631717	0.143046
O	-2.66136	1.737303	-0.07575
H	2.463885	-2.74742	-0.02995
H	-3.06586	0.737309	-1.8333
TS:XB21Mac		M06-2X/6-311++G(d,p)	
O	-0.01087	-0.69358	0.437127
C	-2.49106	1.625349	-0.65053
C	-1.17363	-0.2807	-0.18429
C	-2.33573	-0.9936	0.493353
H	-2.47898	1.405492	-1.72591
H	-1.15011	-0.52039	-1.26072
H	-2.30765	-0.743	1.561631
C	2.09996	-1.62853	-0.17458
C	1.219656	-0.38513	-0.22091
C	1.910328	0.771009	0.502332
C	3.374918	0.839748	0.112437
C	4.055996	-0.34461	-0.35323
H	1.031406	-0.11104	-1.26599
H	1.840281	0.55113	1.574752
H	3.692629	1.820762	-0.23327
H	4.498951	-0.11149	1.147639
C	-3.63982	-0.50955	-0.11154
H	-3.66073	-0.7953	-1.17417
C	-3.72904	1.003967	-0.0162
H	-3.76852	1.281104	1.046034
H	2.312463	-1.89084	0.873002
O	-2.2742	-2.38867	0.293901
H	-1.46727	-2.71515	0.704268
O	-4.76235	-1.04395	0.557002
H	-4.68479	-2.00371	0.549103
O	-4.8532	1.49491	-0.7064
H	-5.62227	1.010539	-0.38797
O	-1.31568	1.121135	-0.02484
O	1.348135	2.025872	0.207644
H	0.385359	1.945411	0.27024
O	4.221309	0.851501	1.68443
H	4.953092	1.486882	1.706821
O	5.095028	-0.05487	-1.23666
H	5.74631	-0.75623	-1.16626
O	3.280855	-1.39783	-0.89131

H	-2.48872	2.70519	-0.51401
H	1.586792	-2.46328	-0.65341
TS:XB23Mac		M06-2X/6-311++G(d,p)	
O	-0.05067	0.829458	0.246545
C	2.431282	-1.64838	-0.43201
C	1.121569	0.308987	-0.25808
C	2.266836	1.075255	0.393963
H	2.48259	-1.548	-1.52455
H	1.15851	0.416929	-1.35591
H	2.177544	0.946657	1.480563
C	-2.20225	1.690706	-0.11347
C	-1.2638	0.541622	-0.47425
C	-1.86281	-0.79338	-0.13767
C	-3.28298	-0.89535	-0.0161
C	-4.09672	0.376551	0.159636
H	-1.02722	0.568279	-1.54776
H	-2.1856	-1.22191	1.276691
H	-3.80465	-1.69761	-0.53208
H	-4.12624	0.658381	1.22158
C	3.592466	0.513341	-0.07893
H	3.676049	0.673626	-1.16457
C	3.646378	-0.97829	0.195828
H	3.621774	-1.1312	1.283192
H	-2.18802	1.83052	0.976387
O	2.240171	2.441017	0.039573
H	1.397188	2.803294	0.330557
O	4.687822	1.10958	0.584397
H	4.623687	2.062784	0.4645
O	4.797118	-1.56306	-0.36747
H	5.555929	-1.05038	-0.06919
O	1.230803	-1.071	0.069819
O	-1.29827	-1.88326	-0.83641
H	-0.40325	-1.98737	-0.49116
O	-3.27113	-1.53874	1.632552
H	-3.39343	-2.49901	1.657644
O	-5.36475	0.136751	-0.34444
H	-5.85396	0.96506	-0.3235
O	-3.51428	1.433959	-0.56792
H	2.407192	-2.70747	-0.17957
H	-1.87238	2.613288	-0.58945

TS:XB32Mac		M06-2X/6-311++G(d,p)	
O	0.026903	1.013208	0.430739
C	2.269008	-1.70201	-0.10031
C	1.123411	0.342822	-0.09691
C	2.370609	1.119833	0.30462
H	2.188246	-1.77246	-1.19386
H	1.04102	0.286376	-1.19581
H	2.403948	1.162648	1.401137
C	-2.22032	1.790653	0.226146
C	-1.21866	0.712816	-0.17424
C	-1.76243	-0.63555	0.255115
C	-3.17662	-0.84325	0.183858
C	-4.07943	0.361178	0.159236
H	-1.11745	0.732753	-1.26403
H	-1.17984	-1.14834	1.015948
H	-2.54099	-1.50517	-1.02767
H	-4.38494	0.611071	1.191117
C	3.595604	0.392853	-0.21658
H	3.557569	0.390068	-1.31655
C	3.593408	-1.04583	0.270264
H	3.698997	-1.03997	1.363581
H	-2.32384	1.827122	1.319363
O	2.381676	2.414758	-0.25686
H	1.616934	2.891275	0.080468
O	4.796069	0.991853	0.224798
H	4.781207	1.917177	-0.04114
O	4.627076	-1.79136	-0.32907
H	5.447357	-1.30425	-0.19773
O	1.182225	-0.96257	0.436114
O	-1.37713	-1.65496	-1.14339
H	-1.09384	-2.53781	-0.86544
O	-3.63395	-1.83584	1.086316
H	-4.38457	-2.27136	0.675649
O	-5.20391	0.067993	-0.60771
H	-5.82813	0.795117	-0.51966
O	-3.44555	1.499954	-0.40112
H	2.211721	-2.70519	0.319593
H	-1.88823	2.765472	-0.13068
TS:XB34Mac		M06-2X/6-311++G(d,p)	
O	0.028801	0.815291	-0.25513

C	-2.46914	-1.65271	0.429845
C	-1.14217	0.319646	0.25597
C	-2.28727	1.068447	-0.41319
H	-2.53335	-1.54347	1.520451
H	-1.17047	0.426752	1.351625
H	-2.1909	0.927766	-1.49789
C	2.105909	1.685207	0.502897
C	1.244465	0.434304	0.43098
C	1.856382	-0.72349	-0.24564
C	3.349693	-0.86848	-0.07898
C	3.975495	0.509796	-0.24995
H	1.033889	-1.10268	1.319806
H	1.528333	-0.97426	-1.25705
H	3.58457	-1.18858	0.943302
H	3.75405	0.911254	-1.2541
C	-3.61654	0.512567	0.054984
H	-3.70678	0.677173	1.13929
C	-3.67182	-0.97942	-0.21664
H	-3.63356	-1.13567	-1.30317
H	2.013427	2.268309	-0.43089
O	-2.26125	2.437987	-0.07594
H	-1.39969	2.784742	-0.33079
O	-4.70696	1.106857	-0.61792
H	-4.63507	2.061397	-0.51261
O	-4.82944	-1.5621	0.333851
H	-5.58323	-1.0428	0.033939
O	-1.25714	-1.08257	-0.05993
O	1.211082	-1.89317	0.633227
H	0.305355	-1.99338	0.25854
O	3.826821	-1.78729	-1.03185
H	4.786468	-1.81094	-0.953
O	5.344925	0.346415	-0.06508
H	5.762163	1.212971	-0.07224
O	3.475717	1.377716	0.727324
H	-2.45023	-2.71387	0.183796
H	1.804498	2.327016	1.330882
TS:XB43Mac		M06-2X/6-311++G(d,p)	
O	-0.16481	0.427026	-0.57403
C	2.775733	-1.5545	-0.54538
C	1.160929	0.161021	-0.72872

C	1.993319	1.090318	0.158673
H	3.066969	-1.4331	-1.59854
H	1.470729	0.295664	-1.78231
H	1.680433	0.920213	1.198513
C	-2.44559	-0.24829	-1.91867
C	-1.6023	-1.00306	-0.92353
C	-1.94728	-1.04084	0.441206
C	-3.21613	-0.36296	0.89053
C	-3.56589	0.735296	-0.10261
H	-0.87015	-1.71786	-1.28334
H	-0.99909	-0.1695	0.407116
H	-4.04795	-1.07897	0.903266
H	-2.77736	1.505402	-0.11534
C	3.46395	0.765194	0.009399
H	3.762366	0.953251	-1.03306
C	3.695524	-0.70221	0.322314
H	3.453942	-0.87202	1.380341
H	-1.88317	0.602479	-2.31154
O	1.813073	2.442637	-0.20631
H	0.863353	2.601455	-0.23695
O	4.274324	1.524848	0.886465
H	4.057684	2.453679	0.754997
O	5.0259	-1.08154	0.048075
H	5.599954	-0.446	0.488259
O	1.420166	-1.19155	-0.35319
O	-1.5623	-2.16049	1.168285
H	-1.39843	-1.87789	2.073564
O	-2.97696	0.152358	2.184294
H	-3.79848	0.532427	2.511265
O	-4.79101	1.258009	0.279899
H	-5.03915	1.960417	-0.3283
O	-3.68951	0.16184	-1.38686
H	2.870976	-2.60618	-0.27815
H	-2.67725	-0.92843	-2.74211
TS:XB45Mac		M06-2X/6-311++G(d,p)	
O	-0.10087	1.622812	-0.16118
C	-1.53462	-1.57001	0.442112
C	-1.0297	0.738687	0.283605
C	-2.39767	1.03032	-0.33959
H	-1.59537	-1.50799	1.537779

H	-1.11261	0.794567	1.386876
H	-2.28716	0.943776	-1.42963
C	2.146049	1.534293	-1.22328
C	1.954433	1.661225	0.167463
C	2.198182	0.512497	1.105875
C	3.084499	-0.51884	0.427316
C	2.560151	-0.7825	-0.97665
H	1.819442	2.637538	0.613658
H	1.241458	0.025073	1.32957
H	4.105072	-0.12298	0.330485
H	1.497214	-1.05592	-0.95225
C	-3.41635	0.022902	0.150464
H	-3.52546	0.13479	1.239849
C	-2.9284	-1.38383	-0.1462
H	-2.87897	-1.50819	-1.2367
H	0.856959	1.495569	-1.19403
O	-2.85335	2.316122	0.020031
H	-2.13026	2.928765	-0.15584
O	-4.67433	0.179426	-0.47816
H	-4.95134	1.093687	-0.35923
O	-3.77564	-2.35337	0.428074
H	-4.67667	-2.13342	0.168358
O	-0.64064	-0.5946	-0.06761
O	2.787621	1.039061	2.273994
H	2.990646	0.295059	2.85106
O	3.054839	-1.67134	1.234412
H	3.541526	-2.36625	0.778366
O	3.346793	-1.79121	-1.51591
H	3.005444	-2.03023	-2.38235
O	2.729879	0.383507	-1.76517
H	-1.13715	-2.54857	0.174214
H	2.423291	2.412976	-1.79479
TS:XB1’2’Mac		M06-2X/6-311++G(d,p)	
O	0.18314	-1.28645	0.649221
C	2.278302	-0.79415	1.390433
H	2.182696	-1.57953	2.130844
C	2.590244	-1.12693	0.031419
H	1.401383	-1.30356	-0.16315
C	3.028816	0.020612	-0.85091
H	4.095071	0.244084	-0.70072

C	2.405317	1.550173	1.004287
H	3.438981	1.848866	1.191428
C	2.198407	1.235327	-0.46968
H	1.143859	1.01243	-0.65893
O	2.132968	0.402296	1.855631
O	3.341128	-2.30181	-0.07561
H	3.047458	-2.76583	-0.86457
O	2.794391	-0.36914	-2.18316
H	3.06125	0.358353	-2.75439
O	2.649629	2.326526	-1.24755
H	1.923546	2.93632	-1.40079
O	-4.97902	-0.08312	-0.66519
H	-5.14338	0.866459	-0.67141
C	-3.5977	-0.25076	-0.66458
H	-3.18863	-0.09974	-1.68016
C	-2.91741	0.72487	0.292894
H	-3.32736	0.55252	1.296518
C	-1.43075	0.4459	0.287123
H	-1.05196	0.606621	-0.7341
C	-1.97694	-1.89684	-0.28389
H	-1.57346	-1.78953	-1.30188
C	-1.16734	-1.00983	0.670134
H	-1.58191	-1.16475	1.683669
O	-3.35733	-1.56616	-0.25438
O	-3.22997	2.034078	-0.1539
H	-2.7713	2.655953	0.418952
O	-0.75496	1.348657	1.159788
H	-0.18849	0.80772	1.723411
H	1.723106	2.325027	1.347829
H	-1.89644	-2.94063	0.015225
TS:XB2’1’Mac		M06-2X/6-311++G(d,p)	
O	0.028762	0.711751	0.540374
C	1.137037	0.252223	-0.16867
H	1.389837	1.293507	-1.54982
C	2.289548	1.108438	0.073469
H	2.225737	1.901133	0.819682
C	3.670506	0.518162	-0.07603
H	3.927431	0.476674	-1.14222
C	2.543455	-1.67286	-0.26781
H	2.664009	-1.60289	-1.35803

C	3.671233	-0.91638	0.427342
H	3.500266	-0.92433	1.511116
O	1.308407	-1.13721	0.144106
O	2.101369	2.057249	-1.34156
H	1.654361	2.899068	-1.1568
O	4.582564	1.333324	0.619274
H	5.444651	0.907282	0.561469
O	4.954148	-1.42386	0.106447
H	5.10617	-2.24633	0.57824
O	-5.38019	0.479982	-0.04266
H	-5.71243	-0.42229	-0.11256
C	-4.06305	0.390583	0.391397
H	-4.02205	0.248003	1.485763
C	-3.32261	-0.745	-0.29789
H	-3.35846	-0.55706	-1.37987
C	-1.87281	-0.77974	0.151072
H	-1.83795	-0.98488	1.232197
C	-2.12346	1.670402	0.537371
H	-2.09784	1.55851	1.630674
C	-1.23969	0.588805	-0.08744
H	-1.13166	0.750406	-1.16775
O	-3.44912	1.607202	0.056458
O	-3.995	-1.94636	0.019652
H	-3.44668	-2.67262	-0.29677
O	-1.26636	-1.83099	-0.56819
H	-0.3267	-1.8549	-0.33037
H	-1.74219	2.659677	0.285192
H	2.545879	-2.72548	0.021807
TS:XB2’3’Mac		M06-2X/6-311++G(d,p)	
O	-0.00054	0.736437	0.429987
C	1.14027	0.324236	-0.22531
H	1.08925	0.557783	-1.29816
C	2.327084	1.036255	0.408951
H	2.076045	1.662677	1.261679
C	3.612187	0.422391	0.318502
H	3.518596	1.49126	-0.76057
C	2.473273	-1.53687	-0.71189
H	2.52956	-1.16738	-1.74395
C	3.694272	-1.05334	0.065987
H	3.740977	-1.57198	1.034369

O	1.283131	-1.07846	-0.08194
O	2.64276	2.28309	-0.80478
H	2.891691	3.131475	-0.40935
O	4.507737	0.873679	1.316273
H	5.392508	0.818805	0.94645
O	4.88767	-1.31829	-0.66698
H	5.173134	-2.21796	-0.48851
O	-5.3867	0.522311	-0.31036
H	-5.76543	-0.33764	-0.09517
C	-4.08973	0.526352	0.185234
H	-4.08619	0.724657	1.271643
C	-3.3804	-0.78954	-0.09654
H	-3.38113	-0.94032	-1.18479
C	-1.94365	-0.73674	0.394937
H	-1.94501	-0.61147	1.488453
C	-2.10465	1.728935	0.015119
H	-2.1163	1.952103	1.091558
C	-1.25011	0.479277	-0.21148
H	-1.09416	0.313783	-1.28489
O	-3.41309	1.56019	-0.48026
O	-4.11241	-1.81048	0.547819
H	-3.61026	-2.62802	0.462765
O	-1.36269	-1.97146	0.041247
H	-0.404	-1.91246	0.160049
H	2.421342	-2.62565	-0.73154
H	-1.66888	2.578419	-0.50921
TS:XB3’2’Mac		M06-2X/6-311++G(d,p)	
O	0.060364	0.792784	0.210564
C	1.182312	0.34344	-0.47099
H	1.019612	0.441186	-1.55768
C	2.375991	1.15479	-0.04414
H	2.70909	1.2037	1.38115
C	3.642417	0.507704	0.089337
H	4.51634	1.044667	-0.26733
C	2.554296	-1.55112	-0.74999
H	2.639446	-1.25598	-1.80325
C	3.744954	-1.01241	0.03371
H	3.696076	-1.43496	1.042666
O	1.372384	-1.0376	-0.16853
O	2.418259	2.416645	-0.66722

H	1.903238	3.031145	-0.13996
O	3.810979	0.986498	1.827506
H	3.938989	0.326875	2.525973
O	4.90937	-1.43114	-0.64065
H	5.68205	-1.25296	-0.09796
O	-5.35418	0.408025	-0.18188
H	-5.6888	-0.45795	0.077712
C	-4.02882	0.467403	0.229145
H	-3.96392	0.712035	1.304169
C	-3.30113	-0.84091	-0.04111
H	-3.36144	-1.03783	-1.12035
C	-1.84134	-0.72827	0.361534
H	-1.78372	-0.55384	1.446866
C	-2.09126	1.710737	-0.11518
H	-2.04412	1.983629	0.94881
C	-1.21613	0.474987	-0.3384
H	-1.12545	0.264307	-1.41158
O	-3.42402	1.488643	-0.51941
O	-3.96416	-1.85339	0.687154
H	-3.44009	-2.65768	0.608108
O	-1.24661	-1.96379	0.03041
H	-0.28579	-1.8759	0.10925
H	2.51532	-2.63794	-0.68976
H	-1.71359	2.545883	-0.70386
TS:XB3’4’Mac		M06-2X/6-311++G(d,p)	
O	-0.01422	0.820168	-0.35091
C	-1.18222	0.313971	0.192051
H	-1.17638	0.40269	1.291196
C	-2.33448	1.100591	-0.42158
H	-2.26969	0.95014	-1.50452
C	-3.6284	0.5262	0.10011
H	-4.17883	1.196311	0.758942
C	-2.41965	-1.6606	0.504164
H	-2.19557	-1.72612	1.579798
C	-3.72054	-0.89428	0.310587
H	-4.47298	-0.5333	-1.01131
O	-1.3288	-1.04043	-0.17367
O	-2.28209	2.463558	-0.08072
H	-1.44997	2.813612	-0.41533
O	-4.66772	0.558419	-1.30442

H	-5.56814	0.848126	-1.09537
O	-4.65814	-1.22348	1.329354
H	-5.21226	-1.93972	1.015974
O	5.342565	0.395086	0.523248
H	5.719168	-0.42153	0.175469
C	4.066592	0.510582	-0.01083
H	4.108068	0.901758	-1.04279
C	3.331768	-0.82181	0.001503
H	3.286886	-1.16701	1.043573
C	1.917154	-0.65268	-0.52519
H	1.964769	-0.32457	-1.57496
C	2.088135	1.697237	0.303886
H	2.143139	2.110856	-0.71372
C	1.214424	0.441247	0.271909
H	1.022674	0.085351	1.29184
O	3.375425	1.420779	0.805412
O	4.076441	-1.72274	-0.78993
H	3.55767	-2.52941	-0.88033
O	1.307496	-1.91927	-0.43262
H	0.35134	-1.81819	-0.55109
H	-2.47875	-2.67447	0.107292
H	1.644456	2.445994	0.959657
TS:XB4’3’Mac		M06-2X/6-311++G(d,p)	
O	-0.04124	0.731239	-0.48898
C	-1.21456	0.210217	0.02046
H	-1.24864	0.307762	1.118196
C	-2.37476	0.953782	-0.6203
H	-2.23762	0.90847	-1.71011
C	-3.67277	0.309041	-0.23379
H	-4.02412	0.193679	1.174981
C	-2.38989	-1.80049	0.330157
H	-2.20006	-1.85155	1.406101
C	-3.7046	-1.07761	0.077088
H	-4.53704	-1.67122	-0.2894
O	-1.30746	-1.16381	-0.32904
O	-2.41057	2.304597	-0.19327
H	-1.65214	2.755481	-0.57695
O	-4.78459	0.769156	-0.96458
H	-4.89356	1.701636	-0.75767
O	-4.29999	-0.83486	1.784265

H	-5.24946	-0.97664	1.908136
O	5.274088	0.550769	0.671403
H	5.70401	-0.24965	0.349113
C	4.024073	0.607158	0.07054
H	4.102596	0.992059	-0.96162
C	3.347793	-0.7561	0.055907
H	3.262853	-1.09675	1.096974
C	1.958516	-0.64871	-0.54711
H	2.049097	-0.32588	-1.59559
C	1.983068	1.711748	0.269435
H	2.074378	2.121783	-0.74682
C	1.168414	0.41832	0.202045
H	0.94066	0.060815	1.21388
O	3.252973	1.49262	0.840594
O	4.172535	-1.62847	-0.68721
H	3.696942	-2.45893	-0.7962
O	1.392231	-1.93783	-0.47707
H	0.443193	-1.87338	-0.65514
H	1.47285	2.443926	0.894615
H	-2.43946	-2.81303	-0.06798
TS:XB4’5’Mac		M06-2X/6-311++G(d,p)	
O	-0.03392	0.881101	-0.49208
C	-1.17768	0.25565	-0.05274
H	-1.12285	0.041393	1.027785
C	-2.37342	1.149961	-0.35661
H	-2.4551	1.246751	-1.4477
C	-3.62663	0.49244	0.204913
H	-3.5406	0.508738	1.295135
C	-2.53895	-1.65556	-0.61504
H	-2.91918	-2.20821	0.665629
C	-3.72406	-0.94886	-0.25694
H	-4.67836	-1.24475	-0.68134
O	-1.31372	-0.96526	-0.76826
O	-2.16925	2.392796	0.262276
H	-2.9669	2.913993	0.125734
O	-4.72946	1.269271	-0.22328
H	-5.46614	1.141707	0.380021
O	-3.89253	-1.86813	1.340456
H	-4.62454	-2.48835	1.475838
O	5.301772	0.42767	0.477281

H	5.642216	-0.46289	0.33485
C	4.031851	0.466411	-0.08526
H	4.093283	0.591689	-1.18086
C	3.241024	-0.79361	0.237419
H	3.178991	-0.8765	1.331247
C	1.837722	-0.69622	-0.3329
H	1.89919	-0.63522	-1.42969
C	2.103744	1.77466	-0.09044
H	2.175325	1.926598	-1.17672
C	1.183633	0.583522	0.179225
H	1.000494	0.488966	1.257287
O	3.381197	1.574776	0.476013
O	3.948874	-1.88939	-0.30432
H	3.388545	-2.66753	-0.21243
O	1.169526	-1.87771	0.058096
H	0.2857	-1.86805	-0.33753
H	-2.62043	-2.41437	-1.38474
H	1.687021	2.67462	0.358274
Benzoic Acid		M06-2X/6-311++G(d,p)	
C	-0.51156	1.220808	-1.2E-05
C	0.215349	0.030772	-2E-06
C	-0.44299	-1.19845	0.000011
C	-1.8321	-1.23281	0.000014
C	-2.55828	-0.0455	0.000005
C	-1.89892	1.181086	-8E-06
C	1.700316	0.123841	-6E-06
O	2.302718	-1.08205	0.000004
O	2.323626	1.151371	-8E-06
H	0.027298	2.160645	-2.1E-05
H	0.133269	-2.11473	0.000018
H	-2.34876	-2.18486	0.000025
H	-3.6416	-0.07578	0.000007
H	-2.46711	2.103321	-1.6E-05
H	3.255304	-0.92166	0.000007
Protonated Benzoic Acid		M06-2X/6-311++G(d,p)	
C	-0.52754	1.225582	-2.7E-05
C	0.184238	0.011755	-3E-06
C	-0.49769	-1.2184	0.000016
C	-1.88044	-1.22586	0.000021
C	-2.58066	-0.02066	0.000003

C	-1.908	1.203287	-2.2E-05
C	1.619027	-0.00135	-3E-06
O	2.238011	-1.12716	-5.9E-05
O	2.381152	1.041514	0.00006
H	-0.03098	2.191312	-6.4E-05
H	0.059896	-2.14652	0.000033
H	-2.41553	-2.16664	0.000039
H	-3.66436	-0.03139	0.000006
H	-2.46483	2.131228	-4.3E-05
H	3.205445	-1.02291	-3.5E-05
H	1.903508	1.88396	0.000149
TMMS		M06-2X/6-311++G(d,p)	
Si	0.067236	-0.02861	0.362824
O	-1.10286	1.096092	0.597978
O	1.432745	0.754988	-0.09838
O	-0.30339	-1.01141	-0.91528
C	0.237152	-0.99351	1.930498
H	0.51638	-0.33617	2.755593
H	-0.70368	-1.48167	2.194767
H	1.003923	-1.76538	1.829507
C	-1.41219	2.088106	-0.3679
H	-2.18299	2.734933	0.050196
H	-0.52862	2.686492	-0.60517
H	-1.78973	1.63252	-1.28894
C	2.515353	0.151412	-0.78364
H	3.187451	0.94323	-1.1138
H	3.069285	-0.52301	-0.12209
H	2.162528	-0.4107	-1.65211
C	-1.44694	-1.84408	-0.93636
H	-2.3559	-1.27559	-0.71152
H	-1.53856	-2.27297	-1.93417
H	-1.35364	-2.66018	-0.21203
Protonated TMMS		M06-2X/6-311++G(d,p)	
Si	-0.11177	-0.23528	0.414459
O	0.075856	1.584109	0.485255
O	1.423877	-0.66342	0.265777
O	-0.89669	-0.42755	-0.9745
C	-0.96726	-0.59298	1.989454
H	-0.33845	-0.34663	2.84833
H	-1.91298	-0.05266	2.073393

H	-1.18544	-1.66247	2.048626
C	0.859155	2.267602	-0.55952
H	0.568176	3.31417	-0.551
H	1.916179	2.124256	-0.34967
H	0.569261	1.793285	-1.49395
C	2.094192	-1.51298	-0.68041
H	3.069324	-1.07418	-0.87961
H	2.221542	-2.50052	-0.24025
H	1.518029	-1.58329	-1.60373
C	-2.29973	-0.40651	-1.272
H	-2.6549	0.624044	-1.31307
H	-2.43046	-0.87582	-2.24367
H	-2.8621	-0.96448	-0.52115
H	0.144114	2.022337	1.345937
TS: BA+TMMS-MeOH		M06-2X/6-311++G(d,p)	
C	-2.78206	1.089417	0.252043
C	-2.47102	-0.23172	-0.08675
C	-3.48121	-1.14075	-0.41903
C	-4.8014	-0.71819	-0.42238
C	-5.1109	0.597734	-0.08675
C	-4.10486	1.500498	0.25382
C	-1.08042	-0.67836	-0.08498
O	-0.83719	-1.92273	-0.23721
O	-0.13899	0.171191	0.059929
C	1.624585	0.462174	2.200585
O	3.334277	0.217896	0.021501
C	3.919691	-0.00676	-1.25326
O	1.564135	-1.59512	-0.00097
C	2.594313	-2.5926	0.145713
H	-1.99201	1.774752	0.532586
H	-3.22549	-2.16158	-0.6742
H	-5.59015	-1.41233	-0.68293
H	-6.14467	0.922706	-0.08685
H	-4.35699	2.518358	0.523341
H	0.191523	-2.02245	-0.19253
H	2.563857	0.201795	2.691108
H	1.454322	1.53046	2.354324
H	0.810232	-0.07745	2.686495
H	4.999001	-0.06877	-1.12187
H	3.561806	-0.9379	-1.70242

H	3.692815	0.817351	-1.93763
H	2.753892	-3.07199	-0.81943
H	3.519437	-2.13338	0.490919
H	2.254741	-3.32937	0.873065
Si	1.731516	0.050914	0.411389
O	1.466698	1.703379	-0.57124
H	0.541994	1.933755	-0.73035
C	2.349226	2.85992	-0.57155
H	1.947518	3.611134	0.106409
H	3.31395	2.507615	-0.22133
H	2.415875	3.239409	-1.58896
Product: BA+TMMS-MeOH (m/z 227)		M06-2X/6-311++G(d,p)	
C	2.422405	-1.10188	0.254187
C	2.013317	0.216865	0.008844
C	2.951207	1.229669	-0.24322
C	4.298566	0.914817	-0.24749
C	4.705587	-0.39683	-0.00508
C	3.772769	-1.40312	0.244663
C	0.605602	0.538075	0.016095
O	0.236622	1.742381	-0.22854
O	-0.25758	-0.38288	0.264693
C	-2.4395	-0.8712	2.11469
O	-2.55407	-1.42815	-0.68389
C	-2.39092	-1.41236	-2.10473
O	-2.24807	1.189047	0.002565
C	-3.55149	1.804856	-0.06601
H	1.684208	-1.87038	0.445365
H	2.61804	2.242863	-0.43001
H	5.034092	1.685914	-0.43752
H	5.762332	-0.63751	-0.01024
H	4.103475	-2.41677	0.431064
H	-0.76155	1.820881	-0.19634
H	-3.52592	-0.87467	2.230663
H	-2.08086	-1.87818	2.336185
H	-2.01593	-0.17782	2.843477
H	-3.11376	-2.10842	-2.5229
H	-2.574	-0.41234	-2.50517
H	-1.38255	-1.73782	-2.36585
H	-3.42634	2.789855	-0.50859
H	-4.21325	1.204654	-0.69228

H	-3.96641	1.903152	0.937504
Si	-1.99157	-0.40071	0.412449
TS: BA+TMMS-2MeOH		M06-2X/6-311++G(d,p)	
C	-2.58225	1.183493	-0.32183
C	-2.02394	-0.06502	-0.02419
C	-2.82938	-1.19427	0.165835
C	-4.20369	-1.06774	0.056843
C	-4.76305	0.174797	-0.24023
C	-3.95847	1.29715	-0.43009
C	-0.58999	-0.20119	0.095872
O	0.041064	-1.25415	0.354415
O	0.217848	0.826947	-0.04864
Si	1.706695	0.021567	0.384261
C	2.01975	-0.16083	2.18089
O	2.808347	0.975815	-0.34592
C	2.854458	2.404546	-0.28456
O	2.305169	-1.40486	-0.55889
C	3.503623	-1.52074	-1.40409
H	-1.93753	2.042053	-0.46376
H	-2.36962	-2.14721	0.398514
H	-4.84202	-1.92961	0.203471
H	-5.83949	0.269225	-0.32398
H	-4.40762	2.255125	-0.65885
H	1.703423	-2.1636	-0.59409
H	2.980883	-0.65809	2.333385
H	2.094751	0.831699	2.633161
H	1.245246	-0.72707	2.695845
H	3.679788	2.731224	-0.9128
H	1.921211	2.829707	-0.65782
H	3.031418	2.739183	0.740143
H	3.863696	-2.54105	-1.30248
H	3.222909	-1.28248	-2.42617
H	4.217429	-0.80221	-1.01871
Prod: BA+TMMS-2MeOH (m/z 195)		M06-2X/6-311++G(d,p)	
C	2.130811	-0.01371	1.22662
C	1.448046	-0.06752	0.000071
C	2.130431	-0.01073	-1.22657
C	3.508186	0.100636	-1.21738
C	4.189771	0.154058	-0.00011
C	3.50857	0.097655	1.217245

C	0.028514	-0.18373	0.000085
O	-0.72238	-0.24785	-1.06209
O	-0.72233	-0.25027	1.062084
O	-3.07233	0.853117	0.000803
C	-2.8416	2.272904	0.001855
Si	-2.12686	-0.41583	-0.00025
C	-2.92412	-2.04308	-0.00202
H	1.576323	-0.06047	2.1563
H	1.575619	-0.05524	-2.15616
H	4.05626	0.145519	-2.14958
H	5.270162	0.24113	-0.00017
H	4.056973	0.14024	2.149358
H	-3.81758	2.749615	-0.01325
H	-2.30318	2.556656	0.906049
H	-2.27691	2.554776	-0.88687
H	-3.55565	-2.14327	-0.88766
H	-2.18201	-2.8427	-0.0006
H	-3.55939	-2.14353	0.880891
m/z 195 Extended Isomer		M06-2X/6-311++G(d,p)	
C	2.000261	1.126519	0.267408
C	1.569832	-0.14921	-0.1108
C	2.487839	-1.18734	-0.31
C	3.838789	-0.94369	-0.1266
C	4.269331	0.326408	0.253467
C	3.354771	1.358577	0.450074
C	0.160168	-0.46566	-0.31549
O	-0.34579	-1.49825	-0.62505
O	-0.6986	0.657062	-0.11579
O	-3.1542	-0.61945	0.325871
C	-3.16545	-2.03845	0.616241
Si	-2.3006	0.632495	-0.03964
C	-3.14047	2.211757	-0.33211
H	1.282625	1.922777	0.413954
H	2.129613	-2.16557	-0.6069
H	4.557998	-1.73836	-0.2788
H	5.32698	0.513666	0.396506
H	3.700014	2.341506	0.744117
H	-4.12868	-2.40961	0.278932
H	-2.34473	-2.51872	0.091246
H	-3.0668	-2.15419	1.693175

H	-4.17254	2.157597	0.013471
H	-2.60726	3.015664	0.179507
H	-3.13054	2.431898	-1.40367
m/z 195 Folded Isomer		M06-2X/6-311++G(d,p)	
C	-2.36631	-0.67529	-0.0769
C	-1.07465	-0.69839	0.410582
C	-0.46567	0.486314	0.914028
C	-1.19391	1.693246	0.907235
C	-2.47134	1.718751	0.369946
C	-3.05936	0.538628	-0.09157
C	-0.16931	-1.87509	0.161936
O	1.056745	-1.39208	-0.24038
O	-0.4406	-3.01915	0.23405
Si	1.117299	0.236845	-0.56664
C	0.542873	0.876137	-2.17208
O	2.428497	0.923478	0.016065
C	3.31744	0.53509	1.079226
H	-2.80686	-1.58415	-0.47114
H	0.364778	0.39459	1.621131
H	-0.76353	2.584953	1.348764
H	-3.0313	2.645218	0.344417
H	-4.06866	0.567495	-0.4868
H	1.195025	0.495381	-2.96283
H	-0.48163	0.564242	-2.38213
H	0.600844	1.96609	-2.17551
H	4.324131	0.801745	0.767933
H	3.053927	1.093316	1.977611
H	3.255356	-0.53911	1.259226
TS: CO_2 Loss		M06-2X/6-311++G(d,p)	
C	-1.5074	-1.13217	-0.41927
C	-0.55188	-0.10296	-0.14711
C	-1.0009	1.254601	-0.18099
C	-2.3247	1.554921	-0.40949
C	-3.23511	0.515382	-0.62879
C	-2.82957	-0.82397	-0.64586
C	0.053332	-0.40142	1.599242
O	1.299184	-0.6217	1.393395
O	-0.70105	-0.34601	2.473235
Si	1.317821	-0.44997	-0.36392
C	1.792958	-1.99924	-1.20059

O	2.203443	0.817971	-0.75628
C	2.527221	2.077209	-0.15838
H	-1.19226	-2.17156	-0.4154
H	-0.29213	2.056265	0.004801
H	-2.66332	2.583166	-0.41624
H	-4.2805	0.752894	-0.79392
H	-3.55333	-1.60744	-0.83141
H	2.8519	-2.19513	-1.01562
H	1.215213	-2.85221	-0.84077
H	1.648387	-1.9029	-2.2788
H	3.598335	2.230167	-0.26969
H	1.992436	2.866007	-0.68688
H	2.269429	2.084112	0.903375
m/z 151		M06-2X/6-311++G(d,p)	
C	2.858667	0.958608	0.000042
C	3.341959	-0.34834	-2.9E-05
C	2.469562	-1.43648	-0.00011
C	1.101394	-1.22386	-0.00012
C	0.602913	0.093673	-5.3E-05
C	1.491749	1.185556	0.000023
H	3.546839	1.794255	0.000108
H	4.411721	-0.52168	-1.8E-05
H	2.860139	-2.44627	-0.00017
H	0.417969	-2.06568	-0.00018
H	1.123493	2.206083	0.000082
Si	-1.1646	0.3782	-1.5E-05
O	-2.05708	-0.93346	0.00001
C	-2.00133	2.004888	0.000152
H	-2.63838	2.09993	0.884496
H	-1.28336	2.825673	-0.00117
H	-2.64065	2.099033	-0.88263
C	-3.46751	-1.21967	0.000019
H	-4.05112	-0.29798	0.000156
H	-3.68507	-1.80326	-0.89139
H	-3.68501	-1.80347	0.891304
m/z 105		M06-2X/6-311++G(d,p)	
C	-2.1871	0.000002	0
C	-1.50732	1.221058	0
C	-0.12816	1.242158	0
C	0.545881	0.000002	0

C	-0.12816	-1.24215	0
C	-1.50732	-1.22105	0
H	-3.27114	0.000002	0
H	-2.0585	2.15261	0
H	0.424757	2.173596	0
H	0.424757	-2.17359	0
H	-2.0585	-2.15261	0
C	1.933381	0.000004	0
O	3.051421	-1.4E-05	0
MW 90 Da		M06-2X/6-311++G(d,p)	
Si	-0.45414	0.208357	-0.00347
O	-0.41881	1.727793	0.00165
O	0.866358	-0.73643	-0.00512
C	2.212003	-0.25761	0.003879
H	2.715371	-0.66272	0.881478
H	2.711839	-0.6151	-0.89626
H	2.237702	0.833492	0.032369
C	-1.91999	-0.90634	0.000954
H	-2.82734	-0.33691	-0.19357
H	-1.8025	-1.68838	-0.75045
H	-2.00961	-1.39454	0.973808

VITA

VITA

Mckay Whetton Easton was born September 4th, 1986 in Aurora, Colorado to David Easton and Chris Easton. He graduated from Eaglecrest High School with honors in 2004. While in high school, he participated in theatre, volleyball, and daily early morning seminary. Following high school, he served a proselyting mission for 2 years for The Church of Jesus Christ of Latter-Day Saints in the Bangkok, Thailand area. While there, he became fluent in Thai, taught classes on religion and English, and instructed other missionaries on effective teaching. He subsequently enrolled at Brigham Young University, where he received a dual degree in Chemical Engineering and Mathematics in 2010. He began a teaching assistantship in the BYU math lab in 2008 and beginning in 2009, supervised and trained groups of other teaching assistants, including composing workshops for a training program that would help the math lab become certified through the College Reading & Learning Association (CRLA). Mckay was accepted to Purdue University in 2010, where he studied under Professor Fabio H. Ribeiro, with strong collaborations with Professor Hilkka I. Kenttämaa and Doctor John J. Nash. His area of research was using density functional theory to investigate reaction mechanisms, especially thermal degradation of biomass model compounds during fast pyrolysis. In 2014, Mckay was awarded the Magoon award for excellence in teaching by the College of Engineering at Purdue University. After graduating with his Ph.D. in 2016, Mckay will

begin a post-doctoral fellowship under Professor Kenttämaa in the chemistry department. Mckay is married to Sheri Easton and has three children, Dallin Easton, Connor Easton, and Bennett Easton.